



## Supporting Document for Surrogate Model Construction of Welded HSS Tubular Y-Joints

### Citation

Garifullin, M., Jokinen, T., & Heinisuo, M. (2016). Supporting Document for Surrogate Model Construction of Welded HSS Tubular Y-Joints: Preliminary version. (Tampere University of Technology. Department of Civil Engineering. Structural Engineering. Research Report; Vol. 164). Tampere University of Technology. Department of Civil Engineering.

### Year

2016

### Version

Publisher's PDF (version of record)

### Link to publication

[TUTCRIS Portal](http://www.tut.fi/tutcris) (<http://www.tut.fi/tutcris>)

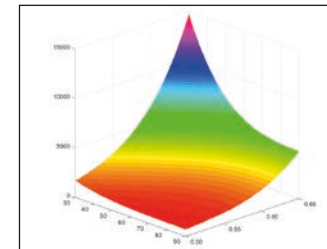
### Take down policy

If you believe that this document breaches copyright, please contact [cris.tau@tuni.fi](mailto:cris.tau@tuni.fi), and we will remove access to the work immediately and investigate your claim.

Marsel Garifullin, Timo Jokinen & Markku Heinisuo

**Supporting Document for Surrogate Model Construction of  
Welded HSS Tubular Y-Joints**

Preliminary version



Tampereen teknillinen yliopisto. Rakennustekniikan laitos. Rakennetekniikka.  
Tutkimusraportti 164  
Tampere University of Technology. Department of Civil Engineering. Structural  
Engineering. Research Report 164

Marsel Garifullin, Timo Jokinen & Markku Heinisuo

Supporting Document for Surrogate Model Construction of  
Welded HSS Tubular Y-Joints  
Preliminary version

Tampere University of Technology. Department of Civil Engineering  
Tampere 2016

ISBN 978-952-15-3699-1 (printed)  
ISBN 978-952-15-3700-4 (PDF)  
ISSN 1797-9161

## TABLE OF CONTENTS

1. Introduction.....	2
2. Theoretical background.....	3
2.1. Surrogate model construction.....	3
2.2. Surrogate model validation.....	4
2.3. Requirements of Eurocodes.....	4
2.4. Example of Kriging.....	5
3. Finite element analysis.....	18
3.1. Finite element modeling .....	18
3.2. Validation of FEM .....	20
3.3. Verification of FEM.....	21
4. Surrogate modeling I.....	26
4.1. Sampling .....	26
4.2. Attempt I .....	26
4.3. Pseudo points.....	29
4.4. Sample points analysis .....	31
5. Surrogate modeling II.....	33
5.1. New sampling .....	33
5.2. Attempt II .....	35
5.3. Interpolated pseudo points .....	36
6. Surrogate modeling III.....	40
6.1. Attempt III .....	40
6.2. Multi-model approach.....	44
6.3. Validation points analysis .....	46
6.4. Improved $\beta$ curves .....	48
6.5. Improved $\varphi$ curves .....	51
6.6. Complex model.....	53
6.7. Alternative methods .....	54
7. Fillet welds study .....	56
7.1. Effect of fillet welds .....	56
7.2. Exact correlation coefficients.....	57
7.3. Correlation coefficients analysis .....	58
7.4. Butt welds vs. fillet welds.....	65
7.5. Discrete correlation coefficients.....	67
8. Axial forces study.....	69
8.1. Effect of axial forces.....	69
8.2. Eurocode approach.....	69
8.3. New formula .....	73
8.4. Figures .....	76
References.....	82
Appendices .....	86
Appendix A. Sample points I .....	86
Appendix B. Sample points II .....	88
Appendix C. Pseudo points.....	89
Appendix D. DACE code.....	120
Appendix E. ooDACE code, single model.....	121
Appendix F. ooDACE code, multi model.....	122
Appendix G. ooDACE code, complex model .....	122
Appendix H. ooDACE code, 3D graphs.....	123
Appendix I. Polyfitn code .....	126
Appendix J. 3D plots.....	126

## **1. Introduction**

Tubular structures with welded joints are used in the wide range of structural applications. The most typical application is tubular trusses. The structural analysis model is frequently constructed using beam finite elements, and the braces are connected to the chords using hinges. In reality, the welded joint does not behave as a hinge when it is loaded by the moment. The joint has resistance against the moment, but in the joint area deformations may occur both at the brace and at the chord, so the stiffness against the moment has to be taken into account in the global analysis of the structure. In the EN 1993-1-8 (2005) only the moment resistance is given for the joint where the angle between the brace and the chord is 90 degrees. In (Grotmann and Sedlacek, 1998) there is the equation which can be used to calculate the initial rotational stiffness for the same case, angle 90 degrees.

When aiming to economic and environmental friendly design the stiffness of the joints must be taken into account. This is especially true when using high strength steel in structures, because then buckling at the ultimate limit state and deflections and vibrations in the serviceability limit state are often critical. In (Boel, 2010) and (Snijder et al., 2011) it has been shown that the rotational stiffness of the welded tubular joint is the main parameter when considering buckling of members of tubular trusses. However, this information is very limited, as given above.

In design it is possible to define the rotational stiffness for the joint using comprehensive finite element analysis (FEA). In practice, this is impossible, especially when performing optimization of structures when the structural analysis must be done thousands and thousands times. In order to avoid these computationally heavy calculations so called surrogate models (or meta models) have been developed. Surrogate models have been used widely in the aerospace applications (Roux et al., 1998), (Jin et al., 2001), (Queipo et al., 2005), (Kleijnen, 2008), (Müller, 2012). Civil engineering applications can be found, too (Mukhopadhyay et al., 2015). In (Díaz et al., 2012) there are 9 references presented (Yun et al., 2008), (Jadid and Fairbairn, 1996), (Anderson et al., 1997), (Stavroulakis et al., 1997), (De Lima et al., 2005), (Guzelbey et al., 2006), (Pirmoz and Gholizadeh, 2007), (Salajegheh et al., 2008), (Kim et al., 2010) dealing with steel structures using surrogate models. In (Díaz et al., 2012) the optimum design of steel frames is presented using semi-rigid joints and surrogate models.

The standard steps in the construction of the surrogate model are:

- Design of experiments (DOE);
- Surrogate model construction;
- Surrogate model validation.

Moreover, the fourth step is the fidelity validation, but it is not needed here.

## 2. Theoretical background

### 2.1. Surrogate model construction

In the surrogate model construction we replace the computationally expensive function  $f(x)$  by a sum of two other functions ( $x$  is the vector of the variables (Müller, 2012)):

$$f(x) = s(x) + \varepsilon(x) \quad (2.1)$$

where  $s(x)$  is the surrogate model at the point  $x$  and  $\varepsilon(x)$  is the difference between the two. The idea is to use the function  $s(x)$  during the calculations or optimization instead of the function  $f(x)$ . The function  $s(x)$  is chosen so that it is cheap to evaluate, and thus the computation times can be reduced considerably.

We can start with a quadratic regression model:

$$s_p(x) = b_0 + \sum_{i=1}^k b_i x_i + \sum_{i=1}^k b_{ii} x_i^2 + \sum_{i=1}^{k-1} \sum_{j=i+1}^k b_{ij} x_i x_j \quad (2.2)$$

or with linear regression ( $b_{ij} = 0$ ) or with constant, only  $b_0 \neq 0$ . If this gives good results (see later criteria) then we can add to the regression a *predictor*  $Z(x)$  (stochastic process) and end up to Kriging.

Kriging is named after the pioneering work of D.G. Krige (a South African mining engineer), and was formally developed by (Matheron, 1963). In (Sacks, Schiller, et al., 1989; Sacks, Welch, et al., 1989) and (Jones et al., 1998) it was made well-known in the context of the modelling, and optimization of deterministic functions, respectively. The Kriging models consist of two components. The first component is some simple model that captures the trend in the data, and the second component measures the deviation between the simple model and the true function. An example of the surrogate model  $\bar{f}(x)$  using Kriging with one variable  $x$  with  $n$  sample points is:

$$\bar{f}(x) = \frac{1}{n} \sum_{j=1}^n x_j + Z(x) \quad (2.3)$$

where the zero order regression is used and the predicted value  $\bar{f}(x)$  is given scaled to [0;1]. The real values  $f(x)$  can be calculated from the normalized data  $\bar{f}(x)$ . In the construction of  $Z(x)$  we need a *correlation function* between points. Define  $R$  as the matrix  $R$  of stochastic-process correlations between the sample points  $x_i$  and  $x_j$ :

$$R_{ij} = R(q, x_i, x_j), \quad i, j = 1, \dots, n \quad (2.4)$$

and let  $\bar{r}(x)$  be a vector of correlation between sample points and untried points  $x$ :

$$\bar{r}(x) = [R(q, x_1, x) \dots R(q, x_n, x)]^T \quad (2.5)$$

The mostly preferred correlation function is the Gaussian correlation:

$$R(x_i, x_j) = \exp \frac{1}{\hat{\theta}} \sum_{k=1}^m q_k \left| x_i^k - x_j^k \right|^2 \quad (2.6)$$

where

- $\theta_k$  are unknown correlation parameters,  $k = 1, \dots, m$ ;
- $m$  is the number of design variables;
- $x_i^k$  and  $x_j^k$  are the components of samples  $x_i$  and  $x_j$ .

After this the surrogate model can be defined, see e.g. (Müller, 2012).

## 2.2. Surrogate model validation

The validation process uses a new sample size approximately equal to one third of the sample size used to build the surrogate model (Lee and Jung, 2006). The validation process consists of comparing the results of the surrogate model with those of the real response. This is a specific problem which depends on the accuracy required of the fitted model. If this accuracy is too low, then the surrogate model must be modified by the introduction of more sample points or by the modification of the surrogate model variables.

The accuracy of the surrogate model can be checked (Díaz et al., 2012) using  $R^2$  value. It consists of calculating the square of the difference between the real response and surrogate model results divided by the difference between the real response results and the mean of the observed values. The larger the value of  $R^2$ , the more accurate is the surrogate model. The validation process consists of using a new set of sample points, but excluding the original sample point set.

$$R^2 = 1 - \frac{\sum_{i=1}^r (y_i - \bar{y}_i)^2}{\sum_{i=1}^r (y_i - \bar{y})^2} \quad (2.7)$$

where  $y_i$  is the real response value,  $\bar{y}_i$  is the surrogate predicted value at the  $i^{\text{th}}$  validation point,  $\bar{y}$  is the mean of the validation point values, and  $r$  is number of validation points.

No single rule exists that specifies a minimum  $R^2$  value which guarantees a good fitting surrogate model. In (Díaz et al., 2012) only the surrogate models with  $R^2$  values larger than 0.85 are considered.

## 2.3. Requirements of Eurocodes

In this research the Eurocodes are used for joints (EN 1993-1-8, 2005) and extension for steel grades up to S700 (EN 1993-1-12, 2007). The variables of the welded T-joint are:

- Chord member dimensions  $b_0, t_0$ ;
- Brace dimensions  $b_1, t_1$ ;
- Angle  $\theta$  between the brace and the chord;
- Weld type  $w_f$  or  $w_b$ , can be either fillet weld ( $w_f$ ) or butt weld ( $w_b$ );
- Relative axial load of the chord  $n_0$ .

Our goal is to predict typical practical cases and this means the chord sizes  $b_0$  are between 300x300x12.5 and 100x100x4, and only squares are considered. This limits the sizes of braces, because:

$$0.25 \leq \frac{b_1}{b_0} = b \leq 0.85 \quad (2.8)$$

The ratio  $b_1/t_1$  is limited  $b_1/t_1 \leq 35$  and in compression to cross-section class 1 or 2. The ratio  $b_0/t_0$  is limited  $35 \geq b_0/t_0 \geq 10$  and moreover to the cross-section class 1 or 2. We consider also HSS up to S700 and this limits the range of the cross-sections. The member sizes are discrete and follow those of Ruukki, meaning cold-formed tubes. The angle  $\theta$  between the brace and the chord is due to welding in the range  $30^\circ \leq \theta \leq 90^\circ$ .

The butt weld is modeled as “no weld” by using TIE constraint of Abaqus. The fillet weld is modeled as steel and using TIE constraint where the weld is in contact with steel. The full strength weld is used for the fillet weld and the size  $a$  is defined as:

$$a^3 \sqrt{2} \times b_w \frac{g_{M2}}{g_{M0}} \frac{f_{y1}}{f_{u1}} t_1 \quad (2.9)$$

where the correlation factor  $\beta_w = 0.9$  for S355 and 1.0 for greater steel grades and material factors are  $\gamma_{M2} = 1.25$  and  $\gamma_{M0} = 1.0$ . The index 1 refers to the brace. In practice this means very large weld sizes for HSS (Ongelin and Valkonen, 2012) as is given in Table 2.1.

Table 2.1. Fillet weld sizes

Brace material	Weld size
S355	$1.16t_1$
S460N	$1.50t_1$
S500N	$1.60t_1$
S550M	$1.62t_1$
S700M	$1.64t_1$

## 2.4. Example of Kriging

Consider the case where we know the exact solution in the range [0.5; 2.5]. The function is  $f(x) = 1/x$ , as shown in Fig. 2.1. The solution for this case was shown in (Halonen, 2012) using DACE toolbox for Matlab.

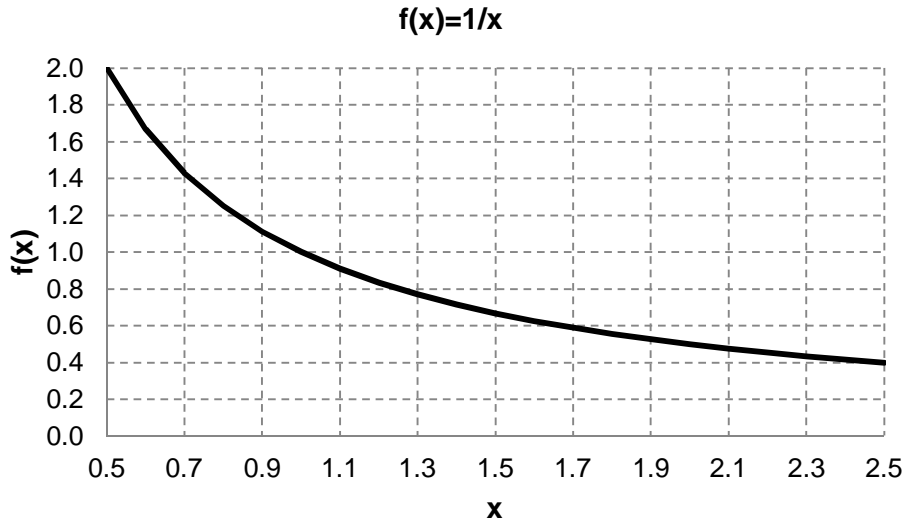


Figure 2.1. Function  $f(x) = 1/x$ .

We have two sample points:

- $x_1 = 1.5$ ;
- $x_2 = 2.0$ .

and generally  $x_i$  sample point where  $i = [1, \dots, n]$  and now  $n = 2$ . The function values at the sample points are:

- $y_1 = 1/1.5 = 0.6667$ ;
- $y_2 = 1/2 = 0.5000$ .

Next we introduce matrix notations as:

$$X = \begin{matrix} \hat{e}^1 & x_1 \\ \hat{e}^1 & x_2 \\ \vdots & \vdots \\ \hat{e}^1 & x_n \end{matrix} = \begin{matrix} \hat{e}^1 & x_1 \\ \hat{e}^1 & x_2 \\ \vdots & \vdots \\ \hat{e}^1 & x_n \end{matrix} = \begin{matrix} \hat{e}^1 & 1.5 \\ \hat{e}^1 & 2.0 \\ \vdots & \vdots \\ \hat{e}^1 & \end{matrix} \quad (2.10)$$

There is an idea to introduce the column of ones to the matrix  $X$ , as seen later.

$$Y = \begin{matrix} \hat{e}^1 & y_1 \\ \hat{e}^1 & y_2 \\ \vdots & \vdots \\ \hat{e}^1 & y_n \end{matrix} = \begin{matrix} \hat{e}^1 & y_1 \\ \hat{e}^1 & y_2 \\ \vdots & \vdots \\ \hat{e}^1 & y_n \end{matrix} = \begin{matrix} \hat{e}^1 & 0.6667 \\ \hat{e}^1 & 0.5000 \\ \vdots & \vdots \\ \hat{e}^1 & \end{matrix} \quad (2.11)$$

We estimate the function  $f(x)$  using a zero order regression, function  $g_0(x) = 1$ , as:

$$f(x) \approx s_p(x) = b_0 \quad (2.12)$$

The parameter  $\beta_0$  represents the trend in the data. Next we estimate the function  $f(x)$  using a linear regression  $g_1(x) = x$  as:

$$f(x) \approx s_p(x) = b_0 + \sum_{i=1}^k b_i x_i \quad (2.13)$$

where  $k$  is number of variables and in this case  $k = 1$ :

$$f(x) \approx s_p(x) = b_0 + b_1 x_i = b_0 + b_1 \times x \quad (2.14)$$

Similarly higher order regression  $g_2(x) = x^2$ , etc can be developed. By expressing the set of equations (4) in matrix form then the least squares estimator  $\bar{b}$  for the parameters  $\beta = (\beta_0, \beta_1, \beta_2, \dots, \beta_k)^T$  is (Queipo et al., 2005), (Müller, 2012):

$$\bar{b} = (X^T X)^{-1} X^T Y \quad (2.15)$$

Using the zero order regression we take only the first column from the matrix  $X$ :

$$\begin{aligned} \bar{b} &= [b_0] = \frac{[1 \ 1]^{-1} \times [1 \ 1] \times 0.6667}{[1 \ 1] \times [1 \ 1] \times 0.5000} \\ \bar{b} &= [b_0] = (2)^{-1} \times (1.1667) = 0.5833 \end{aligned} \quad (2.16)$$

which is the mean of function values at the sample points.

Using the first order regression:

$$\begin{aligned} \bar{b} &= \frac{\hat{b}_0 + \hat{b}_1 \times 1 + \hat{b}_1 \times 1.5}{\hat{b}_0 + \hat{b}_1 \times 1.5 + \hat{b}_1 \times 2.0} = \frac{0.6667 + 0.5833 \times 1 + 0.5833 \times 1.5}{0.6667 + 0.5833 \times 1.5 + 0.5833 \times 2.0} \\ \bar{b} &= \frac{\hat{b}_0 + \hat{b}_1 \times 2.0 + \hat{b}_1 \times 3.5}{\hat{b}_0 + \hat{b}_1 \times 3.5 + \hat{b}_1 \times 6.25} = \frac{0.6667 + 0.5833 \times 2.0 + 0.5833 \times 3.5}{0.6667 + 0.5833 \times 3.5 + 0.5833 \times 6.25} \\ \bar{b} &= \frac{\hat{b}_0 + \hat{b}_1 \times 14.0 + \hat{b}_1 \times 25.0}{\hat{b}_0 + \hat{b}_1 \times 14.0 + \hat{b}_1 \times 36.0} = \frac{0.6667 + 0.5833 \times 14.0 + 0.5833 \times 25.0}{0.6667 + 0.5833 \times 14.0 + 0.5833 \times 36.0} = 0.3333 \end{aligned} \quad (2.17)$$

Now, the constant values  $\beta_0$  is two times the values using zero order regression in this case. We have two estimations for the function  $f(x)$ :

- zero order regression, Eq. (2.12) with parameter of Eq. (2.16);
- first order regression, Eq. (2.14) with parameters of Eq. (2.17).

These are shown in Fig. 2.2.

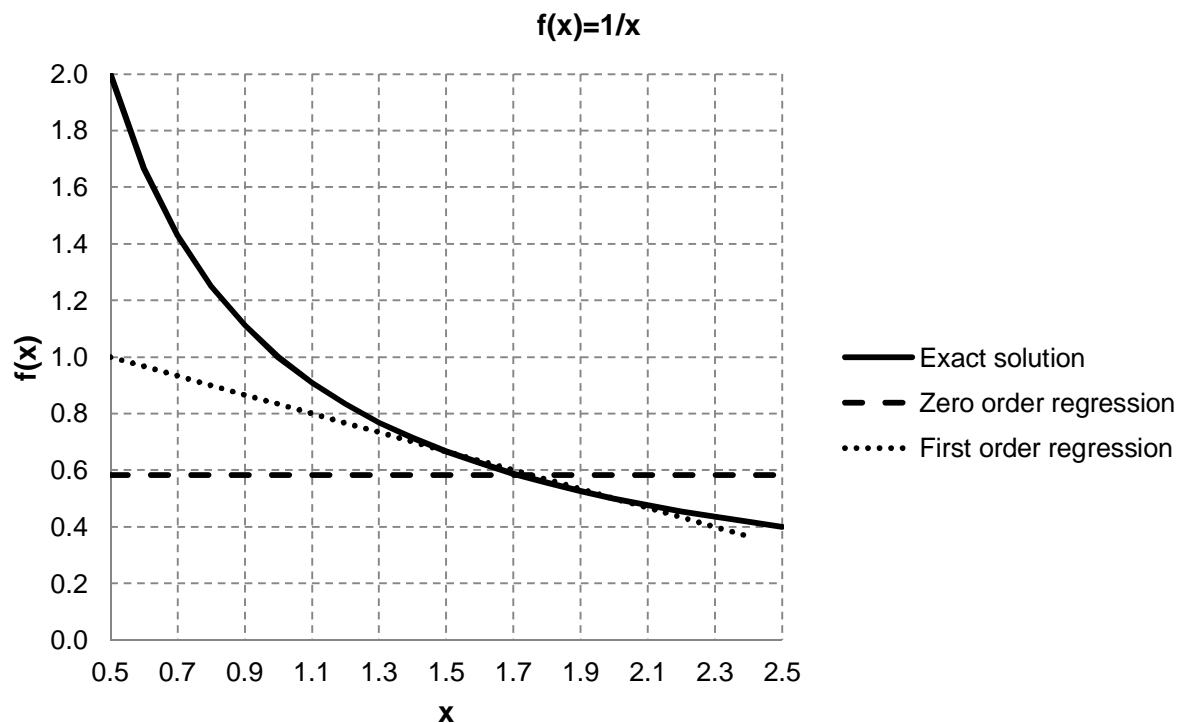


Figure 2.2. Zero order and first order regressions.

However, we have sample points only in the range [1.5; 2.0], so the regression is not expected to be good outside this range. By zooming the figure into the range of interest the result is in Fig. 2.3.

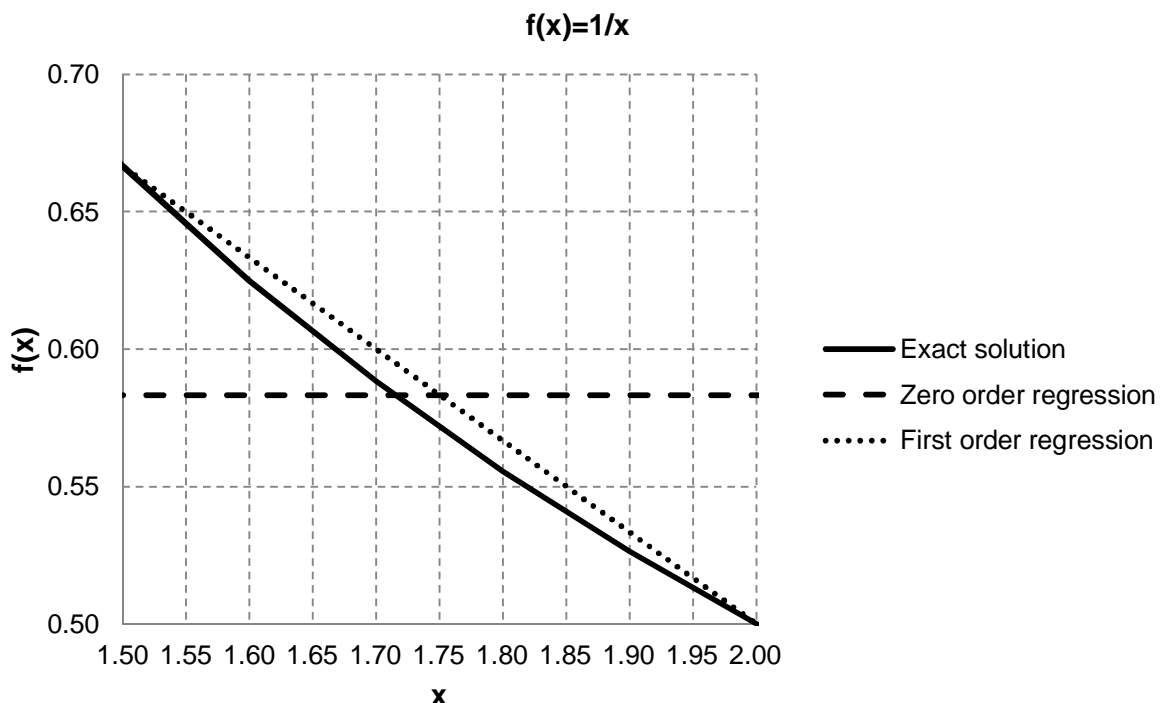


Figure 2.3. Regression in the sample range.

Take next three sample points, meaning two as above and one extra mid of the two:

- $x_1 = 1.5; \quad y_1 = 1/1.5 = 0.666667;$
- $x_2 = 1.75; \quad y_2 = 1/1.75 = 0.571429;$
- $x_3 = 2.0; \quad y_3 = 1/2 = 0.500000.$

$$X = \begin{matrix} x_1 & x_2 & \dots & x_n \\ 1.5 & 1.75 & \dots & 2.0 \end{matrix} \quad (2.18)$$

$$Y = \begin{matrix} y_1 & y_2 & \dots & y_n \\ 0.666667 & 0.571429 & \dots & 0.500000 \end{matrix} \quad (2.19)$$

Using the zero order regression we have:

$$b_0 = \frac{0.666667 + 0.571429 + 0.500000}{3} = 0.579365 \quad (2.20)$$

Using the first order regression we have:

$$\begin{aligned} \bar{b} &= \frac{\sum b_0}{\sum b_1} = \frac{1 + 1 + 1}{1.5 + 1.75 + 2.0} = \frac{3}{4.25} = 0.738095 \\ \bar{b} &= \frac{\sum b_0}{\sum b_1} = \frac{3.00000}{5.25000} = 0.571429 \\ \bar{b} &= \frac{\sum b_0}{\sum b_1} = \frac{24.83333 - 14.0}{8.0} = \frac{10.83333}{8.0} = 1.354166667 \end{aligned} \quad (2.21)$$

The result is shown in Fig. 2.4.

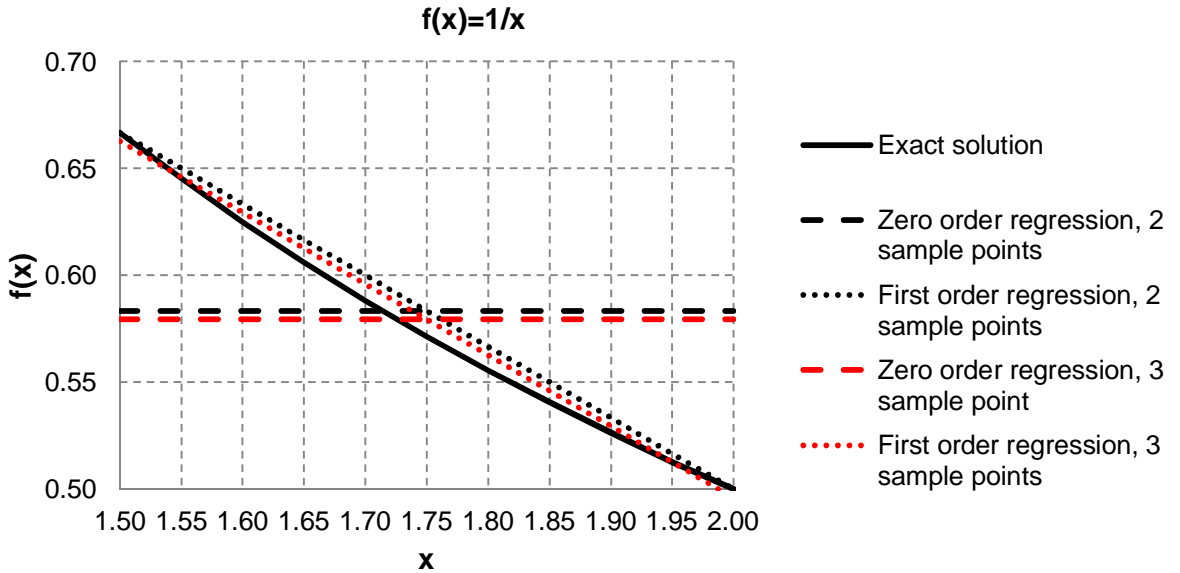


*Figure 2.4. Regressions using two and three sample points.*

Now we have three sample points and estimate the original function using the linear regression then the exact match will not appear in any sample point, but it can be seen that *in mean* the first order regression is nearer to the exact solution. This can be seen in Fig. 2.4.

Next we develop Kriging using two sample points (1.5; 0.66667) and (2.0; 0.5000), zero order regression  $\beta_0 = 0.5833$  and Gaussian process for the function  $Z(x)$ . Graphically this means in our case an effort to find  $Z(x)$  so that the exact fit is achieved at the sample points, as is shown in Fig. 2.5.

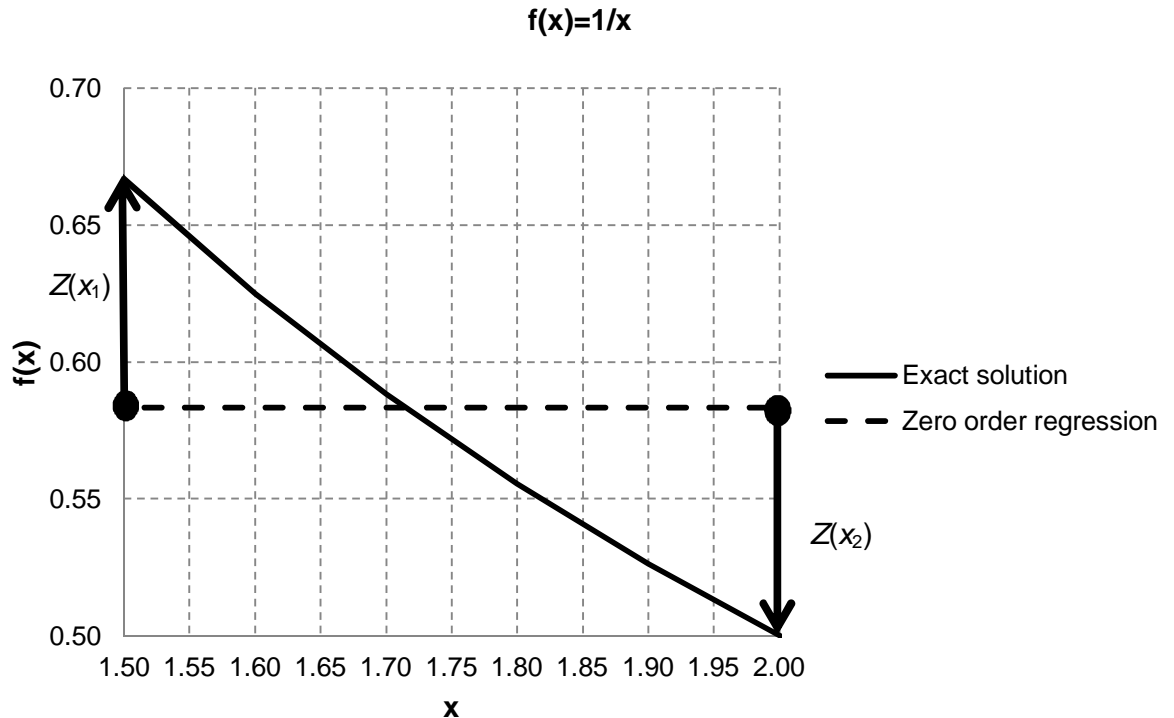


Figure 2.5. Kriging and target of function  $Z(x)$ .

In the general Kriging theory the surrogate model is composed of a regression model and stochastic process (Kwon et al., 2014):

$$\bar{Y}(x) = g(x)^T \beta + Z(x) \quad (2.22)$$

where

- $\bar{Y}$  is the final surrogate model (or metamodel, or response function);
- $x$  can be a vector if we have many variables;
- $g(x)$  is a vector of regression functions, now we have the zero order regression meaning that we have only one regression function which is  $g_0(x) = 1$ ;
- $\beta$  is a vector of parameters for regression functions and now we have  $\beta_0 = 0.5833$ .

So, in this case:

$$\bar{Y}(x) = 0.58333 + Z(x) \quad (2.23)$$

This mean, as noted with Fig. 5, that the first term in Eq. (2.23) approximates globally the design space and a predictor  $Z(x)$  creates localized deviations so that the Kriging model interpolates  $n$  sampled data.

The predictor  $Z(x)$  is assumed (Kwon et al., 2014) to be a Gaussian process with zero mean and covariance 1. This means that we have to normalize the sample data similarly:

$$Mean: \bar{x} = \frac{x_1 + x_2 + \dots + x_n}{n} = \frac{x_1 + x_2}{2} = \frac{1.5 + 2.0}{2} = 1.75 \quad (2.24)$$

$$\begin{aligned} Std: s_x &= \sqrt{\frac{(x_1 - \bar{x})^2 + (x_2 - \bar{x})^2 + \dots + (x_n - \bar{x})^2}{n - 1}} \\ &= \sqrt{\frac{(1.5 - 1.75)^2 + (2.0 - 1.75)^2}{2 - 1}} = 0.353553 \end{aligned} \quad (2.25)$$

$$Mean: \bar{y} = \frac{y_1 + y_2 + \dots + y_n}{n} = \frac{y_1 + y_2}{2} = \frac{0.66667 + 0.5000}{2} = 0.583333 \quad (2.26)$$

$$\begin{aligned} Std: s_y &= \sqrt{\frac{(y_1 - \bar{y})^2 + (y_2 - \bar{y})^2 + \dots + (y_n - \bar{y})^2}{n - 1}} \\ &= \sqrt{\frac{(0.66667 - 0.58333)^2 + (0.5000 - 0.58333)^2}{2 - 1}} = 0.117851 \end{aligned} \quad (2.27)$$

The normalized data is:

$$x_1 = \frac{x_1 - \bar{x}}{s_x} = \frac{1.5 - 1.75}{0.353553} = -0.707107 \quad (2.28)$$

$$x_2 = \frac{x_2 - \bar{x}}{s_x} = \frac{2.0 - 1.75}{0.353553} = 0.707107 \quad (2.29)$$

$$y_1 = \frac{y_1 - \bar{y}}{s_y} = \frac{0.66667 - 0.58333}{0.117851} = 0.707107 \quad (2.30)$$

$$y_2 = \frac{y_2 - \bar{y}}{s_y} = \frac{0.50000 - 0.58333}{0.117851} = -0.707107 \quad (2.31)$$

The normalized data  $\underline{a}$  can be transformed back to real values  $a$  as follows:

$$a = \bar{a} + s_a \times \underline{a} \quad (2.32)$$

Next we need a *correlation function* between points. Define  $R$  as the matrix  $R$  of stochastic-process correlations between the sample points  $x_i$  and  $x_j$ :

$$R_{ij} = R(q, x_i, x_j), \quad i, j = 1, \dots, n \quad (2.33)$$

and let  $\bar{r}(x)$  be a vector of correlation between sample points and untried points  $x$ :

$$\bar{r}(x) = [R(q, x_1, x) \dots R(q, x_n, x)]^T \quad (2.34)$$

The mostly preferred correlation function is the Gaussian correlation (Kwon et al., 2014):

$$R(x_i, x_j) = \exp \left[ -\sum_{k=1}^m q_k |x_i^k - x_j^k|^2 \right] \quad (2.35)$$

where

- $\theta_k$  are unknown correlation parameters,  $k = 1, \dots, m$ ;
- $m$  is the number of design variables;
- $x_i^k$  and  $x_j^k$  are components of samples  $x_i$  and  $x_j$ .

In our case  $n = 2$  and  $m = 1$ , so:

$$R = \begin{bmatrix} \exp \left[ -q |x_1 - x_1|^2 \right] & \exp \left[ -q |x_1 - x_2|^2 \right] \\ \exp \left[ -q |x_2 - x_1|^2 \right] & \exp \left[ -q |x_2 - x_2|^2 \right] \end{bmatrix} \quad (2.36)$$

$$R = \begin{bmatrix} 1 & \exp \left[ -q |x_1 - x_2|^2 \right] \\ \exp \left[ -q |x_2 - x_1|^2 \right] & 1 \end{bmatrix}$$

and

$$\bar{r}(x) = \begin{bmatrix} \exp \left[ -q |x_1 - x|^2 \right] \\ \exp \left[ -q |x_2 - x|^2 \right] \end{bmatrix} \quad (2.37)$$

It can be seen, that the matrix  $R$  is symmetrical and units are at the diagonal, which is a general feature for the matrix  $R$ . Other correlation functions used in Kriging are (Kwon et al., 2014) such as exponential, exponential-Gauss, linear, spherical and cubic.

Generally, the predicted estimate at the untried normalized point is (Kwon et al., 2014):

$$\bar{Y}_{Normalized} = \bar{g}(x)^T \times \bar{b} + \bar{r}(x)^T \times R^{-1} (Y - \bar{G} \times \bar{b}) \quad (2.38)$$

where

$$\bar{G} = [g(x_1)^T, g(x_2)^T, \dots, g(x_n)^T]^T \quad (2.39)$$

and the real value is calculated using Eq. (2.32). We normalized so that mean is zero, so  $\bar{b} = 0$  and from Eq. (2.38) we get:

$$\begin{aligned} \bar{Y}_{Normalized} &= \bar{r}(x)^T \times R^{-1} \times Y \\ \bar{Y}_{Normalized} &= [\exp\{-q(x_1 - x)^2\} \ \exp\{-q(x_2 - x)^2\}] \times R^{-1} \times \begin{bmatrix} e^{y_1} \\ e^{y_2} \end{bmatrix} \end{aligned} \quad (2.40)$$

The inverse of the matrix  $R$ , see Eq. (2.36), is:

$$R^{-1} = \frac{1}{1 - e^2} \begin{bmatrix} 1 & e & -e \\ e & 1 & 0 \\ -e & 0 & 1 \end{bmatrix} \quad (2.41)$$

where

$$e = \exp\{-q(x_1 - x_2)^2\} \quad (2.42)$$

Now we get from Eq. (2.40):

$$\begin{aligned} \bar{Y}_{Normalized} &= [\exp\{-q(x_1 - x)^2\} \ \exp\{-q(x_2 - x)^2\}] \times \frac{1}{1 - e^2} \begin{bmatrix} 1 & e & -e \\ e & 1 & 0 \\ -e & 0 & 1 \end{bmatrix} \times \begin{bmatrix} e^{y_1} \\ e^{y_2} \end{bmatrix} \\ \bar{Y}_{Normalized} &= \frac{1}{1 - e^2} [y_1 \times (e_1 - e_2 \times e) + y_2 \times (e_2 - e_1 \times e)] \end{aligned} \quad (2.43)$$

where

$$e_i = \exp\{-q(x_i - x)^2\}, i = 1, 2. \quad (2.44)$$

It can be seen, that when substituting normalized  $x_1$  and  $x_2$  to Eq. (2.43) the result normalized is  $y_1$  and  $y_2$ .

Next, the correlation parameter  $\theta$  must be defined. Fig. 2.6 illustrates the normalized function  $1/x$  in the normalized range. In the same figure are also shown the values of normalized predictions  $\bar{Y}_{Normalized}$  using different values of the parameter  $\theta$ .

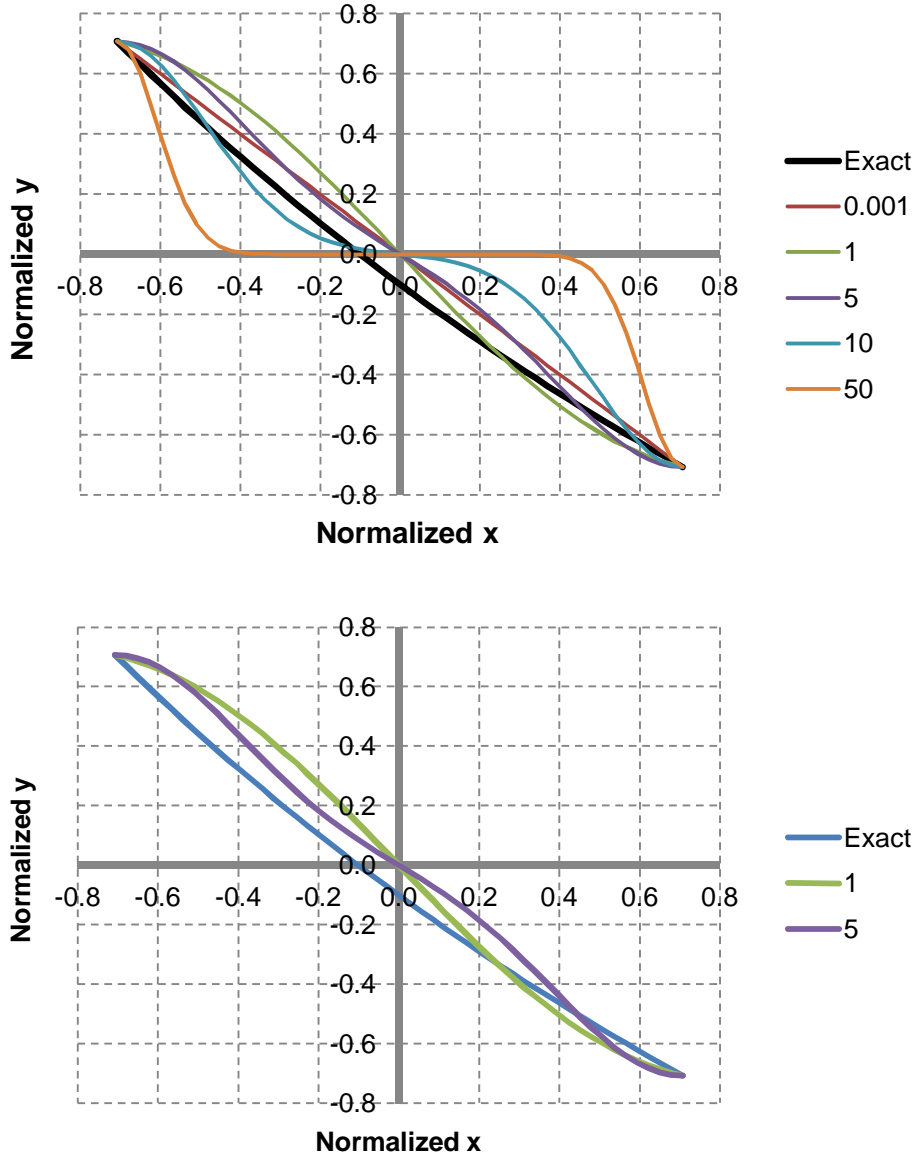


Figure 2.6. Normalized function  $1/x$  and predicted estimates with different parameter  $\theta$ .

It can be seen, that with large  $\theta$  value (e.g. 50) the prediction is such that near the ends it differs from zero and near origin it is zero. With small value 0.001 the prediction is linear. All predictions go through origin in this case, but the exact function does not.

In the Gaussian process the optimal parameters  $\theta$  of the correlation function is solved by finding the maximum of likelihood function  $L$  (Kwon et al., 2014):

$$L = |R|^{1/n} s_z^2 \quad (2.45)$$

where the estimated process variance is:

$$s_z^2 = (Y - G\bar{b})^T R^{-1} (Y - G\bar{b}) / n \quad (2.46)$$

and  $|R|$  is the determinant of  $R$ .

The variance is in our case:

$$s_z^2 = \frac{1}{2} \times [y_1 - y_2] \times \frac{1}{1 - e^2} \times \frac{1 - e \times \hat{y}_1 \times \hat{y}_2}{e - 1} = \frac{y_1^2 - 2ey_1y_2 + y_2^2}{2 \times (1 - e^2)} \quad (2.47)$$

and the determinant is:

$$|R| = 1 - e^2 \quad (2.48)$$

So, the likelihood function Eq. (2.45) is:

$$L = |R|^{1/n} s_z^2 = (1 - e^2)^{1/2} \times \frac{y_1^2 - 2ey_1y_2 + y_2^2}{2 \times (1 - e^2)} = \frac{y_1^2 - 2ey_1y_2 + y_2^2}{2 \times \sqrt{1 - e^2}} \quad (2.49)$$

In our case  $y_1 = -y_2 = y$ , so:

$$L = \frac{y^2 + 2ey^2 + y^2}{2 \times \sqrt{1 - e^2}} = y^2 \frac{e + 1}{\sqrt{1 - e^2}} = y^2 \sqrt{\frac{1 + e}{1 - e}} \quad (2.50)$$

Obviously, the maximum of this function gets when  $e @ 1$ . Taking into account (2.42), this corresponds to  $q @ 0$ . To be specific, we assume it equal to 0.001. The prediction using this value is shown in Fig. 2.7.

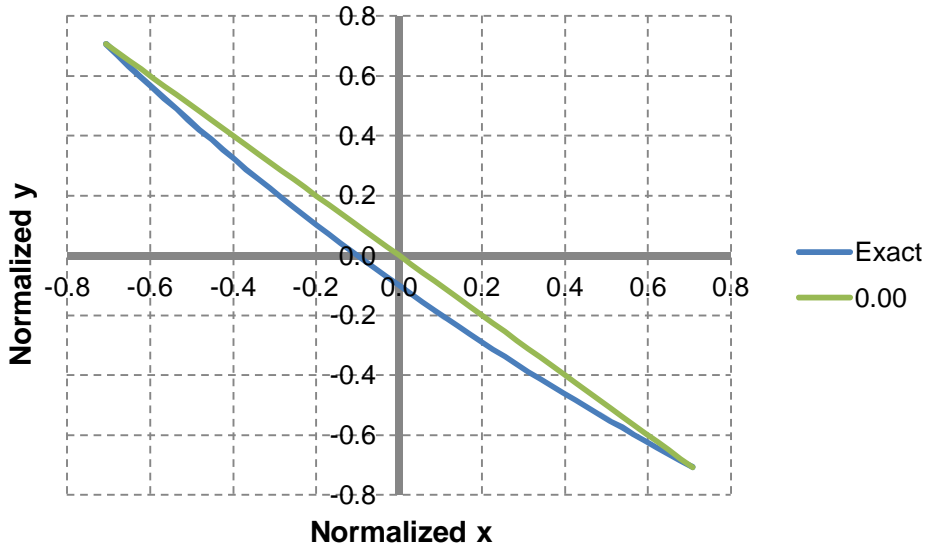
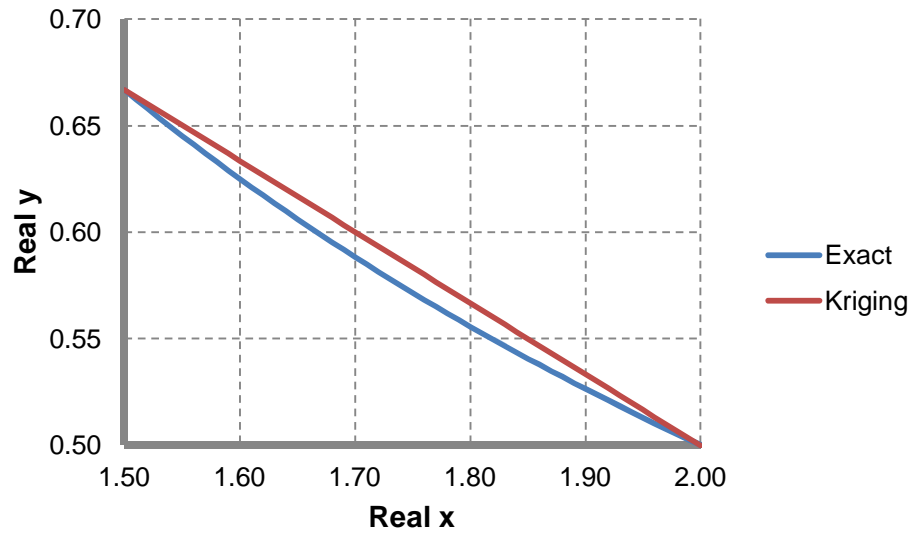


Figure 2.7. Predicted values using  $\theta = 0.001$ .

Real values at the whole range are shown in Fig. 2.8.



*Figure 2.8. Final result.*

The values for the range [0.5; 2.5] are shown in Fig. 2.9.

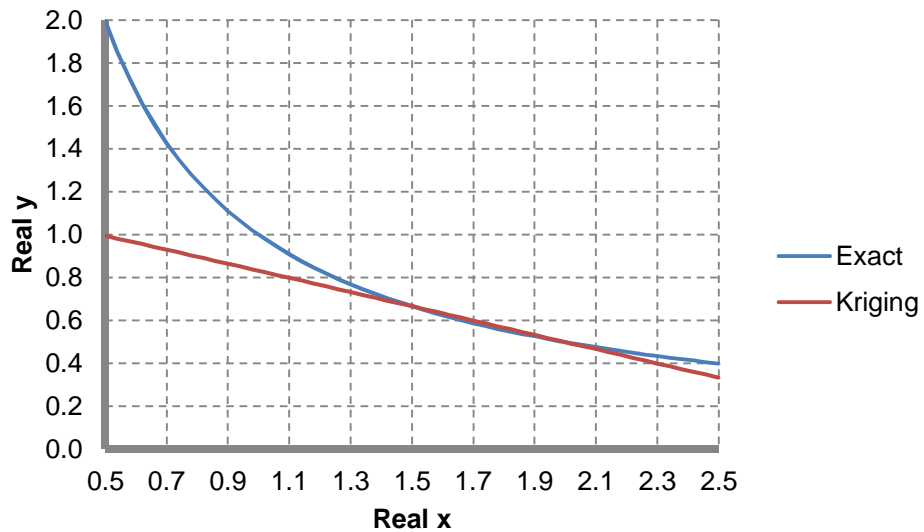


*Figure 2.9. Kriging of function  $1/x$ .*

This result seems to be the same as in (Halonen, 2012, Fig. 3). It should be noted that Kriging is meant for interpolation, not for extrapolation, so the prediction outside the sample points is not good.

The linear interpolation in the range [1.5; 2.0] together with the Kriging is shown in Fig. 2.10.

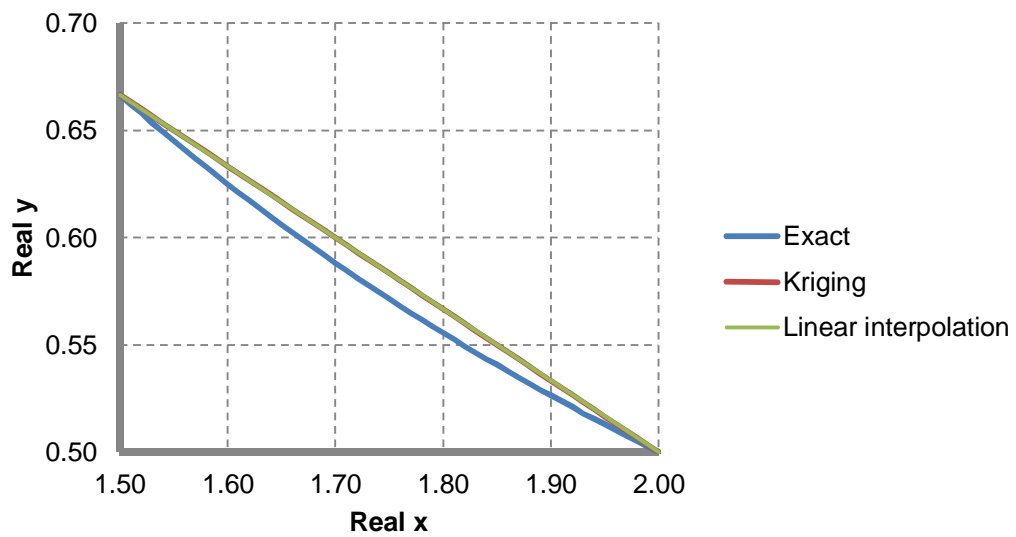


*Figure 2.10. Kriging with linear interpolation.*

The corresponding errors are shown in Fig. 2.11.

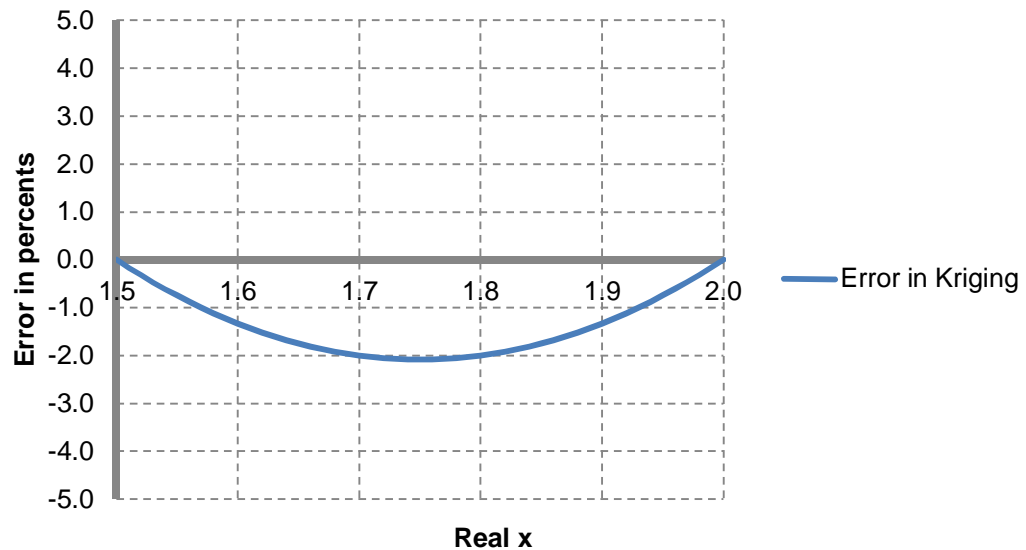


*Figure 2.11. Errors in Kriging.*

### **3. Finite element analysis**

#### **3.1. Finite element modeling**

The Abaqus model was made by using C3D8 brick elements both for the tubes and for the welds. All sections were modeled with round corners, according to EN 10219-2 (2006). Meshing of the truss members was created with solid hexahedral elements as shown in Fig 3.1.

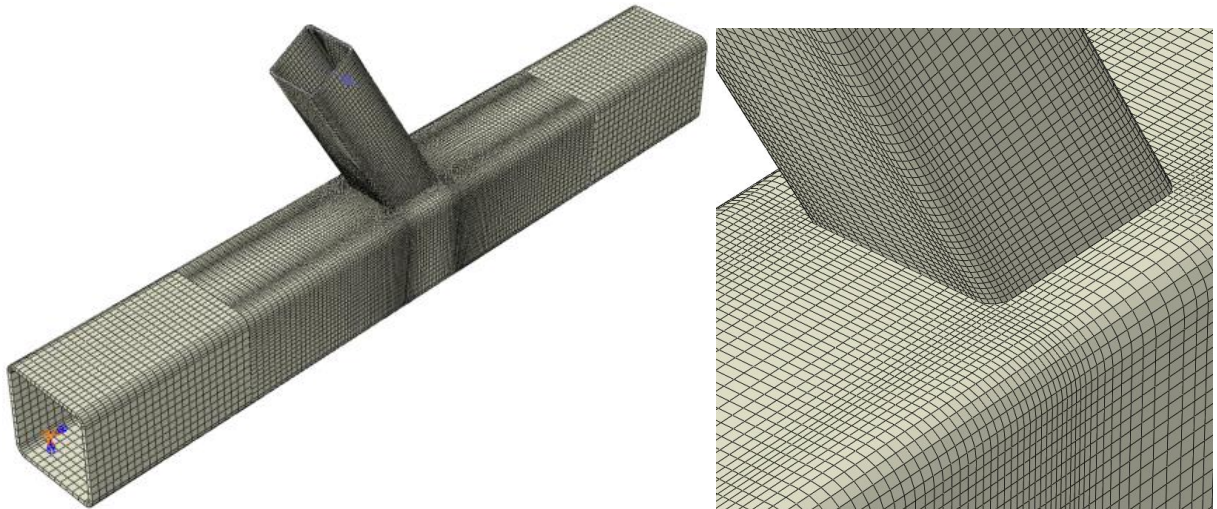


*Figure 3.1. FE model for Y-joint.*

The meshing and the material model were the same as in (Haakana, 2014). Meshing of butt and fillet welds is shown in Fig. 3.2.

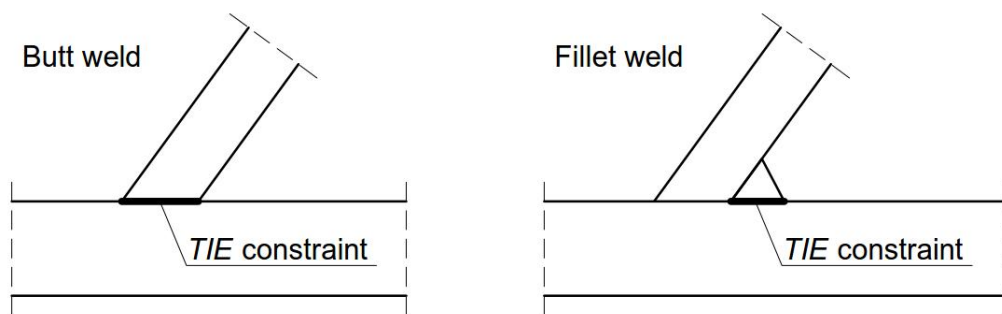


*Figure 3.2. Welds modeling.*

The material model for S355 steel grade is shown in Fig. 3.3. True stresses were used.

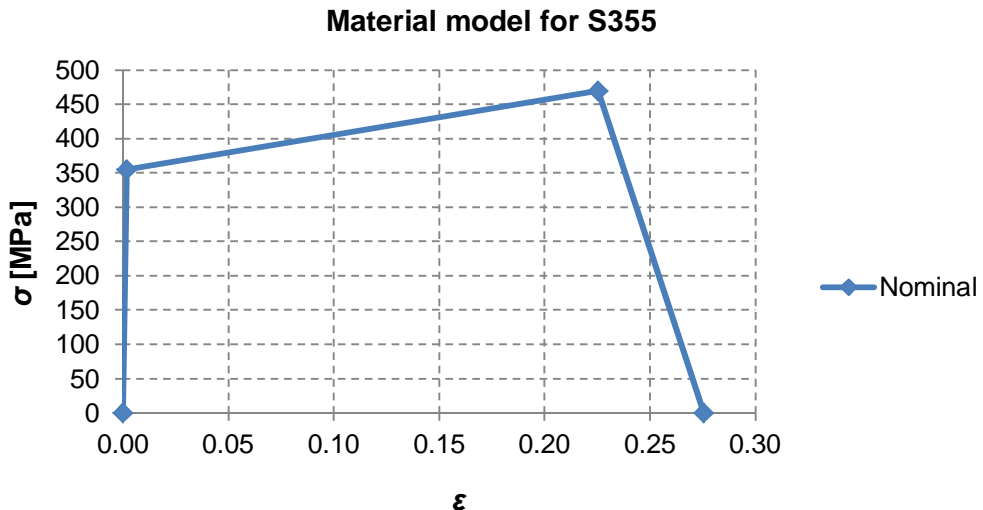


Figure 3.3. Material model for S355.

Similar models were used for all steel grades (Table 3.1). The material does not have influence on the stiffness of joints with butt welds. But, in case of fillet welds the material of the brace has considerable influence on the stiffness due to the weld sizes, see Table 2.1.

Table 3.1. Material data

Grade	Nominal		True	
	ε	σ [MPa]	ε	σ [MPa]
S355	0	0	0	0
	0.00169	355	0.00169	356
	0.22550	470	0.20350	576
	0.27550	0.52220	0.24334	1
S460	0	0	0	0
	0.00219	460	0.00219	461
	0.25930	540	0.23058	680
	0.30930	0.60000	0.26952	1
S500	0	0	0	0
	0.00238	500	0.00238	501
	0.26430	550	0.23451	695
	0.31430	0.61111	0.27329	1
S550	0	0	0	0
	0.00262	550	0.00262	551
	0.28830	600	0.25335	773
	0.33830	0.66667	0.29143	1
S700	0	0	0	0
	0.00333	700	0.00333	682
	0.36050	750	0.30783	1020
	0.41050	0.83333	0.34393	1
S700, t>8 mm	0	0	0	0
	0.00324	680	0.00323	702
	0.36040	750	0.30776	1020
	0.41040	0.83333	0.34386	1

The analyses were force controlled, and the load step was calculated with “Static, Riks” procedure. The joint rotation C was calculated from FEA by extracting the frame behavior from the FEA results, as is given in (Haakana, 2014).

### 3.2. Validation of FEM

The described Abaqus model was validated with the tests of LUT (Tuominen and Björk, 2014) in (Haakana, 2014). The validation was done for K-joint with nominal S500/S500 steel grades. In this case the constant axial load was acting at the chord and the tensile force was increasing at one brace and the other brace was supported axially so there was compression when the tensile was increasing in the test. Figs. 3.4 and 3.5 present respectively the testing apparatus and node sets where displacement differences were measured. Validation results are given on Fig. 3.6.

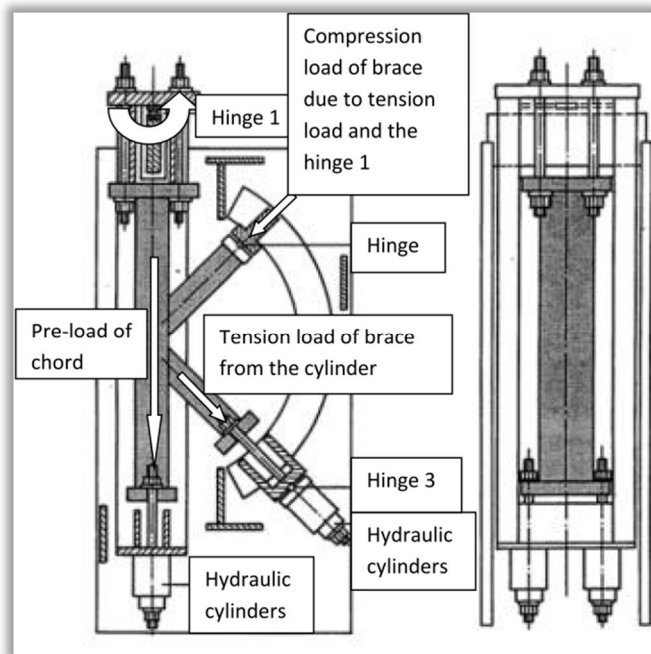


Figure 3.4. Test setup.

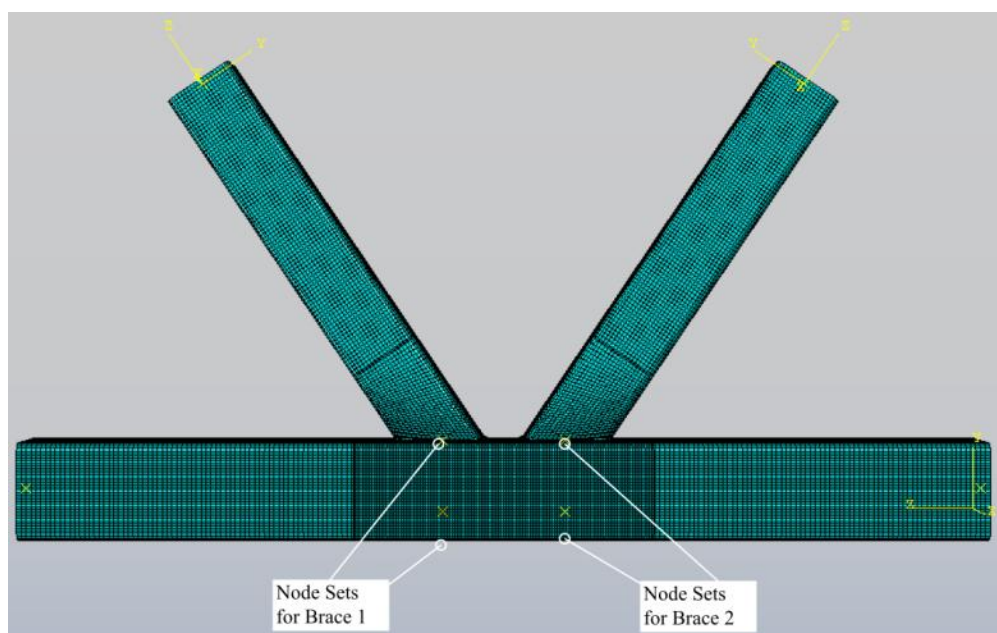


Figure 3.5. Node sets.

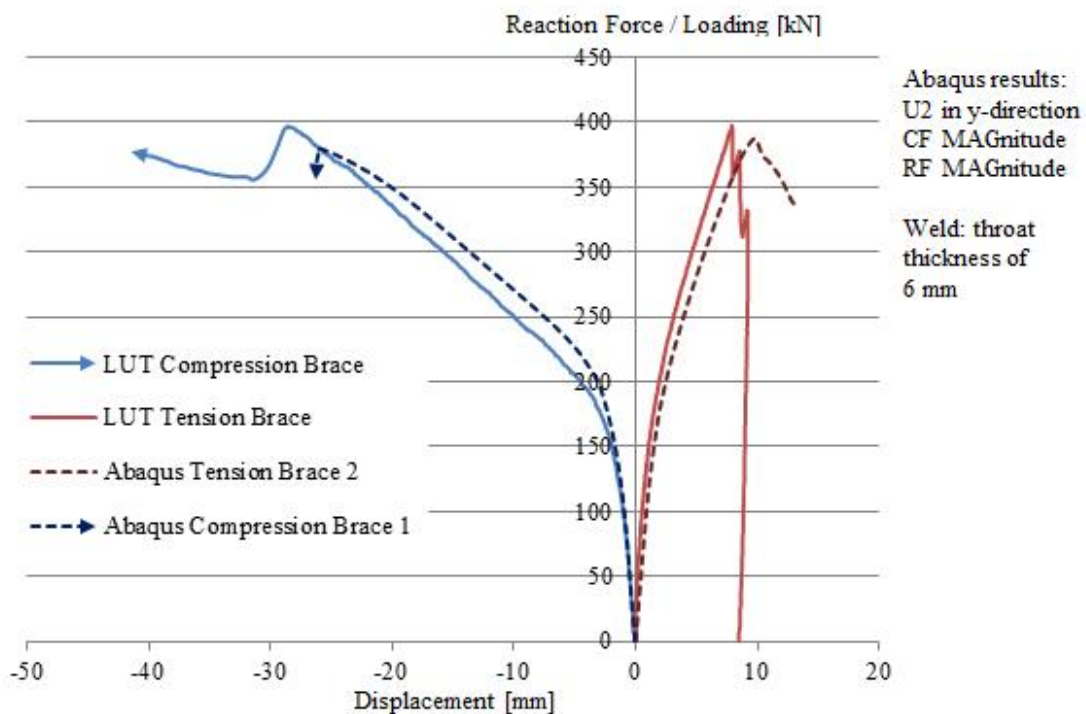


Figure 3.6. Validation of the FE model (Haakana, 2014).

It can be seen, that the FE model predicts rather well the test results in this case and can be used for future research.

### 3.3. Verification of FEM

The first verification was done for the Y-joint where the moment load was acting at two opposite directions. The expected result was that there would not be large difference in the moment resistance and initial rotational stiffness. This verification was done with the Y-joint and:

- Steel grades of chord and brace S500;
- Chord size 150x150x6;
- Two braces sizes 60x60x5 and 110x110x5;
- Angle 60 degrees.

The results are shown in Figs. 3.7, 3.8.

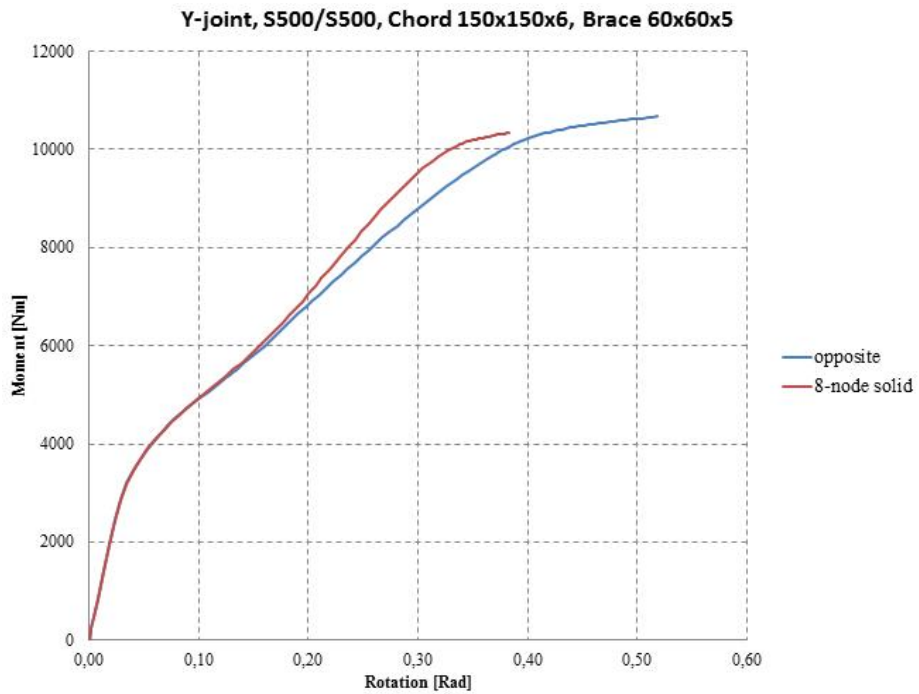


Figure 3.7. Verification case: two opposite moments, case 1.

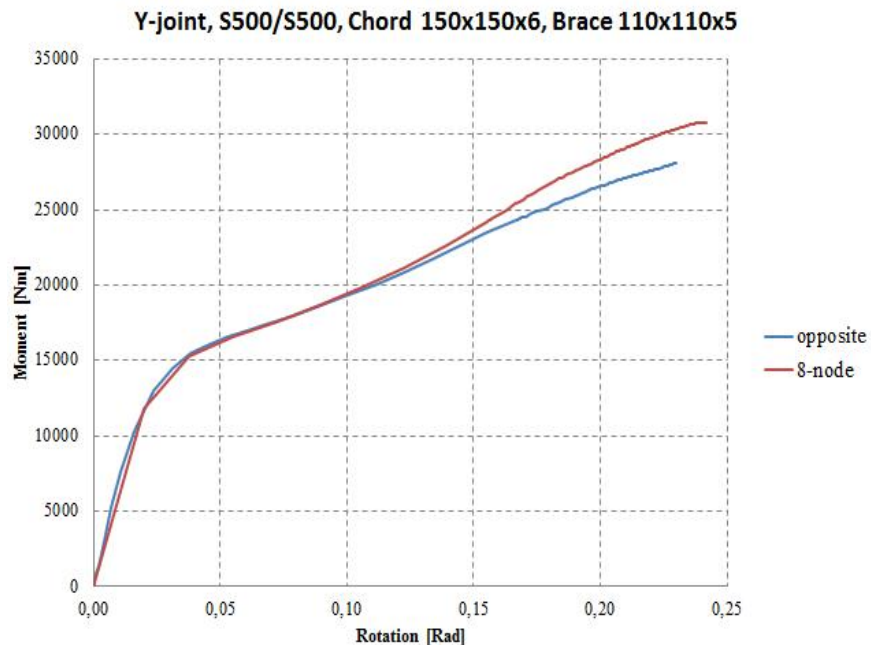
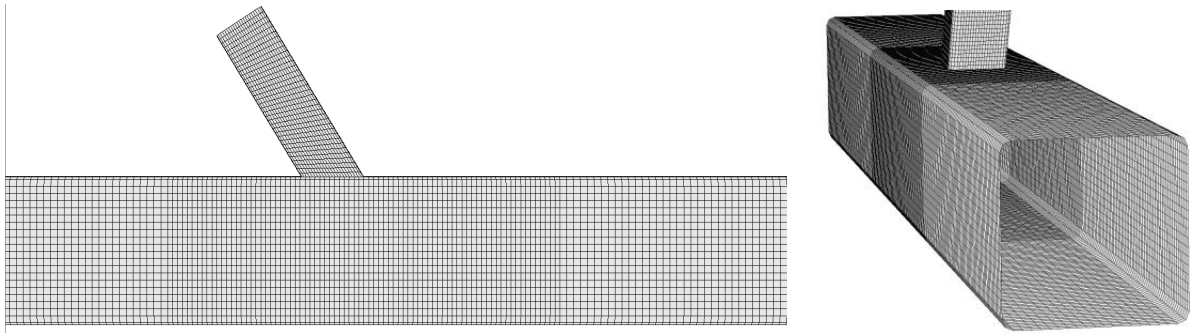


Figure 3.8. Verification case: two opposite moments, case 2.

It can be seen that the maximum moment and the initial rotations are very similar in both cases. The differences in response curves occur at very large rotations, say after 100 mrad.

Next verification was done using shell elements S4R of Abaqus, as is shown in Fig. 3.9. The case was as the previous Y-joint with the brace size 60x60x5, angle 60 degrees. Two shell models were constructed: one along the mid lines of tubes and one along the outer surfaces of the tubes.



*Figure 3.9. Shell element model.*

The computing time required for this model is about the same as for that with 8-noded brick elements. The results are shown in Fig. 3.10 for one case (angle 30 degrees). In this figure the rotation is the rotation at the end of the brace, the point where the moment is acting.

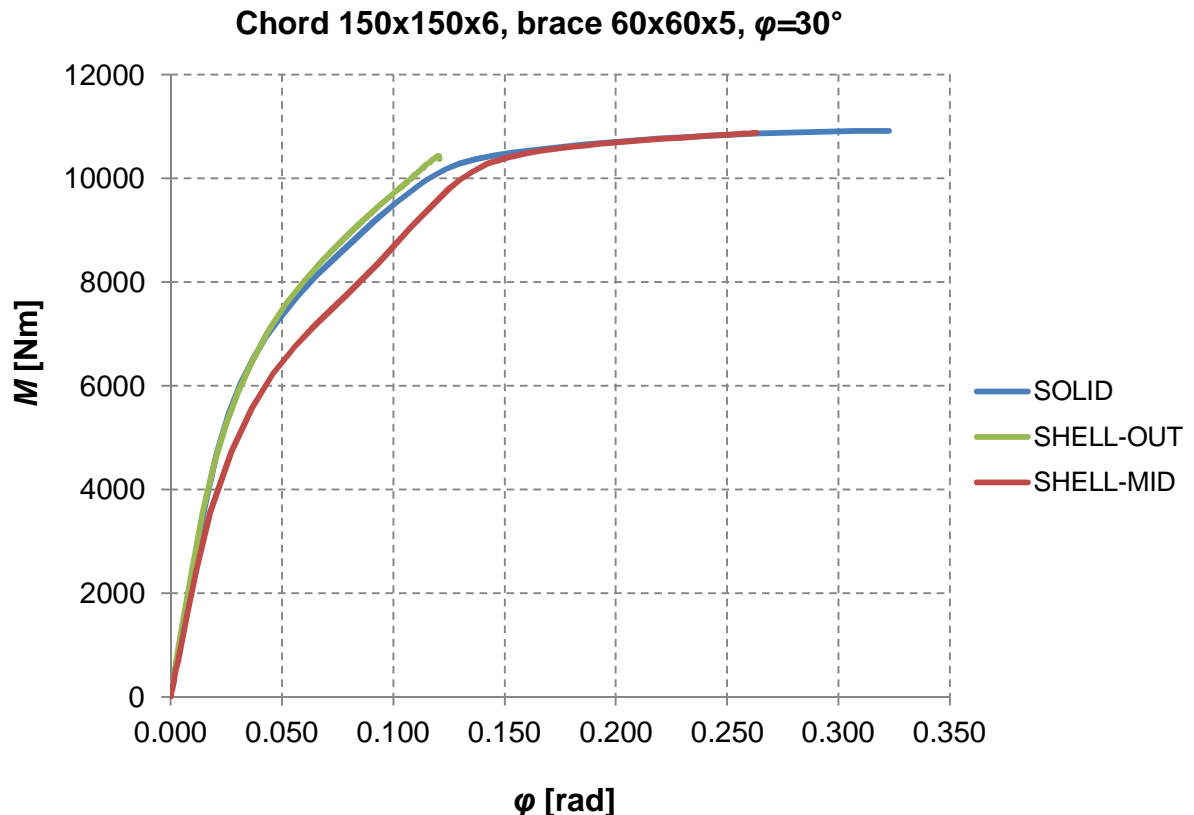


*Figure 3.10. Shell model vs brick model.*

It can be seen, that the stiffness of the brick model (8-node solid) is about same as the stiffness of the shell model. The runs were also done using the shell elements for the same case, chord 150x150x6, brace 60x60x5 and with angles 60 and 90 degrees. The results are shown in Figs. 3.11-3.13 for the moment below 1000 Nm.

**Chord 150x150x6, brace 60x60x5,  $\phi=30^\circ$**

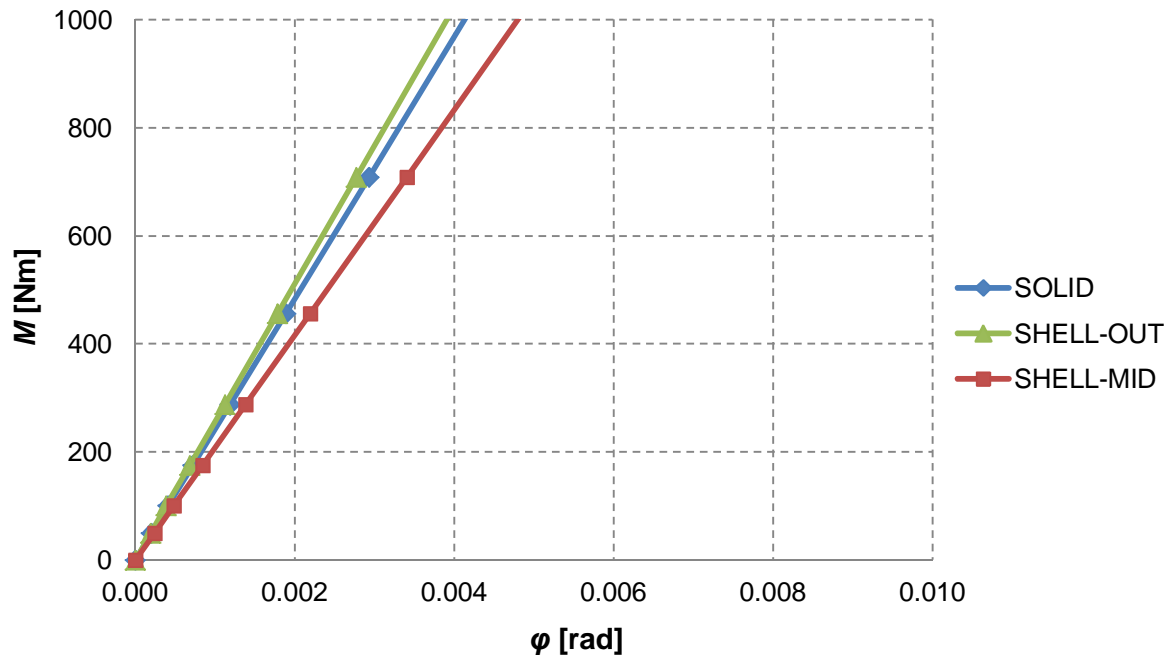


*Figure 3.11. Stiffness of Y-joint, angle 30 degrees.*

**Chord 150x150x6, brace 60x60x5,  $\phi=60^\circ$**

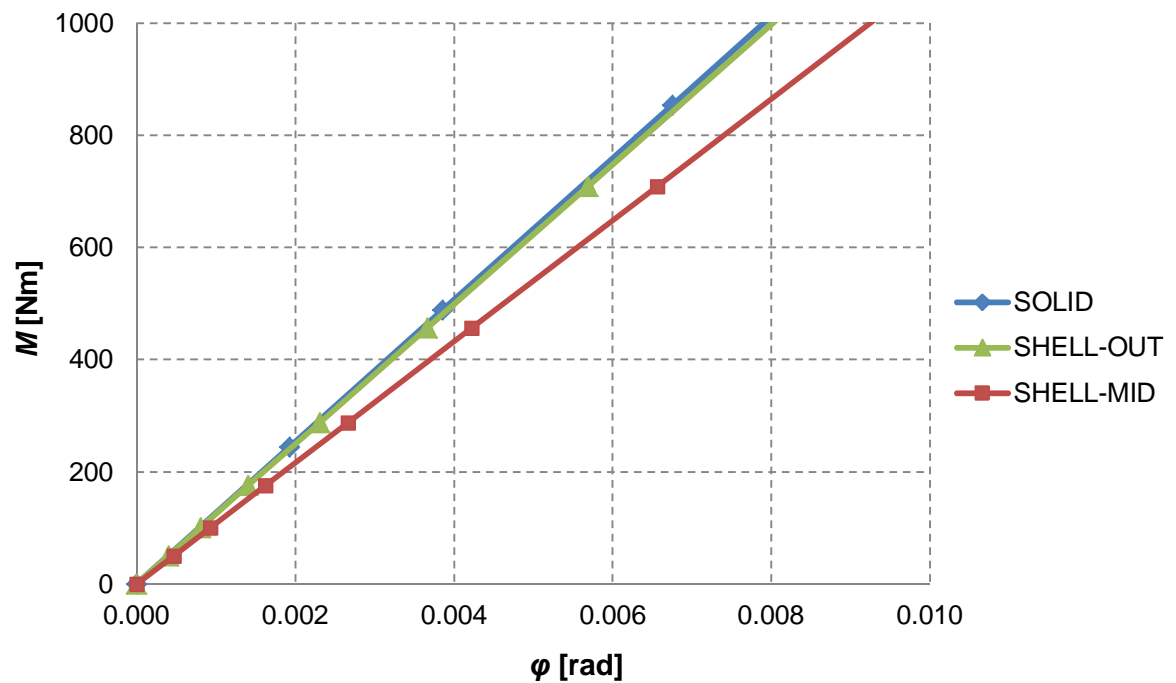


*Figure 3.12. Stiffness of Y-joint, angle 60 degrees.*

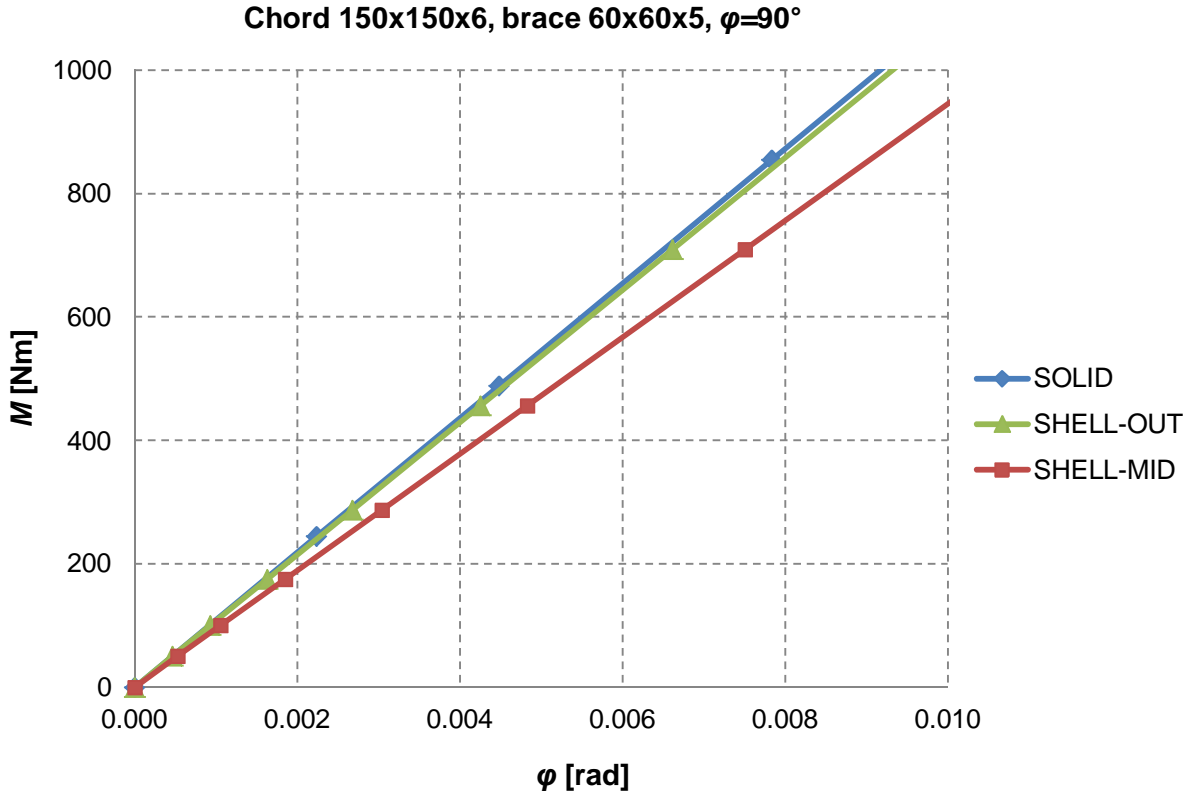


Figure 3.13. Stiffness of Y-joint, angle 90 degrees.

It can be seen that the difference between the solid model and the shell model is very small, practically zero, if the shell model is made along the outer surface of the tubes. The shell model along the mid surface is shown for the comparison, because that technique has been used in some papers. It can be seen in the figure how the initial stiffness increases when the angle between the brace and the chord decreases.

Sample and validation points were defined using the solid model because the maximum moment was obtained using the solid model rather than using the shell model and the modeling of fillet welds could be done based on the exact geometry of the weld. Some tests were done using four layers of 8-noded solid elements near the joints and the 20-noded solid elements, but the results were about the same as using two layers of solid elements.

## 4. Surrogate modeling I

### 4.1. Sampling

The method for determining the sample points to carry out an analysis is called Design of Experiments (DOE). The location of the sample points is very important for generation of an accurate surrogate model. It consists of a compromise between the usage of a reasonable number of sample points to build an accurate model. Several DOE methods are described in (McKay et al., 1979), (Fang et al., 2006) and (Montgomery, 2012). The Latin Hypercube Sampling (LHS) proposed by (McKay et al., 1979) is the most popular space filling sampling technique. In this research engineering justification is used for the definition of the sample points. This technique may mean satisfactory results because the graphs of the initial rotational stiffness indicate rather smooth behavior. The sample points cannot violate any of the requirements of the standards (EN 1993-1-8, 2005) and the values are rounded to the nearest possible value, for e.g. member size. In this research Eurocodes are used and give rather strict rules for the variables of the problem.

However in this research engineering justification was used for the definition of the sample points.

The sample points were defined so that:

- they cover the wide range of variables;
- they can be used for the steel grades in the range from S355 to S700;
- the failure of the brace was not critical.

Based on the engineering judgement the total number of sample points was set as 125. The sample points are given in Table A.1 (App. A). In the table the values of the initial rotational stiffness are also given for 90 degrees using (Grotmann and Sedlacek, 1998).

### 4.2. Attempt I

We started our surrogate modeling using DACE toolbox for Matlab (hereinafter – DACE) (Lophaven et al., 2002). It is a very popular tool for creating surrogate models in scientific and engineering practice (Biles et al., 2007), (Marsden et al., 2004), (Marsden et al., 2008), (Gao and Wang, 2008), (Dubourg et al., 2011), (Husain and Kim, 2008), (Bartz–Beielstein et al., 2004), (Yang et al., 2010).

A Matlab code for creating a surrogate model using DACE toolbox is presented in App. A.

We found soon, that the limit 0.85 of the error term  $R^2$  is not the good criterion for this case. We could exceed it but still the errors at the validation points were over 10%. Using Kriging and zero order regression the errors at the validation points were reduced below 10%, which we set as the acceptance criterion. The validation points and errors between Abaqus results and surrogate model are provided in Table 4.1 using zero order regression and Kriging with the Gaussian correlations.

Table 4.1. Validation of the surrogate model

№	Chord		Brace		$\varphi$ [deg]	C [kNm/rad]		Error, %
	$b_0$ [mm]	$t_0$ [mm]	$b_1$ [mm]	$t_1$ [mm]		Abaqus	Model	
1	140	6	80	4	50	368	358	2.6

2	160	7.1	120	6	50	2280	2193	3.8
3	220	8	180	7.1	50	6265	6223	0.7
4	260	10	200	8	50	7358	7028	4.5
5	140	6	80	4	80	271	264	2.8
6	160	7.1	120	6	80	1619	1629	0.6
7	220	8	180	7.1	80	4402	4300	2.3
8	260	10	200	8	80	5021	4766	5.1

The  $R^2$  error in this case is 0.99, as for linear and second order regression with Kriging. The maximum error was 5.1%, in comparison with 22% and 29% for linear and second order regression respectively.

To identify if the model worked properly we created the graphs which showed how the stiffness depended on every variable. We started from 2D C- $\varphi$  graphs as the easiest ones. To plot such a graph all the variables were kept constant while  $\varphi$  changed gradually from 30 to 90 degrees. All these and subsequent figures were related to zero order polynomial regression models because, as we realized later, higher order regression models gave considerably worse results. During graphical validation some strange cases were observed (Figs. 4.1-4.3).

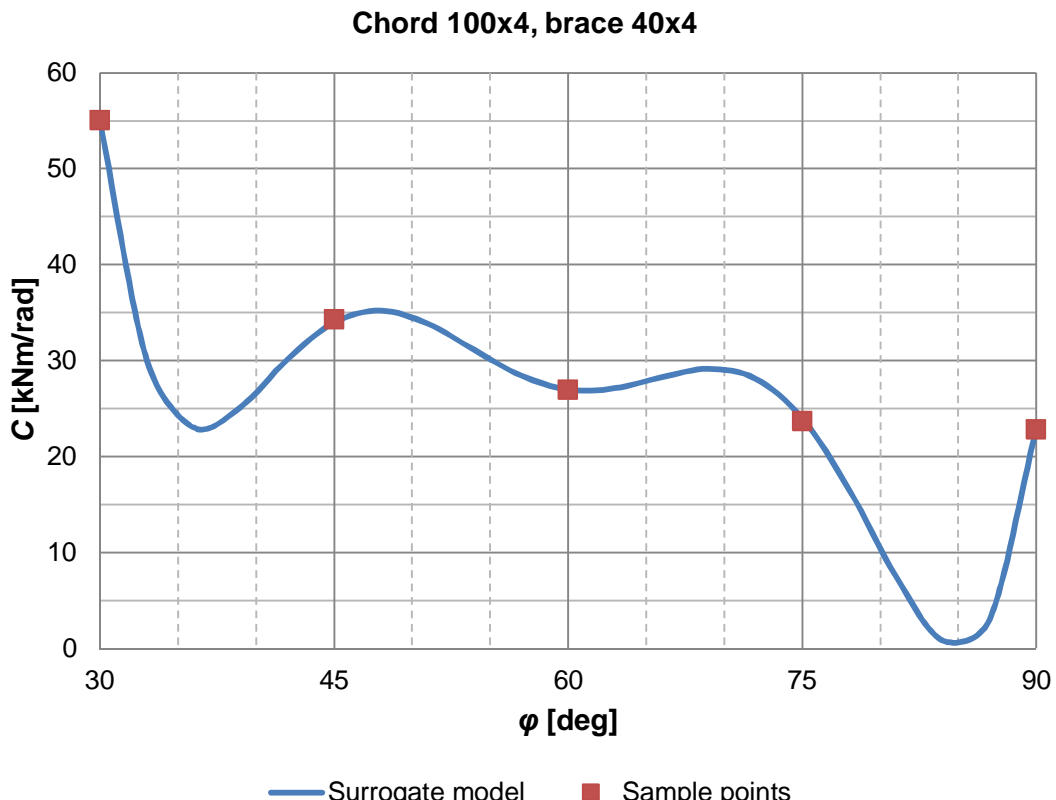


Figure 4.1. C- $\varphi$  response, case 1.

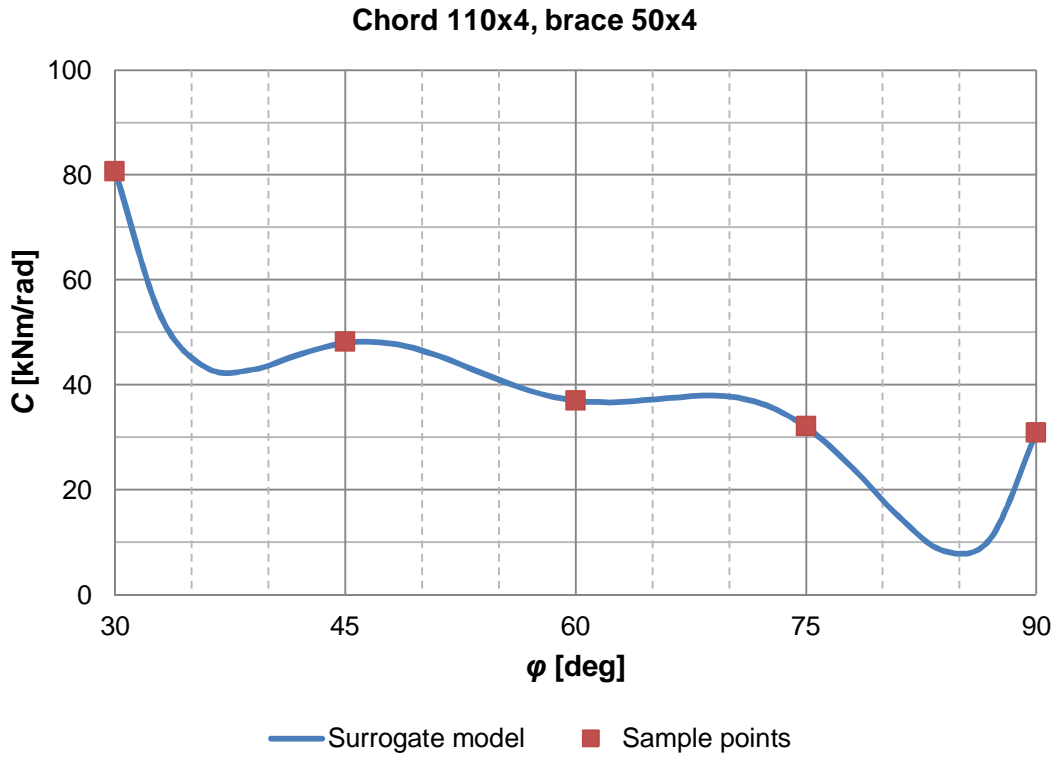


Figure 4.2.  $C$ - $\varphi$  response, case 2.

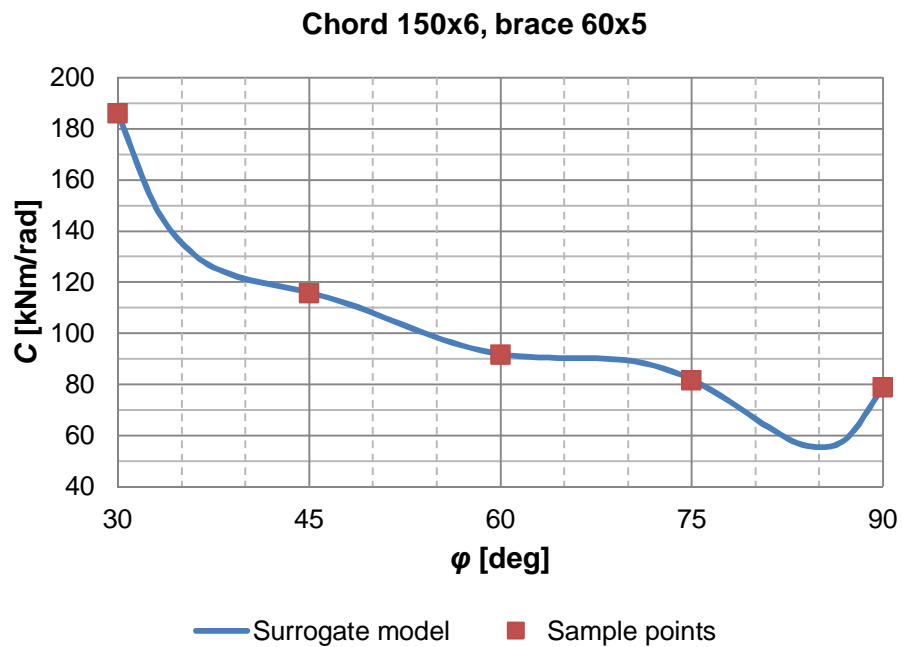


Figure 4.3.  $C$ - $\varphi$  response, case 3.

We continued with the graphs for other variables. It is worth saying, creating the graphs for other variables represented a more complicated task because it required that, except varying one, other variables remain constant. Our sample points were chosen in such a way that this

requirement were met only in few cases, so we had to turn from 2D graphs to 3D graphs, because they allow two variables to vary simultaneously. 3D graphs for some cases are given in Fig. 4.4.

$$b_0=100 \text{ mm}, t_0=5 \text{ mm}, b_1=40\ldots80 \text{ mm}, t_1=4\ldots5 \text{ mm}, \varphi=30^\circ$$

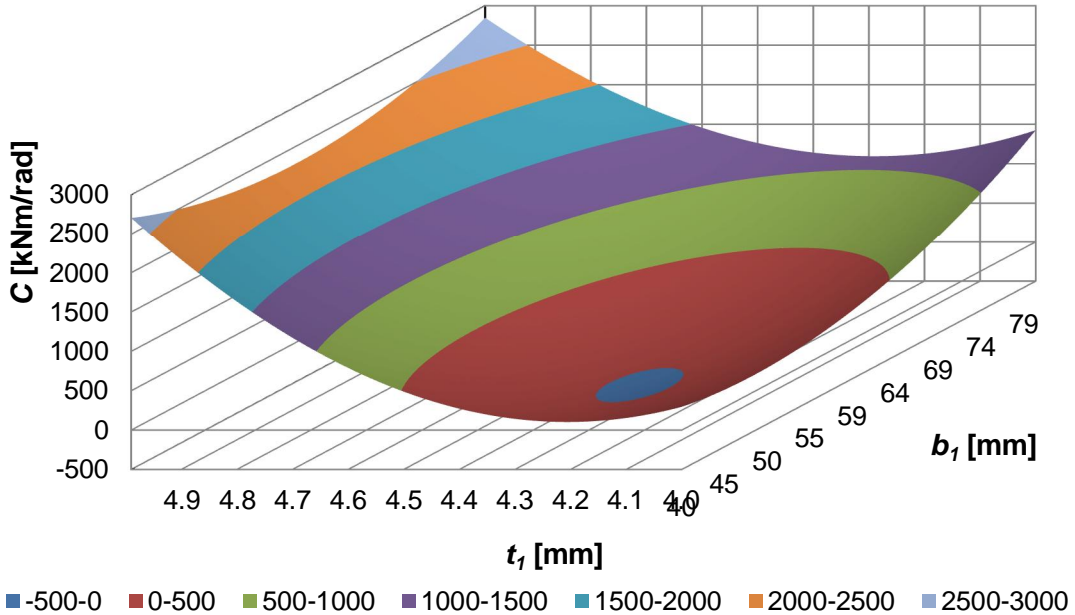


Figure 4.4.  $C-(b_1, t_1)$  response

As can be seen from the figures, we faced with unpredicted behavior of stiffness depending on all variables. Moreover, most of the graphs contained negative values of rotational stiffness.

### 4.3. Pseudo points

To improve the strange behaviour of the model we decided to add the certain boundary conditions for the model. It is obvious that for the angle close to 90 degrees (87-89 degrees) the line must have a zero slope (being very close to a horizontal line). Analytically this means that the partial derivative  $dC/d\varphi$  must equal to zero. Practically, to implement this boundary condition to a discrete function we added some sample points for 95 and 100 degrees angles with the same stiffness value as for 90 degrees. To add the boundary conditions for low angles we extrapolated stiffness for 20 and 25 degrees using 4th order polynomial trendline in Excel.

We called these additional points that were determined not by Abaqus but by other means as “pseudo sample” points (hereinafter – pseudo points). After implementing pseudo points we managed to improve the  $C-\varphi$  graphs (Fig. 4.5).

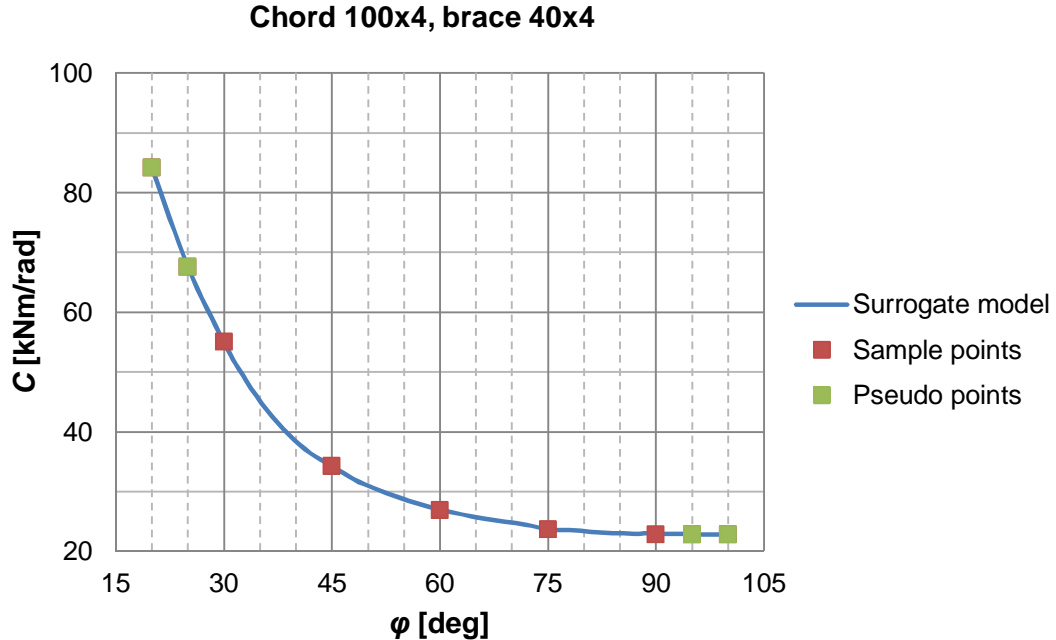


Figure 4.5. Improved  $C$ - $\phi$  graph with pseudo points.

To improve the behavior of the surrogate model on respect to other variables we introduced more pseudo points using the idea that for zero values of all these variables ( $t_0$ ,  $b_1$ , and  $t_1$ ) stiffness responses got zero values as well. The full range of sample and pseudo points for 100 mm chord is presented in Table 4.2.

Table 4.2. Sample and pseudo points, 100 mm chord

Type	Chord		Brace		$\phi$ [deg]	$C$ [kNm/rad]
	$b_0$ [mm]	$t_0$ [mm]	$b_1$ [mm]	$t_1$ [mm]		
pseudo $\phi$	100	4	40	4	20	84
pseudo $\phi$	100	4	40	4	25	68
sample	100	4	40	4	30	55
sample	100	4	40	4	45	34
sample	100	4	40	4	60	27
sample	100	4	40	4	75	24
sample	100	4	40	4	90	23
pseudo $\phi$	100	4	40	4	95	23
pseudo $\phi$	100	4	40	4	100	23
pseudo $t_0$	100	0.1	40	4	30	0
pseudo $t_0$	100	0.1	40	4	45	0
pseudo $t_0$	100	0.1	40	4	60	0
pseudo $t_0$	100	0.1	40	4	75	0
pseudo $t_0$	100	0.1	40	4	90	0
pseudo $b_1, t_1$	100	4	1	0.1	30	0
pseudo $b_1, t_1$	100	4	1	0.1	45	0
pseudo $b_1, t_1$	100	4	1	0.1	60	0
pseudo $b_1, t_1$	100	4	1	0.1	75	0
pseudo $b_1, t_1$	100	4	1	0.1	90	0

But this time we did not manage to improve the behavior of the surrogate model on respect to remaining variables and, moreover, did not run out of the negative values of stiffness. So we had to pay more attention to choice of sample points.

#### 4.4. Sample points analysis

To analyze the distribution of sample points in the range of our interest we created the charts (Figs. 4.6-4.9), adding there, for convenience, validation points (VP), Ruukki's catalogue (Ruukki) and Eurocode limits (Eurocode, see 2.3).

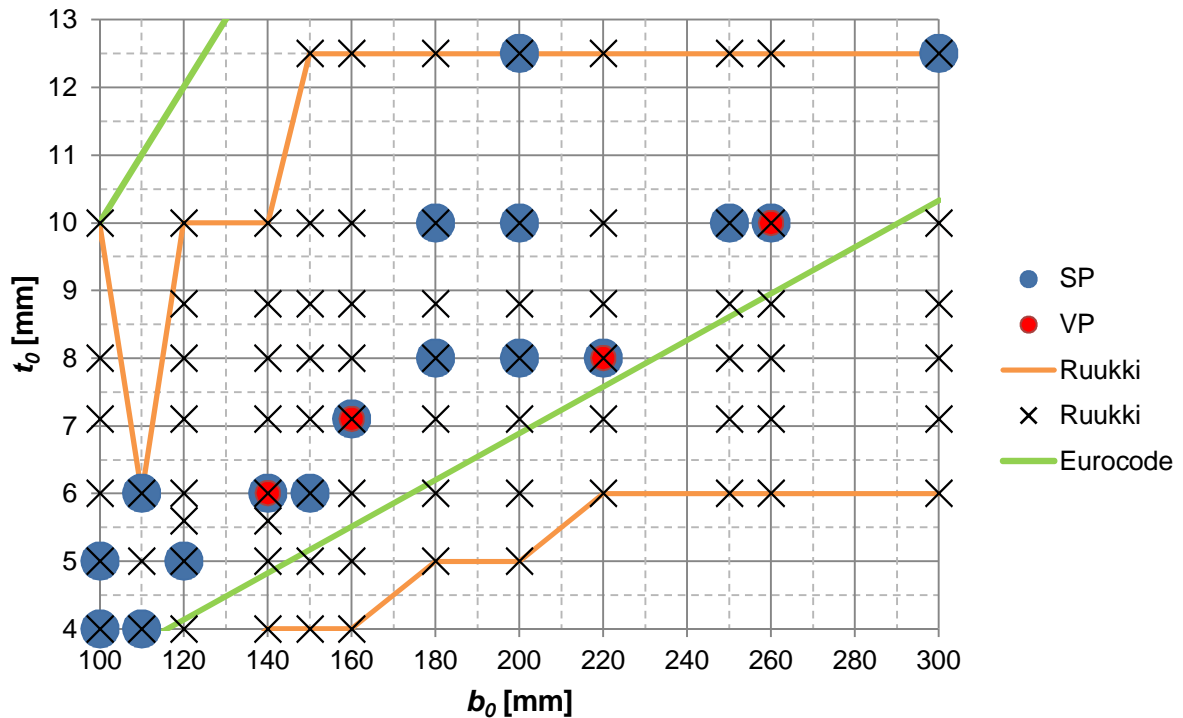


Figure 4.6. Sample points:  $b_0$ - $t_0$ .

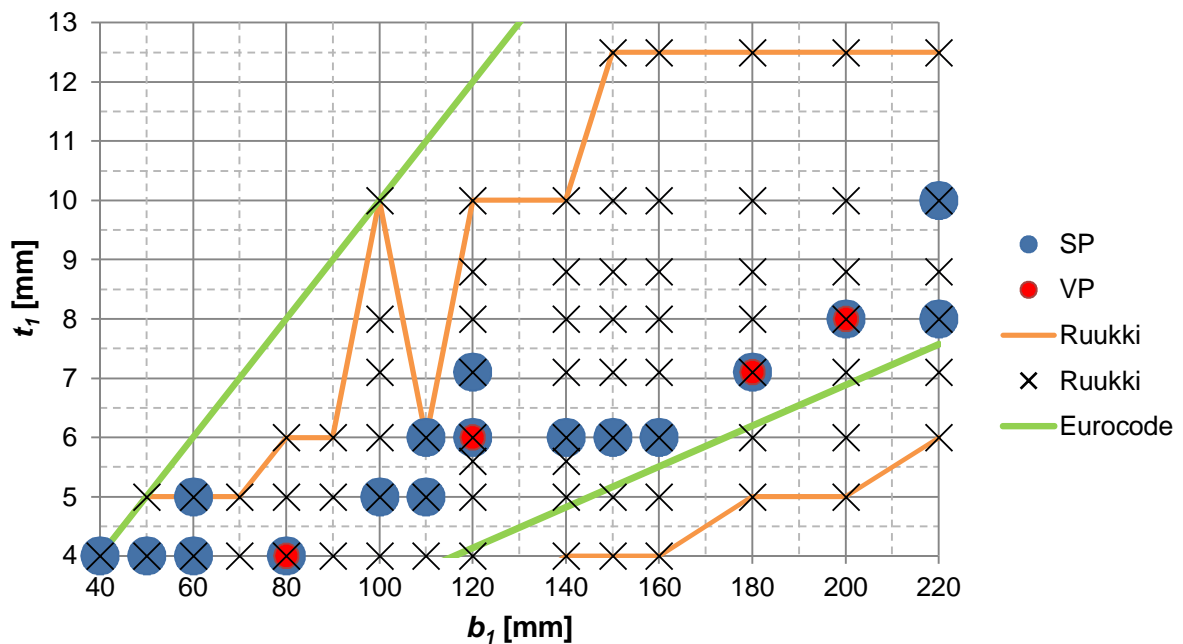


Figure 4.7. Sample points:  $b_1$ - $t_1$ .

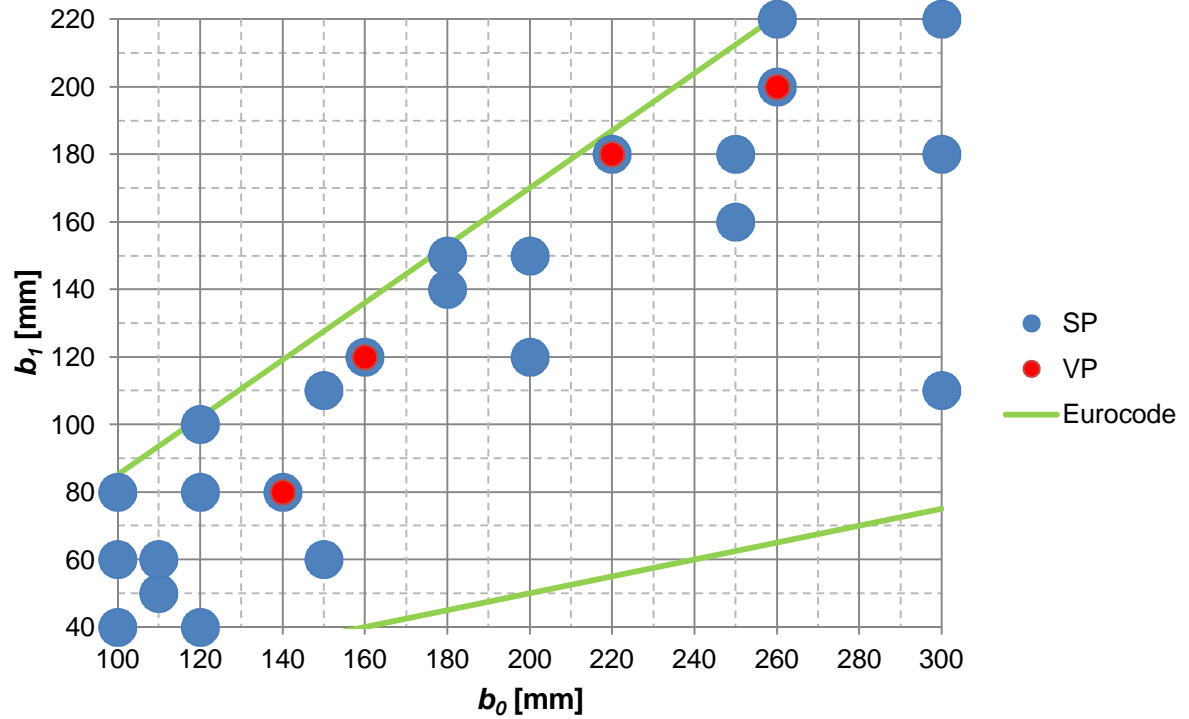


Figure 4.8. Sample points:  $b_1-b_0$ .

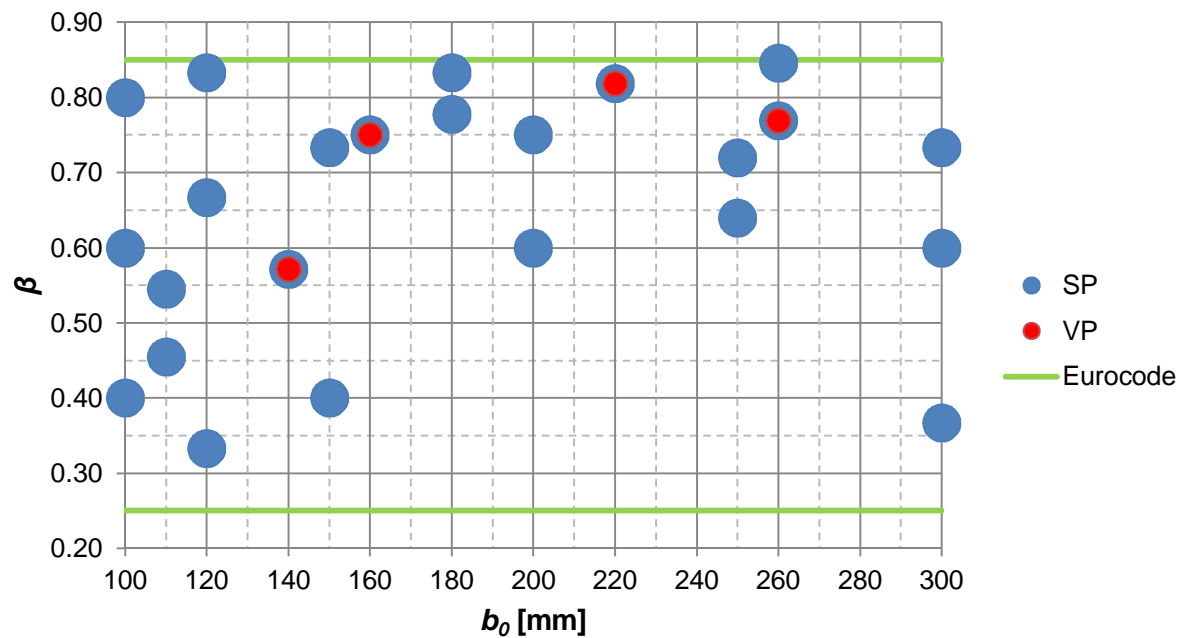


Figure 4.9. Sample points:  $\beta-b_0$ .

As can be seen from the figures, the distribution of sample points in the range of our interest was very uneven, a number of spaces was observed. Moreover, for many cases the values of stiffness for some variables were predicted by extrapolation (for example, some low  $\beta$  for 200 mm chord on Fig. 4.9), which is undesirable for Kriging. To improve the surrogate model and be able to validate it using graphs we decided to create a new series of sample points.

## 5. Surrogate modeling II

### 5.1. New sampling

This time, we analyzed the influence of  $t_1$  on rotational stiffness and came to conclusion that the difference between the values of stiffness for varying  $t_1$  did not exceed 3%. Thus we decided to exclude this variable from the surrogate modeling.

We also replaced  $b_1$  to its relative analogy  $\beta=b_1/b_0$  so that this variable has similar values for all chords. It should be noted that due to low values of  $\beta$  comparing to other variables it was important to input  $\beta$  with at least four characters after the decimal point to avoid the loss of precision.

Moreover, we chose the sample points in such a way that for every variable there were 3 different values (minimum, middle and maximum) while the others remained constant (Figs. 5.1-5.3). Exceptions were made only for cases with the maximum  $t_0$  and  $\beta$  because they had complicated modeling in Abaqus. For those cases only two values (minimum and middle) of  $t_0$  were considered.

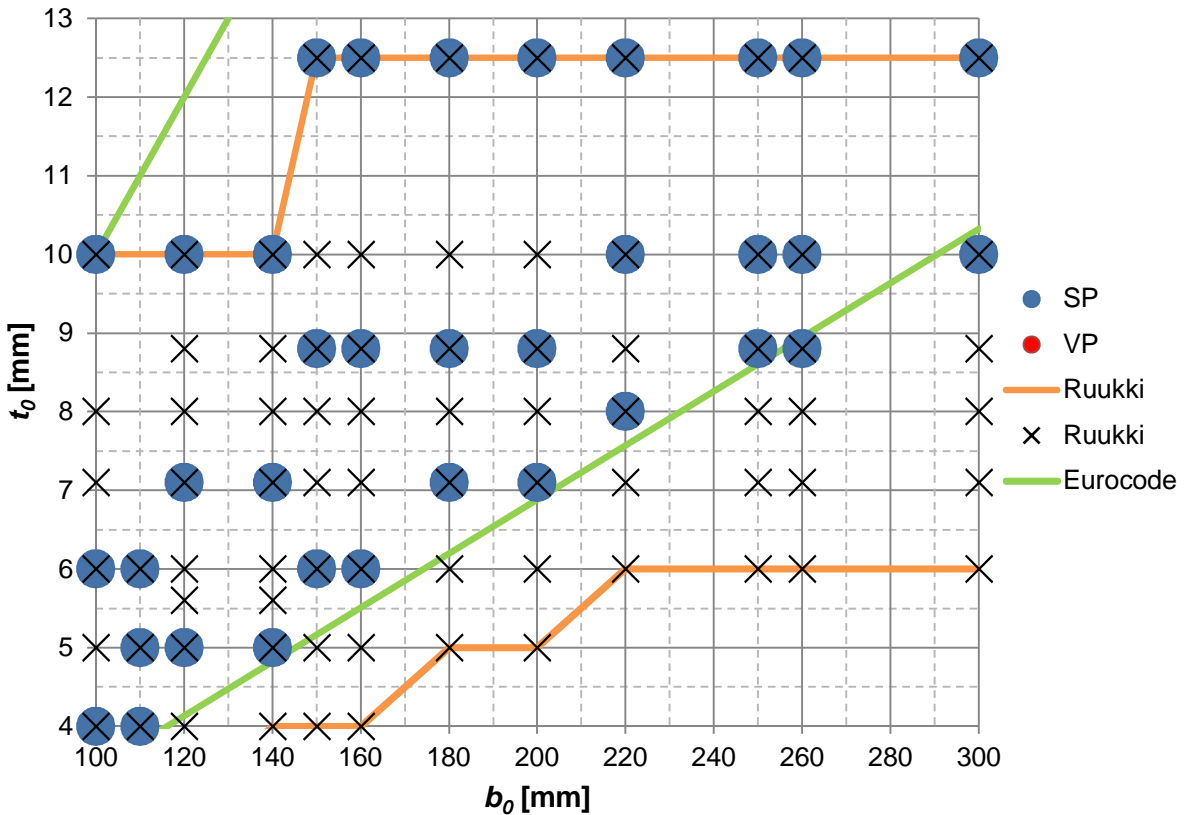


Figure 5.1. New sample points:  $b_0$ - $t_0$ .

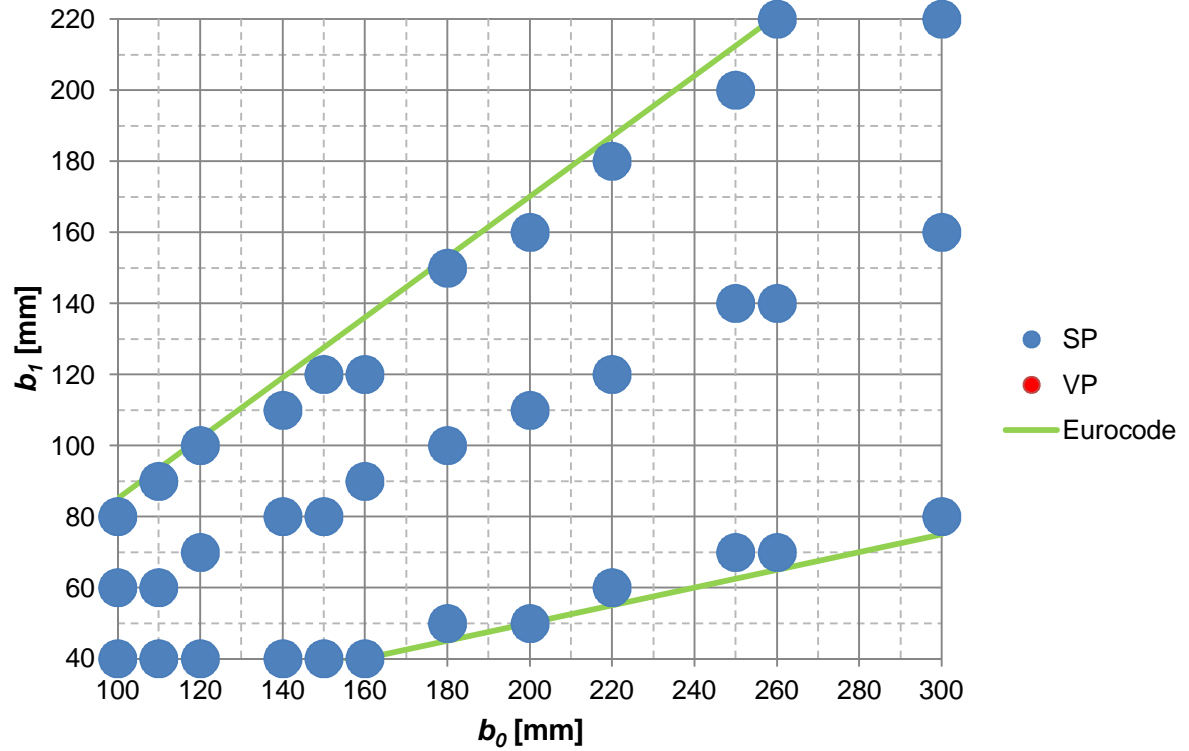


Figure 5.2. New sample points:  $b_1$ - $b_0$ .

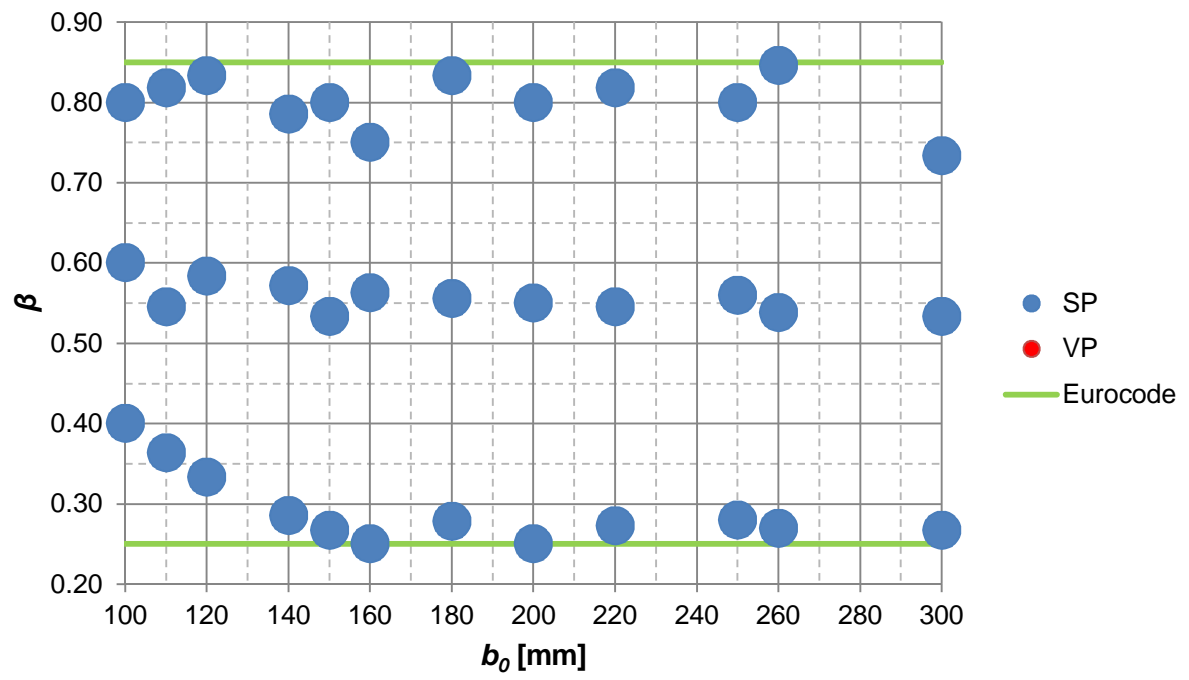


Figure 5.3. New sample points:  $\beta$ - $b_0$ .

This time the number of sample points increased from 125 up to 285, they were distributed evenly and covered the whole area of our interest (Table B.1, App. B).

## 5.2. Attempt II

Having improved our sample points, we created a new surrogate model using DACE. Validation points were taken mostly from the old validation points. As a result we received a surrogate model with the following features:  $R^2=0.8876$ , average error about 56% and maximum error 678%. Graphical validation demonstrated that the model behaved very unpredictably. To improve the situation we implemented pseudo points using the same technique as before. Pseudo points were calculated for the following variables:  $t_0$ ,  $\beta$  and  $\varphi$ . Different combinations of pseudo points were analyzed to find the best solution (Table 5.1).

*Table 5.1. Pseudo points implementing I*

No	$t_0$	$\beta$	$\varphi$	$R^2$	Avg. error, %	Max. error, %
1				0.8876	56	678
2			x	0.9879	8	77
3	x		x	0.8975	48	744
4		x	x	0.6572	75	673
5	x	x	x	0.7271	69	569

The second model with only angle pseudo points seemed to behave best. Graphical validation showed that, despite the relatively good results for  $\varphi$ , its behavior for  $t_0$  and  $\beta$  remained rather questionable (Figs. 5.4, 5.5). More to the point, our model contained many points with negative values of rotational stiffness.

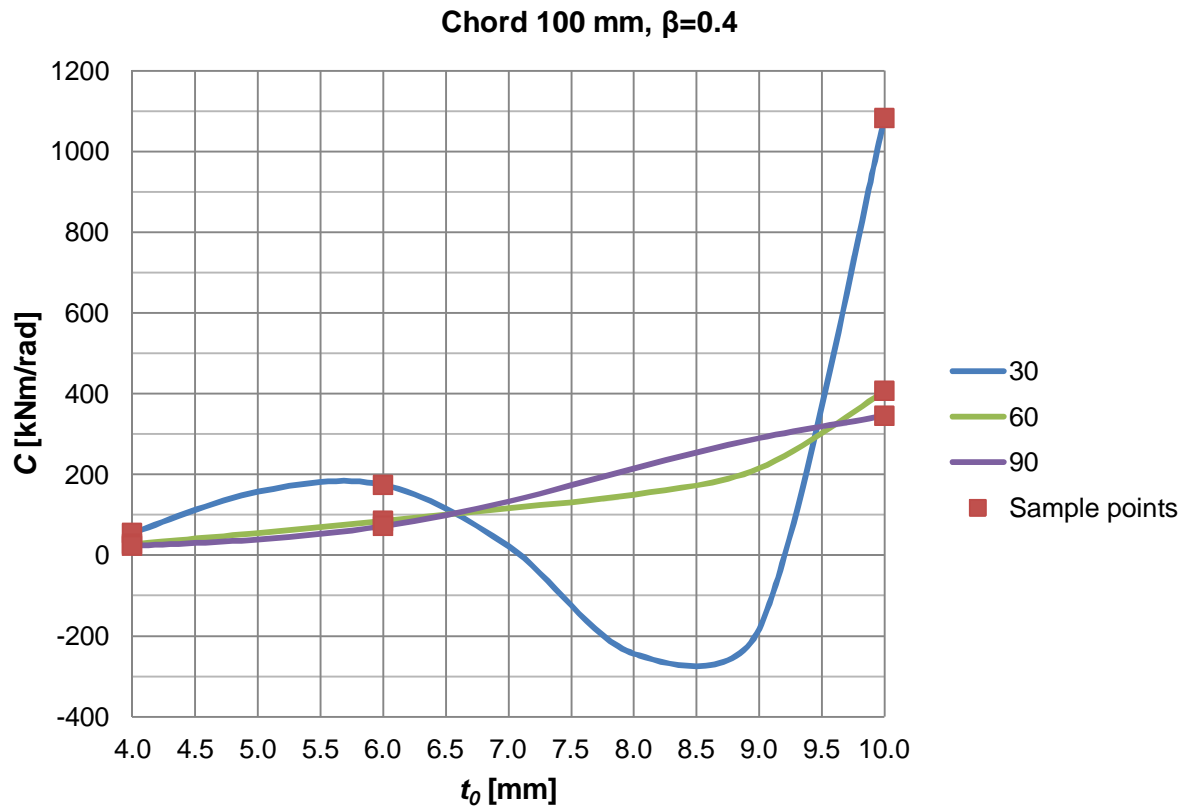


*Figure 5.4. C-t<sub>0</sub> response*

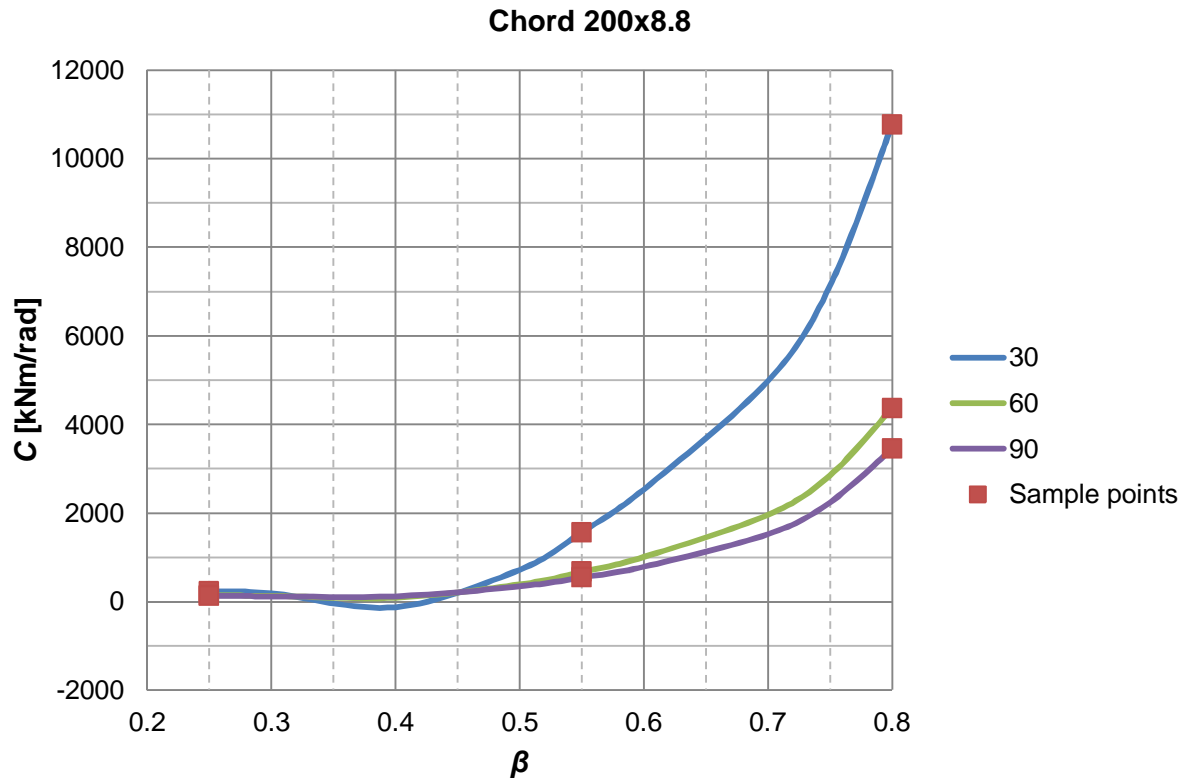


Figure 5.5.  $C$ - $\beta$  response

### 5.3. Interpolated pseudo points

During the validation of our previous model we came to conclusion that we need more sample points to make it work better. Calculating new sample points in Abaqus represented a complicated task and required time, so we decided to implement pseudo points.

Our previous pseudo points were all extrapolated (were out of the range of our interest and affected mostly the boundary conditions of the model). This time we decided to add points between the existing sample points. To distinguish these pseudo points from those, calculated before, we implemented for new ones a new term “interpolated pseudo points”, while using the term “extrapolated pseudo points” for previous ones.

For calculating the stiffness values for interpolated pseudo points we used 4<sup>th</sup> and 2<sup>nd</sup> (for the cases where only two values of thickness were calculated, see 5.1) order polynomial trend lines in Excel. Additional pseudo points were predicted for 45 and 75 degrees angles, two thicknesses (one between the lowest and the middle and one between the middle and the highest) and three betas (one between the lowest and the middle and two between the middle and the highest), see Fig. 5.6. Overall, we added 1869 pseudo points (both extrapolated and interpolated), resulting with 285 sample points the total number of 2154 points. The whole range of sample and pseudo points, both extrapolated and interpolated, is presented in Table C.1, App. C.

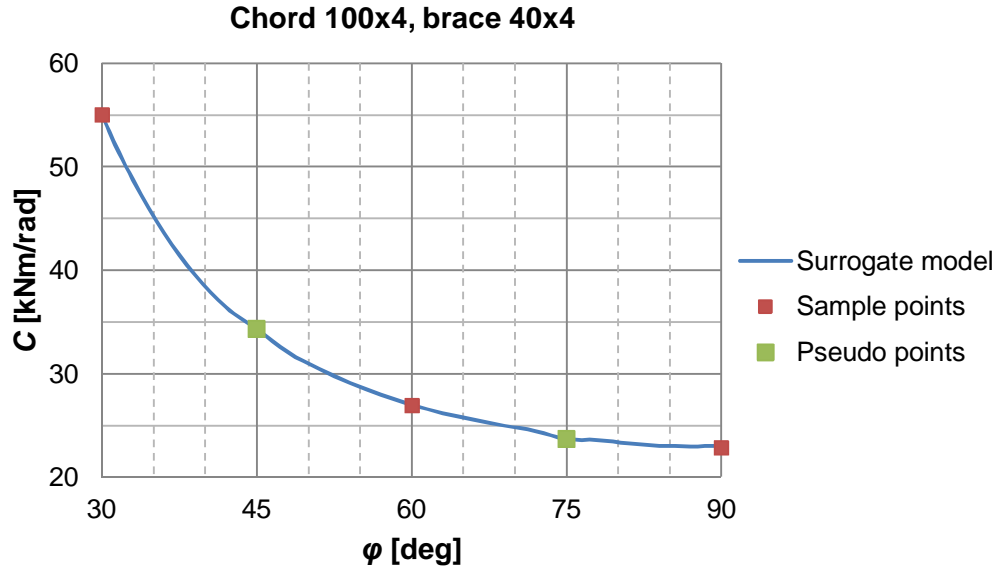


Figure 5.6. Interpolated pseudo points,  $\varphi$

As before, we considered several combinations of pseudo points to find the best result (Table 5.2).

Table 5.2. Pseudo points implementing II

Nº	$t_0$ ext	$t_0$ int	$\beta$ ext	$\beta$ int	$\varphi$ ext	$\varphi$ int	$R^2$	Avg. error, %	Max. error, %
1					x		0.9879	8	77
2					x	x	0.9916	9	163
3		x			x		0.6778	46	250
4	x	x			x		0.6480	92	917
5	x	x		x	x		0.8464	41	455
6	x	x	x	x	x		0.8929	59	828
7	x	x	x	x	x	x	0.9394	17	116

As can be seen, implementing interpolated pseudo points did not improve our model. The model with only extrapolated pseudo points for  $\varphi$  remained the best; its validation is presented in Table 5.3.

Table 5.3. Validation of the model II

Nº	Chord		$\beta$	$\varphi$ [deg]	C [kNm/rad]		Error, %
	$b_0$ [mm]	$t_0$ [mm]			Fact	Model	
1	100	4	0.4000	45	34	36	5.0
2	100	4	0.4000	75	24	23	2.9
3	100	4	0.8000	45	626	668	6.8
4	100	4	0.8000	75	367	358	2.5
5	100	5	0.6000	30	386	488	26.3
6	100	5	0.6000	45	217	282	30.1
7	100	5	0.6000	60	159	179	12.6
8	100	5	0.6000	75	135	139	2.9
9	100	5	0.6000	90	127	129	1.3
10	110	4	0.4545	30	81	143	77.2
11	110	4	0.4545	45	48	58	20.2

12	110	4	0.4545	60	37	30	18.8
13	110	4	0.4545	75	32	24	25.3
14	110	4	0.4545	90	31	25	19.1
15	110	6	0.5455	45	258	276	7.2
16	110	6	0.5455	75	166	163	1.9
17	120	5	0.3333	45	46	47	1.9
18	120	5	0.3333	75	34	33	1.9
19	120	5	0.6667	30	678	708	4.5
20	120	5	0.6667	45	372	409	10.0
21	120	5	0.6667	60	267	273	2.4
22	120	5	0.6667	75	224	226	0.8
23	120	5	0.6667	90	211	218	3.1
24	120	5	0.8333	45	1633	1742	6.7
25	120	5	0.8333	75	979	960	1.9
26	140	6	0.5714	30	568	579	2.0
27	140	6	0.5714	45	322	343	6.5
28	140	6	0.5714	60	238	238	0.0
29	140	6	0.5714	75	204	203	0.6
30	140	6	0.5714	90	194	199	2.5
31	150	6	0.4000	30	186	177	4.7
32	150	6	0.4000	45	116	139	20.1
33	150	6	0.4000	60	92	109	19.1
34	150	6	0.4000	75	82	94	15.0
35	150	6	0.4000	90	79	93	18.0
36	150	6	0.7333	30	2053	2143	4.4
37	150	6	0.7333	45	1118	1243	11.2
38	150	6	0.7333	60	793	822	3.6
39	150	6	0.7333	75	663	674	1.6
40	150	6	0.7333	90	626	651	4.0
41	160	7.1	0.7500	30	3900	3765	3.5
42	160	7.1	0.7500	45	2160	2277	5.4
43	160	7.1	0.7500	60	1556	1551	0.3
44	160	7.1	0.7500	75	1303	1281	1.7
45	160	7.1	0.7500	90	1230	1234	0.3
46	180	8	0.7778	30	7070	6636	6.1
47	180	8	0.7778	45	3926	4012	2.2
48	180	8	0.7778	60	2847	2728	4.2
49	180	8	0.7778	75	2397	2249	6.2
50	180	8	0.7778	90	2268	2162	4.7
51	180	10	0.8333	30	19802	18981	4.1
52	180	10	0.8333	45	10158	10979	8.1
53	180	10	0.8333	60	7423	7297	1.7
54	180	10	0.8333	75	6325	6041	4.5
55	180	10	0.8333	90	6012	5843	2.8
56	200	8	0.7500	30	5756	5704	0.9
57	200	8	0.7500	45	3182	3384	6.4
58	200	8	0.7500	60	2279	2261	0.8
59	200	8	0.7500	75	1905	1845	3.2
60	200	8	0.7500	90	1798	1766	1.8
61	200	10	0.6000	30	3183	3751	17.8
62	200	10	0.6000	45	1789	2141	19.7
63	200	10	0.6000	60	1327	1397	5.3
64	200	10	0.6000	75	1126	1136	0.9
65	200	10	0.6000	90	1069	1081	1.1
66	200	13	0.6000	30	6352	7801	22.8
67	200	13	0.6000	45	3583	4460	24.5
68	200	13	0.6000	60	2681	2925	9.1
69	200	13	0.6000	75	2319	2397	3.3

70	200	13	0.6000	90	2216	2301	3.8
71	220	8	0.8182	45	6210	6609	6.4
72	220	8	0.8182	75	3685	3613	1.9
73	250	10	0.6400	30	4460	4673	4.8
74	250	10	0.6400	45	2501	2641	5.6
75	250	10	0.6400	60	1822	1721	5.6
76	250	10	0.6400	75	1545	1410	8.7
77	250	10	0.6400	90	1466	1351	7.9
78	250	10	0.7200	30	8234	8387	1.9
79	250	10	0.7200	45	4526	4796	6.0
80	250	10	0.7200	60	3264	3151	3.5
81	250	10	0.7200	75	2739	2589	5.5
82	250	10	0.7200	90	2590	2492	3.8
83	260	10	0.7692	30	13024	13168	1.1
84	260	10	0.7692	45	7210	7659	6.2
85	260	10	0.7692	60	5122	5078	0.9
86	260	10	0.7692	75	4297	4172	2.9
87	260	10	0.7692	90	4038	4020	0.5
88	260	10	0.8462	30	27392	26909	1.8
89	260	10	0.8462	45	15492	16197	4.5
90	260	10	0.8462	60	11246	10941	2.7
91	260	10	0.8462	75	9422	8981	4.7
92	260	10	0.8462	90	8897	8628	3.0
93	300	13	0.3667	30	1438	1595	10.9
94	300	13	0.3667	45	917	952	3.8
95	300	13	0.3667	60	735	636	13.5
96	300	13	0.3667	75	660	516	21.8
97	300	13	0.3667	90	637	494	22.5
98	300	13	0.6000	30	6501	7762	19.4
99	300	13	0.6000	45	3696	4426	19.8
100	300	13	0.6000	60	2748	2923	6.4
101	300	13	0.6000	75	2354	2422	2.9
102	300	13	0.6000	90	2244	2338	4.2
103	300	13	0.7333	30	18747	22110	17.9
104	300	13	0.7333	45	10439	12623	20.9
105	300	13	0.7333	60	7526	8302	10.3
106	300	13	0.7333	75	6383	6847	7.3
107	300	13	0.7333	90	6033	6620	9.7
108	140	6	0.5714	50	285	297	4.2
109	140	6	0.5714	80	198	200	0.8
110	160	7.1	0.7500	50	1898	1967	3.6
111	160	7.1	0.7500	80	1263	1251	0.9
112	220	8	0.8182	50	5438	5670	4.3
113	220	8	0.8182	80	3565	3525	1.1
114	260	10	0.7692	50	6284	6544	4.1
115	260	10	0.7692	80	4158	4076	2.0

This was the best surrogate model we managed to improve this model using DACE. Despite the satisfactory results for  $R^2$  and the average error, the high maximum errors and the presence of negative values of stiffness did not allow us to use further. Moreover, graphical validation, as before, demonstrated unpredicted behavior of the model.

## 6. Surrogate modeling III

### 6.1. Attempt III

For our next steps of surrogate modeling we exploited the ooDACE toolbox for Matlab (hereinafter – ooDACE) (Couckuyt et al., 2014), (Ulaganathan et al., 2015). The code required to create a surrogate model with ooDACE is provided in App. E.

Using ooDACE and the sample points from 5.2 together with extrapolated pseudo points for  $\varphi$ ,  $t_0$  and  $\beta$  from Table 5.1 we managed to construct a surrogate model with the following parameters:  $R^2=0.9634$ , average error 13% and maximum error 42%. After adding the interpolated pseudo points from 5.3 we managed to improve it a little:  $R^2=0.9645$ , average error 12% and maximum error 37%. A distinctive feature of this model was a predicted behavior observed on the 2D (Figs. 6.1-6.3) and 3D (App. J) graphs.

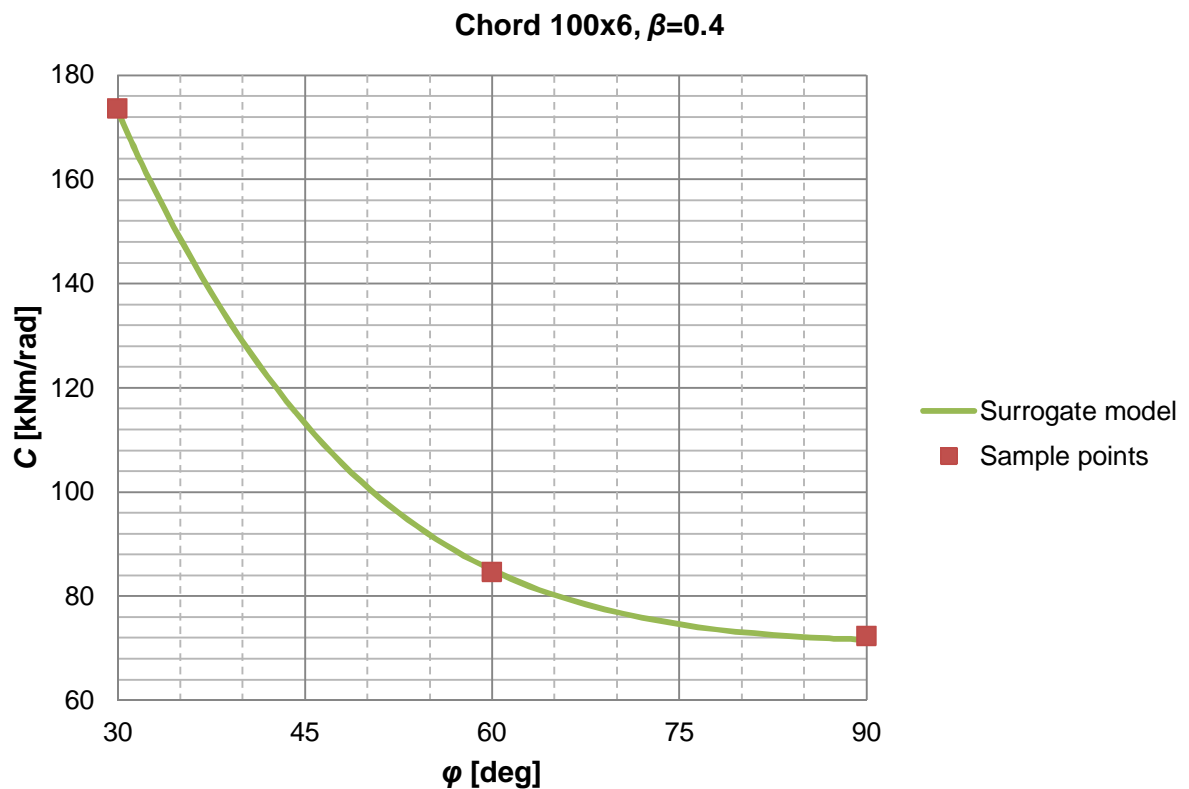


Figure 6.1.  $C$ - $\varphi$  response

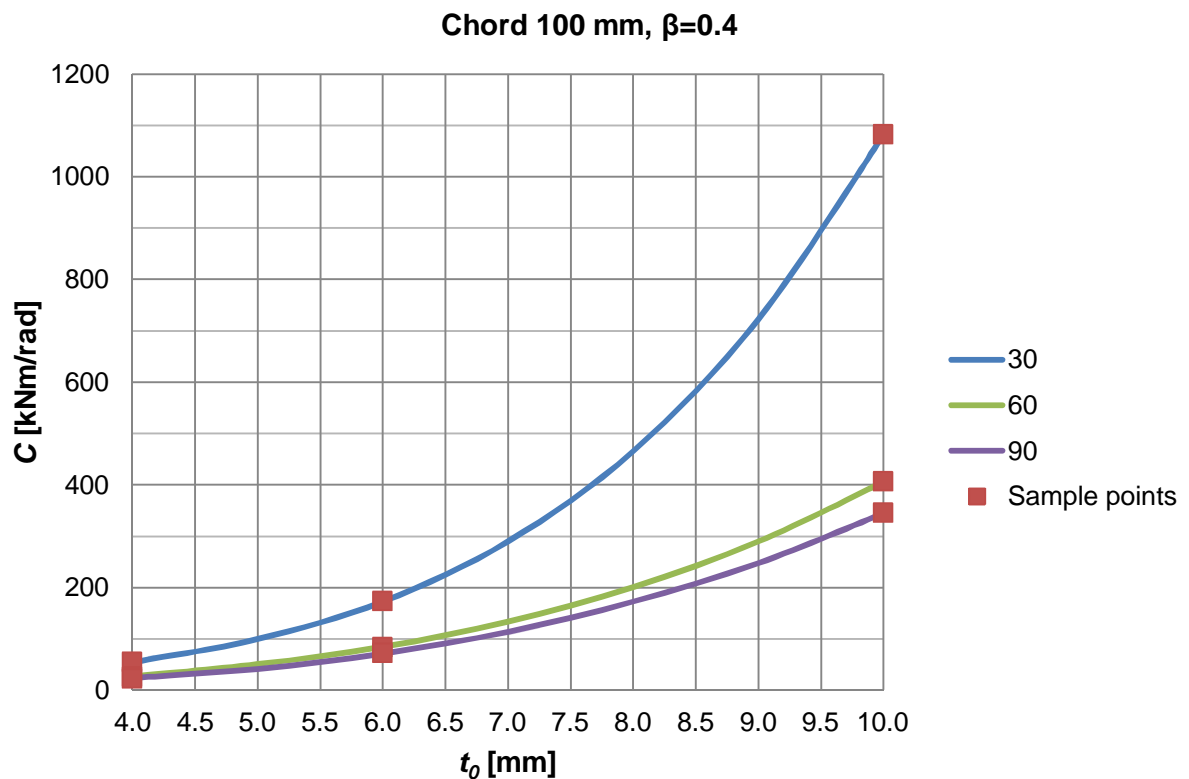


Figure 6.2.  $C-t_0$  response

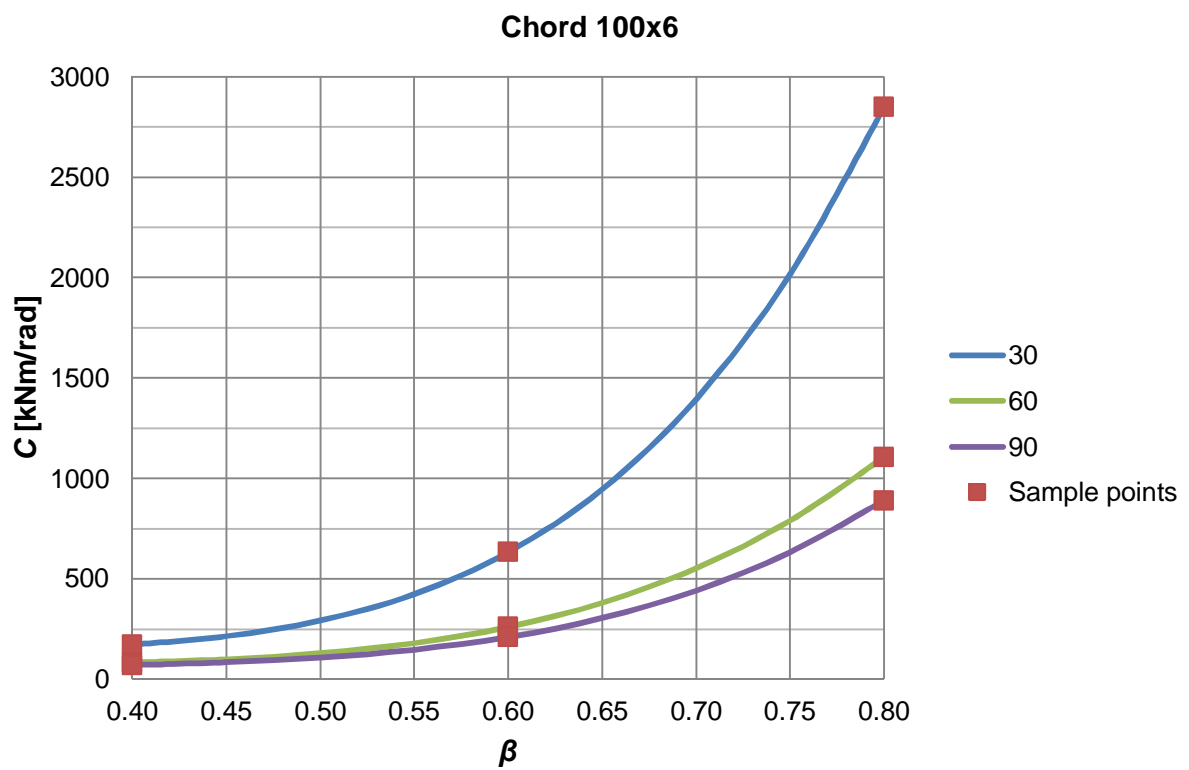


Figure 6.3.  $C-\beta$  response

During creating all the possible graphs with stiffness depending on every variable we did not observed any graph with unpredicted behavior of the model. This meant that the model worked as it should, but its accuracy required serious improvement.

We also realized that for this and our future models the  $R^2$  criterion stopped playing a serious role in assessing the surrogate model and from this case onwards we did not take it into account anymore. The most important criteria became the average and maximum errors, see Eq. 6.1.

$$Error = \frac{|C_{FEM} - C_{SURR}|}{C_{FEM}} \quad (6.1)$$

The results of validation are given in Table 6.1, where points with the error higher than 10% are marked in red.

*Table 6.1. Validation of the model III*

№	Chord		$\beta$	$\varphi$ [deg]	Fact		Surrogate model Error, %
	$b_o$ [mm]	$t_o$ [mm]			$C$ [kNm/rad]	$C$ [kNm/rad]	
1	100	4	0.4000	45	34	36	5.0
2	100	4	0.4000	75	24	24	1.3
3	100	4	0.8000	45	626	669	6.9
4	100	4	0.8000	75	367	359	2.2
5	100	5	0.6000	30	386	374	3.2
6	100	5	0.6000	45	217	233	7.5
7	100	5	0.6000	60	159	157	1.2
8	100	5	0.6000	75	135	127	5.9
9	100	5	0.6000	90	127	126	1.0
10	110	4	0.4545	30	81	68	15.7
11	110	4	0.4545	45	48	46	4.7
12	110	4	0.4545	60	37	32	13.4
13	110	4	0.4545	75	32	25	22.2
14	110	4	0.4545	90	31	26	15.8
15	110	6	0.5455	45	258	275	6.8
16	110	6	0.5455	75	166	163	1.9
17	120	5	0.3333	45	46	48	4.1
18	120	5	0.3333	75	34	33	1.9
19	120	5	0.6667	30	678	806	18.9
20	120	5	0.6667	45	372	470	26.4
21	120	5	0.6667	60	267	323	21.2
22	120	5	0.6667	75	224	274	22.2
23	120	5	0.6667	90	211	257	21.6
24	120	5	0.8333	45	1633	1741	6.6
25	120	5	0.8333	75	979	961	1.8
26	140	6	0.5714	30	568	584	2.9
27	140	6	0.5714	45	322	354	9.9
28	140	6	0.5714	60	238	245	2.9
29	140	6	0.5714	75	204	206	0.9
30	140	6	0.5714	90	194	200	3.1
31	150	6	0.4000	30	186	140	24.7
32	150	6	0.4000	45	116	108	6.6
33	150	6	0.4000	60	92	75	18.1
34	150	6	0.4000	75	82	57	30.2
35	150	6	0.4000	90	79	67	15.0
36	150	6	0.7333	30	2053	2398	16.8
37	150	6	0.7333	45	1118	1391	24.5

38	150	6	0.7333	60	793	933	17.6
39	150	6	0.7333	75	663	777	17.2
40	150	6	0.7333	90	626	734	17.2
41	160	7.1	0.7500	30	3900	3859	1.0
42	160	7.1	0.7500	45	2160	2268	5.0
43	160	7.1	0.7500	60	1556	1507	3.1
44	160	7.1	0.7500	75	1303	1236	5.1
45	160	7.1	0.7500	90	1230	1197	2.7
46	180	8	0.7778	30	7070	7526	6.4
47	180	8	0.7778	45	3926	4438	13.0
48	180	8	0.7778	60	2847	3026	6.3
49	180	8	0.7778	75	2397	2536	5.8
50	180	8	0.7778	90	2268	2405	6.0
51	180	10	0.8333	30	19802	17686	10.7
52	180	10	0.8333	45	10158	10538	3.7
53	180	10	0.8333	60	7423	7177	3.3
54	180	10	0.8333	75	6325	5989	5.3
55	180	10	0.8333	90	6012	5792	3.7
56	200	8	0.7500	30	5756	6216	8.0
57	200	8	0.7500	45	3182	3662	15.1
58	200	8	0.7500	60	2279	2477	8.7
59	200	8	0.7500	75	1905	2057	8.0
60	200	8	0.7500	90	1798	1950	8.4
61	200	10	0.6000	30	3183	3469	9.0
62	200	10	0.6000	45	1789	2075	16.0
63	200	10	0.6000	60	1327	1451	9.3
64	200	10	0.6000	75	1126	1238	10.0
65	200	10	0.6000	90	1069	1169	9.3
66	200	12.5	0.6000	30	6352	6828	7.5
67	200	12.5	0.6000	45	3583	4069	13.6
68	200	12.5	0.6000	60	2681	2821	5.2
69	200	12.5	0.6000	75	2319	2394	3.2
70	200	12.5	0.6000	90	2216	2291	3.4
71	220	8	0.8182	45	6210	6602	6.3
72	220	8	0.8182	75	3685	3620	1.8
73	250	10	0.6400	30	4460	5016	12.5
74	250	10	0.6400	45	2501	2945	17.7
75	250	10	0.6400	60	1822	2045	12.2
76	250	10	0.6400	75	1545	1748	13.2
77	250	10	0.6400	90	1466	1645	12.2
78	250	10	0.7200	30	8234	9566	16.2
79	250	10	0.7200	45	4526	5616	24.1
80	250	10	0.7200	60	3264	3845	17.8
81	250	10	0.7200	75	2739	3243	18.4
82	250	10	0.7200	90	2590	3068	18.4
83	260	10	0.7692	30	13024	16074	23.4
84	260	10	0.7692	45	7210	9514	32.0
85	260	10	0.7692	60	5122	6523	27.4
86	260	10	0.7692	75	4297	5477	27.5
87	260	10	0.7692	90	4038	5151	27.5
88	260	10	0.8462	30	27392	26909	1.8
89	260	10	0.8462	45	15492	16179	4.4
90	260	10	0.8462	60	11246	10941	2.7
91	260	10	0.8462	75	9422	8996	4.5
92	260	10	0.8462	90	8897	8627	3.0
93	300	12.5	0.3667	30	1438	1032	28.2
94	300	12.5	0.3667	45	917	863	5.9
95	300	12.5	0.3667	60	735	580	21.1

96	300	12.5	0.3667	75	660	418	36.7
97	300	12.5	0.3667	90	637	522	18.1
98	300	12.5	0.6000	30	6501	7739	19.0
99	300	12.5	0.6000	45	3696	4560	23.4
100	300	12.5	0.6000	60	2748	3232	17.6
101	300	12.5	0.6000	75	2354	2812	19.4
102	300	12.5	0.6000	90	2244	2622	16.9
103	300	12.5	0.7333	30	18747	23133	23.4
104	300	12.5	0.7333	45	10439	13623	30.5
105	300	12.5	0.7333	60	7526	9442	25.5
106	300	12.5	0.7333	75	6383	8038	25.9
107	300	12.5	0.7333	90	6033	7543	25.0
108	140	6	0.5714	50	285	306	7.3
109	140	6	0.5714	80	198	202	1.8
110	160	7.1	0.7500	50	1898	1941	2.2
111	160	7.1	0.7500	80	1263	1208	4.3
112	220	8	0.8182	50	5438	5662	4.1
113	220	8	0.8182	80	3565	3530	1.0
114	260	10	0.7692	50	6284	8209	30.6
115	260	10	0.7692	80	4158	5337	28.3

## 6.2. Multi-model approach

Before we constructed the surrogate models where rotational stiffness depended on four variables:  $b_0$ ,  $t_0$ ,  $\beta$  and  $\varphi$ . At the same time, if consider attentively, during validation there was no prediction for stiffness between  $b_0$ , e.g. we had the sample points with  $b_0$  100 mm and 110 mm but no validation points with any  $b_0$  between this values. This was also true for other values of  $b_0$ .

Obviously, it seemed possible to construct an independent surrogate model for every chord width instead of one single model for all widths. This would also allow us to exclude  $b_0$  from the list of variables. The code for creating the surrogate model is provided in App. F.

As a result we constructed the surrogate models for every chord (12 in total) not affected each other. As expected this approach gave rather close results to those obtained from a single model (Table 6.2). The average error was 12% while the maximum 36%. However, during our next modeling, in some cases for some chords we observed certain differences (both for better and worse).

We used this approach for our next surrogate modeling as an alternative technique. It is worth saying that it requires much less computational time than a single model approach.

Table 6.2. Many models approach validation

№	Chord		$\beta$	$\varphi$ [deg]	Fact	Surrogate model	
	$b_0$ [mm]	$t_0$ [mm]			$C$ [kNm/rad]	$C$ [kNm/rad]	Error, %
1	100	4	0.4000	45	34	36	5.0
2	100	4	0.4000	75	24	24	1.3
3	100	4	0.8000	45	626	669	6.9
4	100	4	0.8000	75	367	359	2.2
5	100	5	0.6000	30	386	374	3.2
6	100	5	0.6000	45	217	243	12.1
7	100	5	0.6000	60	159	157	1.2
8	100	5	0.6000	75	135	122	9.6
9	100	5	0.6000	90	127	126	1.0
10	110	4	0.4545	30	81	67	17.0

11	110	4	0.4545	45	48	45	6.8
12	110	4	0.4545	60	37	32	13.4
13	110	4	0.4545	75	32	26	19.1
14	110	4	0.4545	90	31	26	15.8
15	110	6	0.5455	45	258	275	6.8
16	110	6	0.5455	75	166	162	2.5
17	120	5	0.3333	45	46	48	4.1
18	120	5	0.3333	75	34	33	1.9
19	120	5	0.6667	30	678	806	18.9
20	120	5	0.6667	45	372	471	26.7
21	120	5	0.6667	60	267	323	21.2
22	120	5	0.6667	75	224	273	21.7
23	120	5	0.6667	90	211	257	21.6
24	120	5	0.8333	45	1633	1740	6.6
25	120	5	0.8333	75	979	961	1.8
26	140	6	0.5714	30	568	584	2.9
27	140	6	0.5714	45	322	355	10.2
28	140	6	0.5714	60	238	245	2.9
29	140	6	0.5714	75	204	206	0.9
30	140	6	0.5714	90	194	200	3.1
31	150	6	0.4000	30	186	140	24.7
32	150	6	0.4000	45	116	107	7.5
33	150	6	0.4000	60	92	75	18.1
34	150	6	0.4000	75	82	59	27.8
35	150	6	0.4000	90	79	67	15.0
36	150	6	0.7333	30	2053	2398	16.8
37	150	6	0.7333	45	1118	1393	24.6
38	150	6	0.7333	60	793	933	17.6
39	150	6	0.7333	75	663	775	16.9
40	150	6	0.7333	90	626	733	17.1
41	160	7.1	0.7500	30	3900	3860	1.0
42	160	7.1	0.7500	45	2160	2268	5.0
43	160	7.1	0.7500	60	1556	1506	3.2
44	160	7.1	0.7500	75	1303	1236	5.1
45	160	7.1	0.7500	90	1230	1197	2.7
46	180	8	0.7778	30	7070	7525	6.4
47	180	8	0.7778	45	3926	4441	13.1
48	180	8	0.7778	60	2847	3026	6.3
49	180	8	0.7778	75	2397	2533	5.7
50	180	8	0.7778	90	2268	2405	6.0
51	180	10	0.8333	30	19802	17686	10.7
52	180	10	0.8333	45	10158	10536	3.7
53	180	10	0.8333	60	7423	7177	3.3
54	180	10	0.8333	75	6325	5992	5.3
55	180	10	0.8333	90	6012	5792	3.7
56	200	8	0.7500	30	5756	6216	8.0
57	200	8	0.7500	45	3182	3664	15.2
58	200	8	0.7500	60	2279	2476	8.6
59	200	8	0.7500	75	1905	2055	7.9
60	200	8	0.7500	90	1798	1950	8.4
61	200	10	0.6000	30	3183	3470	9.0
62	200	10	0.6000	45	1789	2077	16.1
63	200	10	0.6000	60	1327	1451	9.3
64	200	10	0.6000	75	1126	1237	9.9
65	200	10	0.6000	90	1069	1169	9.3
66	200	12.5	0.6000	30	6352	6828	7.5
67	200	12.5	0.6000	45	3583	4070	13.6
68	200	12.5	0.6000	60	2681	2821	5.2

69	200	12.5	0.6000	75	2319	2394	3.2
70	200	12.5	0.6000	90	2216	2291	3.4
71	220	8	0.8182	45	6210	6602	6.3
72	220	8	0.8182	75	3685	3620	1.8
73	250	10	0.6400	30	4460	5015	12.4
74	250	10	0.6400	45	2501	2946	17.8
75	250	10	0.6400	60	1822	2045	12.2
76	250	10	0.6400	75	1545	1747	13.1
77	250	10	0.6400	90	1466	1645	12.2
78	250	10	0.7200	30	8234	9566	16.2
79	250	10	0.7200	45	4526	5618	24.1
80	250	10	0.7200	60	3264	3845	17.8
81	250	10	0.7200	75	2739	3242	18.4
82	250	10	0.7200	90	2590	3068	18.4
83	260	10	0.7692	30	13024	16074	23.4
84	260	10	0.7692	45	7210	9516	32.0
85	260	10	0.7692	60	5122	6523	27.4
86	260	10	0.7692	75	4297	5477	27.5
87	260	10	0.7692	90	4038	5151	27.5
88	260	10	0.8462	30	27392	26910	1.8
89	260	10	0.8462	45	15492	16179	4.4
90	260	10	0.8462	60	11246	10941	2.7
91	260	10	0.8462	75	9422	8996	4.5
92	260	10	0.8462	90	8897	8627	3.0
93	300	12.5	0.3667	30	1438	1032	28.2
94	300	12.5	0.3667	45	917	852	7.1
95	300	12.5	0.3667	60	735	580	21.1
96	300	12.5	0.3667	75	660	425	35.6
97	300	12.5	0.3667	90	637	522	18.1
98	300	12.5	0.6000	30	6501	7738	19.0
99	300	12.5	0.6000	45	3696	4575	23.8
100	300	12.5	0.6000	60	2748	3232	17.6
101	300	12.5	0.6000	75	2354	2803	19.1
102	300	12.5	0.6000	90	2244	2621	16.8
103	300	12.5	0.7333	30	18747	23133	23.4
104	300	12.5	0.7333	45	10439	13654	30.8
105	300	12.5	0.7333	60	7526	9442	25.5
106	300	12.5	0.7333	75	6383	8018	25.6
107	300	12.5	0.7333	90	6033	7543	25.0
108	140	6	0.5714	50	285	307	7.7
109	140	6	0.5714	80	198	202	1.8
110	160	7.1	0.7500	50	1898	1940	2.2
111	160	7.1	0.7500	80	1263	1208	4.3
112	220	8	0.8182	50	5438	5662	4.1
113	220	8	0.8182	80	3565	3530	1.0
114	260	10	0.7692	50	6284	8210	30.6
115	260	10	0.7692	80	4158	5337	28.3

### 6.3. Validation points analysis

We introduced the new criteria for assessing our surrogate models: relative error (hereinafter - error) for any points is less than 10%. For objective assessment of models we calculated in Abaqus a new range of validation points chosen randomly. Validation results are presented in Table 6.3. At that moment our best model had 8% average error, 28% maximum error and 16 “bad” points of total 48 validation points, i.e. a third. The same results were observed using multi-model approach.

To increase the accuracy of our model we conducted the analysis of validation points. The goal of this analysis was to divide the points into groups in accordance with the variables for which they were predicted. In this table the groups are marked by different colors: violet means only  $\varphi$  prediction, blue –  $t_0$  prediction, brown –  $\beta$  prediction and green –  $\beta$  and  $t_0$  prediction. Red cells mean the error higher than 10% ("bad" points).

Table 6.3. Validation points analysis

№	Chord		$\beta$	$\varphi$ [deg]	Fact	Surrogate model	
	$b_0$ [mm]	$t_0$ [mm]				$C$ [kNm/rad]	$C$ [kNm/rad]
1	100	8	0.8000	79	1838	1815	1.3
2	100	6	0.4000	42	115	122	6.2
3	100	10	0.4000	80	349	348	0.4
4	100	8	0.5000	89	300	275	8.3
5	110	5	0.3636	34	71	73	2.8
6	110	6	0.3636	55	76	77	1.4
7	110	6	0.3636	50	82	84	2.8
8	110	5	0.8182	88	746	748	0.3
9	120	5.6	0.5833	80	170	171	0.8
10	120	7.1	0.7500	83	1098	1212	10.4
11	120	8.8	0.8333	42	6030	6664	10.5
12	120	7.1	0.5000	39	399	393	1.5
13	140	7.1	0.3571	90	106	94	11.4
14	140	6	0.7857	89	977	1019	4.3
15	140	7.1	0.5000	40	393	383	2.6
16	140	6	0.5000	30	349	301	13.8
17	150	7.1	0.5333	47	405	419	3.5
18	150	7.1	0.8000	89	1643	1787	8.8
19	150	6	0.4000	71	84	60	28.3
20	150	7.1	0.2667	39	104	108	3.8
21	160	8.8	0.7500	86	1946	2116	8.7
22	160	10	0.3125	76	244	223	8.5
23	160	8.8	0.5000	85	416	384	7.7
24	160	8.8	0.4375	81	303	253	16.5
25	180	10	0.3889	59	405	361	10.8
26	180	12.5	0.6667	33	8504	9550	12.3
27	180	10	0.5000	40	1085	1122	3.4
28	180	10	0.6111	60	1415	1562	10.4
29	200	8.8	0.2500	69	130	129	1.0
30	200	12.5	0.4000	62	855	811	5.1
31	200	8	0.3000	57	138	131	4.8
32	200	7.1	0.6000	66	448	518	15.5
33	220	8.8	0.5455	71	569	553	2.8
34	220	12.5	0.4545	58	1195	1076	9.9
35	220	10	0.4091	37	703	604	14.1
36	220	8	0.7273	62	1757	2247	27.9
37	250	12.5	0.7200	60	6397	6765	5.7
38	250	10	0.6000	90	1073	1183	10.3
39	250	12.5	0.6000	87	2199	2334	6.2
40	250	8.8	0.2800	72	151	150	0.8
41	260	10	0.8462	79	8820	8803	0.2
42	260	12.5	0.5769	67	2135	2309	8.2
43	260	12.5	0.3077	73	498	420	15.6
44	260	12.5	0.6923	51	6208	7559	21.8
45	300	12.5	0.8333	33	39163	40991	4.7
46	300	12.5	0.4667	56	1290	1127	12.6
47	300	12.5	0.8333	85	14946	14910	0.2

48	300	12.5	0.6000	86	2247	2678	19.2
----	-----	------	--------	----	------	------	------

As can be noticed easily, all the red cells are connected to brown and green lines, i.e. points for which  $\beta$  was predicted. Prediction for only  $\varphi$  was satisfactory accurate and there was only one red case for  $t_0$  prediction.

#### 6.4. Improved $\beta$ curves

The analysis conducted in 6.3 showed that prediction in  $\beta$  works bad and requires improvement. As it was mentioned before, when choosing sample points for every case we calculated three betas: minimum (0.25...0.4), middle (0.5...0.55) and maximum (0.8...0.85), let call them  $\beta_1$ ,  $\beta_2$  and  $\beta_3$  respectively. Looking attentively at the bad points in Table 6.3, it can be noticed that for the points with  $\beta_1 < \beta < \beta_2$  the predicted values were lower whereas for the points with  $\beta_2 < \beta < \beta_3$  the opposite trend was observed. This indicates that beta curves used for calculation of pseudo points were inaccurate and this inaccuracy led to inaccuracy in predicted values of stiffness.

To investigate it in details we created a graph for  $\beta$  for one case adding there several old validation points (Fig. 6.4)

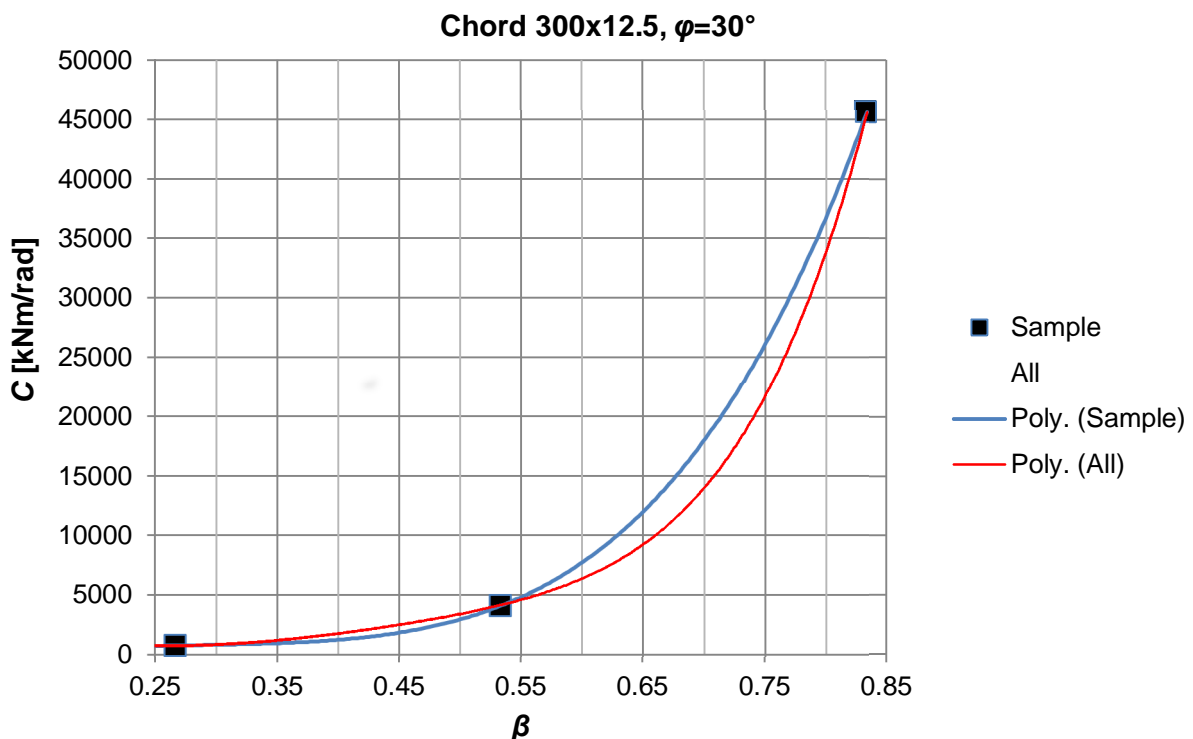


Figure 6.4. Difference in  $\beta$  curves

As can be seen from the graph, the curve predicted in Excel using three sample points (blue line) did not suit accurately the actual curve obtained by using additional points (red line). This discrepancy led to inaccurate values of pseudo points used later in surrogate modeling and, eventually, caused considerable errors in predicted values (up to 28% in this case and even more for others). The same difference was observed for all cases.

To improve this discrepancy we modified beta curves by changing extrapolated pseudo points. It was done manually and had no scientific basis but it allowed us to receive more accurate curves (Fig. 6.5).

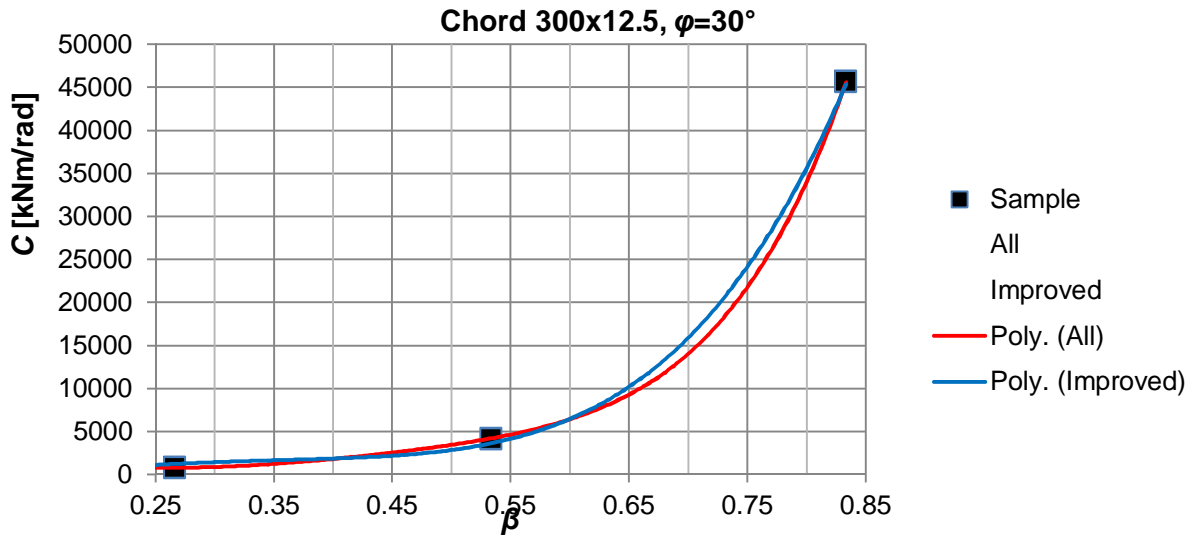


Figure 6.5. Improved  $\beta$  curves

Using improved beta curves new pseudo points were calculated and implemented to the surrogate model. Its validation is given in Table 6.4. The number of red cells decreased two times (from 16 to 8), the average error reduced a little (from 8% to 7%). However for some points extremely high errors were observed (up to 75%).

Table 6.4. Validation, improved  $\beta$ , single model

№	Chord		$\beta$	$\phi$ [deg]	Fact	Surrogate model	
	$b_0$ [mm]	$t_0$ [mm]				$C$ [kNm/rad]	$C$ [kNm/rad]
1	100	8	0.8000	79	1838	1752	4.7
2	100	6	0.4000	42	115	122	6.2
3	100	10	0.4000	80	349	347	0.7
4	100	8	0.5000	89	300	525	75.0
5	110	5	0.3636	34	71	74	4.2
6	110	6	0.3636	55	76	77	1.4
7	110	6	0.3636	50	82	85	4.0
8	110	5	0.8182	88	746	752	0.8
9	120	5.6	0.5833	80	170	171	0.8
10	120	7.1	0.7500	83	1098	1111	1.2
11	120	8.8	0.8333	42	6030	6726	11.6
12	120	7.1	0.5000	39	399	387	3.0
13	140	7.1	0.3571	90	106	113	6.5
14	140	6	0.7857	89	977	1017	4.1
15	140	7.1	0.5000	40	393	400	1.7
16	140	6	0.5000	30	349	366	4.8
17	150	7.1	0.5333	47	405	397	1.9
18	150	7.1	0.8000	89	1643	1778	8.2
19	150	6	0.4000	71	84	67	19.9
20	150	7.1	0.2667	39	104	103	1.1
21	160	8.8	0.7500	86	1946	2115	8.7
22	160	10	0.3125	76	244	329	35.0
23	160	8.8	0.5000	85	416	469	12.7

24	160	8.8	0.4375	81	303	392	29.4
25	180	10	0.3889	59	405	391	3.4
26	180	12.5	0.6667	33	8504	9029	6.2
27	180	10	0.5000	40	1085	1096	1.1
28	180	10	0.6111	60	1415	1470	3.9
29	200	8.8	0.2500	69	130	129	1.0
30	200	12.5	0.4000	62	855	1011	18.3
31	200	8	0.3000	57	138	150	9.0
32	200	7.1	0.6000	66	448	452	0.8
33	220	8.8	0.5455	71	569	547	3.9
34	220	12.5	0.4545	58	1195	1247	4.4
35	220	10	0.4091	37	703	819	16.4
36	220	8	0.7273	62	1757	1974	12.4
37	250	12.5	0.7200	60	6397	6163	3.7
38	250	10	0.6000	90	1073	1090	1.6
39	250	12.5	0.6000	87	2199	2170	1.3
40	250	8.8	0.2800	72	151	150	0.8
41	260	10	0.8462	79	8820	8802	0.2
42	260	12.5	0.5769	67	2135	2115	0.9
43	260	12.5	0.3077	73	498	522	4.8
44	260	12.5	0.6923	51	6208	6222	0.2
45	300	12.5	0.8333	33	39163	40996	4.7
46	300	12.5	0.4667	56	1290	1396	8.2
47	300	12.5	0.8333	85	14946	14908	0.3
48	300	12.5	0.6000	86	2247	2338	4.1

Validation for multi-model approach was also conducted, the results are given in Table 6.5. This time certain difference between these two techniques was noticed: 11 red cells, lesser average error (6%) and no points with extremely high errors.

Table 6.5. Validation, improved  $\beta$ , multi-model

№	Chord		$\beta$	$\varphi$ [deg]	Fact	Surrogate model	
	$b_0$ [mm]	$t_0$ [mm]			$C$ [kNm/rad]	$C$ [kNm/rad]	Error [%]
1	100	8	0.8000	79	1838	1735	5.6
2	100	6	0.4000	42	115	122	6.2
3	100	10	0.4000	80	349	348	0.4
4	100	8	0.5000	89	300	285	5.0
5	110	5	0.3636	34	71	74	4.2
6	110	6	0.3636	55	76	77	1.4
7	110	6	0.3636	50	82	84	2.8
8	110	5	0.8182	88	746	750	0.5
9	120	5.6	0.5833	80	170	169	0.4
10	120	7.1	0.7500	83	1098	1135	3.3
11	120	8.8	0.8333	42	6030	6736	11.7
12	120	7.1	0.5000	39	399	441	10.5
13	140	7.1	0.3571	90	106	114	7.4
14	140	6	0.7857	89	977	1020	4.4
15	140	7.1	0.5000	40	393	468	19.0
16	140	6	0.5000	30	349	339	2.9
17	150	7.1	0.5333	47	405	426	5.2
18	150	7.1	0.8000	89	1643	1789	8.9
19	150	6	0.4000	71	84	72	13.9
20	150	7.1	0.2667	39	104	109	4.7
21	160	8.8	0.7500	86	1946	2115	8.7
22	160	10	0.3125	76	244	255	4.6
23	160	8.8	0.5000	85	416	428	2.9

24	160	8.8	0.4375	81	303	303	0.0
25	180	10	0.3889	59	405	460	13.7
26	180	12.5	0.6667	33	8504	8767	3.1
27	180	10	0.5000	40	1085	1298	19.7
28	180	10	0.6111	60	1415	1413	0.2
29	200	8.8	0.2500	69	130	129	1.0
30	200	12.5	0.4000	62	855	987	15.5
31	200	8	0.3000	57	138	163	18.5
32	200	7.1	0.6000	66	448	478	6.6
33	220	8.8	0.5455	71	569	551	3.2
34	220	12.5	0.4545	58	1195	1278	7.0
35	220	10	0.4091	37	703	901	28.1
36	220	8	0.7273	62	1757	1985	13.0
37	250	12.5	0.7200	60	6397	6163	3.7
38	250	10	0.6000	90	1073	1088	1.4
39	250	12.5	0.6000	87	2199	2193	0.3
40	250	8.8	0.2800	72	151	150	0.8
41	260	10	0.8462	79	8820	8803	0.2
42	260	12.5	0.5769	67	2135	2104	1.4
43	260	12.5	0.3077	73	498	464	6.8
44	260	12.5	0.6923	51	6208	6190	0.3
45	300	12.5	0.8333	33	39163	40994	4.7
46	300	12.5	0.4667	56	1290	1422	10.3
47	300	12.5	0.8333	85	14946	14911	0.2
48	300	12.5	0.6000	86	2247	2323	3.4

Despite the fact that none of these two models suited the required criteria, they had proved that it was possible to modify the model by changing the pseudo points and both of them were used for next steps of surrogate modeling.

## 6.5. Improved $\varphi$ curves

Paying attention to validation results in Table 6.1 we noticed a certain difference for the points for which stiffness was predicted only among angles. For 45 degree points the stiffness values were about 6% higher whereas for 75 degree points they were 2% lower. This trend repeated also for the multi-model approach (Table 6.2). Graphically it is illustrated in Fig. 6.6.

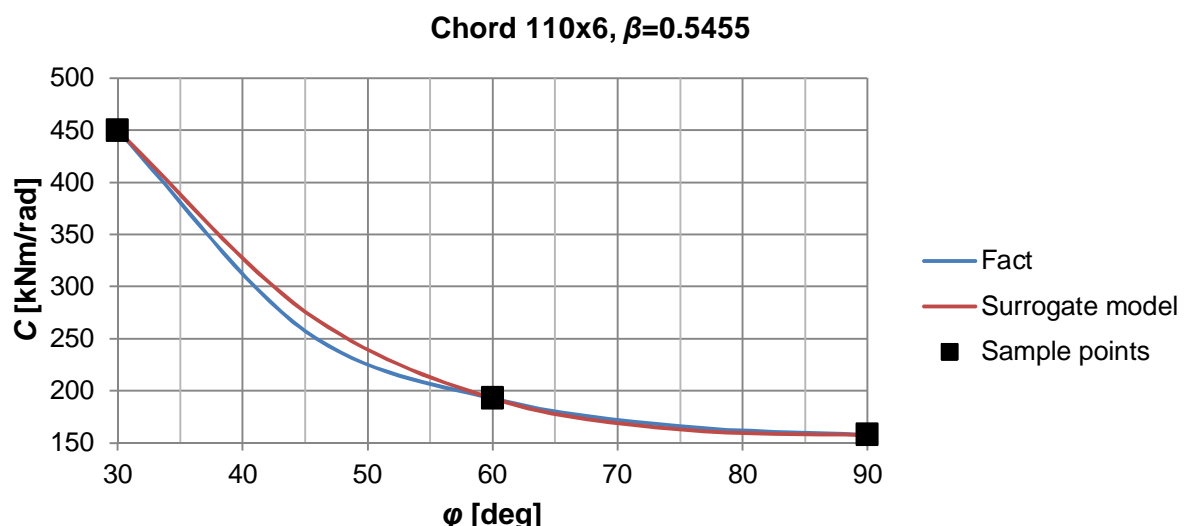


Figure 6.6. Difference in  $\varphi$  curves

To improve this discrepancy we applied the same technique as before for  $\beta$  curves (see 6.4) to the model with improved betas. We did not manage to receive a working surrogate for the single-model approach, although we did for the multi-model. The results of validation are given in Table 6.6.

Table 6.6. Validation, improved  $\beta$  and  $\varphi$ , multi-model

№	Chord		Brace $\beta$	$\varphi$ [deg]	Fact	Surrogate model	
	$b_o$ [mm]	$t_o$ [mm]				$C$ [kNm/rad]	$C$ [kNm/rad]
1	100	8	0.8000	79	1838	1735	5.6
2	100	6	0.4000	42	115	122	6.2
3	100	10	0.4000	80	349	348	0.4
4	100	8	0.5000	89	300	285	5.0
5	110	5	0.3636	34	71	72	1.4
6	110	6	0.3636	55	76	75	1.2
7	110	6	0.3636	50	82	81	0.9
8	110	5	0.8182	88	746	748	0.3
9	120	5.6	0.5833	80	170	167	1.6
10	120	7.1	0.7500	83	1098	1126	2.5
11	120	8.8	0.8333	42	6030	6528	8.3
12	120	7.1	0.5000	39	399	456	14.3
13	140	7.1	0.3571	90	106	114	7.4
14	140	6	0.7857	89	977	1020	4.4
15	140	7.1	0.5000	40	393	468	19.0
16	140	6	0.5000	30	349	339	2.9
17	150	7.1	0.5333	47	405	400	1.2
18	150	7.1	0.8000	89	1643	1783	8.5
19	150	6	0.4000	71	84	77	8.0
20	150	7.1	0.2667	39	104	105	0.9
21	160	8.8	0.7500	86	1946	2102	8.0
22	160	10	0.3125	76	244	243	0.3
23	160	8.8	0.5000	85	416	438	5.3
24	160	8.8	0.4375	81	303	321	6.0
25	180	10	0.3889	59	405	446	10.2
26	180	12.5	0.6667	33	8504	8689	2.2
27	180	10	0.5000	40	1085	1251	15.3
28	180	10	0.6111	60	1415	1421	0.4
29	200	8.8	0.2500	69	130	132	1.3
30	200	12.5	0.4000	62	855	982	14.9
31	200	8	0.3000	57	138	169	22.8
32	200	7.1	0.6000	66	448	501	11.7
33	220	8.8	0.5455	71	569	558	2.0
34	220	12.5	0.4545	58	1195	1282	7.3
35	220	10	0.4091	37	703	1013	44.0
36	220	8	0.7273	62	1757	2034	15.8
37	250	12.5	0.7200	60	6397	6163	3.7
38	250	10	0.6000	90	1073	1086	1.2
39	250	12.5	0.6000	87	2199	2170	1.3
40	250	8.8	0.2800	72	151	151	0.2
41	260	10	0.8462	79	8820	8717	1.2
42	260	12.5	0.5769	67	2135	2229	4.4
43	260	12.5	0.3077	73	498	484	2.8
44	260	12.5	0.6923	51	6208	5061	18.5
45	300	12.5	0.8333	33	39163	40830	4.3
46	300	12.5	0.4667	56	1290	1459	13.1
47	300	12.5	0.8333	85	14946	14795	1.0
48	300	12.5	0.6000	86	2247	2247	0.0

Despite the questionable results, this model, as previous two ones, was used for next steps of surrogate modeling.

## 6.6. Complex model

For that moment we had 5 surrogate models:

- Two without any improvements (single model and multi-model);
- Two with improved betas (single model and multi-model);
- A multi-model with improved betas and angles.

None of them had satisfactory results. However their performance was different for various chords. It seemed logical to create a complex model which contained for every chord a surrogate model which suited it best. For solving this task every chord was analyzed separately to choose the surrogate model with the best performance. The analysis is given in Table 6.7. Here number 1 relates to a model without any improvements, number 2 to the model with improved betas and number 3 to the model with improved betas and angles, SM relates to single model, MM to multi model.

Table 6.7. Complex model legend

$b_o$ [mm]	1SM	1MM	2SM	2MM	3MM
100		x			
110					x
120			x		
140			x		
150					x
160				x	
180			x		
200	x				
220			x		
250				x	
260			x		
300			x		

After the analysis a complex model was created, see App. G. Its validation is presented in Table 6.8. The average error was 4%, maximum 16% and only 4 red cells. This is the best surrogate model we managed to construct.

Table 6.8. Complex model validation

№	Chord		$\beta$	$\varphi$ [deg]	Fact	Surrogate model	
	$b_o$ [mm]	$t_o$ [mm]			$C$ [kNm/rad]	$C$ [kNm/rad]	Error [%]
1	100	8	0.8000	79	1838	1735	5.6
2	100	6	0.4000	42	115	122	6.2
3	100	10	0.4000	80	349	348	0.4
4	100	8	0.5000	89	300	285	5.0
5	110	5	0.3636	34	71	72	1.4
6	110	6	0.3636	55	76	75	1.2
7	110	6	0.3636	50	82	81	0.9
8	110	5	0.8182	88	746	748	0.3
9	120	5.6	0.5833	80	170	171	0.8
10	120	7.1	0.7500	83	1098	1111	1.2
11	120	8.8	0.8333	42	6030	6726	11.6

12	120	7.1	0.5000	39	399	387	3.0
13	140	7.1	0.3571	90	106	113	6.5
14	140	6	0.7857	89	977	1017	4.1
15	140	7.1	0.5000	40	393	400	1.7
16	140	6	0.5000	30	349	366	4.8
17	150	7.1	0.5333	47	405	400	1.2
18	150	7.1	0.8000	89	1643	1783	8.5
19	150	6	0.4000	71	84	77	8.0
20	150	7.1	0.2667	39	104	105	0.9
21	160	8.8	0.7500	86	1946	2102	8.0
22	160	10	0.3125	76	244	243	0.3
23	160	8.8	0.5000	85	416	438	5.3
24	160	8.8	0.4375	81	303	321	6.0
25	180	10	0.3889	59	405	391	3.4
26	180	12.5	0.6667	33	8504	9029	6.2
27	180	10	0.5000	40	1085	1096	1.1
28	180	10	0.6111	60	1415	1470	3.9
29	200	8.8	0.2500	69	130	129	1.0
30	200	12.5	0.4000	62	855	811	5.1
31	200	8	0.3000	57	138	131	4.8
32	200	7.1	0.6000	66	448	518	15.5
33	220	8.8	0.5455	71	569	547	3.9
34	220	12.5	0.4545	58	1195	1247	4.4
35	220	10	0.4091	37	703	819	16.4
36	220	8	0.7273	62	1757	1974	12.4
37	250	12.5	0.7200	60	6397	6163	3.7
38	250	10	0.6000	90	1073	1086	1.2
39	250	12.5	0.6000	87	2199	2170	1.3
40	250	8.8	0.2800	72	151	151	0.2
41	260	10	0.8462	79	8820	8802	0.2
42	260	12.5	0.5769	67	2135	2115	0.9
43	260	12.5	0.3077	73	498	522	4.8
44	260	12.5	0.6923	51	6208	6222	0.2
45	300	12.5	0.8333	33	39163	40996	4.7
46	300	12.5	0.4667	56	1290	1396	8.2
47	300	12.5	0.8333	85	14946	14908	0.3
48	300	12.5	0.6000	86	2247	2338	4.1

## 6.7. Alternative methods

We also tried the alternative approaches for constructing the surrogate model.

First a linear regression model (Tiainen et al., 2012) using existing Matlab tools was tried. It was found that the results were not satisfying. Therefore, the model was restricted to consider only the nearest sampling space to every validation point. Present the validation points as:

$$x^* = [b_0^* \quad t_0^* \quad b^* \quad j^*]$$

The nearest points were chosen to meet the following conditions:

$$\begin{array}{l} \uparrow |b_0^* - b_{0i}| < 30 \\ \uparrow |b_0 - b_i| < 0.08 \\ \uparrow |j_0 - j_i| < 30 \end{array}$$

Then the chosen points were sorted by their normalized distances from the validation point:

$$dist_i = \sqrt{\sum_{k=1}^4 \frac{(x_k - x_k^*)^2}{\max x_k - \min x_k}}, \text{ where } x_1, x_2, x_3, x_4 \text{ relate to } b_0, t_0, \beta \text{ and } \varphi \text{ respectively.}$$

Then 6 nearest points were taken to form the local linear model. Exploiting this procedure we managed to construct a model with the following results:  $R^2=0.9552$ , average error 21% and maximum error 115%.

We tried also an approach using Matlab toolbox called Polyfitn. Developed by John R. D'Errico, it constructs a polynomial regression model using traditional linear least squares techniques. The code and suggestions for implementing this toolbox are given in App. I. Using this toolbox we managed to construct a model with the following results:  $R^2=0.9552$ , average error 37% and maximum error 454%.

We could not be satisfied with none of these methods and had to refuse both.

## 7. Fillet welds study

### 7.1. Effect of fillet welds

In our previous research we investigated the rotational stiffness of tubular joints considering only butt welds. This assumption simplifies FE analysis and surrogate modeling and allows not taking into account the influence of steel grade on rotational stiffness. However, fillet welds, used in practice instead of butt ones, can increase the stiffness of the joints. This increase might be considerable for joints made of tubes with little sections (100-120 mm) for which the weld size is comparative to the size of the section. More to the point, it was shown before that full strength weld size depends on the steel grade (Table 2.1). So, for fillet welds material properties cannot be neglected. It can be seen in Table 2.1 that the full strength weld size for e.g. S500 and S700 are about the same, so in this study the weld size effect was considered only for steel grades S355 and S700.

For calculation of rotational stiffness of tubular joints with fillet welds we proposed the following idea:

1. Replace an original joint with fillet welds by a joint with butt welds. The effect of welding should be implemented by replacing the original brace width  $b_1$  by the equivalent brace width  $b_{eq}$ .
2. Calculate the rotational stiffness using the constructed surrogate model for joints with butt welds using  $b_{eq}$  for fillet welded joints.

Obviously,  $b_{eq}$  lies in the interval:

$$b_1 < b_{eq} < b_1 + 2\sqrt{2}a \quad (7.1)$$

where  $a$  is weld size. So, for calculating  $b_{eq}$  we suggested the following formula:

$$b_{eq} = b_1 + 2\sqrt{2}a \times k_{fw} \quad (7.2)$$

where

- $a$  is weld size, see Fig. 7.1;
- $k_{fw}$  is a correlation coefficient.

This idea is illustrated in Fig. 7.1.

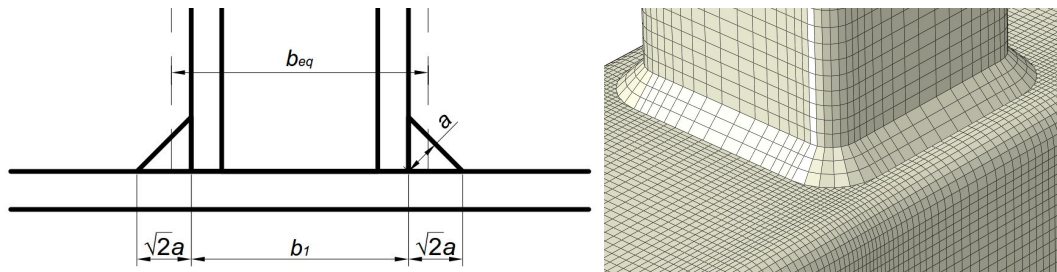


Figure 7.1. Equivalent brace width,  $b_{eq}$ , and FEA model with weld.

The object of this study was to determine the correlation coefficients  $k_{fw}$ .

## 7.2. Exact correlation coefficients

For calculation the values of correlation coefficient a number of cases were chosen covering the whole range of our interest. Then we used the following algorithm:

- Calculate rotational stiffness for joints with fillet welds using FEM.
- Calculate rotational stiffness for joints with butt welds for equivalent brace width using FEM. Equivalent brace width was first determined randomly and then refined through iterations. Detailed procedure for two cases is given in Table 7.1.
- Calculate correlation coefficients.

Table 7.1. Correlation coefficients calculation

№	Chord		Brace		$\varphi$ [deg]	Steel	C [kNm/rad]	Weld	$k_{fw}$
	$b_o$ [mm]	$t_o$ [mm]	$b_1$ [mm]	$t_1$ [mm]					
1	100	4	40	4	90		37.5	fillet	-
2	100	4	53.01	4	90		45.2	butt	1.00
3	100	4	50.41	4	90	S355	39.4	butt	0.80
4	100	4	49.11	4	90		36.5	butt	0.70
5	100	4	49.63	4	90		37.5	butt	<b>0.74</b>
6	120	4	80	4	90		299.1	fillet	-
7	120	4	93.07	4	90	S700	291.9	butt	0.70
8	120	4	91.20	4	90		249.8	butt	0.60
9	120	4	93.44	4	90		301.1	butt	<b>0.72</b>

After calculating the correlation coefficients, we also calculated the values of rotational stiffness ( $C_{SM}$ ) using the equivalent widths and the existing surrogate model for butt welds. All the results are presented in Table 7.2.

Table 7.2. Correlation coefficients and stiffness from surrogate model

№	Chord		Brace		$\varphi$ [deg]	Steel	$C_{FEM}$ [kNm/rad]	$k_{fw}$	$C_{SM}$ [kNm/rad]	Error [%]
	$b_o$ [mm]	$t_o$ [mm]	$b_1$ [mm]	$t_1$ [mm]						
1	100	4	40	4	90	S355	37.5	<b>0.74</b>	31.3	16.6
2	100	7.1	40	4	90	S355	186.7	<b>0.60</b>	168.6	9.7
3	110	4	80	4	90	S355	367.5	<b>0.63</b>	384.7	4.7
4	300	12.5	80	5	90	S355	458.0	<b>0.57</b>	500.7	9.3
5	300	12.5	200	7.1	90	S355	5026.2	<b>0.57</b>	5176.0	3.0
6	150	6	40	4	90	S355	55.9	<b>0.70</b>	60.0	7.4
7	150	12.5	40	4	90	S355	465.2	<b>0.43</b>	482.0	3.6
8	150	6	110	4	90	S355	913.0	<b>0.51</b>	951.9	4.3
9	250	8.8	70	4	90	S355	171.4	<b>0.70</b>	177.8	3.7
10	250	12.5	70	4	90	S355	477.6	<b>0.51</b>	489.5	2.5
11	250	8.8	180	7.1	90	S355	3079.4	<b>0.62</b>	3198.1	3.9
12	100	4	40	4	90	S700	48.5	<b>0.76</b>	42.3	12.8
13	100	7.1	40	4	90	S700	238.8	<b>0.65</b>	213.2	10.7
14	120	4	80	4	90	S700	299.1	<b>0.72</b>	234.7	21.5
15	200	7.1	50	4	90	S700	92.3	<b>0.79</b>	81.1	12.1
16	200	12.5	50	4	90	S700	472.4	<b>0.60</b>	473.5	0.2
17	200	7.1	120	7.1	90	S700	951.2	<b>0.73</b>	1165.3	22.5
18	300	12.5	80	5	90	S700	503.4	<b>0.67</b>	575.2	14.3
19	300	12.5	180	7.1	90	S700	3740.9	<b>0.66</b>	3766.2	0.7
20	150	6	40	4	90	S700	65.0	<b>0.77</b>	72.5	11.5
21	150	12.5	40	4	90	S700	562.2	<b>0.57</b>	596.4	6.1
22	150	6	100	4	90	S700	664.8	<b>0.61</b>	706.3	6.2
23	250	8.8	70	4	90	S700	187.3	<b>0.74</b>	196.9	5.1

24	250	12.5	70	4	90	S700	519.4	<b>0.61</b>	545.6	5.0
25	250	8.8	160	7.1	90	S700	2059.2	<b>0.71</b>	2209.9	7.3
26	150	12.5	60	4	90	S355	936.1	<b>0.42</b>	1031.4	10.2
27	200	12.5	110	4	90	S355	2000.1	<b>0.46</b>	2016.9	0.8
28	250	12.5	150	7.1	90	S355	3197.8	<b>0.58</b>	3046.2	4.7
29	150	7.1	40	4	90	S355	91.0	<b>0.65</b>	99.8	9.6
30	150	7.1	100	4	90	S355	848.2	<b>0.50</b>	828.5	2.3
31	100	7.1	50	4	90	S355	320.5	<b>0.58</b>	296.3	7.5
32	200	7.1	50	4	90	S355	81.6	<b>0.70</b>	75.4	7.6
33	200	7.1	50	4	60	S355	90.8	<b>0.64</b>	82.4	9.3
34	200	7.1	50	4	30	S355	156.7	<b>0.58</b>	132.6	15.4
35	200	12.5	50	4	90	S355	412.9	<b>0.43</b>	415.3	0.6
36	200	12.5	50	4	60	S355	454.7	<b>0.36</b>	454.6	0.0
37	200	12.5	50	4	30	S355	858.2	<b>0.34</b>	860.3	0.2
38	200	7.1	140	7.1	90	S355	1548.5	<b>0.64</b>	1695.9	9.5
39	200	7.1	140	7.1	60	S355	1973.2	<b>0.63</b>	2155.6	9.2
40	200	7.1	140	7.1	30	S355	5518.9	<b>0.69</b>	5838.4	5.8
									<b>Avg.</b>	<b>7.4</b>
									<b>Max.</b>	<b>22.5</b>

The average error arisen when using surrogate model instead of FEM is 7.4%, maximum is 22.5%.

### 7.3. Correlation coefficients analysis

Here we explored how the correlation coefficients depend on the parameters of joints (Figs. 7.2-7.16). The figures are based on the data from Table 7.2.

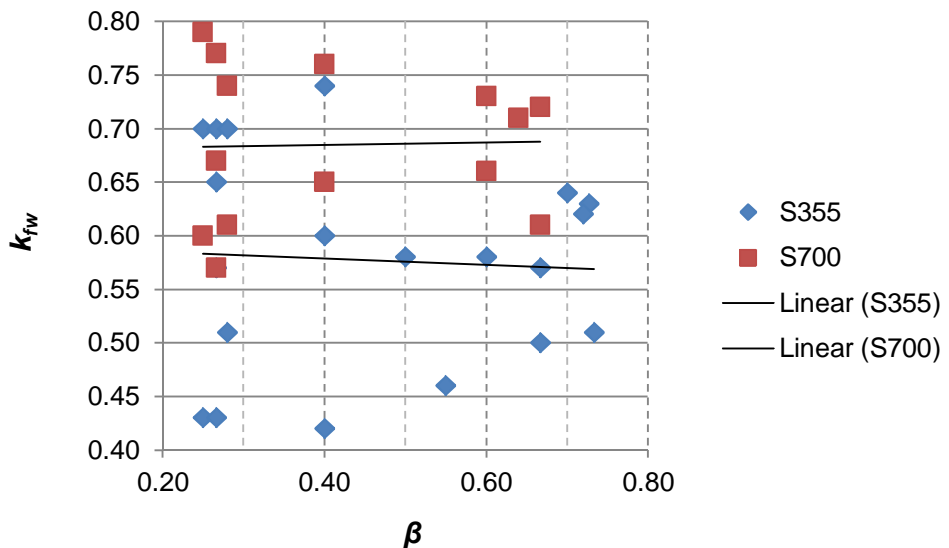


Figure 7.2.  $k_{FW}$ - $\beta$  response: S355 and S700.

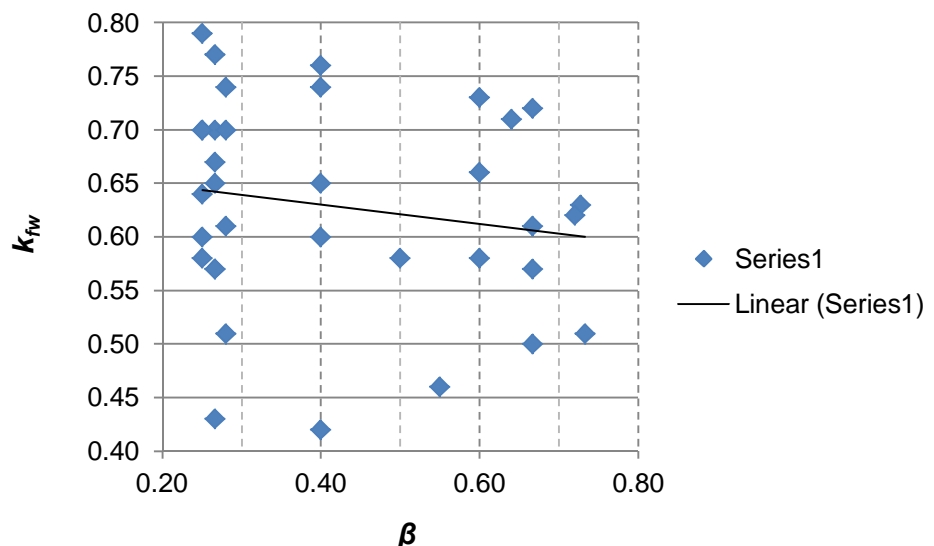


Figure 7.3.  $k_{fw}$ - $\beta$  response: all cases.

As can be seen, correlation coefficients do not depend on  $\beta$ .

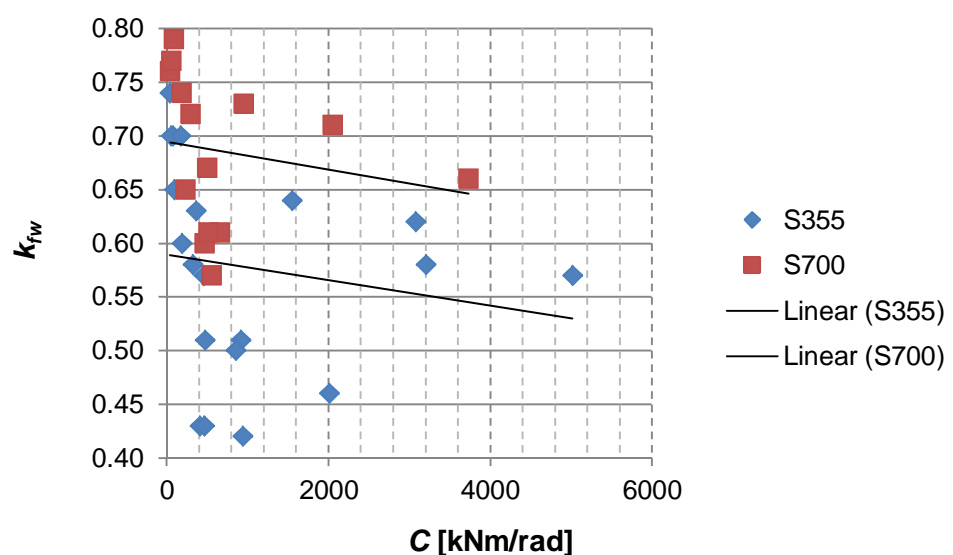


Figure 7.4.  $k_{fw}$ - $C$  response: S355 and S700.

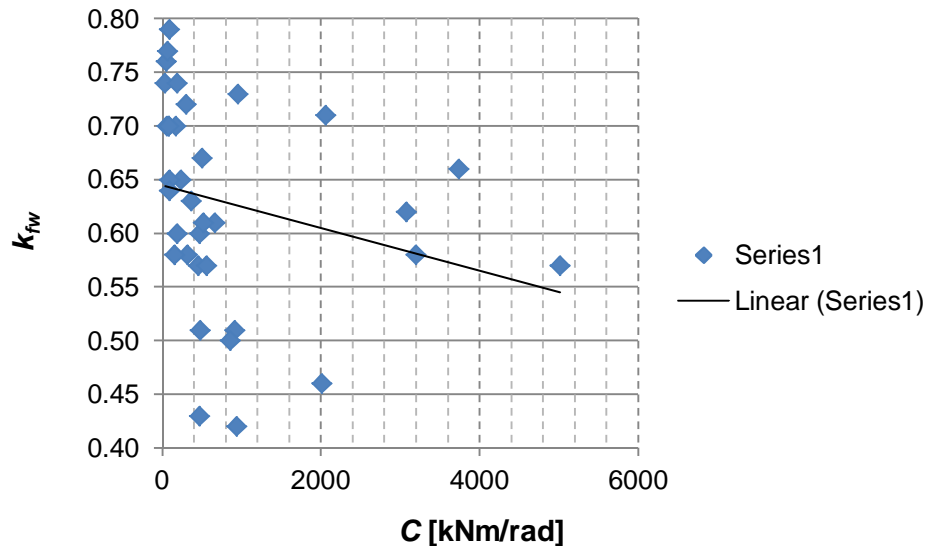


Figure 7.5.  $k_{fw}$ - $C$  response: all cases.

As can be seen, for higher values of rotational stiffness, correlation coefficients are slightly lower.

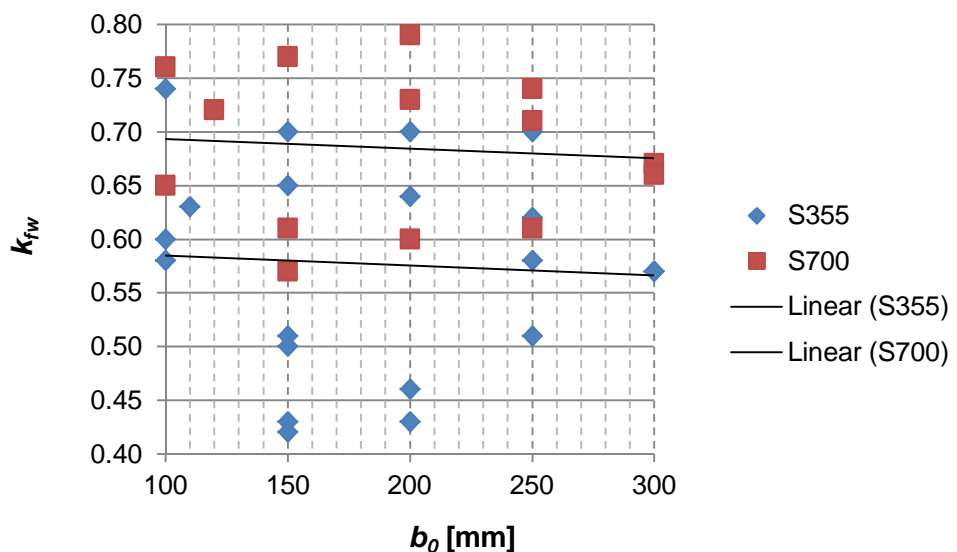


Figure 7.6.  $k_{fw}$ - $b_0$  response: S355 and S700.

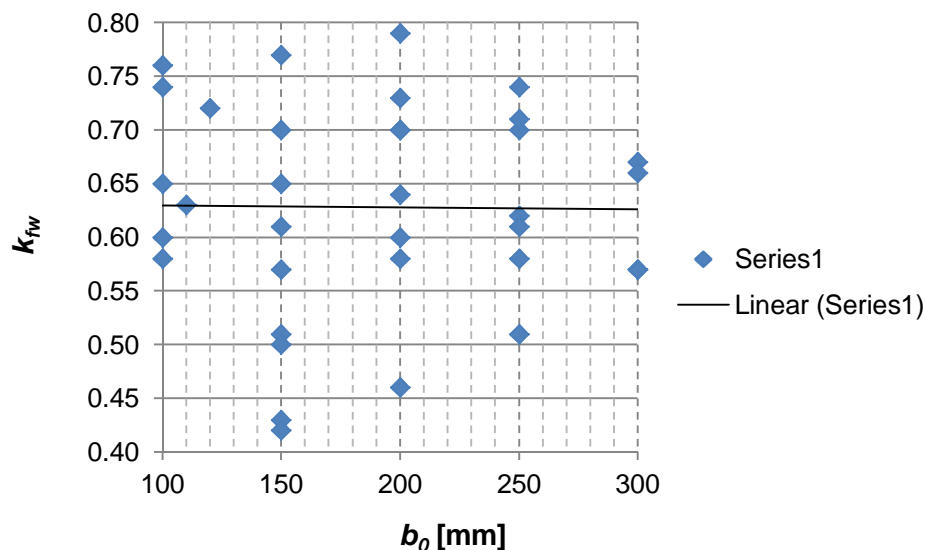


Figure 7.7.  $k_{fw}$ - $b_0$  response: all cases.

As can be seen,  $b_0$  does not affect correlation coefficients.

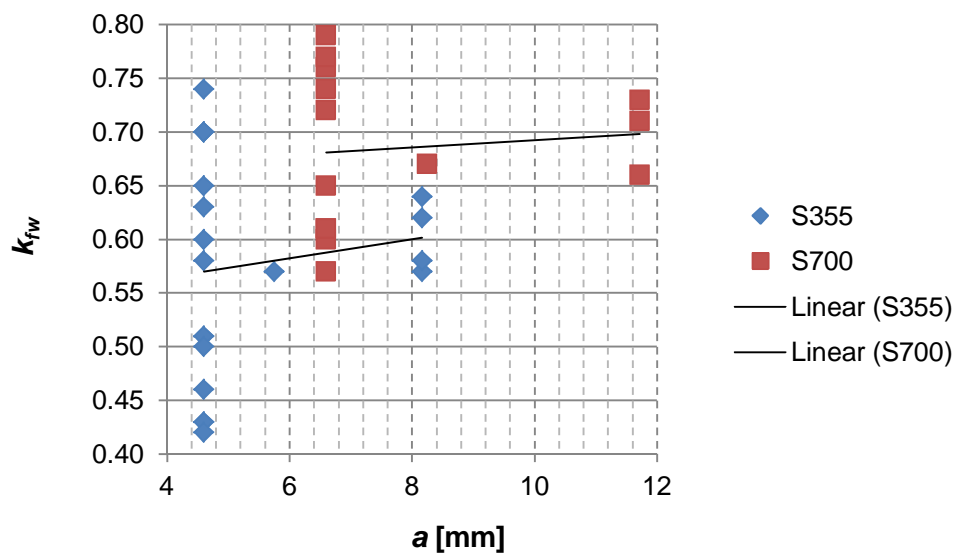


Figure 7.8.  $k_{fw}$ - $a$  response: S355 and S700.

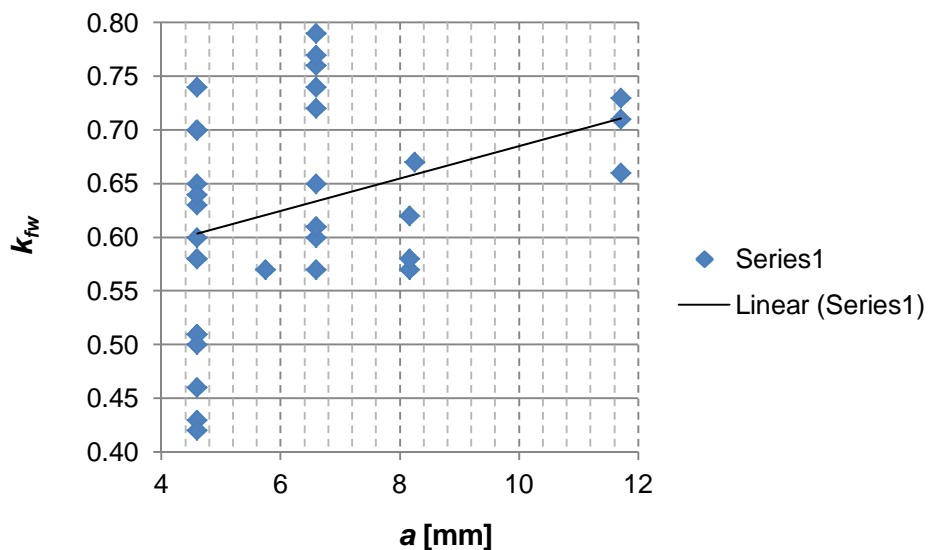


Figure 7.9.  $k_{fw}$ - $a$  response: all cases.

As can be seen, welding size does not affect correlation coefficients.

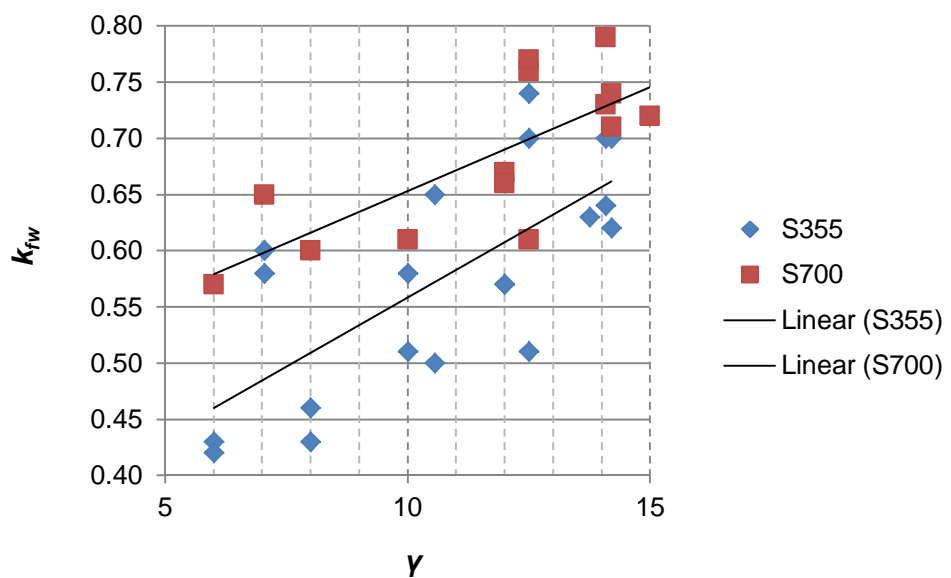


Figure 7.10.  $k_{fw}$ - $\gamma$  response: S355 and S700.

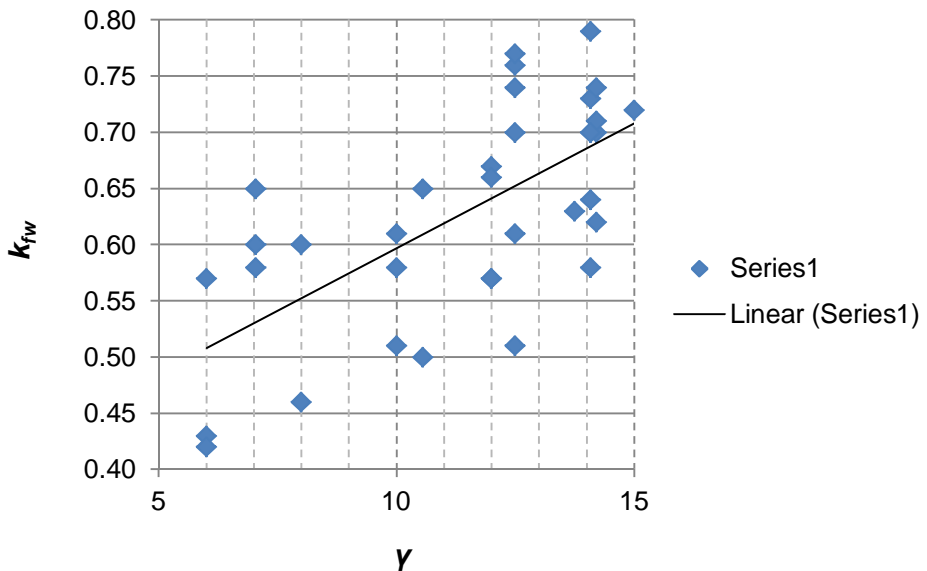


Figure 7.11.  $k_{fw}$ - $\gamma$  response: all cases.

As can be seen, correlation coefficients depend significantly on  $\gamma$ : with  $\gamma$  rising,  $k_{fw}$  increases as well.

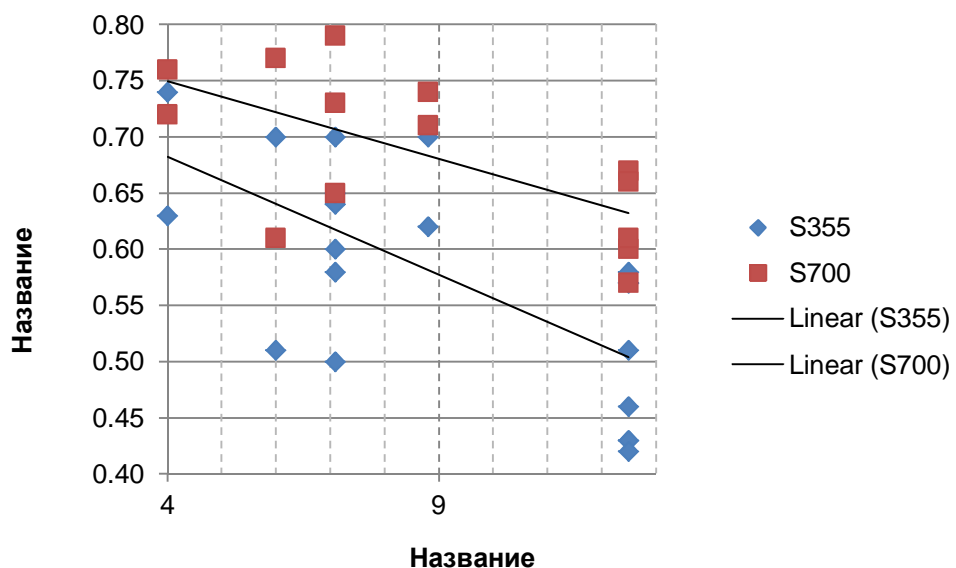


Figure 7.12.  $k_{fw}$ - $t_0$  response: S355 and S700.

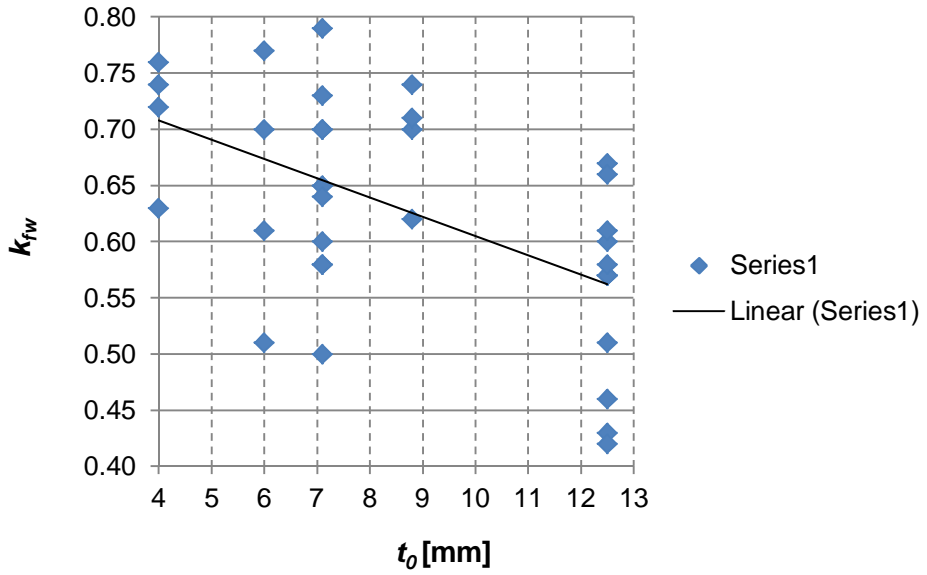


Figure 7.13.  $k_{fw}$ - $t_0$  response: all cases.

As can be seen, with  $t_0$  growing,  $k_{fw}$  declines. This agrees with  $k_{fw}$ - $\gamma$  responses.

Figs. 7.14-7.15 show how the correlation coefficients depend on  $t = \frac{t_1}{t_0}$ .

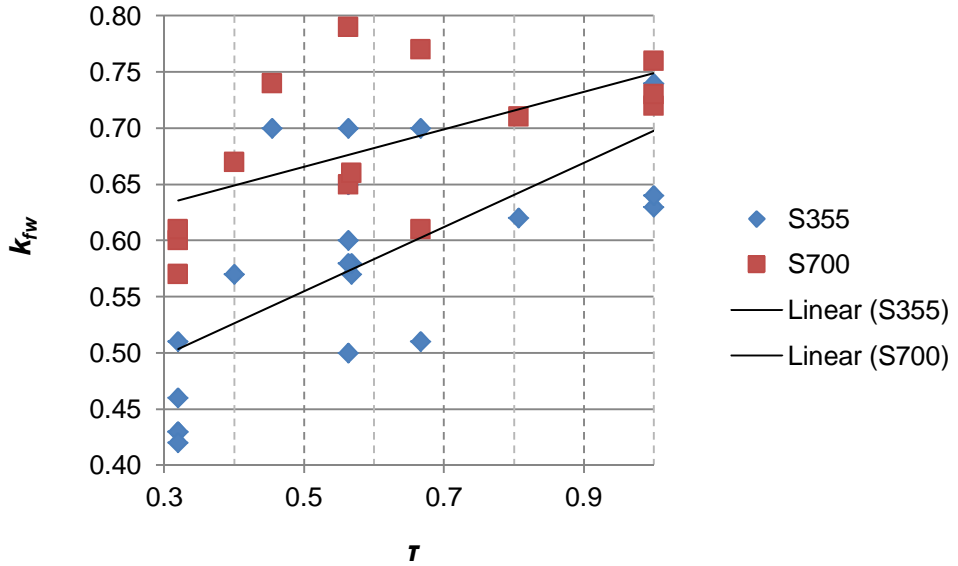


Figure 7.14.  $k_{fw}$ - $\tau$  response: S355 and S700.

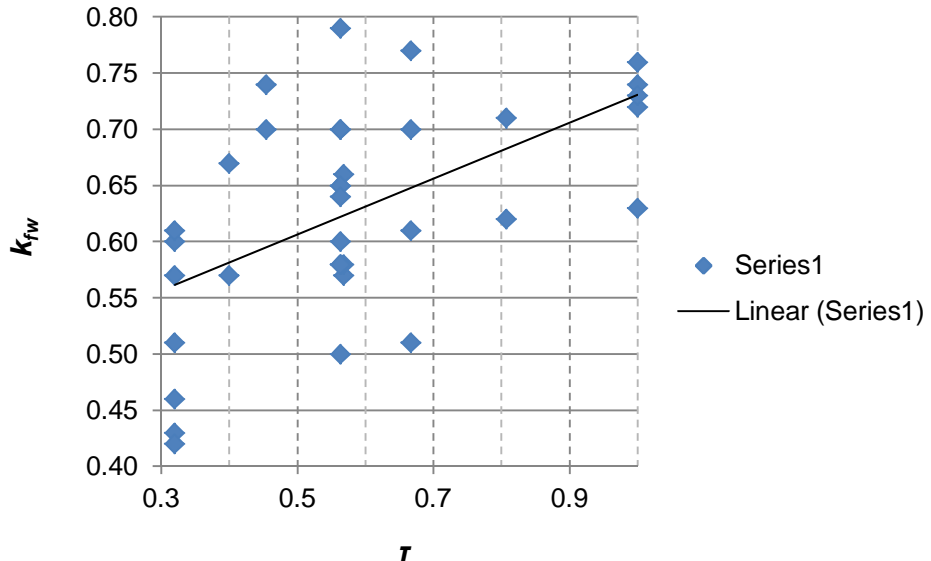


Figure 7.15.  $k_{fw}$ - $\tau$  response: all cases.

As can be seen, for high values of  $\tau$  higher values of  $k_{fw}$  are observed.

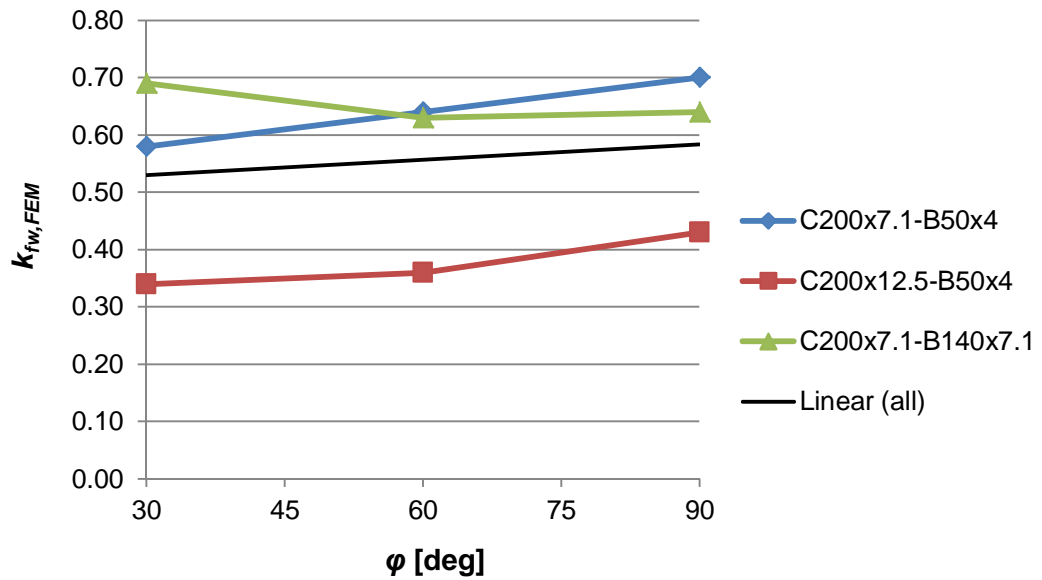


Figure 7.16.  $k_{fw}$ - $\phi$  response.

As can be seen, the effect of angle is rather weak.

#### 7.4. Butt welds vs. fillet welds

To determine the qualitative and quantitative picture of the welds impact on rotational stiffness we provided a comparative analysis for joints with butt and fillet welds for S355 and S700 steel grades. For convenience, absolute and relative stiffnesses were calculated. The results are presented in Table 7.3.

Table 7.3. Butt vs. fillet welds

№	Chord		Brace		$\varphi$ [deg]	$\beta$	C [kNm/rad]			C / C <sub>butt</sub>		
	b <sub>0</sub> [mm]	t <sub>0</sub> [mm]	b <sub>1</sub> [mm]	t <sub>1</sub> [mm]			Butt	Fillet S355	Fillet S700	Butt	Fillet S355	Fillet S700
1	100	4	40	4	90	0.40	23	38	49	1.00	1.64	2.12
2	100	7.1	40	4	90	0.40	124	187	239	1.00	1.51	1.93
3	100	4	70	4	90	0.70	139	287	405	1.00	2.07	2.93
4	100	4	70	4	30	0.70	468	1027	1521	1.00	2.19	3.25
5	200	7.1	50	4	90	0.25	66	82	92	1.00	1.24	1.40
6	200	7.1	50	4	60	0.25	74	91	101*	1.00	1.23	1.37
7	200	7.1	50	4	30	0.25	123	157	172*	1.00	1.27	1.40
8	200	12.5	50	4	90	0.25	360	413	472	1.00	1.15	1.31
9	200	12.5	50	4	60	0.25	402	455	531*	1.00	1.13	1.32
10	200	12.5	50	4	30	0.25	750	858	997*	1.00	1.14	1.33
11	200	7.1	140	7.1	90	0.70	808	1548	2199	1.00	1.92	2.72
12	200	7.1	140	7.1	60	0.70	1048*	1973	2809*	1.00	1.88	2.68
13	200	7.1	140	7.1	30	0.70	2792*	5519	7206*	1.00	1.98	2.58
14	300	12.5	80	5	90	0.26	401	458	503	1.00	1.14	1.26
15	300	12.5	200	7.1	90	0.66	3568	5026	6046	1.00	1.41	1.69
										Avg.	1.53	1.95

\* - no FEM results available, calculated by surrogate model.

Graphically it is shown in Fig. 7.17.

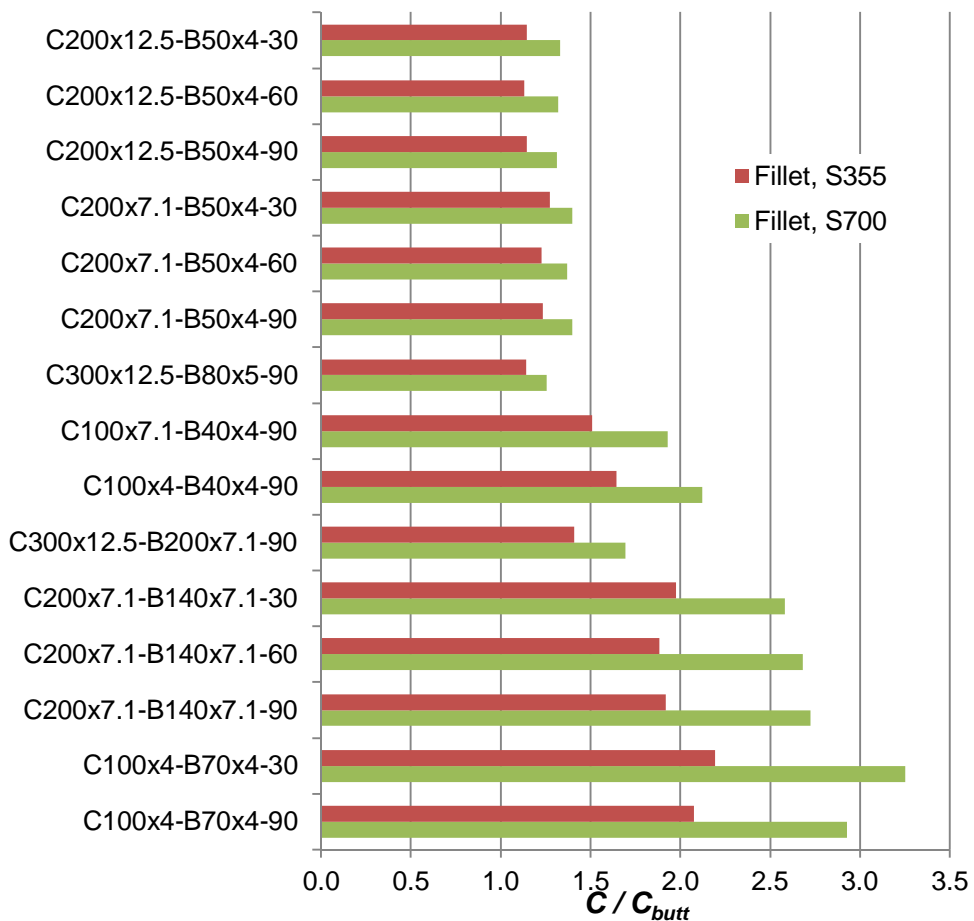


Figure 7.17. Butt vs. fillet welds.

Looking at the results of the analysis the following conclusions can be made:

- Fillet welds increase considerably rotational stiffness of welded joints, in mean 1.5 times for S355 steel grade and 2.0 times for S700.
- The influence of welding is more noticeable for small sections. This might be explained by the fact that for small sections the difference between weld size and chord width is not as high as for large sections.
- The increase of rotational stiffness is higher for sections with high  $\beta$ . This might be explained by a nonlinear C- $\beta$  curve on which a considerable growth for high values of  $\beta$  is observed.

## 7.5. Discrete correlation coefficients

To simplify the analysis we proposed to use instead of the exact values the discrete values of correlation factors: 0.6 for S355 steel and 0.7 for S700 steel. To evaluate the loss of accuracy of this assumption we analyzed the same series of points (numbering of points, see Table 7.2). Rotational stiffness for joints was calculated both by means of FEM and surrogate model in Table 7.4.

Table 7.4. Discrete correlation coefficients

№	$C_{FEM}$ [kNm/rad]	Exact values			Discrete values			
		$k_{fw}$	$C_{SM}$ [kNm/rad]	Error [%]	$k_{fw,dis}$	$C_{FEM}$ [kNm/rad]	Error [%]	$C_{SM}$ [kNm/rad]
1	37.5	<b>0.74</b>	31.3	16.6	<b>0.60</b>	34.0	9.4	28.6
2	186.7	<b>0.60</b>	168.6	9.7	<b>0.60</b>	185.9	0.4	168.6
3	367.5	<b>0.63</b>	384.7	4.7	<b>0.60</b>	351.1	4.5	373.8
4	458.0	<b>0.57</b>	500.7	9.3	<b>0.60</b>	461.8	0.8	506.2
5	5026.2	<b>0.57</b>	5176.0	3.0	<b>0.60</b>	5114.9	1.8	5283.1
6	55.9	<b>0.70</b>	60.0	7.4	<b>0.60</b>	53.7	3.9	57.0
7	465.2	<b>0.43</b>	482.0	3.6	<b>0.60</b>	506.5	8.9	529.5
8	913.0	<b>0.51</b>	951.9	4.3	<b>0.60</b>	986.5	8.0	1016.9
9	171.4	<b>0.70</b>	177.8	3.7	<b>0.60</b>	-	-	172.9
10	477.6	<b>0.51</b>	489.5	2.5	<b>0.60</b>	487.6	2.1	502.9
11	3079.4	<b>0.62</b>	3198.1	3.9	<b>0.60</b>	3018.2	2.0	3147.5
12	48.5	<b>0.76</b>	42.3	12.8	<b>0.70</b>	-	-	38.9
13	238.8	<b>0.65</b>	213.2	10.7	<b>0.70</b>	-	-	225.2
14	299.1	<b>0.72</b>	234.7	21.5	<b>0.70</b>	292.6	2.2	229.7
15	92.3	<b>0.79</b>	81.1	12.1	<b>0.70</b>	89.0	3.6	79.3
16	472.4	<b>0.60</b>	473.5	0.2	<b>0.70</b>	-	-	493.9
17	951.2	<b>0.73</b>	1165.3	22.5	<b>0.70</b>	922.9	3.0	1123.8
18	503.4	<b>0.67</b>	575.2	14.3	<b>0.70</b>	-	-	583.2
19	3740.9	<b>0.66</b>	3766.2	0.7	<b>0.70</b>	3857.1	3.1	3904.9
20	65.0	<b>0.77</b>	72.5	11.5	<b>0.70</b>	-	-	69.3
21	562.2	<b>0.57</b>	596.4	6.1	<b>0.70</b>	-	-	658.5
22	664.8	<b>0.61</b>	706.3	6.2	<b>0.70</b>	735.4	10.6	777.0
23	187.3	<b>0.74</b>	196.9	5.1	<b>0.70</b>	184.6	1.4	193.8
24	519.4	<b>0.61</b>	545.6	5.0	<b>0.70</b>	-	-	567.0
25	2059.2	<b>0.71</b>	2209.9	7.3	<b>0.70</b>	2038.0	1.0	2185.1
26	936.1	<b>0.42</b>	1031.4	10.2	<b>0.60</b>	1025.0	9.5	1111.2
27	2000.1	<b>0.46</b>	2016.9	0.8	<b>0.60</b>	2125.7	6.3	2137.1
28	3197.8	<b>0.58</b>	3046.2	4.7	<b>0.60</b>	3246.3	1.5	3084.6
29	91.0	<b>0.65</b>	99.8	9.6	<b>0.60</b>	88.9	2.3	97.3
30	848.2	<b>0.50</b>	828.5	2.3	<b>0.60</b>	917.5	8.2	891.3
31	320.5	<b>0.58</b>	296.3	7.5	<b>0.60</b>	326.7	2.0	301.2
32	81.6	<b>0.70</b>	75.4	7.6	<b>0.60</b>	-	-	74.1
33	90.8	<b>0.64</b>	82.4	9.3	<b>0.60</b>	89.6	1.3	81.9

34	156.7	<b>0.58</b>	132.6	15.4	<b>0.60</b>	158.0	0.8	133.0	15.1
35	412.9	<b>0.43</b>	415.3	0.6	<b>0.60</b>	436.9	5.8	437.8	6.0
36	454.7	<b>0.36</b>	454.6	0.0	<b>0.60</b>	491.9	8.2	491.4	8.1
37	858.2	<b>0.34</b>	860.3	0.2	<b>0.60</b>	951.0	10.8	952.4	11.0
38	1548.5	<b>0.64</b>	1695.9	9.5	<b>0.60</b>	1477.7	4.6	1643.2	6.1
39	1973.2	<b>0.63</b>	2155.6	9.2	<b>0.60</b>	1901.3	3.6	2105.6	6.7
40	5518.9	<b>0.69</b>	5838.4	5.8	<b>0.60</b>	4971.3	9.9	5434.9	1.5
		<b>Avg.</b>	<b>7.4</b>		<b>Avg.</b>	<b>4.6</b>	<b>Avg.</b>	<b>9.3</b>	
		<b>Max.</b>	<b>22.5</b>		<b>Max.</b>	<b>10.8</b>	<b>Max.</b>	<b>23.8</b>	

As can be seen from the Table, the average error arisen when using discrete values is 4.6%, while the maximum is 11%. The errors between exact and discrete values for surrogate modeling are about the same. Comparing the results of the study we could notice that surrogate modeling neglects the errors of the suggested assumption.

## 8. Axial forces study

### 8.1. Effect of axial forces

Axial forces, acting in braces of joints, have considerable influence as for moment resistance, as for rotational stiffness of joints. The effect is most noticeable for joints with high values of axial forces, close to yield strength.

For today Eurocode (EN 1993-1-8:2005) has the following formula for implementing the effect of axial force to moment resistance:

$$M_{ip,1,Rd} = k_n f_{y0} t_0^2 h_1 \frac{\alpha_1}{\epsilon_2 h} + \frac{2}{\sqrt{1 - b}} + \frac{h}{1 - b} \frac{\ddot{\phi}}{\phi} g_5 \quad (8.1)$$

The effect of axial force is implemented by the reduction factor  $k_n$ , calculated in accordance with the following formula:

$$k_{n,EC} = \begin{cases} 1.3 - \frac{0.4 \times n}{b} & \text{if } 1, \quad n < 0 \\ 1, & \text{if } n \geq 0 \end{cases} \quad (8.2)$$

where  $n$  is defined in as:

$$n = \frac{N_0}{A_0 \times f_{y0}} + \frac{M_0}{W_{el,0} \times f_{y0}} \quad (8.3)$$

In this study we did not consider the influence of moment, so:

$$n = \frac{N_0}{A_0 \times f_{y0}} \quad (8.4)$$

We proposed that the same approach might be applied also for rotational stiffness:

$$S_{j,ini,af} = k_n S_{j,ini} \quad (8.5)$$

where  $S_{j,ini,af}$  and  $S_{j,ini}$  are rotational stiffness of joint with and without axial forces respectively.

The goals of our study were to:

- determine the actual reduction factors  $k_n$  for a series of joints by means of FEM
- check the applicability of Eq. (8.2) for design of reduction factors  $k_n$ ;
- if the need arise, propose a new formula for design of reduction factors  $k_n$ .

### 8.2. Eurocode approach

14 joints were modeled with Abaqus with different  $b_0$ ,  $\beta$ ,  $\gamma$  and  $\varphi$ , so that they cover the whole range of our interest. Each joint was loaded by 14 different axial forces ( $n = -0.99, -0.98, -0.95, -0.80, -0.60, -0.4, -0.2, 0, 0.2, 0.4, 0.6, 0.8, 0.95, 0.99$ ), 196 cases in total. For every case the

reduction factor  $k_n$  was calculated. The results are presented in Table 8.1. In this Table only errors for joints with compressed braces are given.

Table 8.1. Reduction factors, Eurocode

№	Chord		Brace		$\varphi$ [deg]	$f_y$ [MPa]	$n$	$S_{j,ini}$ [kNm/rad]	$k_{n,EC}$	$S_{kn,EC}$ [kNm/rad]	Error [%]
	$b_o$ [mm]	$t_o$ [mm]	$b_1$ [mm]	$t_1$ [mm]							
1	100	4	40	4	90	355	-0.99	14.0	0.31	7.1	49
2	100	4	40	4	90	355	-0.95	16.4	0.35	8.0	51
3	100	4	40	4	90	355	-0.60	20.2	0.70	16.0	21
4	100	4	40	4	90	355	-0.40	21.1	0.90	20.6	3
5	100	4	40	4	90	355	-0.20	22.0	1.00	22.9	4
6	100	4	40	4	90	355	0.00	22.9	1.00	22.9	
7	100	4	40	4	90	355	0.20	23.7	1.00	22.9	
8	100	4	40	4	90	355	0.40	24.5	1.00	22.9	
9	100	4	40	4	90	355	0.60	25.3	1.00	22.9	
10	100	4	40	4	90	355	0.80	26.1	1.00	22.9	
11	100	4	40	4	90	355	0.95	24.6	1.00	22.9	
12	100	4	40	4	90	355	0.99	23.0	1.00	22.9	
13	100	4	80	4	90	355	-0.99	299.7	0.81	274.4	8
14	100	4	80	4	90	355	-0.95	307.7	0.83	281.3	9
15	100	4	80	4	90	355	-0.60	325.2	1.00	340.9	5
16	100	4	80	4	90	355	-0.40	328.9	1.00	340.9	4
17	100	4	80	4	90	355	-0.20	335.8	1.00	340.9	2
18	100	4	80	4	90	355	0.00	340.9	1.00	340.9	
19	100	4	80	4	90	355	0.20	345.9	1.00	340.9	
20	100	4	80	4	90	355	0.40	350.8	1.00	340.9	
21	100	4	80	4	90	355	0.60	355.6	1.00	340.9	
22	100	4	80	4	90	355	0.80	359.0	1.00	340.9	
23	100	4	80	4	90	355	0.95	355.7	1.00	340.9	
24	100	4	80	4	90	355	0.99	348.8	1.00	340.9	
25	100	10	40	4	90	355	-0.98	323.0	0.32	110.5	66
26	100	10	40	4	90	355	-0.95	331.3	0.35	120.8	64
27	100	10	40	4	90	355	-0.80	337.3	0.50	172.6	49
28	100	10	40	4	90	355	-0.60	339.3	0.70	241.6	29
29	100	10	40	4	90	355	-0.40	341.2	0.90	310.7	9
30	100	10	40	4	90	355	-0.20	343.2	1.00	345.2	1
31	100	10	40	4	90	355	0.00	345.2	1.00	345.2	
32	100	10	40	4	90	355	0.20	347.2	1.00	345.2	
33	100	10	40	4	90	355	0.40	349.2	1.00	345.2	
34	100	10	40	4	90	355	0.60	351.2	1.00	345.2	
35	100	10	40	4	90	355	0.80	353.2	1.00	345.2	
36	100	10	40	4	90	355	0.95	349.6	1.00	345.2	
37	100	10	40	4	90	355	0.99	327.8	1.00	345.2	
38	200	7.1	50	4	90	355	-0.98	45.0	0.00	0.0	100
39	200	7.1	50	4	90	355	-0.95	49.5	0.00	0.0	100
40	200	7.1	50	4	90	355	-0.80	53.4	0.02	1.3	98
41	200	7.1	50	4	90	355	-0.60	56.7	0.34	22.4	60
42	200	7.1	50	4	90	355	-0.40	59.9	0.66	43.6	27
43	200	7.1	50	4	90	355	-0.20	63.0	0.98	64.7	3
44	200	7.1	50	4	90	355	0.00	66.0	1.00	66.0	
45	200	7.1	50	4	90	355	0.20	69.0	1.00	66.0	
46	200	7.1	50	4	90	355	0.40	71.8	1.00	66.0	
47	200	7.1	50	4	90	355	0.60	74.7	1.00	66.0	
48	200	7.1	50	4	90	355	0.80	77.5	1.00	66.0	
49	200	7.1	50	4	90	355	0.95	77.8	1.00	66.0	

50	200	7.1	50	4	90	355	0.99	71.3	1.00	66.0	
51	200	7.1	140	7.1	90	355	-0.98	668.7	0.74	597.7	11
52	200	7.1	140	7.1	90	355	-0.95	680.5	0.76	611.5	10
53	200	7.1	140	7.1	90	355	-0.80	714.5	0.84	680.7	5
54	200	7.1	140	7.1	90	355	-0.60	740.6	0.96	773.1	4
55	200	7.1	140	7.1	90	355	-0.40	771.8	1.00	807.7	5
56	200	7.1	140	7.1	90	355	-0.20	786.1	1.00	807.7	3
57	200	7.1	140	7.1	90	355	0.00	807.7	1.00	807.7	
58	200	7.1	140	7.1	90	355	0.20	828.6	1.00	807.7	
59	200	7.1	140	7.1	90	355	0.40	849.1	1.00	807.7	
60	200	7.1	140	7.1	90	355	0.60	869.1	1.00	807.7	
61	200	7.1	140	7.1	90	355	0.80	885.6	1.00	807.7	
62	200	7.1	140	7.1	90	355	0.95	883.2	1.00	807.7	
63	200	7.1	140	7.1	90	355	0.99	872.7	1.00	807.7	
64	200	7.1	160	7.1	90	355	-0.98	1758.6	0.81	1632.8	7
65	200	7.1	160	7.1	90	355	-0.95	1780.9	0.83	1663.0	7
66	200	7.1	160	7.1	90	355	-0.80	1849.5	0.90	1814.2	2
67	200	7.1	160	7.1	90	355	-0.60	1898.5	1.00	2015.8	6
68	200	7.1	160	7.1	90	355	-0.40	1939.3	1.00	2015.8	4
69	200	7.1	160	7.1	90	355	-0.20	1978.4	1.00	2015.8	2
70	200	7.1	160	7.1	90	355	0.00	2015.8	1.00	2015.8	
71	200	7.1	160	7.1	90	355	0.20	2051.9	1.00	2015.8	
72	200	7.1	160	7.1	90	355	0.40	2086.8	1.00	2015.8	
73	200	7.1	160	7.1	90	355	0.60	2120.8	1.00	2015.8	
74	200	7.1	160	7.1	90	355	0.80	2147.5	1.00	2015.8	
75	200	7.1	160	7.1	90	355	0.95	2134.6	1.00	2015.8	
76	200	7.1	160	7.1	90	355	0.99	2109.0	1.00	2015.8	
77	200	12.5	50	4	90	355	-0.99	312.3	0.00	0.0	100
78	200	12.5	50	4	90	355	-0.98	324.7	0.00	0.0	100
79	200	12.5	50	4	90	355	-0.95	333.7	0.00	0.0	100
80	200	12.5	50	4	90	355	-0.80	341.8	0.02	7.2	98
81	200	12.5	50	4	90	355	-0.60	346.3	0.34	122.5	65
82	200	12.5	50	4	90	355	-0.40	351.0	0.66	237.7	32
83	200	12.5	50	4	90	355	-0.20	355.6	0.98	352.9	1
84	200	12.5	50	4	90	355	0.00	360.2	1.00	360.2	
85	200	12.5	50	4	90	355	0.20	364.6	1.00	360.2	
86	200	12.5	50	4	90	355	0.40	369.1	1.00	360.2	
87	200	12.5	50	4	90	355	0.60	373.6	1.00	360.2	
88	200	12.5	50	4	90	355	0.80	378.0	1.00	360.2	
89	200	12.5	50	4	90	355	0.95	376.0	1.00	360.2	
90	200	12.5	50	4	90	355	0.99	351.2	1.00	360.2	
91	300	12.5	80	5	90	355	-0.99	303.9	0.00	0.0	100
92	300	12.5	80	5	90	355	-0.98	317.9	0.00	0.0	100
93	300	12.5	80	5	90	355	-0.80	348.1	0.10	40.1	88
94	300	12.5	80	5	90	355	-0.60	361.7	0.40	160.3	56
95	300	12.5	80	5	90	355	-0.40	375.0	0.70	280.5	25
96	300	12.5	80	5	90	355	-0.20	387.9	1.00	400.8	3
97	300	12.5	80	5	90	355	0.00	400.8	1.00	400.8	
98	300	12.5	80	5	90	355	0.20	413.4	1.00	400.8	
99	300	12.5	80	5	90	355	0.40	425.8	1.00	400.8	
100	300	12.5	80	5	90	355	0.60	438.1	1.00	400.8	
101	300	12.5	80	5	90	355	0.80	450.3	1.00	400.8	
102	300	12.5	80	5	90	355	0.95	453.4	1.00	400.8	
103	300	12.5	80	5	90	355	0.99	426.2	1.00	400.8	
104	300	12.5	220	8.8	90	355	-0.99	5306.6	0.76	4608.9	13
105	300	12.5	220	8.8	90	355	-0.98	5346.0	0.77	4641.9	13
106	300	12.5	220	8.8	90	355	-0.60	5735.3	0.97	5898.9	3
107	300	12.5	220	8.8	90	355	-0.40	5849.5	1.00	6064.3	4

108	300	12.5	220	8.8	90	355	-0.20	5956.8	1.00	6064.3	2
109	300	12.5	220	8.8	90	355	0.00	6064.3	1.00	6064.3	
110	300	12.5	220	8.8	90	355	0.20	6169.5	1.00	6064.3	
111	300	12.5	220	8.8	90	355	0.40	6272.9	1.00	6064.3	
112	300	12.5	220	8.8	90	355	0.60	6374.2	1.00	6064.3	
113	300	12.5	220	8.8	90	355	0.80	6459.1	1.00	6064.3	
114	300	12.5	220	8.8	90	355	0.95	6447.1	1.00	6064.3	
115	300	12.5	220	8.8	90	355	0.99	6364.9	1.00	6064.3	
116	200	7.1	50	4	90	700	-0.80	38.6	0.02	1.3	97
117	200	7.1	50	4	90	700	-0.60	46.6	0.34	22.4	52
118	200	7.1	50	4	90	700	-0.40	53.6	0.66	43.6	19
119	200	7.1	50	4	90	700	-0.20	60.0	0.98	64.7	8
120	200	7.1	50	4	90	700	0.00	66.0	1.00	66.0	
121	200	7.1	50	4	90	700	0.20	71.8	1.00	66.0	
122	200	7.1	50	4	90	700	0.40	77.3	1.00	66.0	
123	200	7.1	50	4	90	700	0.60	82.7	1.00	66.0	
124	200	7.1	50	4	90	700	0.80	87.9	1.00	66.0	
125	200	7.1	50	4	90	700	0.95	90.0	1.00	66.0	
126	200	7.1	50	4	90	700	0.99	85.1	1.00	66.0	
127	200	7.1	160	7.1	90	700	-0.80	1640.5	0.90	1814.2	11
128	200	7.1	160	7.1	90	700	-0.60	1762.8	1.00	2015.8	14
129	200	7.1	160	7.1	90	700	-0.40	1857.8	1.00	2015.8	9
130	200	7.1	160	7.1	90	700	-0.20	1940.6	1.00	2015.8	4
131	200	7.1	160	7.1	90	700	0.00	2015.8	1.00	2015.8	
132	200	7.1	160	7.1	90	700	0.20	2085.8	1.00	2015.8	
133	200	7.1	160	7.1	90	700	0.40	2152.2	1.00	2015.8	
134	200	7.1	160	7.1	90	700	0.60	2215.7	1.00	2015.8	
135	200	7.1	160	7.1	90	700	0.80	2270.0	1.00	2015.8	
136	200	7.1	160	7.1	90	700	0.95	2276.9	1.00	2015.8	
137	200	7.1	160	7.1	90	700	0.99	2260.2	1.00	2015.8	
138	200	12.5	50	4	90	700	-0.99	296.9	0.00	0.0	100
139	200	12.5	50	4	90	700	-0.80	323.6	0.02	7.2	98
140	200	12.5	50	4	90	700	-0.40	342.1	0.66	237.7	31
141	200	12.5	50	4	90	700	-0.20	351.1	0.98	352.9	1
142	200	12.5	50	4	90	700	0.00	360.2	1.00	360.2	
143	200	12.5	50	4	90	700	0.20	369.0	1.00	360.2	
144	200	12.5	50	4	90	700	0.40	377.8	1.00	360.2	
145	200	12.5	50	4	90	700	0.60	386.5	1.00	360.2	
146	200	12.5	50	4	90	700	0.80	395.1	1.00	360.2	
147	200	12.5	50	4	90	700	0.95	396.0	1.00	360.2	
148	200	12.5	50	4	90	700	0.99	377.3	1.00	360.2	
149	200	7.1	160	7.1	60	355	-0.98	2277.0	0.81	2093.8	8
150	200	7.1	160	7.1	60	355	-0.95	2306.4	0.83	2132.6	8
151	200	7.1	160	7.1	60	355	-0.80	2379.9	0.90	2326.4	2
152	200	7.1	160	7.1	60	355	-0.60	2436.8	1.00	2584.9	6
153	200	7.1	160	7.1	60	355	-0.20	2537.7	1.00	2584.9	2
154	200	7.1	160	7.1	60	355	0.00	2584.9	1.00	2584.9	
155	200	7.1	160	7.1	60	355	0.20	2630.2	1.00	2584.9	
156	200	7.1	160	7.1	60	355	0.40	2674.0	1.00	2584.9	
157	200	7.1	160	7.1	60	355	0.60	2716.1	1.00	2584.9	
158	200	7.1	160	7.1	60	355	0.80	2742.9	1.00	2584.9	
159	200	7.1	160	7.1	60	355	0.95	2705.8	1.00	2584.9	
160	200	7.1	160	7.1	60	355	0.99	2656.9	1.00	2584.9	
161	200	7.1	160	7.1	30	355	-0.98	5886.0	0.81	5412.4	8
162	200	7.1	160	7.1	30	355	-0.95	6027.9	0.83	5512.6	9
163	200	7.1	160	7.1	30	355	-0.80	6101.4	0.90	6013.8	1
164	200	7.1	160	7.1	30	355	-0.60	6333.3	1.00	6682.0	6
165	200	7.1	160	7.1	30	355	-0.40	6439.3	1.00	6682.0	4

166	200	7.1	160	7.1	30	355	-0.20	6566.2	1.00	6682.0	2
167	200	7.1	160	7.1	30	355	0.00	6682.0	1.00	6682.0	
168	200	7.1	160	7.1	30	355	0.20	6789.1	1.00	6682.0	
169	200	7.1	160	7.1	30	355	0.40	6911.1	1.00	6682.0	
170	200	7.1	160	7.1	30	355	0.60	7047.4	1.00	6682.0	
171	200	7.1	160	7.1	30	355	0.80	7148.2	1.00	6682.0	
172	200	7.1	160	7.1	30	355	0.95	6854.2	1.00	6682.0	
173	200	7.1	160	7.1	30	355	0.99	6447.5	1.00	6682.0	
										Avg	30
										Max	100

As can be seen from the Table, Eurocode's approach works rather well for joints with tension providing reliable values for stiffness. At the same time, the errors for compressed joints are much higher, 30% in average and 100% maximum ( $k_n$  goes to 0 with small betas). In 8 of 14 cases Eurocode's formula predicted higher values than those of FEM. In 7 of 14 cases extremely low predicted values were observed.

### 8.3. New formula

We suggested a new formula for reduction factor of joints with compression:

$$k_{n,new} = \begin{cases} 1.1 - 0.5 \times n \times \frac{g}{20} \sqrt{\frac{f_y}{355} \times \frac{0.55}{b}} & \text{if } 1, \quad n < 0 \\ 1, \quad n \geq 0 \end{cases} \quad (8.6)$$

The values of rotational stiffness obtained with the use of the proposed formula are presented in Table 8.2. In this Table only errors for joints with compressed braces are given.

Table 8.2. Reduction factors, new formula

№	Chord		Brace		$\varphi$ [deg]	$f_y$ [MPa]	$n$	$S_{i,ini}$ [kNm/rad]	$k_{n,new}$	$S_{kn,new}$ [kNm/rad]	Error [%]
	$b_o$ [mm]	$t_o$ [mm]	$b_1$ [mm]	$t_1$ [mm]							
1	100	4	40	4	90	355	-0.99	14.0	0.74	17	21
2	100	4	40	4	90	355	-0.95	16.4	0.75	17	5
3	100	4	40	4	90	355	-0.60	20.2	0.88	20	1
4	100	4	40	4	90	355	-0.40	21.1	0.95	22	3
5	100	4	40	4	90	355	-0.20	22.0	1.00	23	4
6	100	4	40	4	90	355	0.00	22.9	1.00	23	
7	100	4	40	4	90	355	0.20	23.7	1.00	23	
8	100	4	40	4	90	355	0.40	24.5	1.00	23	
9	100	4	40	4	90	355	0.60	25.3	1.00	23	
10	100	4	40	4	90	355	0.80	26.1	1.00	23	
11	100	4	40	4	90	355	0.95	24.6	1.00	23	
12	100	4	40	4	90	355	0.99	23.0	1.00	23	
13	100	4	80	4	90	355	-0.99	299.7	0.84	288	4
14	100	4	80	4	90	355	-0.95	307.7	0.85	291	5
15	100	4	80	4	90	355	-0.60	325.2	0.94	322	1
16	100	4	80	4	90	355	-0.40	328.9	1.00	340	3
17	100	4	80	4	90	355	-0.20	335.8	1.00	341	2
18	100	4	80	4	90	355	0.00	340.9	1.00	341	
19	100	4	80	4	90	355	0.20	345.9	1.00	341	
20	100	4	80	4	90	355	0.40	350.8	1.00	341	
21	100	4	80	4	90	355	0.60	355.6	1.00	341	
22	100	4	80	4	90	355	0.80	359.0	1.00	341	

23	100	4	80	4	90	355	0.95	355.7	1.00	341	
24	100	4	80	4	90	355	0.99	348.8	1.00	341	
25	100	10	40	4	90	355	-0.98	323.0	0.96	330	2
26	100	10	40	4	90	355	-0.95	331.3	0.96	332	0
27	100	10	40	4	90	355	-0.80	337.3	0.98	339	1
28	100	10	40	4	90	355	-0.60	339.3	1.00	345	2
29	100	10	40	4	90	355	-0.40	341.2	1.00	345	1
30	100	10	40	4	90	355	-0.20	343.2	1.00	345	1
31	100	10	40	4	90	355	0.00	345.2	1.00	345	
32	100	10	40	4	90	355	0.20	347.2	1.00	345	
33	100	10	40	4	90	355	0.40	349.2	1.00	345	
34	100	10	40	4	90	355	0.60	351.2	1.00	345	
35	100	10	40	4	90	355	0.80	353.2	1.00	345	
36	100	10	40	4	90	355	0.95	349.6	1.00	345	
37	100	10	40	4	90	355	0.99	327.8	1.00	345	
38	200	7.1	50	4	90	355	-0.98	45.0	0.59	39	14
39	200	7.1	50	4	90	355	-0.95	49.5	0.60	40	20
40	200	7.1	50	4	90	355	-0.80	53.4	0.68	45	16
41	200	7.1	50	4	90	355	-0.60	56.7	0.79	52	8
42	200	7.1	50	4	90	355	-0.40	59.9	0.89	59	2
43	200	7.1	50	4	90	355	-0.20	63.0	1.00	66	4
44	200	7.1	50	4	90	355	0.00	66.0	1.00	66	
45	200	7.1	50	4	90	355	0.20	69.0	1.00	66	
46	200	7.1	50	4	90	355	0.40	71.8	1.00	66	
47	200	7.1	50	4	90	355	0.60	74.7	1.00	66	
48	200	7.1	50	4	90	355	0.80	77.5	1.00	66	
49	200	7.1	50	4	90	355	0.95	77.8	1.00	66	
50	200	7.1	50	4	90	355	0.99	71.3	1.00	66	
51	200	7.1	140	7.1	90	355	-0.98	668.7	0.79	641	4
52	200	7.1	140	7.1	90	355	-0.95	680.5	0.80	649	5
53	200	7.1	140	7.1	90	355	-0.80	714.5	0.85	687	4
54	200	7.1	140	7.1	90	355	-0.60	740.6	0.91	737	0
55	200	7.1	140	7.1	90	355	-0.40	771.8	0.98	788	2
56	200	7.1	140	7.1	90	355	-0.20	786.1	1.00	808	3
57	200	7.1	140	7.1	90	355	0.00	807.7	1.00	808	
58	200	7.1	140	7.1	90	355	0.20	828.6	1.00	808	
59	200	7.1	140	7.1	90	355	0.40	849.1	1.00	808	
60	200	7.1	140	7.1	90	355	0.60	869.1	1.00	808	
61	200	7.1	140	7.1	90	355	0.80	885.6	1.00	808	
62	200	7.1	140	7.1	90	355	0.95	883.2	1.00	808	
63	200	7.1	140	7.1	90	355	0.99	872.7	1.00	808	
64	200	7.1	160	7.1	90	355	-0.98	1758.6	0.81	1641	7
65	200	7.1	160	7.1	90	355	-0.95	1780.9	0.82	1658	7
66	200	7.1	160	7.1	90	355	-0.80	1849.5	0.87	1747	6
67	200	7.1	160	7.1	90	355	-0.60	1898.5	0.92	1864	2
68	200	7.1	160	7.1	90	355	-0.40	1939.3	0.98	1982	2
69	200	7.1	160	7.1	90	355	-0.20	1978.4	1.00	2016	2
70	200	7.1	160	7.1	90	355	0.00	2015.8	1.00	2016	
71	200	7.1	160	7.1	90	355	0.20	2051.9	1.00	2016	
72	200	7.1	160	7.1	90	355	0.40	2086.8	1.00	2016	
73	200	7.1	160	7.1	90	355	0.60	2120.8	1.00	2016	
74	200	7.1	160	7.1	90	355	0.80	2147.5	1.00	2016	
75	200	7.1	160	7.1	90	355	0.95	2134.6	1.00	2016	
76	200	7.1	160	7.1	90	355	0.99	2109.0	1.00	2016	
77	200	12.5	50	4	90	355	-0.99	312.3	0.81	290	7
78	200	12.5	50	4	90	355	-0.98	324.7	0.81	291	10
79	200	12.5	50	4	90	355	-0.95	333.7	0.82	295	12
80	200	12.5	50	4	90	355	-0.80	341.8	0.86	311	9

81	200	12.5	50	4	90	355	-0.60	346.3	0.92	332	4
82	200	12.5	50	4	90	355	-0.40	351.0	0.98	353	1
83	200	12.5	50	4	90	355	-0.20	355.6	1.00	360	1
84	200	12.5	50	4	90	355	0.00	360.2	1.00	360	
85	200	12.5	50	4	90	355	0.20	364.6	1.00	360	
86	200	12.5	50	4	90	355	0.40	369.1	1.00	360	
87	200	12.5	50	4	90	355	0.60	373.6	1.00	360	
88	200	12.5	50	4	90	355	0.80	378.0	1.00	360	
89	200	12.5	50	4	90	355	0.95	376.0	1.00	360	
90	200	12.5	50	4	90	355	0.99	351.2	1.00	360	
91	300	12.5	80	5	90	355	-0.99	303.9	0.67	270	11
92	300	12.5	80	5	90	355	-0.98	317.9	0.68	272	15
93	300	12.5	80	5	90	355	-0.80	348.1	0.76	303	13
94	300	12.5	80	5	90	355	-0.60	361.7	0.84	337	7
95	300	12.5	80	5	90	355	-0.40	375.0	0.93	372	1
96	300	12.5	80	5	90	355	-0.20	387.9	1.00	401	3
97	300	12.5	80	5	90	355	0.00	400.8	1.00	401	
98	300	12.5	80	5	90	355	0.20	413.4	1.00	401	
99	300	12.5	80	5	90	355	0.40	425.8	1.00	401	
100	300	12.5	80	5	90	355	0.60	438.1	1.00	401	
101	300	12.5	80	5	90	355	0.80	450.3	1.00	401	
102	300	12.5	80	5	90	355	0.95	453.4	1.00	401	
103	300	12.5	80	5	90	355	0.99	426.2	1.00	401	
104	300	12.5	220	8.8	90	355	-0.99	5306.6	0.84	5111	4
105	300	12.5	220	8.8	90	355	-0.98	5346.0	0.85	5127	4
106	300	12.5	220	8.8	90	355	-0.60	5735.3	0.94	5725	0
107	300	12.5	220	8.8	90	355	-0.40	5849.5	1.00	6040	3
108	300	12.5	220	8.8	90	355	-0.20	5956.8	1.00	6064	2
109	300	12.5	220	8.8	90	355	0.00	6064.3	1.00	6064	
110	300	12.5	220	8.8	90	355	0.20	6169.5	1.00	6064	
111	300	12.5	220	8.8	90	355	0.40	6272.9	1.00	6064	
112	300	12.5	220	8.8	90	355	0.60	6374.2	1.00	6064	
113	300	12.5	220	8.8	90	355	0.80	6459.1	1.00	6064	
114	300	12.5	220	8.8	90	355	0.95	6447.1	1.00	6064	
115	300	12.5	220	8.8	90	355	0.99	6364.9	1.00	6064	
116	200	7.1	50	4	90	700	-0.80	38.6	0.51	34	12
117	200	7.1	50	4	90	700	-0.60	46.6	0.66	44	6
118	200	7.1	50	4	90	700	-0.40	53.6	0.81	53	1
119	200	7.1	50	4	90	700	-0.20	60.0	0.95	63	5
120	200	7.1	50	4	90	700	0.00	66.0	1.00	66	
121	200	7.1	50	4	90	700	0.20	71.8	1.00	66	
122	200	7.1	50	4	90	700	0.40	77.3	1.00	66	
123	200	7.1	50	4	90	700	0.60	82.7	1.00	66	
124	200	7.1	50	4	90	700	0.80	87.9	1.00	66	
125	200	7.1	50	4	90	700	0.95	90.0	1.00	66	
126	200	7.1	50	4	90	700	0.99	85.1	1.00	66	
127	200	7.1	160	7.1	90	700	-0.80	1640.5	0.77	1556	5
128	200	7.1	160	7.1	90	700	-0.60	1762.8	0.85	1722	2
129	200	7.1	160	7.1	90	700	-0.40	1857.8	0.94	1887	2
130	200	7.1	160	7.1	90	700	-0.20	1940.6	1.00	2016	4
131	200	7.1	160	7.1	90	700	0.00	2015.8	1.00	2016	
132	200	7.1	160	7.1	90	700	0.20	2085.8	1.00	2016	
133	200	7.1	160	7.1	90	700	0.40	2152.2	1.00	2016	
134	200	7.1	160	7.1	90	700	0.60	2215.7	1.00	2016	
135	200	7.1	160	7.1	90	700	0.80	2270.0	1.00	2016	
136	200	7.1	160	7.1	90	700	0.95	2276.9	1.00	2016	
137	200	7.1	160	7.1	90	700	0.99	2260.2	1.00	2016	
138	200	12.5	50	4	90	700	-0.99	296.9	0.69	248	17

139	200	12.5	50	4	90	700	-0.80	323.6	0.77	276	15
140	200	12.5	50	4	90	700	-0.40	342.1	0.93	336	2
141	200	12.5	50	4	90	700	-0.20	351.1	1.00	360	3
142	200	12.5	50	4	90	700	0.00	360.2	1.00	360	
143	200	12.5	50	4	90	700	0.20	369.0	1.00	360	
144	200	12.5	50	4	90	700	0.40	377.8	1.00	360	
145	200	12.5	50	4	90	700	0.60	386.5	1.00	360	
146	200	12.5	50	4	90	700	0.80	395.1	1.00	360	
147	200	12.5	50	4	90	700	0.95	396.0	1.00	360	
148	200	12.5	50	4	90	700	0.99	377.3	1.00	360	
149	200	7.1	160	7.1	60	355	-0.98	2277.0	0.81	2104	8
150	200	7.1	160	7.1	60	355	-0.95	2306.4	0.82	2126	8
151	200	7.1	160	7.1	60	355	-0.80	2379.9	0.87	2240	6
152	200	7.1	160	7.1	60	355	-0.60	2436.8	0.92	2391	2
153	200	7.1	160	7.1	60	355	-0.20	2537.7	1.00	2585	2
154	200	7.1	160	7.1	60	355	0.00	2584.9	1.00	2585	
155	200	7.1	160	7.1	60	355	0.20	2630.2	1.00	2585	
156	200	7.1	160	7.1	60	355	0.40	2674.0	1.00	2585	
157	200	7.1	160	7.1	60	355	0.60	2716.1	1.00	2585	
158	200	7.1	160	7.1	60	355	0.80	2742.9	1.00	2585	
159	200	7.1	160	7.1	60	355	0.95	2705.8	1.00	2585	
160	200	7.1	160	7.1	60	355	0.99	2656.9	1.00	2585	
161	200	7.1	160	7.1	30	355	-0.98	5886.0	0.81	5438	8
162	200	7.1	160	7.1	30	355	-0.95	6027.9	0.82	5497	9
163	200	7.1	160	7.1	30	355	-0.80	6101.4	0.87	5790	5
164	200	7.1	160	7.1	30	355	-0.60	6333.3	0.92	6180	2
165	200	7.1	160	7.1	30	355	-0.40	6439.3	0.98	6570	2
166	200	7.1	160	7.1	30	355	-0.20	6566.2	1.00	6682	2
167	200	7.1	160	7.1	30	355	0.00	6682.0	1.00	6682	
168	200	7.1	160	7.1	30	355	0.20	6789.1	1.00	6682	
169	200	7.1	160	7.1	30	355	0.40	6911.1	1.00	6682	
170	200	7.1	160	7.1	30	355	0.60	7047.4	1.00	6682	
171	200	7.1	160	7.1	30	355	0.80	7148.2	1.00	6682	
172	200	7.1	160	7.1	30	355	0.95	6854.2	1.00	6682	
173	200	7.1	160	7.1	30	355	0.99	6447.5	1.00	6682	
										Avg	5
										Max	21

As can be seen from the Table, new formula gives much better results for joints with compressed brace (5% average error and 21% maximum). For joints with tension in brace we suggest using Eurocode's formula.

## 8.4. Figures

Figs. 8.1-8.14. illustrate reduction factors calculated by FEM, the Eurocode's formula and the new formula for all 14 cases.

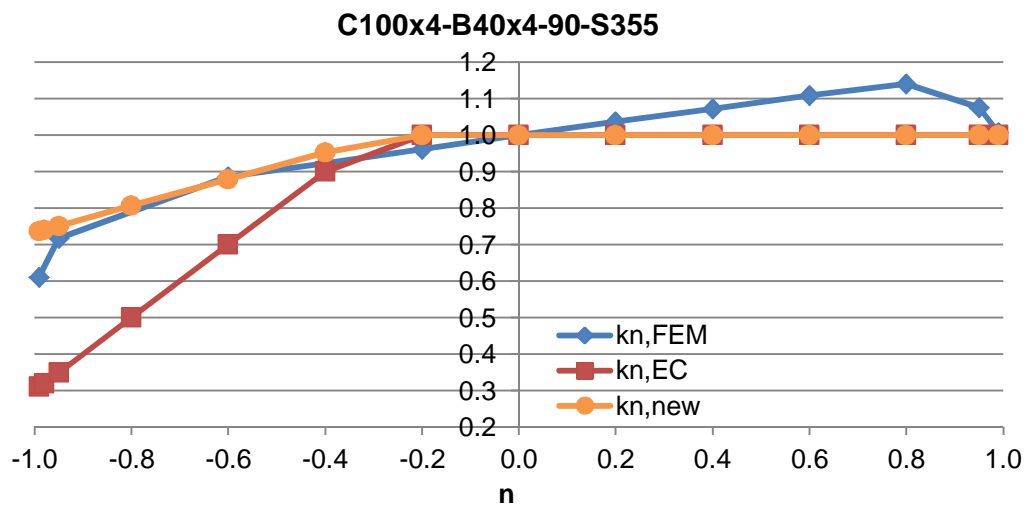


Figure 8.1. Reduction factor, case 1

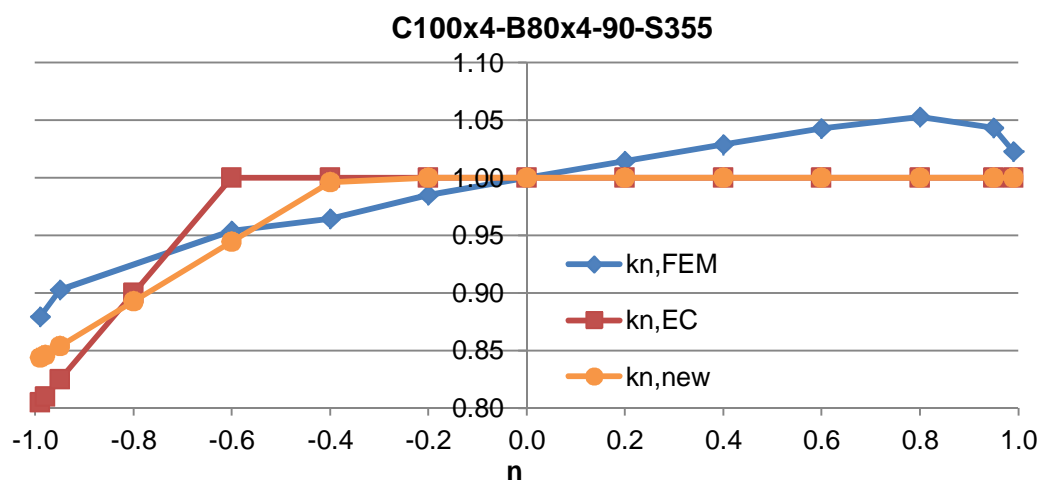


Figure 8.2. Reduction factor, case 2

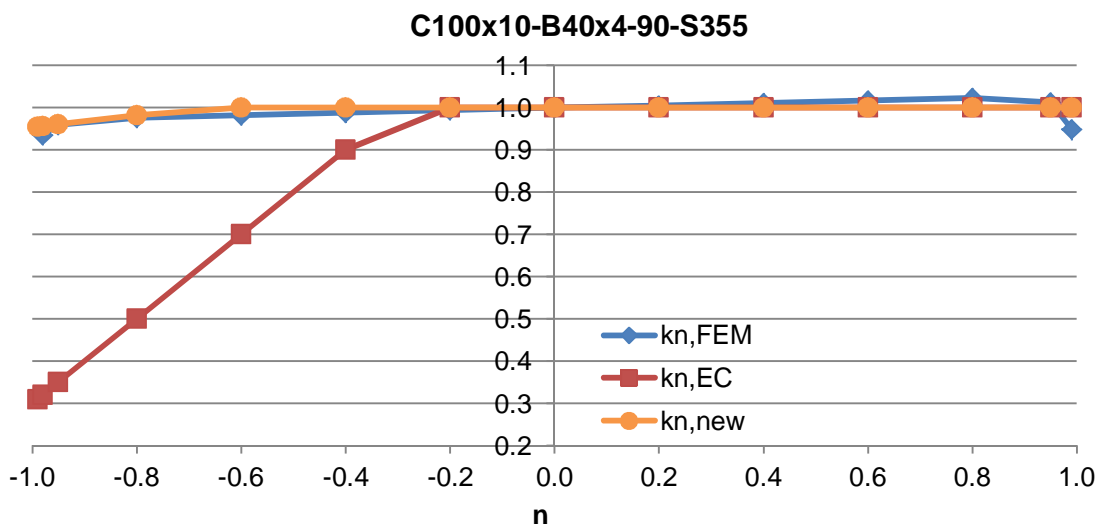


Figure 8.3. Reduction factor, case 3

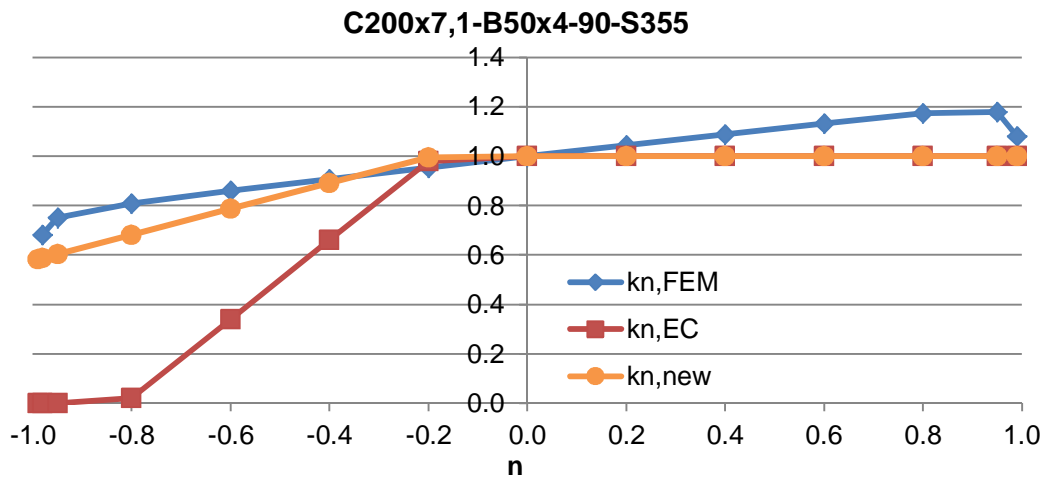


Figure 8.4. Reduction factor, case 4

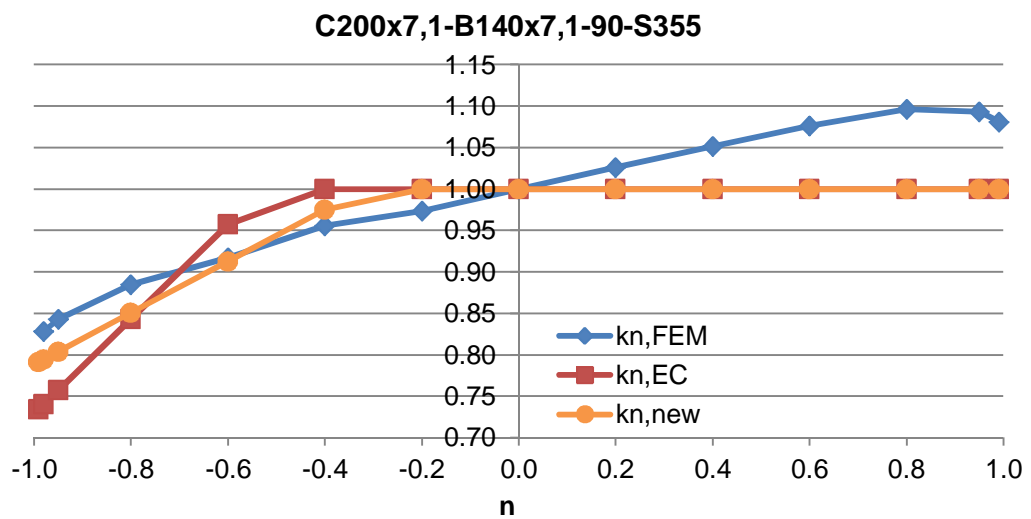


Figure 8.5. Reduction factor, case 5

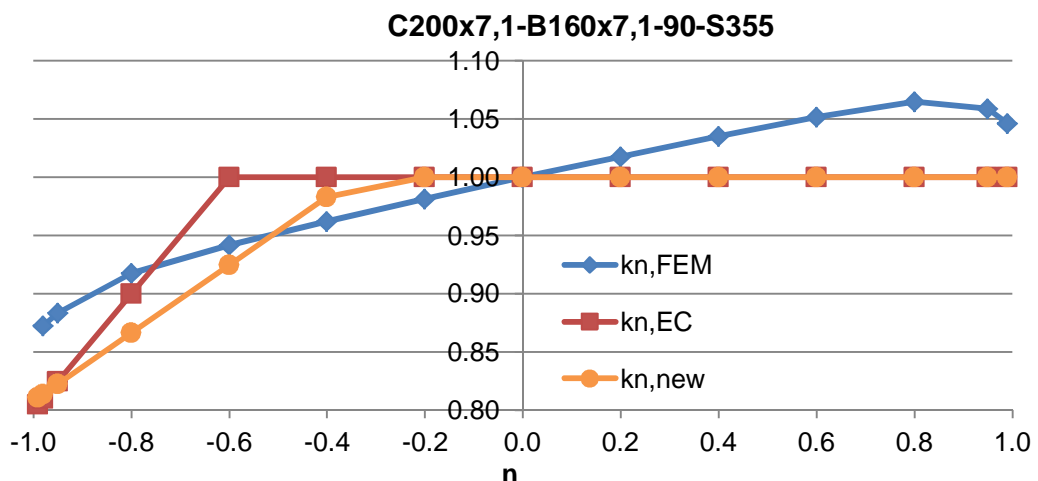


Figure 8.6. Reduction factor, case 6

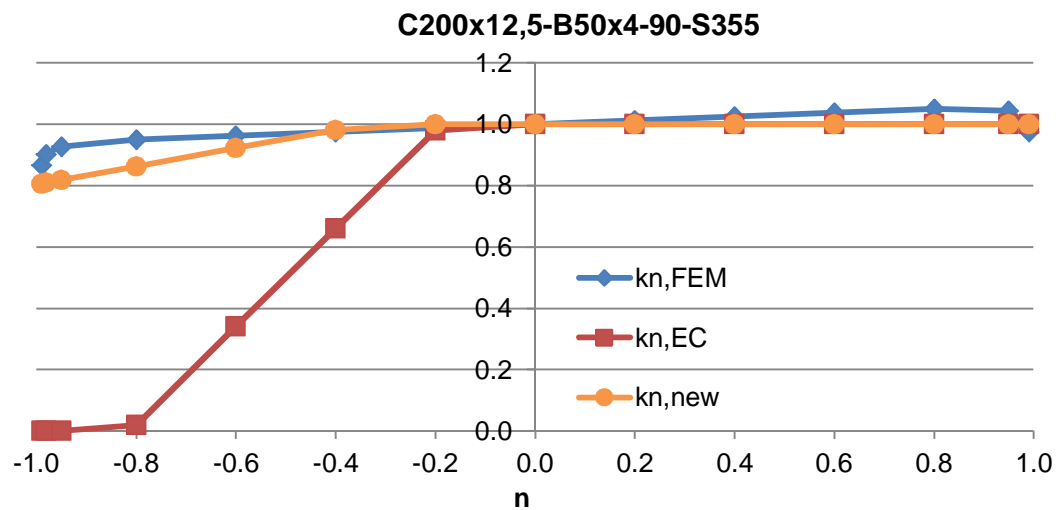


Figure 8.7. Reduction factor, case 7

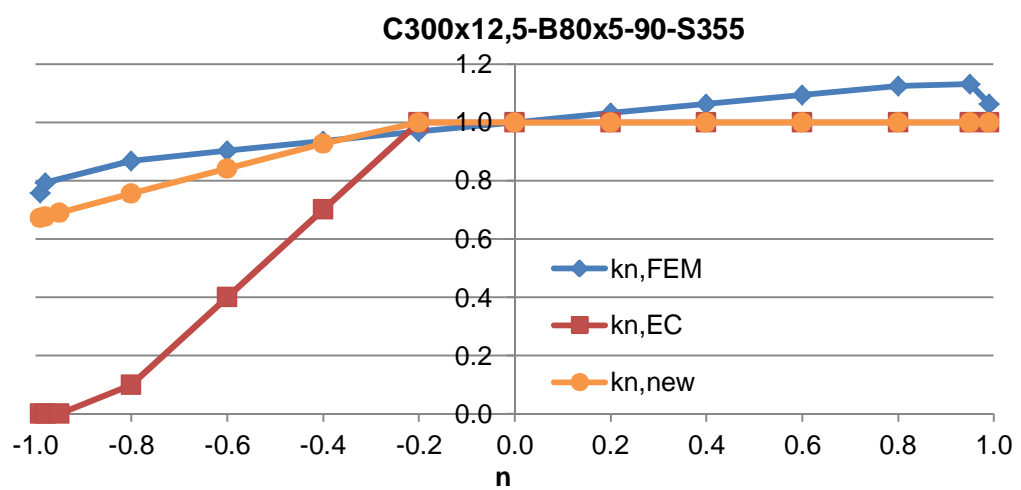


Figure 8.8. Reduction factor, case 8

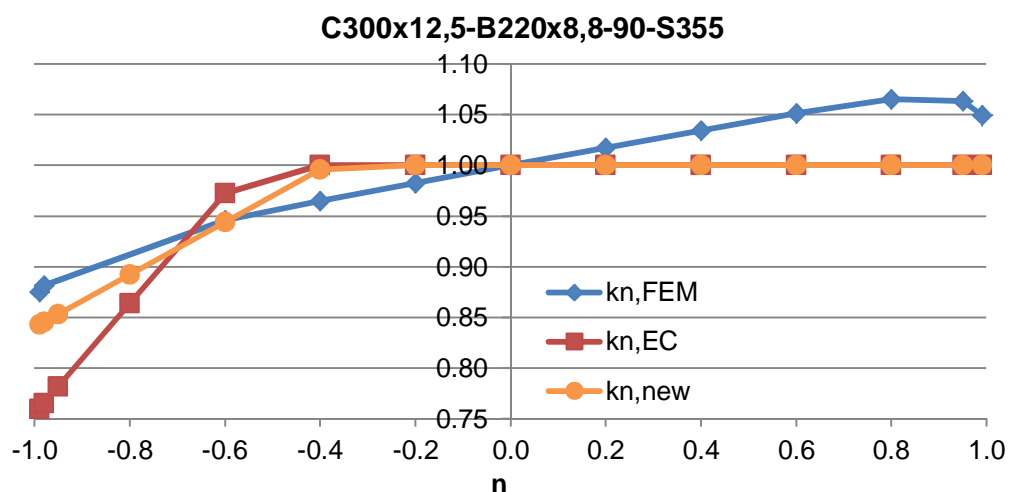


Figure 8.9. Reduction factor, case 9

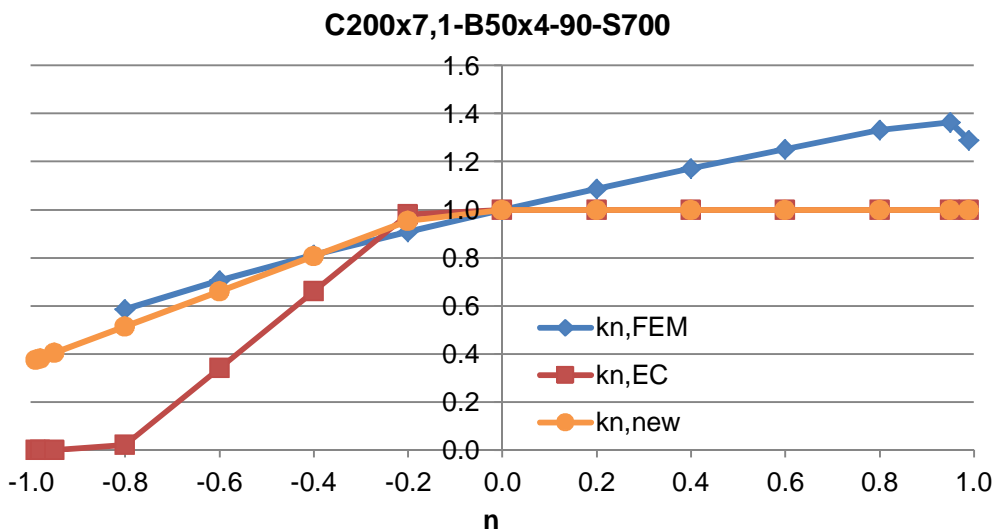


Figure 8.10. Reduction factor, case 10

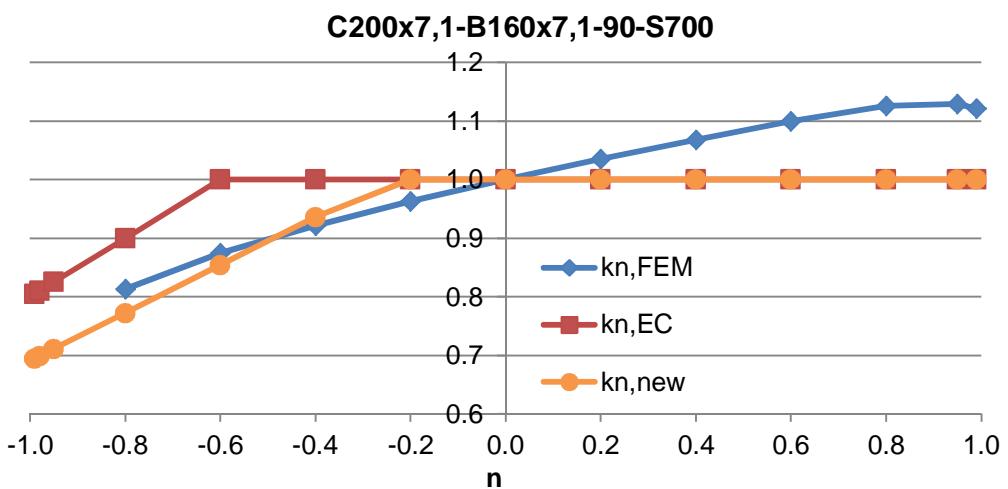


Figure 8.11. Reduction factor, case 11

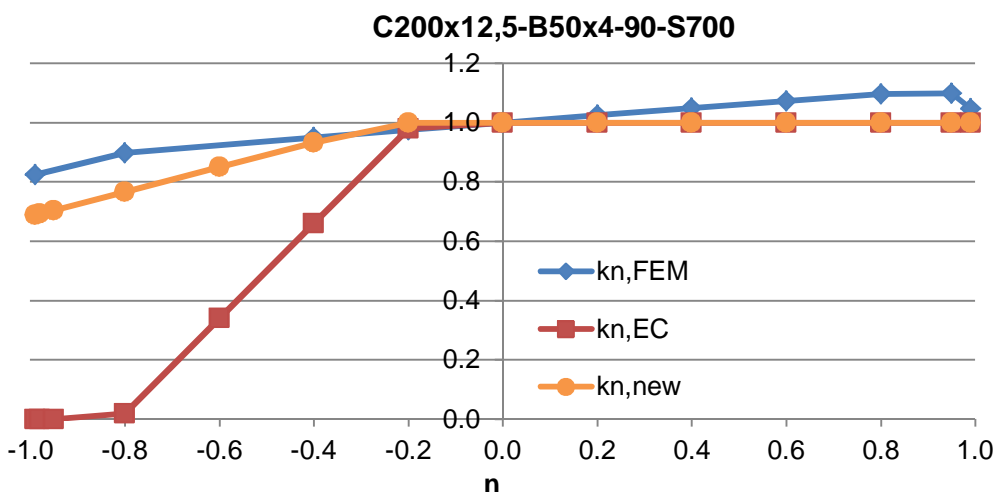


Figure 8.12. Reduction factor, case 12

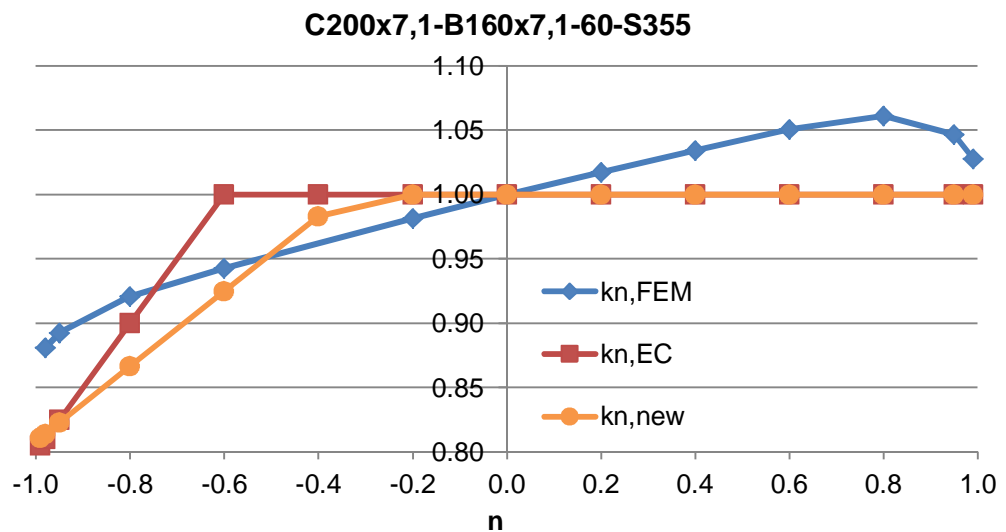


Figure 8.13. Reduction factor, case 13

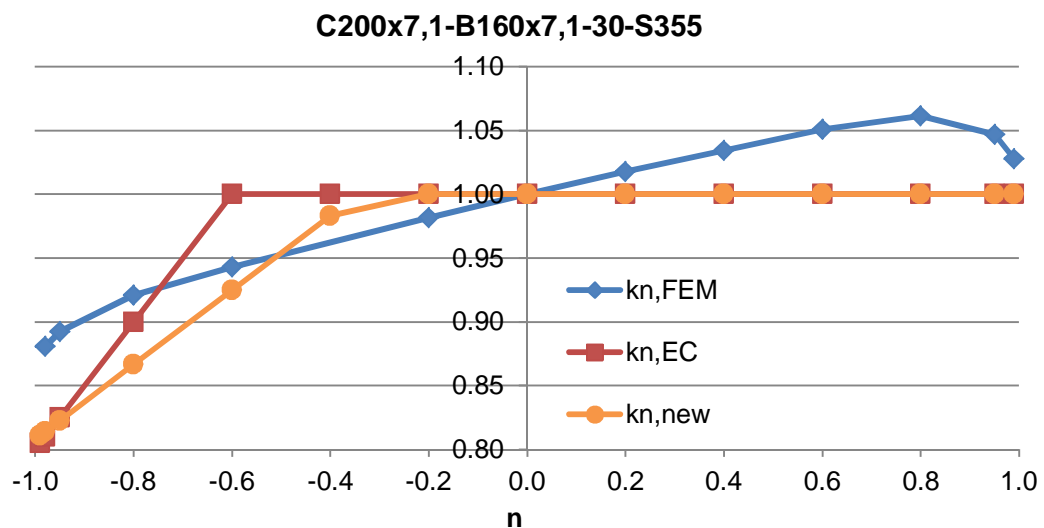


Figure 8.14. Reduction factor, case 14

As can be seen from the Figures, in most cases the new formula (orange line) provides more accurate values than the Eurocode's formula (red line).

## References

- Anderson, D., Hines, E.L., Arthur, S.J. and Eiap, E.L. (1997), "Application of artificial neural networks to the prediction of minor axis steel connections", *Computers & Structures*, Vol. 63, No. 4 (pp. 685–692).
- Bartz-Beielstein, T., Parsopoulos, K.E. and Vrahatis, M.N. (2004), "Design and Analysis of Optimization Algorithms Using Computational Statistics", *Applied Numerical Analysis & Computational Mathematics*, Vol. 1, No. 2 (pp. 413–433).
- Biles, W.E., Kleijnen, J.P.C. and Van Beers, W.C.M. V. (2007), "Kriging in constrained optimization of computer simulations", . In 14th European Concurrent Engineering Conference 2007, ECEC 2007 - 4th Future Business Technology Conference, FUBUTEC 2007. EUROSIS, pp. 44–48.
- Boel, H. (2010), *Buckling Length Factors of Hollow Section Members in Lattice Girders. Ms Sci thesis*. Eindhoven University of Technology, Eindhoven.
- Couckuyt, I., Dhaene, T. and Demeester, P. (2014), "ooDACE Toolbox: A Flexible Object-Oriented Kriging Implementation", *Journal of Machine Learning Research*, Vol. 15 (pp. 3183–3186).
- Díaz, C., Victoria, M., Querin, O.M. and Martí, P. (2012), "Optimum design of semi-rigid connections using metamodels", *Journal of Constructional Steel Research*, Vol. 78 (pp. 97–106).
- Dubourg, V., Sudret, B. and Bourinet, J.-M. (2011), "Reliability-based design optimization using kriging surrogates and subset simulation", *Structural and Multidisciplinary Optimization*, Vol. 44, No. 5 (pp. 673–69).
- European Committee for Standardisation, (CEN). (2006), *Cold formed welded structural hollow sections of non-alloy and fine grain steels. Part 2: Tolerances, dimensions and sectional properties (EN 10219-2:2006)*. Brussels.
- European Committee for Standardisation, (CEN). (2007), *Eurocode 3. Design of steel structures, Part 1-12: Additional rules for the extension of EN 1993 up to steel grades S 700 (EN 1993-1-12: 2007)*. Brussels, 2007.
- European Committee for Standardisation, (CEN). (2005), *Eurocode 3. Design of steel structures, Part 1-8: Design of joints (EN 1993-1-8:2005)*. Brussels, 2005.
- Fang, K.-T., Li, R. and Sudjianto, A. (2006), *Design and modeling for computer experiments*. Chapman & Hall/CRC.
- Gao, Y. and Wang, X. (2008), "An effective warpage optimization method in injection molding based on the Kriging model", *International Journal of Advanced Manufacturing Technology*, Vol. 37, No. 9-10 (pp. 953–960).

- Grotmann, D. and Sedlacek, G. (1998), *Rotational stiffness of welded RHS beam-to-column joints*. Cidect 5BB-8/98. RWTH-Aachen, Aachen.
- Guzelbey, I.H., Cevik, A. and Göğüş, M.T. (2006), "Prediction of rotation capacity of wide flange beams using neural networks", *Journal of Constructional Steel Research*, Vol. 62, No. 10 (pp. 950–961).
- Haakana, Ä. (2014), *In-Plane Buckling and Semi-Rigid Joints of Tubular High Strength Steel Trusses*. Ms Sci thesis. Tampere University of Technology, Tampere.
- Halonen, L. (2012), *Applying metamodels to parametric structural analysis*. M Sci thesis. Tampere University of Technology. 84 p., Tampere.
- Husain, A. and Kim, K.Y. (2008), "Shape optimization of micro-channel heat sink for micro-electronic cooling", *IEEE Transactions on Components and Packaging Technologies*, Vol. 31, No. 2 SPEC. ISS. (pp. 322–330).
- Jadid, M.N. and Fairbairn, D.R. (1996), "Neural-network applications in predicting moment-curvature parameters from experimental data", *Engineering Applications of Artificial Intelligence*, Vol. 9, No. 3 (pp. 309–319).
- Jin, R., Chen, W. and Simpson, T.W. (2001), "Comparative studies of metamodeling techniques under multiple modelling criteria", *Structural and Multidisciplinary Optimization*, Vol. 23, No. 1 (pp. 1–13).
- Jones, D.R., Schonlau, M. and Welch, W.J. (1998), "Efficient global optimization of expensive black-box functions", *Journal of Global optimization*, Vol. 13, No. 4 (pp. 455–492).
- Kim, J., Ghaboussi, J. and Elnashai, A.S. (2010), "Mechanical and informational modeling of steel beam-to-column connections", *Engineering Structures*, Vol. 32, No. 2 (pp. 449–458).
- Kleijnen, J.P.C. (2008), "Simulation experiments in practice: statistical design and regression analysis", *Journal of Simulation*, Vol. 2 (pp. 19–27).
- Kwon, H., Yi, S. and Choi, S. (2014), "Numerical investigation for erratic behavior of Kriging surrogate model", *Journal of Mechanical Science and Technology*, Vol. 28, No. 9 (pp. 3697–3707).
- Lee, T. and Jung, J. (2006), "Metamodel-based shape optimization of connecting rod considering fatigue life", *Key Engineering Materials*, Vol. 306-308 (pp. 211–216).
- De Lima, L.R.O., Vellasco, P.C.G. da S., De Andrade, S.A.L., Da Silva, J.G.S. and Vellasco, M.M.B.R. (2005), "Neural networks assessment of beam-to-column joints", *Journal of the Brazilian Society of Mechanical Sciences and Engineering*, Vol. 27, No. 3 (pp. 314–324).
- Lophaven, S.N., Søndergaard, J. and Nielsen, H.B. (2002), *DACE, A MATLAB Kriging Toolbox, Version 2.0, August 1*. Technical University of Denmark, Copenhagen.

- Marsden, A.L., Feinstein, J.A. and Taylor, C.A. (2008), "A computational framework for derivative-free optimization of cardiovascular geometries", *Computer Methods in Applied Mechanics and Engineering*, Vol. 197 (pp. 1890–1905).
- Marsden, A.L., Wang, M., Dennis Jr, J.E. and Moin, P. (2004), "Optimal aeroacoustic shape design using the surrogate management framework", *Optimization and Engineering*, Vol. 5, No. 2 (pp. 235–262).
- Matheron, G. (1963), "Principles of geostatistics", *Economic geology*, Vol. 58, No. 8 (pp. 1246–1266).
- McKay, M.D., Bechman, R.J. and Conover, W.J. (1979), "A Comparison of Three Methods for Selecting Values of Input Variables in the Analysis of Output From a Computer Code", *Technometrics*, Vol. 21, No. 2 (pp. 239–245).
- Montgomery, D.C. (2012), *Design and Analysis of Experiments*. John Wiley & Sons.
- Mukhopadhyay, T., Dey, T.K., Dey, S. and Chakrabarti, A. (2015), "Optimization of fiber reinforced polymer web core bridge deck – A hybrid approach", *Structural Engineering International*, Vol. 25, No. 2 (pp. 173–183).
- Müller, J. (2012), *Surrogate Model Algorithms for Computationally Expensive Black-Box Global Optimization Problems*. Tampere University of Technology. Publication 1092.
- Ongelin, P. and Valkonen, I. (2012), *Structural hollow sections. EN 1993 - Handbook 2012*. Rautaruukki Oyj.
- Pirmoz, A. and Gholizadeh, S. (2007), *Predicting of moment--rotation behavior of bolted connections using neural networks*. 3rd national congress on civil engineering.
- Queipo, N. V., Haftka, R.T., Shyy, W., Goel, T., Vaidyanathan, R. and Kevin Tucker, P. (2005), "Surrogate-based analysis and optimization", *Progress in Aerospace Sciences*, Vol. 41 (pp. 1–28).
- Roux, W.J., Stander, N. and Haftka, R.T. (1998), "Response surface approximations for structural optimization", *International Journal for Numerical Methods in Engineering*, Vol. 42, No. 3 (pp. 517–534).
- Sacks, J., Schiller, S.B. and Welch, W.J. (1989), "Designs for computer experiments", *Technometrics*, Vol. 31, No. 1 (pp. 41–47).
- Sacks, J., Welch, W.J., Mitchell, T.J. and Wynn, H.P. (1989), "Design and analysis of computer experiments", *Statistical science* (pp. 409–423).
- Salajegheh, E., Gholizadeh, S. and Pirmoz, A. (2008), "Self-organizing parallel back propagation neural networks for predicting the moment-rotation behavior of bolted connections", *Asian Journal of Civil Engineering*, Vol. 9, No. 6 (pp. 625–640).
- Snijder, H.H., Boel, H.D., Hoenderkamp, J.C.D. and Spoorenberg, R.C. (2011), "Buckling

length factors for welded lattice girders with hollow section braces and chords", *Proceedings of Eurosteel 2011* (pp. 1881–1886).

Stavroulakis, G.E., Avdelas, A.V., Abdalla, K.M. and Panagiotopoulos, P.D. (1997), "A neural network approach to the modelling, calculation and identification of semi-rigid connections in steel structures", *Journal of Constructional Steel Research*, Vol. 44, No. 1-2 (pp. 91–105).

Tiainen, T., Heinisuo, M., Jokinen, T. and Salminen, M. (2012), "Steel building optimization applying metamodel techniques", *Rakenteiden Mekaniikka (Journal of Structural Mechanics)*, Vol. 45, No. 3 (pp. 152–161).

Tuominen, N. and Björk, T. (2014), "Ultimate Capacity of Welded Joints Made of High Strength Steel CFRHS", *Proceedings of Eurosteel 2014* (pp. 83–84).

Ulaganathan, S., Couckuyt, I., Deschrijver, D., Laermans, E. and Dhaene, T. (2015), "A Matlab Toolbox for Kriging Metamodelling", *Procedia Computer Science*, Vol. 51 (pp. 2708–2713).

Yang, W., Feinstein, J. a. and Marsden, A.L. (2010), "Constrained optimization of an idealized Y-shaped baffle for the Fontan surgery at rest and exercise", *Computer Methods in Applied Mechanics and Engineering*, Vol. 199, No. 33-36 (pp. 2135–2149).

Yun, G.J., Ghaboussi, J. and Elnashai, A.S. (2008), "Self-learning simulation method for inverse nonlinear modeling of cyclic behavior of connections", *Computer Methods in Applied Mechanics and Engineering*, Vol. 197, No. 33-40 (pp. 2836–2857).

# Appendices

## Appendix A. Sample points I

Table A.1. Sample points I

№	Chord		Brace		$\varphi$ [deg]	C [kNm/rad]	
	$b_0$ [mm]	$t_0$ [mm]	$b_1$ [mm]	$t_1$ [mm]		Abaqus	Cidect
1	100	4	40	4	30	55	-
2	100	4	40	4	45	34	-
3	100	4	40	4	60	27	-
4	100	4	40	4	75	24	-
5	100	4	40	4	90	23	17
6	100	4	80	4	30	1135	-
7	100	4	80	4	45	626	-
8	100	4	80	4	60	442	-
9	100	4	80	4	75	367	-
10	100	4	80	4	90	343	246
11	100	5	60	4	30	386	-
12	100	5	60	4	45	217	-
13	100	5	60	4	60	159	-
14	100	5	60	4	75	135	-
15	100	5	60	4	90	127	115
16	110	4	50	4	30	81	-
17	110	4	50	4	45	48	-
18	110	4	50	4	60	37	-
19	110	4	50	4	75	32	-
20	110	4	50	4	90	31	-
21	110	6	60	4	30	450	-
22	110	6	60	4	45	258	-
23	110	6	60	4	60	193	-
24	110	6	60	4	75	166	-
25	110	6	60	4	90	158	-
26	120	5	40	4	30	70	-
27	120	5	40	4	45	46	-
28	120	5	40	4	60	37	-
29	120	5	40	4	75	34	-
30	120	5	40	4	90	33	-
31	120	5	80	4	30	678	-
32	120	5	80	4	45	372	-
33	120	5	80	4	60	267	-
34	120	5	80	4	75	224	-
35	120	5	80	4	90	211	-
36	120	5	100	5	30	2923	-
37	120	5	100	5	45	1633	-
38	120	5	100	5	60	1170	-
39	120	5	100	5	75	979	-
40	120	5	100	5	90	923	-
41	140	6	80	4	30	568	-
42	140	6	80	4	45	322	-
43	140	6	80	4	60	238	-
44	140	6	80	4	75	204	-
45	140	6	80	4	90	194	-
46	150	6	60	5	30	186	-

47	150	6	60	5	45	116	-
48	150	6	60	5	60	92	-
49	150	6	60	5	75	82	-
50	150	6	60	5	90	79	58
51	150	6	110	5	30	2053	-
52	150	6	110	5	45	1118	-
53	150	6	110	5	60	793	-
54	150	6	110	5	75	663	-
55	150	6	110	5	90	626	499
56	160	7.1	120	6	30	3900	-
57	160	7.1	120	6	45	2160	-
58	160	7.1	120	6	60	1556	-
59	160	7.1	120	6	75	1303	-
60	160	7.1	120	6	90	1230	-
61	180	8	140	6	30	7070	-
62	180	8	140	6	45	3926	-
63	180	8	140	6	60	2847	-
64	180	8	140	6	75	2397	-
65	180	8	140	6	90	2268	-
66	180	10	150	6	30	19802	-
67	180	10	150	6	45	10158	-
68	180	10	150	6	60	7423	-
69	180	10	150	6	75	6325	-
70	180	10	150	6	90	6012	-
71	200	8	150	6	30	5756	-
72	200	8	150	6	45	3182	-
73	200	8	150	6	60	2279	-
74	200	8	150	6	75	1905	-
75	200	8	150	6	90	1798	1346
76	200	10	120	5	30	3183	-
77	200	10	120	5	45	1789	-
78	200	10	120	5	60	1327	-
79	200	10	120	5	75	1126	-
80	200	10	120	5	90	1069	957
81	200	12.5	120	7.1	30	6352	-
82	200	12.5	120	7.1	45	3583	-
83	200	12.5	120	7.1	60	2681	-
84	200	12.5	120	7.1	75	2319	-
85	200	12.5	120	7.1	90	2216	1760
86	220	8	180	7.1	30	11157	-
87	220	8	180	7.1	45	6210	-
88	220	8	180	7.1	60	4415	-
89	220	8	180	7.1	75	3685	-
90	220	8	180	7.1	90	3474	-
91	250	10	160	6	30	4460	-
92	250	10	160	6	45	2501	-
93	250	10	160	6	60	1822	-
94	250	10	160	6	75	1545	-
95	250	10	160	6	90	1466	-
96	250	10	180	7.1	30	8234	-
97	250	10	180	7.1	45	4526	-
98	250	10	180	7.1	60	3264	-
99	250	10	180	7.1	75	2739	-
100	250	10	180	7.1	90	2590	-
101	260	10	200	8	30	13024	-

102	260	10	200	8	45	7210	-
103	260	10	200	8	60	5122	-
104	260	10	200	8	75	4297	-
105	260	10	200	8	90	4038	-
106	260	10	220	8	30	27392	-
107	260	10	220	8	45	15492	-
108	260	10	220	8	60	11246	-
109	260	10	220	8	75	9422	-
110	260	10	220	8	90	8897	-
111	300	12.5	110	6	30	1438	-
112	300	12.5	110	6	45	917	-
113	300	12.5	110	6	60	735	-
114	300	12.5	110	6	75	660	-
115	300	12.5	110	6	90	637	448
116	300	12.5	180	7.1	30	6501	-
117	300	12.5	180	7.1	45	3696	-
118	300	12.5	180	7.1	60	2748	-
119	300	12.5	180	7.1	75	2354	-
120	300	12.5	180	7.1	90	2244	1910
121	300	12.5	220	10	30	18747	-
122	300	12.5	220	10	45	10439	-
123	300	12.5	220	10	60	7526	-
124	300	12.5	220	10	75	6383	-
125	300	12.5	220	10	90	6033	4488

## Appendix B. Sample points II

Table B.1. Sample points II

$b_0$	$\beta$	$t_1$	$t_0$	30°			60°			90°			$t_0$	30°			60°			$t_0$	30°			60°		
				$\varphi$		$C$ [kNm/rad]		$C$ [kNm/rad]																		
100	0.400	4	4	55	27	23	6	174	85	72	10	1082	406	345												
100	0.600	4	4	215	86	68	6	634	262	211	10	4007	1229	1013												
100	0.800	4	4	1135	442	343	6	2847	1107	891																
110	0.364	4	4	44	23	20	5	83	43	37	6	140	72	62												
110	0.545	4	4	150	63	50	5	272	116	94	6	450	193	158												
110	0.818	4	4	1457	568	439	5	2349	948	751	6	3536	1389	1117												
120	0.333	4	5	70	37	33	7.1	203	106	92	10	638	291	253												
120	0.583	4	5	364	150	121	7.1	1009	422	345	10	3197	1155	953												
120	0.833	5	5	2923	1170	923	7.1	6637	2532	2047																
140	0.286	4	5	53	30	27	7.1	152	85	76	10	453	231	205												
140	0.571	5	5	353	143	117	7.1	944	399	328	10	2646	1075	891												
140	0.786	5	5	2097	794	618	7.1	4846	1954	1569																
150	0.267	4	6	81	47	42	8.8	262	146	130	12.5	1004	433	382												
150	0.533	5	6	448	191	158	8.8	1372	593	494	12.5	5046	1897	1586												
150	0.800	6	6	3785	1471	1149	8.8	9697	3742	3034																
160	0.250	4	6	73	44	39	8.8	236	135	122	12.5	862	397	353												
160	0.563	5	6	559	232	190	8.8	1677	714	590	12.5	5884	2242	1866												
160	0.750	6	6	2493	943	735	8.8	6531	2617	2111																
180	0.278	4	7.1	148	85	76	8.8	280	158	141	12.5	946	467	415												
180	0.556	6	7.1	896	378	309	8.8	1617	693	571	12.5	5165	2134	1774												
180	0.833	7.1	7.1	8286	3312	2600	8.8	13374	5401	4322																

200	0.250	4	7.1	123	74	66	8.8	233	138	124	12.5	750	402	360
200	0.550	5	7.1	869	367	295	8.8	1566	673	546	12.5	4910	2040	1672
200	0.800	7.1	7.1	6690	2589	2020	8.8	10763	4362	3457				
220	0.273	4	8	203	118	105	10	395	226	203	12.5	840	454	405
220	0.545	7.1	8	1157	490	402	10	2131	922	762	12.5	4347	1899	1580
220	0.818	7.1	8	11157	4415	3474	10	18372	7443	5944				
250	0.280	4	8.8	285	164	146	10	416	237	212	12.5	859	472	422
250	0.560	7.1	8.8	1718	721	589	10	2429	1034	848	12.5	4815	2094	1731
250	0.800	7.1	8.8	12549	4943	3876	10	16880	6768	5384				
260	0.269	4	8.8	267	155	139	10	389	226	203	12.5	798	448	402
260	0.538	7.1	8.8	1496	639	524	10	2118	916	755	12.5	4175	1842	1527
260	0.846	8.8	8.8	20765	8271	6441	10	26909	10941	8628				
300	0.267	5	10	390	227	205	12.5	774	445	401				
300	0.533	8	10	2136	908	747	12.5	4114	1795	1486				
300	0.833	10	10	27313	10664	8367	12.5	45620	18624	14858				

## Appendix C. Pseudo points

Table C.1. Pseudo points

Nº	$b_0$ [mm]	$t_0$ [mm]	$\beta$	$\varphi$ [deg]	C [kNm/rad]	$b_1$ [mm]	$t_1$ [mm]
Pseudo φ int	100	4	0.40	45	36	40	4
Pseudo φ int	100	4	0.40	75	24	40	4
Pseudo φ ext	100	4	0.40	20	75	40	4
Pseudo φ ext	100	4	0.40	25	64	40	4
Pseudo φ ext	100	4	0.40	95	23	40	4
Pseudo φ ext	100	4	0.40	100	23	40	4
Pseudo φ int	100	6	0.40	45	113	40	4
Pseudo φ int	100	6	0.40	75	74	40	4
Pseudo φ ext	100	6	0.40	20	239	40	4
Pseudo φ ext	100	6	0.40	25	203	40	4
Pseudo φ ext	100	6	0.40	95	72	40	4
Pseudo φ ext	100	6	0.40	100	72	40	4
Pseudo φ int	100	10	0.40	45	602	40	4
Pseudo φ int	100	10	0.40	75	352	40	4
Pseudo φ ext	100	10	0.40	20	1654	40	4
Pseudo φ ext	100	10	0.40	25	1338	40	4
Pseudo φ ext	100	10	0.40	95	345	40	4
Pseudo φ ext	100	10	0.40	100	345	40	4
Pseudo φ int	100	4	0.60	45	128	60	4
Pseudo φ int	100	4	0.60	75	71	60	4
Pseudo φ ext	100	4	0.60	20	310	60	4
Pseudo φ ext	100	4	0.60	25	258	60	4
Pseudo φ ext	100	4	0.60	95	68	60	4
Pseudo φ ext	100	4	0.60	100	68	60	4
Pseudo φ int	100	6	0.60	45	381	60	4
Pseudo φ int	100	6	0.60	75	219	60	4
Pseudo φ ext	100	6	0.60	20	911	60	4
Pseudo φ ext	100	6	0.60	25	759	60	4
Pseudo φ ext	100	6	0.60	95	211	60	4
Pseudo φ ext	100	6	0.60	100	211	60	4
Pseudo φ int	100	10	0.60	45	2010	60	4
Pseudo φ int	100	10	0.60	75	1030	60	4
Pseudo φ ext	100	10	0.60	20	6435	60	4
Pseudo φ ext	100	10	0.60	25	5087	60	4
Pseudo φ ext	100	10	0.60	95	1013	60	4

Pseudo $\varphi$ ext	100	10	0.60	100	1013	60	4
Pseudo $\varphi$ int	100	4	0.80	45	669	80	4
Pseudo $\varphi$ int	100	4	0.80	75	359	80	4
Pseudo $\varphi$ ext	100	4	0.80	20	1637	80	4
Pseudo $\varphi$ ext	100	4	0.80	25	1364	80	4
Pseudo $\varphi$ ext	100	4	0.80	95	343	80	4
Pseudo $\varphi$ ext	100	4	0.80	100	343	80	4
Pseudo $\varphi$ int	100	6	0.80	45	1653	80	4
Pseudo $\varphi$ int	100	6	0.80	75	922	80	4
Pseudo $\varphi$ ext	100	6	0.80	20	4184	80	4
Pseudo $\varphi$ ext	100	6	0.80	25	3451	80	4
Pseudo $\varphi$ ext	100	6	0.80	95	891	80	4
Pseudo $\varphi$ ext	100	6	0.80	100	891	80	4
Pseudo $\varphi$ int	110	4	0.36	45	30	40	4
Pseudo $\varphi$ int	110	4	0.36	75	20	40	4
Pseudo $\varphi$ ext	110	4	0.36	20	60	40	4
Pseudo $\varphi$ ext	110	4	0.36	25	52	40	4
Pseudo $\varphi$ ext	110	4	0.36	95	20	40	4
Pseudo $\varphi$ ext	110	4	0.36	100	20	40	4
Pseudo $\varphi$ int	110	5	0.36	45	56	40	4
Pseudo $\varphi$ int	110	5	0.36	75	38	40	4
Pseudo $\varphi$ ext	110	5	0.36	20	112	40	4
Pseudo $\varphi$ ext	110	5	0.36	25	96	40	4
Pseudo $\varphi$ ext	110	5	0.36	95	37	40	4
Pseudo $\varphi$ ext	110	5	0.36	100	37	40	4
Pseudo $\varphi$ int	110	6	0.36	45	94	40	4
Pseudo $\varphi$ int	110	6	0.36	75	64	40	4
Pseudo $\varphi$ ext	110	6	0.36	20	191	40	4
Pseudo $\varphi$ ext	110	6	0.36	25	163	40	4
Pseudo $\varphi$ ext	110	6	0.36	95	62	40	4
Pseudo $\varphi$ ext	110	6	0.36	100	62	40	4
Pseudo $\varphi$ int	110	4	0.55	45	91	60	4
Pseudo $\varphi$ int	110	4	0.55	75	52	60	4
Pseudo $\varphi$ ext	110	4	0.55	20	215	60	4
Pseudo $\varphi$ ext	110	4	0.55	25	179	60	4
Pseudo $\varphi$ ext	110	4	0.55	95	50	60	4
Pseudo $\varphi$ ext	110	4	0.55	100	50	60	4
Pseudo $\varphi$ int	110	5	0.55	45	167	60	4
Pseudo $\varphi$ int	110	5	0.55	75	98	60	4
Pseudo $\varphi$ ext	110	5	0.55	20	387	60	4
Pseudo $\varphi$ ext	110	5	0.55	25	325	60	4
Pseudo $\varphi$ ext	110	5	0.55	95	94	60	4
Pseudo $\varphi$ ext	110	5	0.55	100	94	60	4
Pseudo $\varphi$ int	110	6	0.55	45	275	60	4
Pseudo $\varphi$ int	110	6	0.55	75	163	60	4
Pseudo $\varphi$ ext	110	6	0.55	20	640	60	4
Pseudo $\varphi$ ext	110	6	0.55	25	536	60	4
Pseudo $\varphi$ ext	110	6	0.55	95	158	60	4
Pseudo $\varphi$ ext	110	6	0.55	100	158	60	4
Pseudo $\varphi$ int	110	4	0.82	45	860	90	4
Pseudo $\varphi$ int	110	4	0.82	75	460	90	4
Pseudo $\varphi$ ext	110	4	0.82	20	2098	90	4
Pseudo $\varphi$ ext	110	4	0.82	25	1749	90	4
Pseudo $\varphi$ ext	110	4	0.82	95	439	90	4
Pseudo $\varphi$ ext	110	4	0.82	100	439	90	4
Pseudo $\varphi$ int	110	6	0.82	45	2066	90	4
Pseudo $\varphi$ int	110	6	0.82	75	1157	90	4
Pseudo $\varphi$ ext	110	6	0.82	20	5173	90	4
Pseudo $\varphi$ ext	110	6	0.82	25	4277	90	4
Pseudo $\varphi$ ext	110	6	0.82	95	1117	90	4

Pseudo $\varphi$ ext	110	6	0.82	100	1117	90	4
Pseudo $\varphi$ int	120	5	0.33	45	48	40	4
Pseudo $\varphi$ int	120	5	0.33	75	33	40	4
Pseudo $\varphi$ ext	120	5	0.33	20	94	40	4
Pseudo $\varphi$ ext	120	5	0.33	25	81	40	4
Pseudo $\varphi$ ext	120	5	0.33	95	33	40	4
Pseudo $\varphi$ ext	120	5	0.33	100	33	40	4
Pseudo $\varphi$ int	120	7.1	0.33	45	137	40	4
Pseudo $\varphi$ int	120	7.1	0.33	75	94	40	4
Pseudo $\varphi$ ext	120	7.1	0.33	20	275	40	4
Pseudo $\varphi$ ext	120	7.1	0.33	25	235	40	4
Pseudo $\varphi$ ext	120	7.1	0.33	95	92	40	4
Pseudo $\varphi$ ext	120	7.1	0.33	100	92	40	4
Pseudo $\varphi$ int	120	10	0.33	45	396	40	4
Pseudo $\varphi$ int	120	10	0.33	75	258	40	4
Pseudo $\varphi$ ext	120	10	0.33	20	919	40	4
Pseudo $\varphi$ ext	120	10	0.33	25	765	40	4
Pseudo $\varphi$ ext	120	10	0.33	95	253	40	4
Pseudo $\varphi$ ext	120	10	0.33	100	253	40	4
Pseudo $\varphi$ int	120	5	0.58	45	218	70	4
Pseudo $\varphi$ int	120	5	0.58	75	125	70	4
Pseudo $\varphi$ ext	120	5	0.58	20	522	70	4
Pseudo $\varphi$ ext	120	5	0.58	25	436	70	4
Pseudo $\varphi$ ext	120	5	0.58	95	121	70	4
Pseudo $\varphi$ ext	120	5	0.58	100	121	70	4
Pseudo $\varphi$ int	120	7.1	0.58	45	609	70	4
Pseudo $\varphi$ int	120	7.1	0.58	75	357	70	4
Pseudo $\varphi$ ext	120	7.1	0.58	20	1450	70	4
Pseudo $\varphi$ ext	120	7.1	0.58	25	1209	70	4
Pseudo $\varphi$ ext	120	7.1	0.58	95	345	70	4
Pseudo $\varphi$ ext	120	7.1	0.58	100	345	70	4
Pseudo $\varphi$ int	120	10	0.58	45	1760	70	4
Pseudo $\varphi$ int	120	10	0.58	75	976	70	4
Pseudo $\varphi$ ext	120	10	0.58	20	4882	70	4
Pseudo $\varphi$ ext	120	10	0.58	25	3952	70	4
Pseudo $\varphi$ ext	120	10	0.58	95	953	70	4
Pseudo $\varphi$ ext	120	10	0.58	100	953	70	4
Pseudo $\varphi$ int	120	5	0.83	45	1740	100	5
Pseudo $\varphi$ int	120	5	0.83	75	961	100	5
Pseudo $\varphi$ ext	120	5	0.83	20	4202	100	5
Pseudo $\varphi$ ext	120	5	0.83	25	3505	100	5
Pseudo $\varphi$ ext	120	5	0.83	95	923	100	5
Pseudo $\varphi$ ext	120	5	0.83	100	923	100	5
Pseudo $\varphi$ int	120	7.1	0.83	45	3802	100	5
Pseudo $\varphi$ int	120	7.1	0.83	75	2114	100	5
Pseudo $\varphi$ ext	120	7.1	0.83	20	9845	100	5
Pseudo $\varphi$ ext	120	7.1	0.83	25	8084	100	5
Pseudo $\varphi$ ext	120	7.1	0.83	95	2047	100	5
Pseudo $\varphi$ ext	120	7.1	0.83	100	2047	100	5
Pseudo $\varphi$ int	140	5	0.29	45	38	40	4
Pseudo $\varphi$ int	140	5	0.29	75	28	40	4
Pseudo $\varphi$ ext	140	5	0.29	20	70	40	4
Pseudo $\varphi$ ext	140	5	0.29	25	61	40	4
Pseudo $\varphi$ ext	140	5	0.29	95	27	40	4
Pseudo $\varphi$ ext	140	5	0.29	100	27	40	4
Pseudo $\varphi$ int	140	7.1	0.29	45	107	40	4
Pseudo $\varphi$ int	140	7.1	0.29	75	77	40	4
Pseudo $\varphi$ ext	140	7.1	0.29	20	201	40	4
Pseudo $\varphi$ ext	140	7.1	0.29	25	174	40	4
Pseudo $\varphi$ ext	140	7.1	0.29	95	76	40	4

Pseudo $\varphi$ ext	140	7.1	0.29	100	76	40	4
Pseudo $\varphi$ int	140	10	0.29	45	300	40	4
Pseudo $\varphi$ int	140	10	0.29	75	209	40	4
Pseudo $\varphi$ ext	140	10	0.29	20	627	40	4
Pseudo $\varphi$ ext	140	10	0.29	25	531	40	4
Pseudo $\varphi$ ext	140	10	0.29	95	205	40	4
Pseudo $\varphi$ ext	140	10	0.29	100	205	40	4
Pseudo $\varphi$ int	140	5	0.57	45	210	80	5
Pseudo $\varphi$ int	140	5	0.57	75	121	80	5
Pseudo $\varphi$ ext	140	5	0.57	20	513	80	5
Pseudo $\varphi$ ext	140	5	0.57	25	425	80	5
Pseudo $\varphi$ ext	140	5	0.57	95	117	80	5
Pseudo $\varphi$ ext	140	5	0.57	100	117	80	5
Pseudo $\varphi$ int	140	7.1	0.57	45	572	80	5
Pseudo $\varphi$ int	140	7.1	0.57	75	339	80	5
Pseudo $\varphi$ ext	140	7.1	0.57	20	1354	80	5
Pseudo $\varphi$ ext	140	7.1	0.57	25	1130	80	5
Pseudo $\varphi$ ext	140	7.1	0.57	95	328	80	5
Pseudo $\varphi$ ext	140	7.1	0.57	100	328	80	5
Pseudo $\varphi$ int	140	10	0.57	45	1559	80	5
Pseudo $\varphi$ int	140	10	0.57	75	916	80	5
Pseudo $\varphi$ ext	140	10	0.57	20	3877	80	5
Pseudo $\varphi$ ext	140	10	0.57	25	3201	80	5
Pseudo $\varphi$ ext	140	10	0.57	95	891	80	5
Pseudo $\varphi$ ext	140	10	0.57	100	891	80	5
Pseudo $\varphi$ int	140	5	0.79	45	1212	110	5
Pseudo $\varphi$ int	140	5	0.79	75	644	110	5
Pseudo $\varphi$ ext	140	5	0.79	20	3066	110	5
Pseudo $\varphi$ ext	140	5	0.79	25	2537	110	5
Pseudo $\varphi$ ext	140	5	0.79	95	618	110	5
Pseudo $\varphi$ ext	140	5	0.79	100	618	110	5
Pseudo $\varphi$ int	140	7.1	0.79	45	2879	110	5
Pseudo $\varphi$ int	140	7.1	0.79	75	1627	110	5
Pseudo $\varphi$ ext	140	7.1	0.79	20	7009	110	5
Pseudo $\varphi$ ext	140	7.1	0.79	25	5827	110	5
Pseudo $\varphi$ ext	140	7.1	0.79	95	1569	110	5
Pseudo $\varphi$ ext	140	7.1	0.79	100	1569	110	5
Pseudo $\varphi$ int	150	6	0.27	45	58	40	4
Pseudo $\varphi$ int	150	6	0.27	75	43	40	4
Pseudo $\varphi$ ext	150	6	0.27	20	104	40	4
Pseudo $\varphi$ ext	150	6	0.27	25	92	40	4
Pseudo $\varphi$ ext	150	6	0.27	95	42	40	4
Pseudo $\varphi$ ext	150	6	0.27	100	42	40	4
Pseudo $\varphi$ int	150	8.8	0.27	45	183	40	4
Pseudo $\varphi$ int	150	8.8	0.27	75	133	40	4
Pseudo $\varphi$ ext	150	8.8	0.27	20	348	40	4
Pseudo $\varphi$ ext	150	8.8	0.27	25	301	40	4
Pseudo $\varphi$ ext	150	8.8	0.27	95	130	40	4
Pseudo $\varphi$ ext	150	8.8	0.27	100	130	40	4
Pseudo $\varphi$ int	150	12.5	0.27	45	597	40	4
Pseudo $\varphi$ int	150	12.5	0.27	75	387	40	4
Pseudo $\varphi$ ext	150	12.5	0.27	20	1489	40	4
Pseudo $\varphi$ ext	150	12.5	0.27	25	1220	40	4
Pseudo $\varphi$ ext	150	12.5	0.27	95	382	40	4
Pseudo $\varphi$ ext	150	12.5	0.27	100	382	40	4
Pseudo $\varphi$ int	150	6	0.53	45	273	80	5
Pseudo $\varphi$ int	150	6	0.53	75	163	80	5
Pseudo $\varphi$ ext	150	6	0.53	20	641	80	5
Pseudo $\varphi$ ext	150	6	0.53	25	535	80	5
Pseudo $\varphi$ ext	150	6	0.53	95	158	80	5

Pseudo $\varphi$ ext	150	6	0.53	100	158	80	5
Pseudo $\varphi$ int	150	8.8	0.53	45	839	80	5
Pseudo $\varphi$ int	150	8.8	0.53	75	508	80	5
Pseudo $\varphi$ ext	150	8.8	0.53	20	1965	80	5
Pseudo $\varphi$ ext	150	8.8	0.53	25	1641	80	5
Pseudo $\varphi$ ext	150	8.8	0.53	95	494	80	5
Pseudo $\varphi$ ext	150	8.8	0.53	100	494	80	5
Pseudo $\varphi$ int	150	12.5	0.53	45	2829	80	5
Pseudo $\varphi$ int	150	12.5	0.53	75	1622	80	5
Pseudo $\varphi$ ext	150	12.5	0.53	20	7645	80	5
Pseudo $\varphi$ ext	150	12.5	0.53	25	6210	80	5
Pseudo $\varphi$ ext	150	12.5	0.53	95	1586	80	5
Pseudo $\varphi$ ext	150	12.5	0.53	100	1586	80	5
Pseudo $\varphi$ int	150	6	0.80	45	2221	120	6
Pseudo $\varphi$ int	150	6	0.80	75	1199	120	6
Pseudo $\varphi$ ext	150	6	0.80	20	5481	120	6
Pseudo $\varphi$ ext	150	6	0.80	25	4556	120	6
Pseudo $\varphi$ ext	150	6	0.80	95	1149	120	6
Pseudo $\varphi$ ext	150	6	0.80	100	1149	120	6
Pseudo $\varphi$ int	150	8.8	0.80	45	5587	120	6
Pseudo $\varphi$ int	150	8.8	0.80	75	3133	120	6
Pseudo $\varphi$ ext	150	8.8	0.80	20	14341	120	6
Pseudo $\varphi$ ext	150	8.8	0.80	25	11791	120	6
Pseudo $\varphi$ ext	150	8.8	0.80	95	3034	120	6
Pseudo $\varphi$ ext	150	8.8	0.80	100	3034	120	6
Pseudo $\varphi$ int	160	6	0.25	45	54	40	4
Pseudo $\varphi$ int	160	6	0.25	75	40	40	4
Pseudo $\varphi$ ext	160	6	0.25	20	94	40	4
Pseudo $\varphi$ ext	160	6	0.25	25	83	40	4
Pseudo $\varphi$ ext	160	6	0.25	95	39	40	4
Pseudo $\varphi$ ext	160	6	0.25	100	39	40	4
Pseudo $\varphi$ int	160	8.8	0.25	45	168	40	4
Pseudo $\varphi$ int	160	8.8	0.25	75	124	40	4
Pseudo $\varphi$ ext	160	8.8	0.25	20	310	40	4
Pseudo $\varphi$ ext	160	8.8	0.25	25	269	40	4
Pseudo $\varphi$ ext	160	8.8	0.25	95	122	40	4
Pseudo $\varphi$ ext	160	8.8	0.25	100	122	40	4
Pseudo $\varphi$ int	160	12.5	0.25	45	533	40	4
Pseudo $\varphi$ int	160	12.5	0.25	75	358	40	4
Pseudo $\varphi$ ext	160	12.5	0.25	20	1251	40	4
Pseudo $\varphi$ ext	160	12.5	0.25	25	1036	40	4
Pseudo $\varphi$ ext	160	12.5	0.25	95	353	40	4
Pseudo $\varphi$ ext	160	12.5	0.25	100	353	40	4
Pseudo $\varphi$ int	160	6	0.56	45	336	90	5
Pseudo $\varphi$ int	160	6	0.56	75	196	90	5
Pseudo $\varphi$ ext	160	6	0.56	20	806	90	5
Pseudo $\varphi$ ext	160	6	0.56	25	671	90	5
Pseudo $\varphi$ ext	160	6	0.56	95	190	90	5
Pseudo $\varphi$ ext	160	6	0.56	100	190	90	5
Pseudo $\varphi$ int	160	8.8	0.56	45	1019	90	5
Pseudo $\varphi$ int	160	8.8	0.56	75	609	90	5
Pseudo $\varphi$ ext	160	8.8	0.56	20	2408	90	5
Pseudo $\varphi$ ext	160	8.8	0.56	25	2008	90	5
Pseudo $\varphi$ ext	160	8.8	0.56	95	590	90	5
Pseudo $\varphi$ ext	160	8.8	0.56	100	590	90	5
Pseudo $\varphi$ int	160	12.5	0.56	45	3331	90	5
Pseudo $\varphi$ int	160	12.5	0.56	75	1912	90	5
Pseudo $\varphi$ ext	160	12.5	0.56	20	8855	90	5
Pseudo $\varphi$ ext	160	12.5	0.56	25	7217	90	5
Pseudo $\varphi$ ext	160	12.5	0.56	95	1866	90	5

Pseudo $\varphi$ ext	160	12.5	0.56	100	1866	90	5
Pseudo $\varphi$ int	160	6	0.75	45	1439	120	6
Pseudo $\varphi$ int	160	6	0.75	75	767	120	6
Pseudo $\varphi$ ext	160	6	0.75	20	3648	120	6
Pseudo $\varphi$ ext	160	6	0.75	25	3017	120	6
Pseudo $\varphi$ ext	160	6	0.75	95	735	120	6
Pseudo $\varphi$ ext	160	6	0.75	100	735	120	6
Pseudo $\varphi$ int	160	8.8	0.75	45	3858	120	6
Pseudo $\varphi$ int	160	8.8	0.75	75	2186	120	6
Pseudo $\varphi$ ext	160	8.8	0.75	20	9491	120	6
Pseudo $\varphi$ ext	160	8.8	0.75	25	7872	120	6
Pseudo $\varphi$ ext	160	8.8	0.75	95	2111	120	6
Pseudo $\varphi$ ext	160	8.8	0.75	100	2111	120	6
Pseudo $\varphi$ int	180	7.1	0.28	45	105	50	4
Pseudo $\varphi$ int	180	7.1	0.28	75	77	50	4
Pseudo $\varphi$ ext	180	7.1	0.28	20	193	50	4
Pseudo $\varphi$ ext	180	7.1	0.28	25	169	50	4
Pseudo $\varphi$ ext	180	7.1	0.28	95	76	50	4
Pseudo $\varphi$ ext	180	7.1	0.28	100	76	50	4
Pseudo $\varphi$ int	180	8.8	0.28	45	197	50	4
Pseudo $\varphi$ int	180	8.8	0.28	75	144	50	4
Pseudo $\varphi$ ext	180	8.8	0.28	20	370	50	4
Pseudo $\varphi$ ext	180	8.8	0.28	25	321	50	4
Pseudo $\varphi$ ext	180	8.8	0.28	95	141	50	4
Pseudo $\varphi$ ext	180	8.8	0.28	100	141	50	4
Pseudo $\varphi$ int	180	12.5	0.28	45	611	50	4
Pseudo $\varphi$ int	180	12.5	0.28	75	422	50	4
Pseudo $\varphi$ ext	180	12.5	0.28	20	1332	50	4
Pseudo $\varphi$ ext	180	12.5	0.28	25	1119	50	4
Pseudo $\varphi$ ext	180	12.5	0.28	95	415	50	4
Pseudo $\varphi$ ext	180	12.5	0.28	100	415	50	4
Pseudo $\varphi$ int	180	7.1	0.56	45	543	100	6
Pseudo $\varphi$ int	180	7.1	0.56	75	319	100	6
Pseudo $\varphi$ ext	180	7.1	0.56	20	1286	100	6
Pseudo $\varphi$ ext	180	7.1	0.56	25	1073	100	6
Pseudo $\varphi$ ext	180	7.1	0.56	95	309	100	6
Pseudo $\varphi$ ext	180	7.1	0.56	100	309	100	6
Pseudo $\varphi$ int	180	8.8	0.56	45	988	100	6
Pseudo $\varphi$ int	180	8.8	0.56	75	589	100	6
Pseudo $\varphi$ ext	180	8.8	0.56	20	2309	100	6
Pseudo $\varphi$ ext	180	8.8	0.56	25	1931	100	6
Pseudo $\varphi$ ext	180	8.8	0.56	95	571	100	6
Pseudo $\varphi$ ext	180	8.8	0.56	100	571	100	6
Pseudo $\varphi$ int	180	12.5	0.56	45	3073	100	6
Pseudo $\varphi$ int	180	12.5	0.56	75	1824	100	6
Pseudo $\varphi$ ext	180	12.5	0.56	20	7528	100	6
Pseudo $\varphi$ ext	180	12.5	0.56	25	6231	100	6
Pseudo $\varphi$ ext	180	12.5	0.56	95	1774	100	6
Pseudo $\varphi$ ext	180	12.5	0.56	100	1774	100	6
Pseudo $\varphi$ int	180	7.1	0.83	45	4937	150	7.1
Pseudo $\varphi$ int	180	7.1	0.83	75	2713	150	7.1
Pseudo $\varphi$ ext	180	7.1	0.83	20	11893	150	7.1
Pseudo $\varphi$ ext	180	7.1	0.83	25	9929	150	7.1
Pseudo $\varphi$ ext	180	7.1	0.83	95	2600	150	7.1
Pseudo $\varphi$ ext	180	7.1	0.83	100	2600	150	7.1
Pseudo $\varphi$ int	180	8.8	0.83	45	7964	150	7.1
Pseudo $\varphi$ int	180	8.8	0.83	75	4487	150	7.1
Pseudo $\varphi$ ext	180	8.8	0.83	20	19292	150	7.1
Pseudo $\varphi$ ext	180	8.8	0.83	25	16061	150	7.1
Pseudo $\varphi$ ext	180	8.8	0.83	95	4322	150	7.1

Pseudo $\varphi$ ext	180	8.8	0.83	100	4322	150	7.1
Pseudo $\varphi$ int	200	7.1	0.25	45	91	50	4
Pseudo $\varphi$ int	200	7.1	0.25	75	67	50	4
Pseudo $\varphi$ ext	200	7.1	0.25	20	158	50	4
Pseudo $\varphi$ ext	200	7.1	0.25	25	139	50	4
Pseudo $\varphi$ ext	200	7.1	0.25	95	66	50	4
Pseudo $\varphi$ ext	200	7.1	0.25	100	66	50	4
Pseudo $\varphi$ int	200	8.8	0.25	45	169	50	4
Pseudo $\varphi$ int	200	8.8	0.25	75	126	50	4
Pseudo $\varphi$ ext	200	8.8	0.25	20	301	50	4
Pseudo $\varphi$ ext	200	8.8	0.25	25	264	50	4
Pseudo $\varphi$ ext	200	8.8	0.25	95	124	50	4
Pseudo $\varphi$ ext	200	8.8	0.25	100	124	50	4
Pseudo $\varphi$ int	200	12.5	0.25	45	510	50	4
Pseudo $\varphi$ int	200	12.5	0.25	75	366	50	4
Pseudo $\varphi$ ext	200	12.5	0.25	20	1020	50	4
Pseudo $\varphi$ ext	200	12.5	0.25	25	872	50	4
Pseudo $\varphi$ ext	200	12.5	0.25	95	360	50	4
Pseudo $\varphi$ ext	200	12.5	0.25	100	360	50	4
Pseudo $\varphi$ int	200	7.1	0.55	45	531	110	5
Pseudo $\varphi$ int	200	7.1	0.55	75	306	110	5
Pseudo $\varphi$ ext	200	7.1	0.55	20	1233	110	5
Pseudo $\varphi$ ext	200	7.1	0.55	25	1034	110	5
Pseudo $\varphi$ ext	200	7.1	0.55	95	295	110	5
Pseudo $\varphi$ ext	200	7.1	0.55	100	295	110	5
Pseudo $\varphi$ int	200	8.8	0.55	45	965	110	5
Pseudo $\varphi$ int	200	8.8	0.55	75	566	110	5
Pseudo $\varphi$ ext	200	8.8	0.55	20	2215	110	5
Pseudo $\varphi$ ext	200	8.8	0.55	25	1861	110	5
Pseudo $\varphi$ ext	200	8.8	0.55	95	546	110	5
Pseudo $\varphi$ ext	200	8.8	0.55	100	546	110	5
Pseudo $\varphi$ int	200	12.5	0.55	45	2947	110	5
Pseudo $\varphi$ int	200	12.5	0.55	75	1726	110	5
Pseudo $\varphi$ ext	200	12.5	0.55	20	7088	110	5
Pseudo $\varphi$ ext	200	12.5	0.55	25	5896	110	5
Pseudo $\varphi$ ext	200	12.5	0.55	95	1672	110	5
Pseudo $\varphi$ ext	200	12.5	0.55	100	1672	110	5
Pseudo $\varphi$ int	200	7.1	0.80	45	3917	160	7.1
Pseudo $\varphi$ int	200	7.1	0.80	75	2108	160	7.1
Pseudo $\varphi$ ext	200	7.1	0.80	20	9702	160	7.1
Pseudo $\varphi$ ext	200	7.1	0.80	25	8060	160	7.1
Pseudo $\varphi$ ext	200	7.1	0.80	95	2020	160	7.1
Pseudo $\varphi$ ext	200	7.1	0.80	100	2020	160	7.1
Pseudo $\varphi$ int	200	8.8	0.80	45	6446	160	7.1
Pseudo $\varphi$ int	200	8.8	0.80	75	3599	160	7.1
Pseudo $\varphi$ ext	200	8.8	0.80	20	15428	160	7.1
Pseudo $\varphi$ ext	200	8.8	0.80	25	12887	160	7.1
Pseudo $\varphi$ ext	200	8.8	0.80	95	3457	160	7.1
Pseudo $\varphi$ ext	200	8.8	0.80	100	3457	160	7.1
Pseudo $\varphi$ int	220	8	0.27	45	146	60	4
Pseudo $\varphi$ int	220	8	0.27	75	107	60	4
Pseudo $\varphi$ ext	220	8	0.27	20	264	60	4
Pseudo $\varphi$ ext	220	8	0.27	25	231	60	4
Pseudo $\varphi$ ext	220	8	0.27	95	105	60	4
Pseudo $\varphi$ ext	220	8	0.27	100	105	60	4
Pseudo $\varphi$ int	220	10	0.27	45	281	60	4
Pseudo $\varphi$ int	220	10	0.27	75	206	60	4
Pseudo $\varphi$ ext	220	10	0.27	20	519	60	4
Pseudo $\varphi$ ext	220	10	0.27	25	452	60	4
Pseudo $\varphi$ ext	220	10	0.27	95	203	60	4

Pseudo $\varphi$ ext	220	10	0.27	100	203	60	4
Pseudo $\varphi$ int	220	12.5	0.27	45	576	60	4
Pseudo $\varphi$ int	220	12.5	0.27	75	412	60	4
Pseudo $\varphi$ ext	220	12.5	0.27	20	1135	60	4
Pseudo $\varphi$ ext	220	12.5	0.27	25	974	60	4
Pseudo $\varphi$ ext	220	12.5	0.27	95	405	60	4
Pseudo $\varphi$ ext	220	12.5	0.27	100	405	60	4
Pseudo $\varphi$ int	220	8	0.55	45	702	120	7.1
Pseudo $\varphi$ int	220	8	0.55	75	415	120	7.1
Pseudo $\varphi$ ext	220	8	0.55	20	1659	120	7.1
Pseudo $\varphi$ ext	220	8	0.55	25	1384	120	7.1
Pseudo $\varphi$ ext	220	8	0.55	95	402	120	7.1
Pseudo $\varphi$ ext	220	8	0.55	100	402	120	7.1
Pseudo $\varphi$ int	220	10	0.55	45	1308	120	7.1
Pseudo $\varphi$ int	220	10	0.55	75	786	120	7.1
Pseudo $\varphi$ ext	220	10	0.55	20	3038	120	7.1
Pseudo $\varphi$ ext	220	10	0.55	25	2543	120	7.1
Pseudo $\varphi$ ext	220	10	0.55	95	762	120	7.1
Pseudo $\varphi$ ext	220	10	0.55	100	762	120	7.1
Pseudo $\varphi$ int	220	12.5	0.55	45	2677	120	7.1
Pseudo $\varphi$ int	220	12.5	0.55	75	1627	120	7.1
Pseudo $\varphi$ ext	220	12.5	0.55	20	6192	120	7.1
Pseudo $\varphi$ ext	220	12.5	0.55	25	5183	120	7.1
Pseudo $\varphi$ ext	220	12.5	0.55	95	1580	120	7.1
Pseudo $\varphi$ ext	220	12.5	0.55	100	1580	120	7.1
Pseudo $\varphi$ int	220	8	0.82	45	6601	180	7.1
Pseudo $\varphi$ int	220	8	0.82	75	3620	180	7.1
Pseudo $\varphi$ ext	220	8	0.82	20	16097	180	7.1
Pseudo $\varphi$ ext	220	8	0.82	25	13404	180	7.1
Pseudo $\varphi$ ext	220	8	0.82	95	3474	180	7.1
Pseudo $\varphi$ ext	220	8	0.82	100	3474	180	7.1
Pseudo $\varphi$ int	220	10	0.82	45	10970	180	7.1
Pseudo $\varphi$ int	220	10	0.82	75	6175	180	7.1
Pseudo $\varphi$ ext	220	10	0.82	20	26441	180	7.1
Pseudo $\varphi$ ext	220	10	0.82	25	22039	180	7.1
Pseudo $\varphi$ ext	220	10	0.82	95	5944	180	7.1
Pseudo $\varphi$ ext	220	10	0.82	100	5944	180	7.1
Pseudo $\varphi$ int	250	8.8	0.28	45	204	70	4
Pseudo $\varphi$ int	250	8.8	0.28	75	148	70	4
Pseudo $\varphi$ ext	250	8.8	0.28	20	372	70	4
Pseudo $\varphi$ ext	250	8.8	0.28	25	325	70	4
Pseudo $\varphi$ ext	250	8.8	0.28	95	146	70	4
Pseudo $\varphi$ ext	250	8.8	0.28	100	146	70	4
Pseudo $\varphi$ int	250	10	0.28	45	296	70	4
Pseudo $\varphi$ int	250	10	0.28	75	216	70	4
Pseudo $\varphi$ ext	250	10	0.28	20	546	70	4
Pseudo $\varphi$ ext	250	10	0.28	25	475	70	4
Pseudo $\varphi$ ext	250	10	0.28	95	212	70	4
Pseudo $\varphi$ ext	250	10	0.28	100	212	70	4
Pseudo $\varphi$ int	250	12.5	0.28	45	596	70	4
Pseudo $\varphi$ int	250	12.5	0.28	75	429	70	4
Pseudo $\varphi$ ext	250	12.5	0.28	20	1150	70	4
Pseudo $\varphi$ ext	250	12.5	0.28	25	991	70	4
Pseudo $\varphi$ ext	250	12.5	0.28	95	422	70	4
Pseudo $\varphi$ ext	250	12.5	0.28	100	422	70	4
Pseudo $\varphi$ int	250	8.8	0.56	45	1039	140	7.1
Pseudo $\varphi$ int	250	8.8	0.56	75	609	140	7.1
Pseudo $\varphi$ ext	250	8.8	0.56	20	2465	140	7.1
Pseudo $\varphi$ ext	250	8.8	0.56	25	2057	140	7.1
Pseudo $\varphi$ ext	250	8.8	0.56	95	589	140	7.1

Pseudo $\varphi$ ext	250	8.8	0.56	100	589	140	7.1
Pseudo $\varphi$ int	250	10	0.56	45	1480	140	7.1
Pseudo $\varphi$ int	250	10	0.56	75	876	140	7.1
Pseudo $\varphi$ ext	250	10	0.56	20	3471	140	7.1
Pseudo $\varphi$ ext	250	10	0.56	25	2902	140	7.1
Pseudo $\varphi$ ext	250	10	0.56	95	848	140	7.1
Pseudo $\varphi$ ext	250	10	0.56	100	848	140	7.1
Pseudo $\varphi$ int	250	12.5	0.56	45	2964	140	7.1
Pseudo $\varphi$ int	250	12.5	0.56	75	1786	140	7.1
Pseudo $\varphi$ ext	250	12.5	0.56	20	6848	140	7.1
Pseudo $\varphi$ ext	250	12.5	0.56	25	5737	140	7.1
Pseudo $\varphi$ ext	250	12.5	0.56	95	1731	140	7.1
Pseudo $\varphi$ ext	250	12.5	0.56	100	1731	140	7.1
Pseudo $\varphi$ int	250	8.8	0.80	45	7413	200	7.1
Pseudo $\varphi$ int	250	8.8	0.80	75	4043	200	7.1
Pseudo $\varphi$ ext	250	8.8	0.80	20	18113	200	7.1
Pseudo $\varphi$ ext	250	8.8	0.80	25	15081	200	7.1
Pseudo $\varphi$ ext	250	8.8	0.80	95	3876	200	7.1
Pseudo $\varphi$ ext	250	8.8	0.80	100	3876	200	7.1
Pseudo $\varphi$ int	250	10	0.80	45	10029	200	7.1
Pseudo $\varphi$ int	250	10	0.80	75	5597	200	7.1
Pseudo $\varphi$ ext	250	10	0.80	20	24352	200	7.1
Pseudo $\varphi$ ext	250	10	0.80	25	20274	200	7.1
Pseudo $\varphi$ ext	250	10	0.80	95	5384	200	7.1
Pseudo $\varphi$ ext	250	10	0.80	100	5384	200	7.1
Pseudo $\varphi$ int	260	10	0.27	45	279	70	4
Pseudo $\varphi$ int	260	10	0.27	75	206	70	4
Pseudo $\varphi$ ext	260	10	0.27	20	508	70	4
Pseudo $\varphi$ ext	260	10	0.27	25	443	70	4
Pseudo $\varphi$ ext	260	10	0.27	95	203	70	4
Pseudo $\varphi$ ext	260	10	0.27	100	203	70	4
Pseudo $\varphi$ int	260	12.5	0.27	45	560	70	4
Pseudo $\varphi$ int	260	12.5	0.27	75	409	70	4
Pseudo $\varphi$ ext	260	12.5	0.27	20	1060	70	4
Pseudo $\varphi$ ext	260	12.5	0.27	25	917	70	4
Pseudo $\varphi$ ext	260	12.5	0.27	95	402	70	4
Pseudo $\varphi$ ext	260	12.5	0.27	100	402	70	4
Pseudo $\varphi$ int	260	10	0.54	45	1302	140	7.1
Pseudo $\varphi$ int	260	10	0.54	75	779	140	7.1
Pseudo $\varphi$ ext	260	10	0.54	20	3012	140	7.1
Pseudo $\varphi$ ext	260	10	0.54	25	2523	140	7.1
Pseudo $\varphi$ ext	260	10	0.54	95	755	140	7.1
Pseudo $\varphi$ ext	260	10	0.54	100	755	140	7.1
Pseudo $\varphi$ int	260	12.5	0.54	45	2592	140	7.1
Pseudo $\varphi$ int	260	12.5	0.54	75	1575	140	7.1
Pseudo $\varphi$ ext	260	12.5	0.54	20	5908	140	7.1
Pseudo $\varphi$ ext	260	12.5	0.54	25	4962	140	7.1
Pseudo $\varphi$ ext	260	12.5	0.54	95	1527	140	7.1
Pseudo $\varphi$ ext	260	12.5	0.54	100	1527	140	7.1
Pseudo $\varphi$ int	260	8.8	0.85	45	12383	220	8.8
Pseudo $\varphi$ int	260	8.8	0.85	75	6734	220	8.8
Pseudo $\varphi$ ext	260	8.8	0.85	20	29724	220	8.8
Pseudo $\varphi$ ext	260	8.8	0.85	25	24852	220	8.8
Pseudo $\varphi$ ext	260	8.8	0.85	95	6441	220	8.8
Pseudo $\varphi$ ext	260	8.8	0.85	100	6441	220	8.8
Pseudo $\varphi$ int	260	10	0.85	45	16179	220	8.8
Pseudo $\varphi$ int	260	10	0.85	75	8996	220	8.8
Pseudo $\varphi$ ext	260	10	0.85	20	38418	220	8.8
Pseudo $\varphi$ ext	260	10	0.85	25	32156	220	8.8
Pseudo $\varphi$ ext	260	10	0.85	95	8628	220	8.8

Pseudo $\varphi$ ext	260	10	0.85	100	8628	220	8.8
Pseudo $\varphi$ int	300	10	0.27	45	280	80	5
Pseudo $\varphi$ int	300	10	0.27	75	208	80	5
Pseudo $\varphi$ ext	300	10	0.27	20	509	80	5
Pseudo $\varphi$ ext	300	10	0.27	25	444	80	5
Pseudo $\varphi$ ext	300	10	0.27	95	205	80	5
Pseudo $\varphi$ ext	300	10	0.27	100	205	80	5
Pseudo $\varphi$ int	300	12.5	0.27	45	550	80	5
Pseudo $\varphi$ int	300	12.5	0.27	75	407	80	5
Pseudo $\varphi$ ext	300	12.5	0.27	20	1019	80	5
Pseudo $\varphi$ ext	300	12.5	0.27	25	885	80	5
Pseudo $\varphi$ ext	300	12.5	0.27	95	401	80	5
Pseudo $\varphi$ ext	300	12.5	0.27	100	401	80	5
Pseudo $\varphi$ int	300	10	0.53	45	1299	160	8
Pseudo $\varphi$ int	300	10	0.53	75	771	160	8
Pseudo $\varphi$ ext	300	10	0.53	20	3060	160	8
Pseudo $\varphi$ ext	300	10	0.53	25	2555	160	8
Pseudo $\varphi$ ext	300	10	0.53	95	747	160	8
Pseudo $\varphi$ ext	300	10	0.53	100	747	160	8
Pseudo $\varphi$ int	300	12.5	0.53	45	2537	160	8
Pseudo $\varphi$ int	300	12.5	0.53	75	1532	160	8
Pseudo $\varphi$ ext	300	12.5	0.53	20	5847	160	8
Pseudo $\varphi$ ext	300	12.5	0.53	25	4900	160	8
Pseudo $\varphi$ ext	300	12.5	0.53	95	1486	160	8
Pseudo $\varphi$ ext	300	12.5	0.53	100	1486	160	8
Pseudo $\varphi$ int	300	10	0.83	45	16045	250	10
Pseudo $\varphi$ int	300	10	0.83	75	8722	250	10
Pseudo $\varphi$ ext	300	10	0.83	20	39574	250	10
Pseudo $\varphi$ ext	300	10	0.83	25	32886	250	10
Pseudo $\varphi$ ext	300	10	0.83	95	8367	250	10
Pseudo $\varphi$ ext	300	10	0.83	100	8367	250	10
Pseudo $\varphi$ int	300	12.5	0.83	45	27378	250	10
Pseudo $\varphi$ int	300	12.5	0.83	75	15444	250	10
Pseudo $\varphi$ ext	300	12.5	0.83	20	65406	250	10
Pseudo $\varphi$ ext	300	12.5	0.83	25	54619	250	10
Pseudo $\varphi$ ext	300	12.5	0.83	95	14858	250	10
Pseudo $\varphi$ ext	300	12.5	0.83	100	14858	250	10
Pseudo $\varphi$ int	110	5	0.82	45	1403	90	4
Pseudo $\varphi$ int	110	5	0.82	75	782	90	4
Pseudo $\varphi$ ext	110	5	0.82	20	3374	90	4
Pseudo $\varphi$ ext	110	5	0.82	25	2816	90	4
Pseudo $\varphi$ ext	110	5	0.82	95	751	90	4
Pseudo $\varphi$ ext	110	5	0.82	100	751	90	4
Pseudo $\varphi$ int	260	8.8	0.27	45	192	70	4
Pseudo $\varphi$ int	260	8.8	0.27	75	142	70	4
Pseudo $\varphi$ ext	260	8.8	0.27	20	348	70	4
Pseudo $\varphi$ ext	260	8.8	0.27	25	304	70	4
Pseudo $\varphi$ ext	260	8.8	0.27	95	139	70	4
Pseudo $\varphi$ ext	260	8.8	0.27	100	139	70	4
Pseudo $\varphi$ int	260	8.8	0.54	45	913	140	7.1
Pseudo $\varphi$ int	260	8.8	0.54	75	542	140	7.1
Pseudo $\varphi$ ext	260	8.8	0.54	20	2136	140	7.1
Pseudo $\varphi$ ext	260	8.8	0.54	25	1787	140	7.1
Pseudo $\varphi$ ext	260	8.8	0.54	95	524	140	7.1
Pseudo $\varphi$ ext	260	8.8	0.54	100	524	140	7.1
Pseudo t0 int	100	5	0.40	30	100	40	4
Pseudo t0 int	100	8	0.40	30	466	40	4
Pseudo t0 ext	100	0	0.40	30	0	40	4
Pseudo t0 ext	100	0.1	0.40	30	0	40	4
Pseudo t0 ext	100	12	0.40	30	2225	40	4

Pseudo t0 ext	100	12.5	0.40	30	2622	40	4
Pseudo t0 int	100	5	0.60	30	374	60	4
Pseudo t0 int	100	8	0.60	30	1694	60	4
Pseudo t0 ext	100	0	0.60	30	0	60	4
Pseudo t0 ext	100	0.1	0.60	30	0	60	4
Pseudo t0 ext	100	12	0.60	30	8418	60	4
Pseudo t0 ext	100	12.5	0.60	30	9969	60	4
Pseudo t0 int	100	5	0.80	30	1896	80	4
Pseudo t0 int	100	8	0.80	30	5324	80	4
Pseudo t0 ext	100	0	0.80	30	0	80	4
Pseudo t0 ext	100	0.1	0.80	30	0	80	4
Pseudo t0 ext	100	10	0.80	30	8564	80	4
Pseudo t0 ext	100	12	0.80	30	12570	80	4
Pseudo t0 ext	100	12.5	0.80	30	13691	80	4
Pseudo t0 int	100	5	0.40	60	50	40	4
Pseudo t0 int	100	8	0.40	60	201	40	4
Pseudo t0 ext	100	0	0.40	60	0	40	4
Pseudo t0 ext	100	0.1	0.40	60	0	40	4
Pseudo t0 ext	100	12	0.40	60	736	40	4
Pseudo t0 ext	100	12.5	0.40	60	843	40	4
Pseudo t0 int	100	5	0.60	60	157	60	4
Pseudo t0 int	100	8	0.60	60	612	60	4
Pseudo t0 ext	100	0	0.60	60	0	60	4
Pseudo t0 ext	100	0.1	0.60	60	0	60	4
Pseudo t0 ext	100	12	0.60	60	2225	60	4
Pseudo t0 ext	100	12.5	0.60	60	2548	60	4
Pseudo t0 int	100	5	0.80	60	738	80	4
Pseudo t0 int	100	8	0.80	60	2068	80	4
Pseudo t0 ext	100	0	0.80	60	0	80	4
Pseudo t0 ext	100	0.1	0.80	60	0	80	4
Pseudo t0 ext	100	10	0.80	60	3325	80	4
Pseudo t0 ext	100	12	0.80	60	4878	80	4
Pseudo t0 ext	100	12.5	0.80	60	5312	80	4
Pseudo t0 int	100	5	0.40	90	43	40	4
Pseudo t0 int	100	8	0.40	90	172	40	4
Pseudo t0 ext	100	0	0.40	90	0	40	4
Pseudo t0 ext	100	0.1	0.40	90	0	40	4
Pseudo t0 ext	100	12	0.40	90	622	40	4
Pseudo t0 ext	100	12.5	0.40	90	712	40	4
Pseudo t0 int	100	5	0.60	90	126	60	4
Pseudo t0 int	100	8	0.60	90	501	60	4
Pseudo t0 ext	100	0	0.60	90	0	60	4
Pseudo t0 ext	100	0.1	0.60	90	0	60	4
Pseudo t0 ext	100	12	0.60	90	1842	60	4
Pseudo t0 ext	100	12.5	0.60	90	2112	60	4
Pseudo t0 int	100	5	0.80	90	586	80	4
Pseudo t0 int	100	8	0.80	90	1690	80	4
Pseudo t0 ext	100	0	0.80	90	0	80	4
Pseudo t0 ext	100	0.1	0.80	90	0	80	4
Pseudo t0 ext	100	10	0.80	90	2740	80	4
Pseudo t0 ext	100	12	0.80	90	4041	80	4
Pseudo t0 ext	100	12.5	0.80	90	4406	80	4
Pseudo t0 int	110	4.5	0.36	30	62	40	4
Pseudo t0 int	110	5.5	0.36	30	109	40	4
Pseudo t0 ext	110	0	0.36	30	0	40	4
Pseudo t0 ext	110	0.1	0.36	30	0	40	4
Pseudo t0 ext	110	8	0.36	30	329	40	4
Pseudo t0 ext	110	8.5	0.36	30	395	40	4
Pseudo t0 int	110	4.5	0.55	30	205	60	4
Pseudo t0 int	110	5.5	0.55	30	353	60	4

Pseudo t0 ext	110	0	0.55	30	0	60	4
Pseudo t0 ext	110	0.1	0.55	30	0	60	4
Pseudo t0 ext	110	8	0.55	30	1018	60	4
Pseudo t0 ext	110	8.5	0.55	30	1215	60	4
Pseudo t0 int	110	4.5	0.82	30	1870	90	4
Pseudo t0 int	110	5.5	0.82	30	2902	90	4
Pseudo t0 ext	110	0	0.82	30	0	90	4
Pseudo t0 ext	110	0.1	0.82	30	0	90	4
Pseudo t0 ext	110	8	0.82	30	7105	90	4
Pseudo t0 ext	110	8.5	0.82	30	8318	90	4
Pseudo t0 int	110	4.5	0.36	60	32	40	4
Pseudo t0 int	110	5.5	0.36	60	56	40	4
Pseudo t0 ext	110	0	0.36	60	0	40	4
Pseudo t0 ext	110	0.1	0.36	60	0	40	4
Pseudo t0 ext	110	8	0.36	60	164	40	4
Pseudo t0 ext	110	8.5	0.36	60	195	40	4
Pseudo t0 int	110	4.5	0.55	60	87	60	4
Pseudo t0 int	110	5.5	0.55	60	151	60	4
Pseudo t0 ext	110	0	0.55	60	0	60	4
Pseudo t0 ext	110	0.1	0.55	60	0	60	4
Pseudo t0 ext	110	8	0.55	60	431	60	4
Pseudo t0 ext	110	8.5	0.55	60	510	60	4
Pseudo t0 int	110	4.5	0.82	60	745	90	4
Pseudo t0 int	110	5.5	0.82	60	1155	90	4
Pseudo t0 ext	110	0	0.82	60	0	90	4
Pseudo t0 ext	110	0.1	0.82	60	0	90	4
Pseudo t0 ext	110	8	0.82	60	2567	90	4
Pseudo t0 ext	110	8.5	0.82	60	2916	90	4
Pseudo t0 int	110	4.5	0.36	90	27	40	4
Pseudo t0 int	110	5.5	0.36	90	48	40	4
Pseudo t0 ext	110	0	0.36	90	0	40	4
Pseudo t0 ext	110	0.1	0.36	90	0	40	4
Pseudo t0 ext	110	8	0.36	90	142	40	4
Pseudo t0 ext	110	8.5	0.36	90	170	40	4
Pseudo t0 int	110	4.5	0.55	90	70	60	4
Pseudo t0 int	110	5.5	0.55	90	123	60	4
Pseudo t0 ext	110	0	0.55	90	0	60	4
Pseudo t0 ext	110	0.1	0.55	90	0	60	4
Pseudo t0 ext	110	8	0.55	90	357	60	4
Pseudo t0 ext	110	8.5	0.55	90	424	60	4
Pseudo t0 int	110	4.5	0.82	90	584	90	4
Pseudo t0 int	110	5.5	0.82	90	923	90	4
Pseudo t0 ext	110	0	0.82	90	0	90	4
Pseudo t0 ext	110	0.1	0.82	90	0	90	4
Pseudo t0 ext	110	8	0.82	90	2100	90	4
Pseudo t0 ext	110	8.5	0.82	90	2392	90	4
Pseudo t0 int	120	6.05	0.33	30	123	40	4
Pseudo t0 int	120	8.55	0.33	30	373	40	4
Pseudo t0 ext	120	0	0.33	30	0	40	4
Pseudo t0 ext	120	0.1	0.33	30	0	40	4
Pseudo t0 ext	120	12	0.33	30	1221	40	4
Pseudo t0 ext	120	12.5	0.33	30	1416	40	4
Pseudo t0 int	120	6.05	0.58	30	620	70	4
Pseudo t0 int	120	8.55	0.58	30	1853	70	4
Pseudo t0 ext	120	0	0.58	30	0	70	4
Pseudo t0 ext	120	0.1	0.58	30	0	70	4
Pseudo t0 ext	120	12	0.58	30	6223	70	4
Pseudo t0 ext	120	12.5	0.58	30	7251	70	4
Pseudo t0 int	120	6.05	0.83	30	4596	100	5
Pseudo t0 int	120	8.55	0.83	30	10060	100	5

Pseudo t0 ext	120	0	0.83	30	0	100	5
Pseudo t0 ext	120	0.1	0.83	30	0	100	5
Pseudo t0 ext	120	10	0.83	30	14186	100	5
Pseudo t0 ext	120	12	0.83	30	21028	100	5
Pseudo t0 ext	120	12.5	0.83	30	22948	100	5
Pseudo t0 int	120	6.05	0.33	60	66	40	4
Pseudo t0 int	120	8.55	0.33	60	183	40	4
Pseudo t0 ext	120	0	0.33	60	0	40	4
Pseudo t0 ext	120	0.1	0.33	60	0	40	4
Pseudo t0 ext	120	12	0.33	60	498	40	4
Pseudo t0 ext	120	12.5	0.33	60	562	40	4
Pseudo t0 int	120	6.05	0.58	60	263	70	4
Pseudo t0 int	120	8.55	0.58	60	730	70	4
Pseudo t0 ext	120	0	0.58	60	0	70	4
Pseudo t0 ext	120	0.1	0.58	60	0	70	4
Pseudo t0 ext	120	12	0.58	60	1967	70	4
Pseudo t0 ext	120	12.5	0.58	60	2214	70	4
Pseudo t0 int	120	6.05	0.83	60	1787	100	5
Pseudo t0 int	120	8.55	0.83	60	3774	100	5
Pseudo t0 ext	120	0	0.83	60	0	100	5
Pseudo t0 ext	120	0.1	0.83	60	0	100	5
Pseudo t0 ext	120	10	0.83	60	5262	100	5
Pseudo t0 ext	120	12	0.83	60	7717	100	5
Pseudo t0 ext	120	12.5	0.83	60	8404	100	5
Pseudo t0 int	120	6.05	0.33	90	57	40	4
Pseudo t0 int	120	8.55	0.33	90	160	40	4
Pseudo t0 ext	120	0	0.33	90	0	40	4
Pseudo t0 ext	120	0.1	0.33	90	0	40	4
Pseudo t0 ext	120	12	0.33	90	433	40	4
Pseudo t0 ext	120	12.5	0.33	90	488	40	4
Pseudo t0 int	120	6.05	0.58	90	214	70	4
Pseudo t0 int	120	8.55	0.58	90	600	70	4
Pseudo t0 ext	120	0	0.58	90	0	70	4
Pseudo t0 ext	120	0.1	0.58	90	0	70	4
Pseudo t0 ext	120	12	0.58	90	1626	70	4
Pseudo t0 ext	120	12.5	0.58	90	1831	70	4
Pseudo t0 int	120	6.05	0.83	90	1430	100	5
Pseudo t0 int	120	8.55	0.83	90	3078	100	5
Pseudo t0 ext	120	0	0.83	90	0	100	5
Pseudo t0 ext	120	0.1	0.83	90	0	100	5
Pseudo t0 ext	120	10	0.83	90	4317	100	5
Pseudo t0 ext	120	12	0.83	90	6367	100	5
Pseudo t0 ext	120	12.5	0.83	90	6942	100	5
Pseudo t0 int	140	6.05	0.29	30	93	40	4
Pseudo t0 int	140	8.55	0.29	30	273	40	4
Pseudo t0 ext	140	0	0.29	30	0	40	4
Pseudo t0 ext	140	0.1	0.29	30	0	40	4
Pseudo t0 ext	140	12	0.29	30	833	40	4
Pseudo t0 ext	140	12.5	0.29	30	957	40	4
Pseudo t0 int	140	6.05	0.57	30	597	80	5
Pseudo t0 int	140	8.55	0.57	30	1637	80	5
Pseudo t0 ext	140	0	0.57	30	0	80	5
Pseudo t0 ext	140	0.1	0.57	30	0	80	5
Pseudo t0 ext	140	12	0.57	30	4715	80	5
Pseudo t0 ext	140	12.5	0.57	30	5380	80	5
Pseudo t0 int	140	6.05	0.79	30	3334	110	5
Pseudo t0 int	140	8.55	0.79	30	7390	110	5
Pseudo t0 ext	140	0	0.79	30	0	110	5
Pseudo t0 ext	140	0.1	0.79	30	0	110	5
Pseudo t0 ext	140	10	0.79	30	10461	110	5

Pseudo t0 ext	140	12	0.79	30	15563	110	5
Pseudo t0 ext	140	12.5	0.79	30	16995	110	5
Pseudo t0 int	140	6.05	0.29	60	53	40	4
Pseudo t0 int	140	8.55	0.29	60	146	40	4
Pseudo t0 ext	140	0	0.29	60	0	40	4
Pseudo t0 ext	140	0.1	0.29	60	0	40	4
Pseudo t0 ext	140	12	0.29	60	394	40	4
Pseudo t0 ext	140	12.5	0.29	60	443	40	4
Pseudo t0 int	140	6.05	0.57	60	250	80	5
Pseudo t0 int	140	8.55	0.57	60	684	80	5
Pseudo t0 ext	140	0	0.57	60	0	80	5
Pseudo t0 ext	140	0.1	0.57	60	0	80	5
Pseudo t0 ext	140	12	0.57	60	1809	80	5
Pseudo t0 ext	140	12.5	0.57	60	2032	80	5
Pseudo t0 int	140	6.05	0.79	60	1313	110	5
Pseudo t0 int	140	8.55	0.79	60	3041	110	5
Pseudo t0 ext	140	0	0.79	60	0	110	5
Pseudo t0 ext	140	0.1	0.79	60	0	110	5
Pseudo t0 ext	140	10	0.79	60	4362	110	5
Pseudo t0 ext	140	12	0.79	60	6567	110	5
Pseudo t0 ext	140	12.5	0.79	60	7187	110	5
Pseudo t0 int	140	6.05	0.29	90	47	40	4
Pseudo t0 int	140	8.55	0.29	90	130	40	4
Pseudo t0 ext	140	0	0.29	90	0	40	4
Pseudo t0 ext	140	0.1	0.29	90	0	40	4
Pseudo t0 ext	140	12	0.29	90	349	40	4
Pseudo t0 ext	140	12.5	0.29	90	392	40	4
Pseudo t0 int	140	6.05	0.57	90	205	80	5
Pseudo t0 int	140	8.55	0.57	90	565	80	5
Pseudo t0 ext	140	0	0.57	90	0	80	5
Pseudo t0 ext	140	0.1	0.57	90	0	80	5
Pseudo t0 ext	140	12	0.57	90	1505	80	5
Pseudo t0 ext	140	12.5	0.57	90	1691	80	5
Pseudo t0 int	140	6.05	0.79	90	1042	110	5
Pseudo t0 int	140	8.55	0.79	90	2466	110	5
Pseudo t0 ext	140	0	0.79	90	0	110	5
Pseudo t0 ext	140	0.1	0.79	90	0	110	5
Pseudo t0 ext	140	10	0.79	90	3558	110	5
Pseudo t0 ext	140	12	0.79	90	5385	110	5
Pseudo t0 ext	140	12.5	0.79	90	5900	110	5
Pseudo t0 int	150	7.4	0.27	30	147	40	4
Pseudo t0 int	150	10.65	0.27	30	531	40	4
Pseudo t0 ext	150	0	0.27	30	0	40	4
Pseudo t0 ext	150	0.1	0.27	30	0	40	4
Pseudo t0 ext	150	14.5	0.27	30	1851	40	4
Pseudo t0 ext	150	15	0.27	30	2133	40	4
Pseudo t0 int	150	7.4	0.53	30	792	80	5
Pseudo t0 int	150	10.65	0.53	30	2713	80	5
Pseudo t0 ext	150	0	0.53	30	0	80	5
Pseudo t0 ext	150	0.1	0.53	30	0	80	5
Pseudo t0 ext	150	14.5	0.53	30	9205	80	5
Pseudo t0 ext	150	15	0.53	30	10587	80	5
Pseudo t0 int	150	7.4	0.80	30	6411	120	6
Pseudo t0 int	150	10.65	0.80	30	15051	120	6
Pseudo t0 ext	150	0	0.80	30	0	120	6
Pseudo t0 ext	150	0.1	0.80	30	0	120	6
Pseudo t0 ext	150	12.5	0.80	30	21559	120	6
Pseudo t0 ext	150	14.5	0.80	30	29893	120	6
Pseudo t0 ext	150	15	0.80	30	32187	120	6
Pseudo t0 int	150	7.4	0.27	60	87	40	4

Pseudo t0 int	150	10.65	0.27	60	262	40	4
Pseudo t0 ext	150	0	0.27	60	0	40	4
Pseudo t0 ext	150	0.1	0.27	60	0	40	4
Pseudo t0 ext	150	14.5	0.27	60	695	40	4
Pseudo t0 ext	150	15	0.27	60	776	40	4
Pseudo t0 int	150	7.4	0.53	60	349	80	5
Pseudo t0 int	150	10.65	0.53	60	1101	80	5
Pseudo t0 ext	150	0	0.53	60	0	80	5
Pseudo t0 ext	150	0.1	0.53	60	0	80	5
Pseudo t0 ext	150	14.5	0.53	60	3201	80	5
Pseudo t0 ext	150	15	0.53	60	3615	80	5
Pseudo t0 int	150	7.4	0.80	60	2481	120	6
Pseudo t0 int	150	10.65	0.80	60	5796	120	6
Pseudo t0 ext	150	0	0.80	60	0	120	6
Pseudo t0 ext	150	0.1	0.80	60	0	120	6
Pseudo t0 ext	150	12.5	0.80	60	8291	120	6
Pseudo t0 ext	150	14.5	0.80	60	11484	120	6
Pseudo t0 ext	150	15	0.80	60	12363	120	6
Pseudo t0 int	150	7.4	0.27	90	78	40	4
Pseudo t0 int	150	10.65	0.27	90	233	40	4
Pseudo t0 ext	150	0	0.27	90	0	40	4
Pseudo t0 ext	150	0.1	0.27	90	0	40	4
Pseudo t0 ext	150	14.5	0.27	90	609	40	4
Pseudo t0 ext	150	15	0.27	90	678	40	4
Pseudo t0 int	150	7.4	0.53	90	290	80	5
Pseudo t0 int	150	10.65	0.53	90	919	80	5
Pseudo t0 ext	150	0	0.53	90	0	80	5
Pseudo t0 ext	150	0.1	0.53	90	0	80	5
Pseudo t0 ext	150	14.5	0.53	90	2677	80	5
Pseudo t0 ext	150	15	0.53	90	3023	80	5
Pseudo t0 int	150	7.4	0.80	90	1984	120	6
Pseudo t0 int	150	10.65	0.80	90	4752	120	6
Pseudo t0 ext	150	0	0.80	90	0	120	6
Pseudo t0 ext	150	0.1	0.80	90	0	120	6
Pseudo t0 ext	150	12.5	0.80	90	6844	120	6
Pseudo t0 ext	150	14.5	0.80	90	9529	120	6
Pseudo t0 ext	150	15	0.80	90	10269	120	6
Pseudo t0 int	160	7.4	0.25	30	134	40	4
Pseudo t0 int	160	10.65	0.25	30	467	40	4
Pseudo t0 ext	160	0	0.25	30	0	40	4
Pseudo t0 ext	160	0.1	0.25	30	0	40	4
Pseudo t0 ext	160	14.5	0.25	30	1555	40	4
Pseudo t0 ext	160	15	0.25	30	1783	40	4
Pseudo t0 int	160	7.4	0.56	30	983	90	5
Pseudo t0 int	160	10.65	0.56	30	3236	90	5
Pseudo t0 ext	160	0	0.56	30	0	90	5
Pseudo t0 ext	160	0.1	0.56	30	0	90	5
Pseudo t0 ext	160	14.5	0.56	30	10527	90	5
Pseudo t0 ext	160	15	0.56	30	12056	90	5
Pseudo t0 int	160	7.4	0.75	30	4283	120	6
Pseudo t0 int	160	10.65	0.75	30	10203	120	6
Pseudo t0 ext	160	0	0.75	30	0	120	6
Pseudo t0 ext	160	0.1	0.75	30	0	120	6
Pseudo t0 ext	160	12.5	0.75	30	14675	120	6
Pseudo t0 ext	160	14.5	0.75	30	20410	120	6
Pseudo t0 ext	160	15	0.75	30	21990	120	6
Pseudo t0 int	160	7.4	0.25	60	81	40	4
Pseudo t0 int	160	10.65	0.25	60	242	40	4
Pseudo t0 ext	160	0	0.25	60	0	40	4
Pseudo t0 ext	160	0.1	0.25	60	0	40	4

Pseudo t0 ext	160	14.5	0.25	60	633	40	4
Pseudo t0 ext	160	15	0.25	60	705	40	4
Pseudo t0 int	160	7.4	0.56	60	422	90	5
Pseudo t0 int	160	10.65	0.56	60	1313	90	5
Pseudo t0 ext	160	0	0.56	60	0	90	5
Pseudo t0 ext	160	0.1	0.56	60	0	90	5
Pseudo t0 ext	160	14.5	0.56	60	3746	90	5
Pseudo t0 ext	160	15	0.56	60	4220	90	5
Pseudo t0 int	160	7.4	0.75	60	1681	120	6
Pseudo t0 int	160	10.65	0.75	60	4153	120	6
Pseudo t0 ext	160	0	0.75	60	0	120	6
Pseudo t0 ext	160	0.1	0.75	60	0	120	6
Pseudo t0 ext	160	12.5	0.75	60	6034	120	6
Pseudo t0 ext	160	14.5	0.75	60	8453	120	6
Pseudo t0 ext	160	15	0.75	60	9121	120	6
Pseudo t0 int	160	7.4	0.25	90	73	40	4
Pseudo t0 int	160	10.65	0.25	90	216	40	4
Pseudo t0 ext	160	0	0.25	90	0	40	4
Pseudo t0 ext	160	0.1	0.25	90	0	40	4
Pseudo t0 ext	160	14.5	0.25	90	559	40	4
Pseudo t0 ext	160	15	0.25	90	621	40	4
Pseudo t0 int	160	7.4	0.56	90	348	90	5
Pseudo t0 int	160	10.65	0.56	90	1090	90	5
Pseudo t0 ext	160	0	0.56	90	0	90	5
Pseudo t0 ext	160	0.1	0.56	90	0	90	5
Pseudo t0 ext	160	14.5	0.56	90	3123	90	5
Pseudo t0 ext	160	15	0.56	90	3520	90	5
Pseudo t0 int	160	7.4	0.75	90	1341	120	6
Pseudo t0 int	160	10.65	0.75	90	3381	120	6
Pseudo t0 ext	160	0	0.75	90	0	120	6
Pseudo t0 ext	160	0.1	0.75	90	0	120	6
Pseudo t0 ext	160	12.5	0.75	90	4938	120	6
Pseudo t0 ext	160	14.5	0.75	90	6945	120	6
Pseudo t0 ext	160	15	0.75	90	7499	120	6
Pseudo t0 int	180	7.95	0.28	30	205	50	4
Pseudo t0 int	180	10.65	0.28	30	530	50	4
Pseudo t0 ext	180	0	0.28	30	0	50	4
Pseudo t0 ext	180	0.1	0.28	30	0	50	4
Pseudo t0 ext	180	14.5	0.28	30	1665	50	4
Pseudo t0 ext	180	15	0.28	30	1901	50	4
Pseudo t0 int	180	7.95	0.56	30	1209	100	6
Pseudo t0 int	180	10.65	0.56	30	2952	100	6
Pseudo t0 ext	180	0	0.56	30	0	100	6
Pseudo t0 ext	180	0.1	0.56	30	0	100	6
Pseudo t0 ext	180	14.5	0.56	30	8989	100	6
Pseudo t0 ext	180	15	0.56	30	10242	100	6
Pseudo t0 int	180	7.95	0.83	30	10680	150	7.1
Pseudo t0 int	180	10.65	0.83	30	20270	150	7.1
Pseudo t0 ext	180	0	0.83	30	0	150	7.1
Pseudo t0 ext	180	0.1	0.83	30	0	150	7.1
Pseudo t0 ext	180	12.5	0.83	30	28588	150	7.1
Pseudo t0 ext	180	14.5	0.83	30	39178	150	7.1
Pseudo t0 ext	180	15	0.83	30	42085	150	7.1
Pseudo t0 int	180	7.95	0.28	60	117	50	4
Pseudo t0 int	180	10.65	0.28	60	282	50	4
Pseudo t0 ext	180	0	0.28	60	0	50	4
Pseudo t0 ext	180	0.1	0.28	60	0	50	4
Pseudo t0 ext	180	14.5	0.28	60	756	50	4
Pseudo t0 ext	180	15	0.28	60	846	50	4
Pseudo t0 int	180	7.95	0.56	60	516	100	6

Pseudo t0 int	180	10.65	0.56	60	1252	100	6
Pseudo t0 ext	180	0	0.56	60	0	100	6
Pseudo t0 ext	180	0.1	0.56	60	0	100	6
Pseudo t0 ext	180	14.5	0.56	60	3592	100	6
Pseudo t0 ext	180	15	0.56	60	4058	100	6
Pseudo t0 int	180	7.95	0.83	60	4294	150	7.1
Pseudo t0 int	180	10.65	0.83	60	8243	150	7.1
Pseudo t0 ext	180	0	0.83	60	0	150	7.1
Pseudo t0 ext	180	0.1	0.83	60	0	150	7.1
Pseudo t0 ext	180	12.5	0.83	60	11680	150	7.1
Pseudo t0 ext	180	14.5	0.83	60	16062	150	7.1
Pseudo t0 ext	180	15	0.83	60	17266	150	7.1
Pseudo t0 int	180	7.95	0.28	90	105	50	4
Pseudo t0 int	180	10.65	0.28	90	252	50	4
Pseudo t0 ext	180	0	0.28	90	0	50	4
Pseudo t0 ext	180	0.1	0.28	90	0	50	4
Pseudo t0 ext	180	14.5	0.28	90	669	50	4
Pseudo t0 ext	180	15	0.28	90	747	50	4
Pseudo t0 int	180	7.95	0.56	90	424	100	6
Pseudo t0 int	180	10.65	0.56	90	1037	100	6
Pseudo t0 ext	180	0	0.56	90	0	100	6
Pseudo t0 ext	180	0.1	0.56	90	0	100	6
Pseudo t0 ext	180	14.5	0.56	90	2993	100	6
Pseudo t0 ext	180	15	0.56	90	3383	100	6
Pseudo t0 int	180	7.95	0.83	90	3408	150	7.1
Pseudo t0 int	180	10.65	0.83	90	6677	150	7.1
Pseudo t0 ext	180	0	0.83	90	0	150	7.1
Pseudo t0 ext	180	0.1	0.83	90	0	150	7.1
Pseudo t0 ext	180	12.5	0.83	90	9536	150	7.1
Pseudo t0 ext	180	14.5	0.83	90	13192	150	7.1
Pseudo t0 ext	180	15	0.83	90	14198	150	7.1
Pseudo t0 int	200	7.95	0.25	30	171	50	4
Pseudo t0 int	200	10.65	0.25	30	431	50	4
Pseudo t0 ext	200	0	0.25	30	0	50	4
Pseudo t0 ext	200	0.1	0.25	30	0	50	4
Pseudo t0 ext	200	14.5	0.25	30	1283	50	4
Pseudo t0 ext	200	15	0.25	30	1454	50	4
Pseudo t0 int	200	7.95	0.55	30	1173	110	5
Pseudo t0 int	200	10.65	0.55	30	2838	110	5
Pseudo t0 ext	200	0	0.55	30	0	110	5
Pseudo t0 ext	200	0.1	0.55	30	0	110	5
Pseudo t0 ext	200	14.5	0.55	30	8444	110	5
Pseudo t0 ext	200	15	0.55	30	9594	110	5
Pseudo t0 int	200	7.95	0.80	30	8607	160	7.1
Pseudo t0 int	200	10.65	0.80	30	16279	160	7.1
Pseudo t0 ext	200	0	0.80	30	0	160	7.1
Pseudo t0 ext	200	0.1	0.80	30	0	160	7.1
Pseudo t0 ext	200	12.5	0.80	30	22927	160	7.1
Pseudo t0 ext	200	14.5	0.80	30	31386	160	7.1
Pseudo t0 ext	200	15	0.80	30	33708	160	7.1
Pseudo t0 int	200	7.95	0.25	60	102	50	4
Pseudo t0 int	200	10.65	0.25	60	245	50	4
Pseudo t0 ext	200	0	0.25	60	0	50	4
Pseudo t0 ext	200	0.1	0.25	60	0	50	4
Pseudo t0 ext	200	14.5	0.25	60	644	50	4
Pseudo t0 ext	200	15	0.25	60	718	50	4
Pseudo t0 int	200	7.95	0.55	60	502	110	5
Pseudo t0 int	200	10.65	0.55	60	1208	110	5
Pseudo t0 ext	200	0	0.55	60	0	110	5
Pseudo t0 ext	200	0.1	0.55	60	0	110	5

Pseudo t0 ext	200	14.5	0.55	60	3395	110	5
Pseudo t0 ext	200	15	0.55	60	3825	110	5
Pseudo t0 int	200	7.95	0.80	60	3420	160	7.1
Pseudo t0 int	200	10.65	0.80	60	6795	160	7.1
Pseudo t0 ext	200	0	0.80	60	0	160	7.1
Pseudo t0 ext	200	0.1	0.80	60	0	160	7.1
Pseudo t0 ext	200	12.5	0.80	60	9757	160	7.1
Pseudo t0 ext	200	14.5	0.80	60	13553	160	7.1
Pseudo t0 ext	200	15	0.80	60	14599	160	7.1
Pseudo t0 int	200	7.95	0.25	90	92	50	4
Pseudo t0 int	200	10.65	0.25	90	220	50	4
Pseudo t0 ext	200	0	0.25	90	0	50	4
Pseudo t0 ext	200	0.1	0.25	90	0	50	4
Pseudo t0 ext	200	14.5	0.25	90	574	50	4
Pseudo t0 ext	200	15	0.25	90	639	50	4
Pseudo t0 int	200	7.95	0.55	90	405	110	5
Pseudo t0 int	200	10.65	0.55	90	986	110	5
Pseudo t0 ext	200	0	0.55	90	0	110	5
Pseudo t0 ext	200	0.1	0.55	90	0	110	5
Pseudo t0 ext	200	14.5	0.55	90	2793	110	5
Pseudo t0 ext	200	15	0.55	90	3150	110	5
Pseudo t0 int	200	7.95	0.80	90	2692	160	7.1
Pseudo t0 int	200	10.65	0.80	90	5439	160	7.1
Pseudo t0 ext	200	0	0.80	90	0	160	7.1
Pseudo t0 ext	200	0.1	0.80	90	0	160	7.1
Pseudo t0 ext	200	12.5	0.80	90	7857	160	7.1
Pseudo t0 ext	200	14.5	0.80	90	10963	160	7.1
Pseudo t0 ext	200	15	0.80	90	11820	160	7.1
Pseudo t0 int	220	9	0.27	30	286	60	4
Pseudo t0 int	220	11.25	0.27	30	583	60	4
Pseudo t0 ext	220	0	0.27	30	0	60	4
Pseudo t0 ext	220	0.1	0.27	30	0	60	4
Pseudo t0 ext	220	14.5	0.27	30	1447	60	4
Pseudo t0 ext	220	15	0.27	30	1644	60	4
Pseudo t0 int	220	9	0.55	30	1578	120	7.1
Pseudo t0 int	220	11.25	0.55	30	3066	120	7.1
Pseudo t0 ext	220	0	0.55	30	0	120	7.1
Pseudo t0 ext	220	0.1	0.55	30	0	120	7.1
Pseudo t0 ext	220	14.5	0.55	30	7358	120	7.1
Pseudo t0 ext	220	15	0.55	30	8340	120	7.1
Pseudo t0 int	220	9	0.82	30	14543	180	7.1
Pseudo t0 int	220	11.25	0.82	30	23780	180	7.1
Pseudo t0 ext	220	0	0.82	30	0	180	7.1
Pseudo t0 ext	220	0.1	0.82	30	0	180	7.1
Pseudo t0 ext	220	12.5	0.82	30	29880	180	7.1
Pseudo t0 ext	220	14.5	0.82	30	41080	180	7.1
Pseudo t0 ext	220	15	0.82	30	44157	180	7.1
Pseudo t0 int	220	9	0.27	60	166	60	4
Pseudo t0 int	220	11.25	0.27	60	325	60	4
Pseudo t0 ext	220	0	0.27	60	0	60	4
Pseudo t0 ext	220	0.1	0.27	60	0	60	4
Pseudo t0 ext	220	14.5	0.27	60	739	60	4
Pseudo t0 ext	220	15	0.27	60	828	60	4
Pseudo t0 int	220	9	0.55	60	676	120	7.1
Pseudo t0 int	220	11.25	0.55	60	1335	120	7.1
Pseudo t0 ext	220	0	0.55	60	0	120	7.1
Pseudo t0 ext	220	0.1	0.55	60	0	120	7.1
Pseudo t0 ext	220	14.5	0.55	60	3214	120	7.1
Pseudo t0 ext	220	15	0.55	60	3640	120	7.1
Pseudo t0 int	220	9	0.82	60	5833	180	7.1

Pseudo t0 int	220	11.25	0.82	60	9727	180	7.1
Pseudo t0 ext	220	0	0.82	60	0	180	7.1
Pseudo t0 ext	220	0.1	0.82	60	0	180	7.1
Pseudo t0 ext	220	12.5	0.82	60	12311	180	7.1
Pseudo t0 ext	220	14.5	0.82	60	17073	180	7.1
Pseudo t0 ext	220	15	0.82	60	18384	180	7.1
Pseudo t0 int	220	9	0.27	90	148	60	4
Pseudo t0 int	220	11.25	0.27	90	291	60	4
Pseudo t0 ext	220	0	0.27	90	0	60	4
Pseudo t0 ext	220	0.1	0.27	90	0	60	4
Pseudo t0 ext	220	14.5	0.27	90	657	60	4
Pseudo t0 ext	220	15	0.27	90	735	60	4
Pseudo t0 int	220	9	0.55	90	557	120	7.1
Pseudo t0 int	220	11.25	0.55	90	1108	120	7.1
Pseudo t0 ext	220	0	0.55	90	0	120	7.1
Pseudo t0 ext	220	0.1	0.55	90	0	120	7.1
Pseudo t0 ext	220	14.5	0.55	90	2685	120	7.1
Pseudo t0 ext	220	15	0.55	90	3043	120	7.1
Pseudo t0 int	220	9	0.82	90	4629	180	7.1
Pseudo t0 int	220	11.25	0.82	90	7813	180	7.1
Pseudo t0 ext	220	0	0.82	90	0	180	7.1
Pseudo t0 ext	220	0.1	0.82	90	0	180	7.1
Pseudo t0 ext	220	12.5	0.82	90	9933	180	7.1
Pseudo t0 ext	220	14.5	0.82	90	13846	180	7.1
Pseudo t0 ext	220	15	0.82	90	14924	180	7.1
Pseudo t0 int	250	9.4	0.28	30	345	70	4
Pseudo t0 int	250	11.25	0.28	30	604	70	4
Pseudo t0 ext	250	0	0.28	30	0	70	4
Pseudo t0 ext	250	0.1	0.28	30	0	70	4
Pseudo t0 ext	250	14.5	0.28	30	1452	70	4
Pseudo t0 ext	250	15	0.28	30	1643	70	4
Pseudo t0 int	250	9.4	0.56	30	2046	140	7.1
Pseudo t0 int	250	11.25	0.56	30	3441	140	7.1
Pseudo t0 ext	250	0	0.56	30	0	140	7.1
Pseudo t0 ext	250	0.1	0.56	30	0	140	7.1
Pseudo t0 ext	250	14.5	0.56	30	8016	140	7.1
Pseudo t0 ext	250	15	0.56	30	9055	140	7.1
Pseudo t0 int	250	9.4	0.80	30	14636	200	7.1
Pseudo t0 int	250	11.25	0.80	30	22053	200	7.1
Pseudo t0 ext	250	0	0.80	30	0	200	7.1
Pseudo t0 ext	250	0.1	0.80	30	0	200	7.1
Pseudo t0 ext	250	12.5	0.80	30	27909	200	7.1
Pseudo t0 ext	250	14.5	0.80	30	38698	200	7.1
Pseudo t0 ext	250	15	0.80	30	41668	200	7.1
Pseudo t0 int	250	9.4	0.28	60	198	70	4
Pseudo t0 int	250	11.25	0.28	60	339	70	4
Pseudo t0 ext	250	0	0.28	60	0	70	4
Pseudo t0 ext	250	0.1	0.28	60	0	70	4
Pseudo t0 ext	250	14.5	0.28	60	766	70	4
Pseudo t0 ext	250	15	0.28	60	858	70	4
Pseudo t0 int	250	9.4	0.56	60	865	140	7.1
Pseudo t0 int	250	11.25	0.56	60	1482	140	7.1
Pseudo t0 ext	250	0	0.56	60	0	140	7.1
Pseudo t0 ext	250	0.1	0.56	60	0	140	7.1
Pseudo t0 ext	250	14.5	0.56	60	3519	140	7.1
Pseudo t0 ext	250	15	0.56	60	3982	140	7.1
Pseudo t0 int	250	9.4	0.80	60	5821	200	7.1
Pseudo t0 int	250	11.25	0.80	60	8960	200	7.1
Pseudo t0 ext	250	0	0.80	60	0	200	7.1
Pseudo t0 ext	250	0.1	0.80	60	0	200	7.1

Pseudo t0 ext	250	12.5	0.80	60	11453	200	7.1
Pseudo t0 ext	250	14.5	0.80	60	16065	200	7.1
Pseudo t0 ext	250	15	0.80	60	17338	200	7.1
Pseudo t0 int	250	9.4	0.28	90	176	70	4
Pseudo t0 int	250	11.25	0.28	90	303	70	4
Pseudo t0 ext	250	0	0.28	90	0	70	4
Pseudo t0 ext	250	0.1	0.28	90	0	70	4
Pseudo t0 ext	250	14.5	0.28	90	682	70	4
Pseudo t0 ext	250	15	0.28	90	762	70	4
Pseudo t0 int	250	9.4	0.56	90	708	140	7.1
Pseudo t0 int	250	11.25	0.56	90	1221	140	7.1
Pseudo t0 ext	250	0	0.56	90	0	140	7.1
Pseudo t0 ext	250	0.1	0.56	90	0	140	7.1
Pseudo t0 ext	250	14.5	0.56	90	2925	140	7.1
Pseudo t0 ext	250	15	0.56	90	3314	140	7.1
Pseudo t0 int	250	9.4	0.80	90	4601	200	7.1
Pseudo t0 int	250	11.25	0.80	90	7202	200	7.1
Pseudo t0 ext	250	0	0.80	90	0	200	7.1
Pseudo t0 ext	250	0.1	0.80	90	0	200	7.1
Pseudo t0 ext	250	12.5	0.80	90	9275	200	7.1
Pseudo t0 ext	250	14.5	0.80	90	13122	200	7.1
Pseudo t0 ext	250	15	0.80	90	14186	200	7.1
Pseudo t0 int	260	9.4	0.27	30	323	70	4
Pseudo t0 int	260	11.25	0.27	30	563	70	4
Pseudo t0 ext	260	0	0.27	30	0	70	4
Pseudo t0 ext	260	0.1	0.27	30	0	70	4
Pseudo t0 ext	260	14.5	0.27	30	1337	70	4
Pseudo t0 ext	260	15	0.27	30	1510	70	4
Pseudo t0 int	260	9.4	0.54	30	1783	140	7.1
Pseudo t0 int	260	11.25	0.54	30	2995	140	7.1
Pseudo t0 ext	260	0	0.54	30	0	140	7.1
Pseudo t0 ext	260	0.1	0.54	30	0	140	7.1
Pseudo t0 ext	260	14.5	0.54	30	6894	140	7.1
Pseudo t0 ext	260	15	0.54	30	7771	140	7.1
Pseudo t0 int	260	9.4	0.85	30	23738	220	8.8
Pseudo t0 int	260	11.25	0.85	30	34155	220	8.8
Pseudo t0 ext	260	0	0.85	30	0	220	8.8
Pseudo t0 ext	260	0.1	0.85	30	0	220	8.8
Pseudo t0 ext	260	12.5	0.85	30	42263	220	8.8
Pseudo t0 ext	260	14.5	0.85	30	57030	220	8.8
Pseudo t0 ext	260	15	0.85	30	61067	220	8.8
Pseudo t0 int	260	9.4	0.27	60	188	70	4
Pseudo t0 int	260	11.25	0.27	60	322	70	4
Pseudo t0 ext	260	0	0.27	60	0	70	4
Pseudo t0 ext	260	0.1	0.27	60	0	70	4
Pseudo t0 ext	260	14.5	0.27	60	723	70	4
Pseudo t0 ext	260	15	0.27	60	808	70	4
Pseudo t0 int	260	9.4	0.54	60	767	140	7.1
Pseudo t0 int	260	11.25	0.54	60	1311	140	7.1
Pseudo t0 ext	260	0	0.54	60	0	140	7.1
Pseudo t0 ext	260	0.1	0.54	60	0	140	7.1
Pseudo t0 ext	260	14.5	0.54	60	3070	140	7.1
Pseudo t0 ext	260	15	0.54	60	3465	140	7.1
Pseudo t0 int	260	9.4	0.85	60	9560	220	8.8
Pseudo t0 int	260	11.25	0.85	60	14113	220	8.8
Pseudo t0 ext	260	0	0.85	60	0	220	8.8
Pseudo t0 ext	260	0.1	0.85	60	0	220	8.8
Pseudo t0 ext	260	12.5	0.85	60	17688	220	8.8
Pseudo t0 ext	260	14.5	0.85	60	24243	220	8.8
Pseudo t0 ext	260	15	0.85	60	26042	220	8.8

Pseudo t0 int	260	9.4	0.27	90	169	70	4
Pseudo t0 int	260	11.25	0.27	90	289	70	4
Pseudo t0 ext	260	0	0.27	90	0	70	4
Pseudo t0 ext	260	0.1	0.27	90	0	70	4
Pseudo t0 ext	260	14.5	0.27	90	647	70	4
Pseudo t0 ext	260	15	0.27	90	722	70	4
Pseudo t0 int	260	9.4	0.54	90	630	140	7.1
Pseudo t0 int	260	11.25	0.54	90	1083	140	7.1
Pseudo t0 ext	260	0	0.54	90	0	140	7.1
Pseudo t0 ext	260	0.1	0.54	90	0	140	7.1
Pseudo t0 ext	260	14.5	0.54	90	2555	140	7.1
Pseudo t0 ext	260	15	0.54	90	2887	140	7.1
Pseudo t0 int	260	9.4	0.85	90	7495	220	8.8
Pseudo t0 int	260	11.25	0.85	90	11236	220	8.8
Pseudo t0 ext	260	0	0.85	90	0	220	8.8
Pseudo t0 ext	260	0.1	0.85	90	0	220	8.8
Pseudo t0 ext	260	12.5	0.85	90	14186	220	8.8
Pseudo t0 ext	260	14.5	0.85	90	19614	220	8.8
Pseudo t0 ext	260	15	0.85	90	21107	220	8.8
Pseudo t0 int	300	11.25	0.27	30	559	80	5
Pseudo t0 ext	300	0	0.27	30	0	80	5
Pseudo t0 ext	300	0.1	0.27	30	0	80	5
Pseudo t0 ext	300	14.5	0.27	30	1223	80	5
Pseudo t0 ext	300	15	0.27	30	1358	80	5
Pseudo t0 int	300	11.25	0.53	30	3020	160	8
Pseudo t0 ext	300	0	0.53	30	0	160	8
Pseudo t0 ext	300	0.1	0.53	30	0	160	8
Pseudo t0 ext	300	14.5	0.53	30	6349	160	8
Pseudo t0 ext	300	15	0.53	30	7009	160	8
Pseudo t0 int	300	11.25	0.83	30	35893	250	10
Pseudo t0 ext	300	0	0.83	30	0	250	10
Pseudo t0 ext	300	0.1	0.83	30	0	250	10
Pseudo t0 ext	300	14.5	0.83	30	63569	250	10
Pseudo t0 ext	300	15	0.83	30	68516	250	10
Pseudo t0 int	300	11.25	0.27	60	324	80	5
Pseudo t0 ext	300	0	0.27	60	0	80	5
Pseudo t0 ext	300	0.1	0.27	60	0	80	5
Pseudo t0 ext	300	14.5	0.27	60	695	80	5
Pseudo t0 ext	300	15	0.27	60	770	80	5
Pseudo t0 int	300	11.25	0.53	60	1301	160	8
Pseudo t0 ext	300	0	0.53	60	0	160	8
Pseudo t0 ext	300	0.1	0.53	60	0	160	8
Pseudo t0 ext	300	14.5	0.53	60	2829	160	8
Pseudo t0 ext	300	15	0.53	60	3139	160	8
Pseudo t0 int	300	11.25	0.83	60	14379	250	10
Pseudo t0 ext	300	0	0.83	60	0	250	10
Pseudo t0 ext	300	0.1	0.83	60	0	250	10
Pseudo t0 ext	300	14.5	0.83	60	26515	250	10
Pseudo t0 ext	300	15	0.83	60	28700	250	10
Pseudo t0 int	300	11.25	0.27	90	292	80	5
Pseudo t0 ext	300	0	0.27	90	0	80	5
Pseudo t0 ext	300	0.1	0.27	90	0	80	5
Pseudo t0 ext	300	14.5	0.27	90	627	80	5
Pseudo t0 ext	300	15	0.27	90	694	80	5
Pseudo t0 int	300	11.25	0.53	90	1073	160	8
Pseudo t0 ext	300	0	0.53	90	0	160	8
Pseudo t0 ext	300	0.1	0.53	90	0	160	8
Pseudo t0 ext	300	14.5	0.53	90	2353	160	8
Pseudo t0 ext	300	15	0.53	90	2614	160	8
Pseudo t0 int	300	11.25	0.83	90	11392	250	10

Pseudo t0 ext	300	0	0.83	90	0	250	10
Pseudo t0 ext	300	0.1	0.83	90	0	250	10
Pseudo t0 ext	300	14.5	0.83	90	21316	250	10
Pseudo t0 ext	300	15	0.83	90	23107	250	10
Pseudo β int	100	4	0.50	30	89	50	4
Pseudo β int	100	4	0.70	30	524	70	4
Pseudo β ext	100	4	0.00	30	0	0	0
Pseudo β ext	100	4	0.01	30	0	1	0
Pseudo β ext	100	4	0.90	30	2194	90	4
Pseudo β ext	100	4	0.95	30	2945	95	4
Pseudo β int	100	6	0.50	30	293	50	4
Pseudo β int	100	6	0.70	30	1397	70	4
Pseudo β ext	100	6	0.00	30	0	0	0
Pseudo β ext	100	6	0.01	30	0	1	0
Pseudo β ext	100	6	0.90	30	5308	90	4
Pseudo β ext	100	6	0.95	30	7035	95	4
Pseudo β int	100	10	0.50	30	2303	50	4
Pseudo β int	100	10	0.70	30	6136	70	4
Pseudo β ext	100	10	0.00	30	0	0	0
Pseudo β ext	100	10	0.01	30	0	1	0
Pseudo β ext	100	10	0.90	30	11102	90	4
Pseudo β ext	100	10	0.95	30	12334	95	4
Pseudo β int	100	4	0.50	60	39	50	4
Pseudo β int	100	4	0.70	60	205	70	4
Pseudo β ext	100	4	0.00	60	0	0	0
Pseudo β ext	100	4	0.01	60	0	1	0
Pseudo β ext	100	4	0.90	60	859	90	4
Pseudo β ext	100	4	0.95	60	1156	95	4
Pseudo β int	100	6	0.50	60	132	50	4
Pseudo β int	100	6	0.70	60	552	70	4
Pseudo β ext	100	6	0.00	60	0	0	0
Pseudo β ext	100	6	0.01	60	0	1	0
Pseudo β ext	100	6	0.90	60	2054	90	4
Pseudo β ext	100	6	0.95	60	2721	95	4
Pseudo β int	100	10	0.50	60	716	50	4
Pseudo β int	100	10	0.70	60	2053	70	4
Pseudo β ext	100	10	0.00	60	0	0	0
Pseudo β ext	100	10	0.01	60	0	1	0
Pseudo β ext	100	10	0.90	60	5207	90	4
Pseudo β ext	100	10	0.95	60	6437	95	4
Pseudo β int	100	4	0.50	90	32	50	4
Pseudo β int	100	4	0.70	90	160	70	4
Pseudo β ext	100	4	0.00	90	0	0	0
Pseudo β ext	100	4	0.01	90	0	1	0
Pseudo β ext	100	4	0.90	90	666	90	4
Pseudo β ext	100	4	0.95	90	897	95	4
Pseudo β int	100	6	0.50	90	109	50	4
Pseudo β int	100	6	0.70	90	444	70	4
Pseudo β ext	100	6	0.00	90	0	0	0
Pseudo β ext	100	6	0.01	90	0	1	0
Pseudo β ext	100	6	0.90	90	1659	90	4
Pseudo β ext	100	6	0.95	90	2201	95	4
Pseudo β int	100	10	0.50	90	596	50	4
Pseudo β int	100	10	0.70	90	1688	70	4
Pseudo β ext	100	10	0.00	90	0	0	0
Pseudo β ext	100	10	0.01	90	0	1	0
Pseudo β ext	100	10	0.90	90	4312	90	4
Pseudo β ext	100	10	0.95	90	5344	95	4
Pseudo β int	110	4	0.45	30	68	50	4
Pseudo β int	110	4	0.68	30	524	75	4

Pseudo β ext	110	4	0.00	30	0	0	0
Pseudo β ext	110	4	0.01	30	0	1.1	0
Pseudo β ext	110	4	0.90	30	2440	99	4
Pseudo β ext	110	4	0.95	30	3249	104.5	4
Pseudo β int	110	5	0.45	30	130	50	4
Pseudo β int	110	5	0.68	30	877	75	4
Pseudo β ext	110	5	0.00	30	0	0	0
Pseudo β ext	110	5	0.01	30	0	1.1	0
Pseudo β ext	110	5	0.90	30	3886	99	4
Pseudo β ext	110	5	0.95	30	5145	104.5	4
Pseudo β int	110	6	0.45	30	224	50	4
Pseudo β int	110	6	0.68	30	1362	75	4
Pseudo β ext	110	6	0.00	30	0	0	0
Pseudo β ext	110	6	0.01	30	0	1.1	0
Pseudo β ext	110	6	0.90	30	5787	99	4
Pseudo β ext	110	6	0.95	30	7625	104.5	4
Pseudo β int	110	4	0.45	60	32	50	4
Pseudo β int	110	4	0.68	60	205	75	4
Pseudo β ext	110	4	0.00	60	0	0	0
Pseudo β ext	110	4	0.01	60	0	1.1	0
Pseudo β ext	110	4	0.90	60	953	99	4
Pseudo β ext	110	4	0.95	60	1271	104.5	4
Pseudo β int	110	5	0.45	60	61	50	4
Pseudo β int	110	5	0.68	60	355	75	4
Pseudo β ext	110	5	0.00	60	0	0	0
Pseudo β ext	110	5	0.01	60	0	1.1	0
Pseudo β ext	110	5	0.90	60	1573	99	4
Pseudo β ext	110	5	0.95	60	2087	104.5	4
Pseudo β int	110	6	0.45	60	106	50	4
Pseudo β int	110	6	0.68	60	544	75	4
Pseudo β ext	110	6	0.00	60	0	0	0
Pseudo β ext	110	6	0.01	60	0	1.1	0
Pseudo β ext	110	6	0.90	60	2271	99	4
Pseudo β ext	110	6	0.95	60	2993	104.5	4
Pseudo β int	110	4	0.45	90	27	50	4
Pseudo β int	110	4	0.68	90	160	75	4
Pseudo β ext	110	4	0.00	90	0	0	0
Pseudo β ext	110	4	0.01	90	0	1.1	0
Pseudo β ext	110	4	0.90	90	736	99	4
Pseudo β ext	110	4	0.95	90	982	104.5	4
Pseudo β int	110	5	0.45	90	51	50	4
Pseudo β int	110	5	0.68	90	282	75	4
Pseudo β ext	110	5	0.00	90	0	0	0
Pseudo β ext	110	5	0.01	90	0	1.1	0
Pseudo β ext	110	5	0.90	90	1247	99	4
Pseudo β ext	110	5	0.95	90	1657	104.5	4
Pseudo β int	110	6	0.45	90	89	50	4
Pseudo β int	110	6	0.68	90	438	75	4
Pseudo β ext	110	6	0.00	90	0	0	0
Pseudo β ext	110	6	0.01	90	0	1.1	0
Pseudo β ext	110	6	0.90	90	1829	99	4
Pseudo β ext	110	6	0.95	90	2414	104.5	4
Pseudo β int	120	5	0.46	30	108	55	4
Pseudo β int	120	5	0.71	30	1153	85	4
Pseudo β ext	120	5	0.00	30	0	0	0
Pseudo β ext	120	5	0.01	30	0	1.2	0
Pseudo β ext	120	5	0.90	30	4460	108	5
Pseudo β ext	120	5	0.95	30	5963	114	5
Pseudo β int	120	7.1	0.46	30	361	55	4
Pseudo β int	120	7.1	0.71	30	2797	85	4

Pseudo β ext	120	7.1	0.00	30	0	0	0
Pseudo β ext	120	7.1	0.01	30	0	1.2	0
Pseudo β ext	120	7.1	0.90	30	9917	108	5
Pseudo β ext	120	7.1	0.95	30	13100	114	5
Pseudo β int	120	10	0.46	30	1399	55	4
Pseudo β int	120	10	0.71	30	7016	85	4
Pseudo β ext	120	10	0.00	30	0	0	0
Pseudo β ext	120	10	0.01	30	0	1.2	0
Pseudo β ext	120	10	0.90	30	19947	108	5
Pseudo β ext	120	10	0.95	30	25381	114	5
Pseudo β int	120	5	0.46	60	52	55	4
Pseudo β int	120	5	0.71	60	461	85	4
Pseudo β ext	120	5	0.00	60	0	0	0
Pseudo β ext	120	5	0.01	60	0	1.2	0
Pseudo β ext	120	5	0.90	60	1791	108	5
Pseudo β ext	120	5	0.95	60	2400	114	5
Pseudo β int	120	7.1	0.46	60	175	55	4
Pseudo β int	120	7.1	0.71	60	1093	85	4
Pseudo β ext	120	7.1	0.00	60	0	0	0
Pseudo β ext	120	7.1	0.01	60	0	1.2	0
Pseudo β ext	120	7.1	0.90	60	3765	108	5
Pseudo β ext	120	7.1	0.95	60	4963	114	5
Pseudo β int	120	10	0.46	60	543	55	4
Pseudo β int	120	10	0.71	60	2537	85	4
Pseudo β ext	120	10	0.00	60	0	0	0
Pseudo β ext	120	10	0.01	60	0	1.2	0
Pseudo β ext	120	10	0.90	60	7511	108	5
Pseudo β ext	120	10	0.95	60	9661	114	5
Pseudo β int	120	5	0.46	90	44	55	4
Pseudo β int	120	5	0.71	90	365	85	4
Pseudo β ext	120	5	0.00	90	0	0	0
Pseudo β ext	120	5	0.01	90	0	1.2	0
Pseudo β ext	120	5	0.90	90	1413	108	5
Pseudo β ext	120	5	0.95	90	1894	114	5
Pseudo β int	120	7.1	0.46	90	148	55	4
Pseudo β int	120	7.1	0.71	90	884	85	4
Pseudo β ext	120	7.1	0.00	90	0	0	0
Pseudo β ext	120	7.1	0.01	90	0	1.2	0
Pseudo β ext	120	7.1	0.90	90	3046	108	5
Pseudo β ext	120	7.1	0.95	90	4019	114	5
Pseudo β int	120	10	0.46	90	459	55	4
Pseudo β int	120	10	0.71	90	2079	85	4
Pseudo β ext	120	10	0.00	90	0	0	0
Pseudo β ext	120	10	0.01	90	0	1.2	0
Pseudo β ext	120	10	0.90	90	6173	108	5
Pseudo β ext	120	10	0.95	90	7953	114	5
Pseudo β int	140	5	0.43	30	90	60	4
Pseudo β int	140	5	0.68	30	932	95	4
Pseudo β ext	140	5	0.00	30	0	0	0
Pseudo β ext	140	5	0.01	30	0	1.4	0
Pseudo β ext	140	5	0.90	30	4324	126	5
Pseudo β ext	140	5	0.95	30	5724	133	5
Pseudo β int	140	7.1	0.43	30	292	60	4
Pseudo β int	140	7.1	0.68	30	2264	95	4
Pseudo β ext	140	7.1	0.00	30	0	0	0
Pseudo β ext	140	7.1	0.01	30	0	1.4	0
Pseudo β ext	140	7.1	0.90	30	9703	126	5
Pseudo β ext	140	7.1	0.95	30	12734	133	5
Pseudo β int	140	10	0.43	30	1015	60	4
Pseudo β int	140	10	0.68	30	5421	95	4

Pseudo β ext	140	10	0.00	30	0	0	0
Pseudo β ext	140	10	0.01	30	0	1.4	0
Pseudo β ext	140	10	0.90	30	19535	126	5
Pseudo β ext	140	10	0.95	30	25083	133	5
Pseudo β int	140	5	0.43	60	47	60	4
Pseudo β int	140	5	0.68	60	357	95	4
Pseudo β ext	140	5	0.00	60	0	0	0
Pseudo β ext	140	5	0.01	60	0	1.4	0
Pseudo β ext	140	5	0.90	60	1636	126	5
Pseudo β ext	140	5	0.95	60	2168	133	5
Pseudo β int	140	7.1	0.43	60	146	60	4
Pseudo β int	140	7.1	0.68	60	920	95	4
Pseudo β ext	140	7.1	0.00	60	0	0	0
Pseudo β ext	140	7.1	0.01	60	0	1.4	0
Pseudo β ext	140	7.1	0.90	60	3922	126	5
Pseudo β ext	140	7.1	0.95	60	5159	133	5
Pseudo β int	140	10	0.43	60	444	60	4
Pseudo β int	140	10	0.68	60	2213	95	4
Pseudo β ext	140	10	0.00	60	0	0	0
Pseudo β ext	140	10	0.01	60	0	1.4	0
Pseudo β ext	140	10	0.90	60	8340	126	5
Pseudo β ext	140	10	0.95	60	10810	133	5
Pseudo β int	140	5	0.43	90	42	60	4
Pseudo β int	140	5	0.68	90	282	95	4
Pseudo β ext	140	5	0.00	90	0	0	0
Pseudo β ext	140	5	0.01	90	0	1.4	0
Pseudo β ext	140	5	0.90	90	1267	126	5
Pseudo β ext	140	5	0.95	90	1678	133	5
Pseudo β int	140	7.1	0.43	90	126	60	4
Pseudo β int	140	7.1	0.68	90	743	95	4
Pseudo β ext	140	7.1	0.00	90	0	0	0
Pseudo β ext	140	7.1	0.01	90	0	1.4	0
Pseudo β ext	140	7.1	0.90	90	3148	126	5
Pseudo β ext	140	7.1	0.95	90	4141	133	5
Pseudo β int	140	10	0.43	90	383	60	4
Pseudo β int	140	10	0.68	90	1811	95	4
Pseudo β ext	140	10	0.00	90	0	0	0
Pseudo β ext	140	10	0.01	90	0	1.4	0
Pseudo β ext	140	10	0.90	90	6808	126	5
Pseudo β ext	140	10	0.95	90	8830	133	5
Pseudo β int	150	6	0.40	30	140	60	4
Pseudo β int	150	6	0.67	30	1445	100	4
Pseudo β ext	150	6	0.00	30	0	0	0
Pseudo β ext	150	6	0.01	30	0	1.5	0
Pseudo β ext	150	6	0.90	30	6932	135	6
Pseudo β ext	150	6	0.95	30	9104	142.5	6
Pseudo β int	150	8.8	0.40	30	500	60	4
Pseudo β int	150	8.8	0.67	30	3924	100	4
Pseudo β ext	150	8.8	0.00	30	0	0	0
Pseudo β ext	150	8.8	0.01	30	0	1.5	0
Pseudo β ext	150	8.8	0.90	30	17349	135	6
Pseudo β ext	150	8.8	0.95	30	22601	142.5	6
Pseudo β int	150	12.5	0.40	30	2308	60	4
Pseudo β int	150	12.5	0.67	30	10733	100	4
Pseudo β ext	150	12.5	0.00	30	0	0	0
Pseudo β ext	150	12.5	0.01	30	0	1.5	0
Pseudo β ext	150	12.5	0.90	30	34748	135	6
Pseudo β ext	150	12.5	0.95	30	43471	142.5	6
Pseudo β int	150	6	0.40	60	75	60	4
Pseudo β int	150	6	0.67	60	569	100	4

Pseudo β ext	150	6	0.00	60	0	0	0
Pseudo β ext	150	6	0.01	60	0	1.5	0
Pseudo β ext	150	6	0.90	60	2699	135	6
Pseudo β ext	150	6	0.95	60	3551	142.5	6
Pseudo β int	150	8.8	0.40	60	258	60	4
Pseudo β int	150	8.8	0.67	60	1553	100	4
Pseudo β ext	150	8.8	0.00	60	0	0	0
Pseudo β ext	150	8.8	0.01	60	0	1.5	0
Pseudo β ext	150	8.8	0.90	60	6669	135	6
Pseudo β ext	150	8.8	0.95	60	8687	142.5	6
Pseudo β int	150	12.5	0.40	60	909	60	4
Pseudo β int	150	12.5	0.67	60	4040	100	4
Pseudo β ext	150	12.5	0.00	60	0	0	0
Pseudo β ext	150	12.5	0.01	60	0	1.5	0
Pseudo β ext	150	12.5	0.90	60	13614	135	6
Pseudo β ext	150	12.5	0.95	60	17184	142.5	6
Pseudo β int	150	6	0.40	90	67	60	4
Pseudo β int	150	6	0.67	90	450	100	4
Pseudo β ext	150	6	0.00	90	0	0	0
Pseudo β ext	150	6	0.01	90	0	1.5	0
Pseudo β ext	150	6	0.90	90	2101	135	6
Pseudo β ext	150	6	0.95	90	2764	142.5	6
Pseudo β int	150	8.8	0.40	90	225	60	4
Pseudo β int	150	8.8	0.67	90	1265	100	4
Pseudo β ext	150	8.8	0.00	90	0	0	0
Pseudo β ext	150	8.8	0.01	90	0	1.5	0
Pseudo β ext	150	8.8	0.90	90	5411	135	6
Pseudo β ext	150	8.8	0.95	90	7054	142.5	6
Pseudo β int	150	12.5	0.40	90	780	60	4
Pseudo β int	150	12.5	0.67	90	3338	100	4
Pseudo β ext	150	12.5	0.00	90	0	0	0
Pseudo β ext	150	12.5	0.01	90	0	1.5	0
Pseudo β ext	150	12.5	0.90	90	11263	135	6
Pseudo β ext	150	12.5	0.95	90	14238	142.5	6
Pseudo β int	160	6	0.41	30	145	65	4
Pseudo β int	160	6	0.66	30	1240	105	4
Pseudo β ext	160	6	0.00	30	0	0	0
Pseudo β ext	160	6	0.01	30	0	1.6	0
Pseudo β ext	160	6	0.90	30	6338	144	6
Pseudo β ext	160	6	0.95	30	8309	152	6
Pseudo β int	160	8.8	0.41	30	520	65	4
Pseudo β int	160	8.8	0.66	30	3422	105	4
Pseudo β ext	160	8.8	0.00	30	0	0	0
Pseudo β ext	160	8.8	0.01	30	0	1.6	0
Pseudo β ext	160	8.8	0.90	30	15880	144	6
Pseudo β ext	160	8.8	0.95	30	20626	152	6
Pseudo β int	160	12.5	0.41	30	2480	65	4
Pseudo β int	160	12.5	0.66	30	9432	105	4
Pseudo β ext	160	12.5	0.00	30	0	0	0
Pseudo β ext	160	12.5	0.01	30	0	1.6	0
Pseudo β ext	160	12.5	0.90	30	28052	144	6
Pseudo β ext	160	12.5	0.95	30	34282	152	6
Pseudo β int	160	6	0.41	60	79	65	4
Pseudo β int	160	6	0.66	60	481	105	4
Pseudo β ext	160	6	0.00	60	0	0	0
Pseudo β ext	160	6	0.01	60	0	1.6	0
Pseudo β ext	160	6	0.90	60	2379	144	6
Pseudo β ext	160	6	0.95	60	3121	152	6
Pseudo β int	160	8.8	0.41	60	266	65	4
Pseudo β int	160	8.8	0.66	60	1392	105	4

Pseudo β ext	160	8.8	0.00	60	0	0	0
Pseudo β ext	160	8.8	0.01	60	0	1.6	0
Pseudo β ext	160	8.8	0.90	60	6359	144	6
Pseudo β ext	160	8.8	0.95	60	8276	152	6
Pseudo β int	160	12.5	0.41	60	975	65	4
Pseudo β int	160	12.5	0.66	60	3704	105	4
Pseudo β ext	160	12.5	0.00	60	0	0	0
Pseudo β ext	160	12.5	0.01	60	0	1.6	0
Pseudo β ext	160	12.5	0.90	60	12477	144	6
Pseudo β ext	160	12.5	0.95	60	15624	152	6
Pseudo β int	160	6	0.41	90	71	65	4
Pseudo β int	160	6	0.66	90	381	105	4
Pseudo β ext	160	6	0.00	90	0	0	0
Pseudo β ext	160	6	0.01	90	0	1.6	0
Pseudo β ext	160	6	0.90	90	1840	144	6
Pseudo β ext	160	6	0.95	90	2412	152	6
Pseudo β int	160	8.8	0.41	90	233	65	4
Pseudo β int	160	8.8	0.66	90	1131	105	4
Pseudo β ext	160	8.8	0.00	90	0	0	0
Pseudo β ext	160	8.8	0.01	90	0	1.6	0
Pseudo β ext	160	8.8	0.90	90	5123	144	6
Pseudo β ext	160	8.8	0.95	90	6671	152	6
Pseudo β int	160	12.5	0.41	90	839	65	4
Pseudo β int	160	12.5	0.66	90	3048	105	4
Pseudo β ext	160	12.5	0.00	90	0	0	0
Pseudo β ext	160	12.5	0.01	90	0	1.6	0
Pseudo β ext	160	12.5	0.90	90	10199	144	6
Pseudo β ext	160	12.5	0.95	90	12780	152	6
Pseudo β int	180	7.1	0.42	30	246	75	4
Pseudo β int	180	7.1	0.69	30	3089	125	4
Pseudo β ext	180	7.1	0.00	30	0	0	0
Pseudo β ext	180	7.1	0.01	30	0	1.8	0
Pseudo β ext	180	7.1	0.90	30	12399	162	7.1
Pseudo β ext	180	7.1	0.95	30	16376	171	7.1
Pseudo β int	180	8.8	0.42	30	504	75	4
Pseudo β int	180	8.8	0.69	30	5152	125	4
Pseudo β ext	180	8.8	0.00	30	0	0	0
Pseudo β ext	180	8.8	0.01	30	0	1.8	0
Pseudo β ext	180	8.8	0.90	30	19835	162	7.1
Pseudo β ext	180	8.8	0.95	30	26068	171	7.1
Pseudo β int	180	12.5	0.42	30	2091	75	4
Pseudo β int	180	12.5	0.69	30	12746	125	4
Pseudo β ext	180	12.5	0.00	30	0	0	0
Pseudo β ext	180	12.5	0.01	30	0	1.8	0
Pseudo β ext	180	12.5	0.90	30	40529	162	7.1
Pseudo β ext	180	12.5	0.95	30	51852	171	7.1
Pseudo β int	180	7.1	0.42	60	128	75	4
Pseudo β int	180	7.1	0.69	60	1237	125	4
Pseudo β ext	180	7.1	0.00	60	0	0	0
Pseudo β ext	180	7.1	0.01	60	0	1.8	0
Pseudo β ext	180	7.1	0.90	60	4968	162	7.1
Pseudo β ext	180	7.1	0.95	60	6578	171	7.1
Pseudo β int	180	8.8	0.42	60	259	75	4
Pseudo β int	180	8.8	0.69	60	2092	125	4
Pseudo β ext	180	8.8	0.00	60	0	0	0
Pseudo β ext	180	8.8	0.01	60	0	1.8	0
Pseudo β ext	180	8.8	0.90	60	8026	162	7.1
Pseudo β ext	180	8.8	0.95	60	10569	171	7.1
Pseudo β int	180	12.5	0.42	60	933	75	4
Pseudo β int	180	12.5	0.69	60	5171	125	4

Pseudo β ext	180	12.5	0.00	60	0	0	0
Pseudo β ext	180	12.5	0.01	60	0	1.8	0
Pseudo β ext	180	12.5	0.90	60	16653	162	7.1
Pseudo β ext	180	12.5	0.95	60	21400	171	7.1
Pseudo β int	180	7.1	0.42	90	114	75	4
Pseudo β int	180	7.1	0.69	90	979	125	4
Pseudo β ext	180	7.1	0.00	90	0	0	0
Pseudo β ext	180	7.1	0.01	90	0	1.8	0
Pseudo β ext	180	7.1	0.90	90	3898	162	7.1
Pseudo β ext	180	7.1	0.95	90	5160	171	7.1
Pseudo β int	180	8.8	0.42	90	227	75	4
Pseudo β int	180	8.8	0.69	90	1681	125	4
Pseudo β ext	180	8.8	0.00	90	0	0	0
Pseudo β ext	180	8.8	0.01	90	0	1.8	0
Pseudo β ext	180	8.8	0.90	90	6423	162	7.1
Pseudo β ext	180	8.8	0.95	90	8461	171	7.1
Pseudo β int	180	12.5	0.42	90	804	75	4
Pseudo β int	180	12.5	0.69	90	4232	125	4
Pseudo β ext	180	12.5	0.00	90	0	0	0
Pseudo β ext	180	12.5	0.01	90	0	1.8	0
Pseudo β ext	180	12.5	0.90	90	13606	162	7.1
Pseudo β ext	180	12.5	0.95	90	17500	171	7.1
Pseudo β int	200	7.1	0.40	30	211	80	4
Pseudo β int	200	7.1	0.68	30	2678	135	4
Pseudo β ext	200	7.1	0.00	30	0	0	0
Pseudo β ext	200	7.1	0.01	30	0	2	0
Pseudo β ext	200	7.1	0.90	30	12348	180	7.1
Pseudo β ext	200	7.1	0.95	30	16262	190	7.1
Pseudo β int	200	8.8	0.40	30	443	80	4
Pseudo β int	200	8.8	0.68	30	4465	135	4
Pseudo β ext	200	8.8	0.00	30	0	0	0
Pseudo β ext	200	8.8	0.01	30	0	2	0
Pseudo β ext	200	8.8	0.90	30	19569	180	7.1
Pseudo β ext	200	8.8	0.95	30	25637	190	7.1
Pseudo β int	200	12.5	0.40	30	1846	80	4
Pseudo β int	200	12.5	0.68	30	11016	135	4
Pseudo β ext	200	12.5	0.00	30	0	0	0
Pseudo β ext	200	12.5	0.01	30	0	2	0
Pseudo β ext	200	12.5	0.90	30	38725	180	7.1
Pseudo β ext	200	12.5	0.95	30	49360	190	7.1
Pseudo β int	200	7.1	0.40	60	119	80	4
Pseudo β int	200	7.1	0.68	60	1051	135	4
Pseudo β ext	200	7.1	0.00	60	0	0	0
Pseudo β ext	200	7.1	0.01	60	0	2	0
Pseudo β ext	200	7.1	0.90	60	4781	180	7.1
Pseudo β ext	200	7.1	0.95	60	6306	190	7.1
Pseudo β int	200	8.8	0.40	60	237	80	4
Pseudo β int	200	8.8	0.68	60	1820	135	4
Pseudo β ext	200	8.8	0.00	60	0	0	0
Pseudo β ext	200	8.8	0.01	60	0	2	0
Pseudo β ext	200	8.8	0.90	60	7964	180	7.1
Pseudo β ext	200	8.8	0.95	60	10463	190	7.1
Pseudo β int	200	12.5	0.40	60	843	80	4
Pseudo β int	200	12.5	0.68	60	4576	135	4
Pseudo β ext	200	12.5	0.00	60	0	0	0
Pseudo β ext	200	12.5	0.01	60	0	2	0
Pseudo β ext	200	12.5	0.90	60	16833	180	7.1
Pseudo β ext	200	12.5	0.95	60	21667	190	7.1
Pseudo β int	200	7.1	0.40	90	105	80	4
Pseudo β int	200	7.1	0.68	90	823	135	4

Pseudo β ext	200	7.1	0.00	90	0	0	0
Pseudo β ext	200	7.1	0.01	90	0	2	0
Pseudo β ext	200	7.1	0.90	90	3732	180	7.1
Pseudo β ext	200	7.1	0.95	90	4926	190	7.1
Pseudo β int	200	8.8	0.40	90	207	80	4
Pseudo β int	200	8.8	0.68	90	1445	135	4
Pseudo β ext	200	8.8	0.00	90	0	0	0
Pseudo β ext	200	8.8	0.01	90	0	2	0
Pseudo β ext	200	8.8	0.90	90	6325	180	7.1
Pseudo β ext	200	8.8	0.95	90	8320	190	7.1
Pseudo β int	200	12.5	0.40	90	726	80	4
Pseudo β int	200	12.5	0.68	90	3691	135	4
Pseudo β ext	200	12.5	0.00	90	0	0	0
Pseudo β ext	200	12.5	0.01	90	0	2	0
Pseudo β ext	200	12.5	0.90	90	13588	180	7.1
Pseudo β ext	200	12.5	0.95	90	17519	190	7.1
Pseudo β int	220	8	0.41	30	314	90	4
Pseudo β int	220	8	0.68	30	4096	150	4
Pseudo β ext	220	8	0.00	30	0	0	0
Pseudo β ext	220	8	0.01	30	0	2.2	0
Pseudo β ext	220	8	0.90	30	18459	198	7.1
Pseudo β ext	220	8	0.95	30	24414	209	7.1
Pseudo β int	220	10	0.41	30	664	90	4
Pseudo β int	220	10	0.68	30	6964	150	4
Pseudo β ext	220	10	0.00	30	0	0	0
Pseudo β ext	220	10	0.01	30	0	2.2	0
Pseudo β ext	220	10	0.90	30	30101	198	7.1
Pseudo β ext	220	10	0.95	30	39643	209	7.1
Pseudo β int	220	12.5	0.41	30	1618	90	4
Pseudo β int	220	12.5	0.68	30	12203	150	4
Pseudo β ext	220	12.5	0.00	30	0	0	0
Pseudo β ext	220	12.5	0.01	30	0	2.2	0
Pseudo β ext	220	12.5	0.90	30	47719	198	7.1
Pseudo β ext	220	12.5	0.95	30	62125	209	7.1
Pseudo β int	220	8	0.41	60	170	90	4
Pseudo β int	220	8	0.68	60	1629	150	4
Pseudo β ext	220	8	0.00	60	0	0	0
Pseudo β ext	220	8	0.01	60	0	2.2	0
Pseudo β ext	220	8	0.90	60	7325	198	7.1
Pseudo β ext	220	8	0.95	60	9711	209	7.1
Pseudo β int	220	10	0.41	60	350	90	4
Pseudo β int	220	10	0.68	60	2837	150	4
Pseudo β ext	220	10	0.00	60	0	0	0
Pseudo β ext	220	10	0.01	60	0	2.2	0
Pseudo β ext	220	10	0.90	60	12229	198	7.1
Pseudo β ext	220	10	0.95	60	16143	209	7.1
Pseudo β int	220	12.5	0.41	60	804	90	4
Pseudo β int	220	12.5	0.68	60	5069	150	4
Pseudo β ext	220	12.5	0.00	60	0	0	0
Pseudo β ext	220	12.5	0.01	60	0	2.2	0
Pseudo β ext	220	12.5	0.90	60	19692	198	7.1
Pseudo β ext	220	12.5	0.95	60	25682	209	7.1
Pseudo β int	220	8	0.41	90	151	90	4
Pseudo β int	220	8	0.68	90	1292	150	4
Pseudo β ext	220	8	0.00	90	0	0	0
Pseudo β ext	220	8	0.01	90	0	2.2	0
Pseudo β ext	220	8	0.90	90	5758	198	7.1
Pseudo β ext	220	8	0.95	90	7633	209	7.1
Pseudo β int	220	10	0.41	90	309	90	4
Pseudo β int	220	10	0.68	90	2279	150	4

Pseudo β ext	220	10	0.00	90	0	0	0
Pseudo β ext	220	10	0.01	90	0	2.2	0
Pseudo β ext	220	10	0.90	90	9764	198	7.1
Pseudo β ext	220	10	0.95	90	12894	209	7.1
Pseudo β int	220	12.5	0.41	90	702	90	4
Pseudo β int	220	12.5	0.68	90	4115	150	4
Pseudo β ext	220	12.5	0.00	90	0	0	0
Pseudo β ext	220	12.5	0.01	90	0	2.2	0
Pseudo β ext	220	12.5	0.90	90	15882	198	7.1
Pseudo β ext	220	12.5	0.95	90	20719	209	7.1
Pseudo β int	250	8.8	0.42	30	461	105	4
Pseudo β int	250	8.8	0.68	30	5125	170	4
Pseudo β ext	250	8.8	0.00	30	0	0	0
Pseudo β ext	250	8.8	0.01	30	0	2.5	0
Pseudo β ext	250	8.8	0.90	30	23449	225	7.1
Pseudo β ext	250	8.8	0.95	30	31031	237.5	7.1
Pseudo β int	250	10	0.42	30	699	105	4
Pseudo β int	250	10	0.68	30	6998	170	4
Pseudo β ext	250	10	0.00	30	0	0	0
Pseudo β ext	250	10	0.01	30	0	2.5	0
Pseudo β ext	250	10	0.90	30	31338	225	7.1
Pseudo β ext	250	10	0.95	30	41381	237.5	7.1
Pseudo β int	250	12.5	0.42	30	1652	105	4
Pseudo β int	250	12.5	0.68	30	12313	170	4
Pseudo β ext	250	12.5	0.00	30	0	0	0
Pseudo β ext	250	12.5	0.01	30	0	2.5	0
Pseudo β ext	250	12.5	0.90	30	50322	225	7.1
Pseudo β ext	250	12.5	0.95	30	65769	237.5	7.1
Pseudo β int	250	8.8	0.42	60	244	105	4
Pseudo β int	250	8.8	0.68	60	2034	170	4
Pseudo β ext	250	8.8	0.00	60	0	0	0
Pseudo β ext	250	8.8	0.01	60	0	2.5	0
Pseudo β ext	250	8.8	0.90	60	9257	225	7.1
Pseudo β ext	250	8.8	0.95	60	12274	237.5	7.1
Pseudo β int	250	10	0.42	60	365	105	4
Pseudo β int	250	10	0.68	60	2827	170	4
Pseudo β ext	250	10	0.00	60	0	0	0
Pseudo β ext	250	10	0.01	60	0	2.5	0
Pseudo β ext	250	10	0.90	60	12597	225	7.1
Pseudo β ext	250	10	0.95	60	16668	237.5	7.1
Pseudo β int	250	12.5	0.42	60	830	105	4
Pseudo β int	250	12.5	0.68	60	5106	170	4
Pseudo β ext	250	12.5	0.00	60	0	0	0
Pseudo β ext	250	12.5	0.01	60	0	2.5	0
Pseudo β ext	250	12.5	0.90	60	20664	225	7.1
Pseudo β ext	250	12.5	0.95	60	27047	237.5	7.1
Pseudo β int	250	8.8	0.42	90	216	105	4
Pseudo β int	250	8.8	0.68	90	1610	170	4
Pseudo β ext	250	8.8	0.00	90	0	0	0
Pseudo β ext	250	8.8	0.01	90	0	2.5	0
Pseudo β ext	250	8.8	0.90	90	7246	225	7.1
Pseudo β ext	250	8.8	0.95	90	9606	237.5	7.1
Pseudo β int	250	10	0.42	90	321	105	4
Pseudo β int	250	10	0.68	90	2263	170	4
Pseudo β ext	250	10	0.00	90	0	0	0
Pseudo β ext	250	10	0.01	90	0	2.5	0
Pseudo β ext	250	10	0.90	90	10017	225	7.1
Pseudo β ext	250	10	0.95	90	13258	237.5	7.1
Pseudo β int	250	12.5	0.42	90	720	105	4
Pseudo β int	250	12.5	0.68	90	4149	170	4

Pseudo β ext	250	12.5	0.00	90	0	0	0
Pseudo β ext	250	12.5	0.01	90	0	2.5	0
Pseudo β ext	250	12.5	0.90	90	16746	225	7.1
Pseudo β ext	250	12.5	0.95	90	21935	237.5	7.1
Pseudo β int	260	8.8	0.40	30	358	105	4
Pseudo β int	260	8.8	0.69	30	6759	180	4
Pseudo β ext	260	8.8	0.00	30	0	0	0
Pseudo β ext	260	8.8	0.01	30	0	2.6	0
Pseudo β ext	260	8.8	0.90	30	28858	234	8.8
Pseudo β ext	260	8.8	0.95	30	38298	247	8.8
Pseudo β int	260	10	0.40	30	573	105	4
Pseudo β int	260	10	0.69	30	8948	180	4
Pseudo β ext	260	10	0.00	30	0	0	0
Pseudo β ext	260	10	0.01	30	0	2.6	0
Pseudo β ext	260	10	0.90	30	37253	234	8.8
Pseudo β ext	260	10	0.95	30	49303	247	8.8
Pseudo β int	260	12.5	0.40	30	1404	105	4
Pseudo β int	260	12.5	0.69	30	14968	180	4
Pseudo β ext	260	12.5	0.00	30	0	0	0
Pseudo β ext	260	12.5	0.01	30	0	2.6	0
Pseudo β ext	260	12.5	0.90	30	57797	234	8.8
Pseudo β ext	260	12.5	0.95	30	75816	247	8.8
Pseudo β int	260	8.8	0.40	60	203	105	4
Pseudo β int	260	8.8	0.69	60	2698	180	4
Pseudo β ext	260	8.8	0.00	60	0	0	0
Pseudo β ext	260	8.8	0.01	60	0	2.6	0
Pseudo β ext	260	8.8	0.90	60	11515	234	8.8
Pseudo β ext	260	8.8	0.95	60	15312	247	8.8
Pseudo β int	260	10	0.40	60	314	105	4
Pseudo β int	260	10	0.69	60	3641	180	4
Pseudo β ext	260	10	0.00	60	0	0	0
Pseudo β ext	260	10	0.01	60	0	2.6	0
Pseudo β ext	260	10	0.90	60	15180	234	8.8
Pseudo β ext	260	10	0.95	60	20135	247	8.8
Pseudo β int	260	12.5	0.40	60	726	105	4
Pseudo β int	260	12.5	0.69	60	6271	180	4
Pseudo β ext	260	12.5	0.00	60	0	0	0
Pseudo β ext	260	12.5	0.01	60	0	2.6	0
Pseudo β ext	260	12.5	0.90	60	24244	234	8.8
Pseudo β ext	260	12.5	0.95	60	31877	247	8.8
Pseudo β int	260	8.8	0.40	90	184	105	4
Pseudo β int	260	8.8	0.69	90	2117	180	4
Pseudo β ext	260	8.8	0.00	90	0	0	0
Pseudo β ext	260	8.8	0.01	90	0	2.6	0
Pseudo β ext	260	8.8	0.90	90	8963	234	8.8
Pseudo β ext	260	8.8	0.95	90	11917	247	8.8
Pseudo β int	260	10	0.40	90	282	105	4
Pseudo β int	260	10	0.69	90	2887	180	4
Pseudo β ext	260	10	0.00	90	0	0	0
Pseudo β ext	260	10	0.01	90	0	2.6	0
Pseudo β ext	260	10	0.90	90	11968	234	8.8
Pseudo β ext	260	10	0.95	90	15878	247	8.8
Pseudo β int	260	12.5	0.40	90	639	105	4
Pseudo β int	260	12.5	0.69	90	5051	180	4
Pseudo β ext	260	12.5	0.00	90	0	0	0
Pseudo β ext	260	12.5	0.01	90	0	2.6	0
Pseudo β ext	260	12.5	0.90	90	19447	234	8.8
Pseudo β ext	260	12.5	0.95	90	25582	247	8.8
Pseudo β int	300	10	0.40	30	552	120	5
Pseudo β int	300	10	0.68	30	9095	205	5

Pseudo β ext	300	10	0.00	30	0	0	0
Pseudo β ext	300	10	0.01	30	0	3	0
Pseudo β ext	300	10	0.90	30	41060	270	10
Pseudo β ext	300	10	0.95	30	54364	285	10
Pseudo β int	300	12.5	0.40	30	1250	120	5
Pseudo β int	300	12.5	0.68	30	15771	205	5
Pseudo β ext	300	12.5	0.00	30	0	0	0
Pseudo β ext	300	12.5	0.01	30	0	3	0
Pseudo β ext	300	12.5	0.90	30	67986	270	10
Pseudo β ext	300	12.5	0.95	30	89575	285	10
Pseudo β int	300	10	0.40	60	311	120	5
Pseudo β int	300	10	0.68	60	3571	205	5
Pseudo β ext	300	10	0.00	60	0	0	0
Pseudo β ext	300	10	0.01	60	0	3	0
Pseudo β ext	300	10	0.90	60	16061	270	10
Pseudo β ext	300	10	0.95	60	21305	285	10
Pseudo β int	300	12.5	0.40	60	669	120	5
Pseudo β int	300	12.5	0.68	60	6458	205	5
Pseudo β ext	300	12.5	0.00	60	0	0	0
Pseudo β ext	300	12.5	0.01	60	0	3	0
Pseudo β ext	300	12.5	0.90	60	27824	270	10
Pseudo β ext	300	12.5	0.95	60	36741	285	10
Pseudo β int	300	10	0.40	90	281	120	5
Pseudo β int	300	10	0.68	90	2820	205	5
Pseudo β ext	300	10	0.00	90	0	0	0
Pseudo β ext	300	10	0.01	90	0	3	0
Pseudo β ext	300	10	0.90	90	12599	270	10
Pseudo β ext	300	10	0.95	90	16716	285	10
Pseudo β int	300	12.5	0.40	90	596	120	5
Pseudo β int	300	12.5	0.68	90	5176	205	5
Pseudo β ext	300	12.5	0.00	90	0	0	0
Pseudo β ext	300	12.5	0.01	90	0	3	0
Pseudo β ext	300	12.5	0.90	90	22203	270	10
Pseudo β ext	300	12.5	0.95	90	29333	285	10

## Appendix D. DACE code

The Matlab operations needed to create a single model with DACE toolbox:

```
theta = 10 ; lob = 1e-1; upb = 20;
[modelC, perfC] = dacefit (data, C, @regpoly0, @corrgauss, theta, lob, upb);
```

where

- *theta, lob, upb* are the parameters of the surrogate model;
- *data* is the matrix of sample points;
- *@regpoly0* is the regression model used (zero order polynomial in this case);
- *@corrgauss* is correlation model used (Gaussian in this case);
- *C* is the matrix of the responses (stiffness) of the sample points;
- *modelC* is a surrogate model constructed;

To return the predicted responses of rotational stiffness the following code is used:

```
CC=predictor (VP, modelC);
```

where

- $VP$  is the matrix of validation points;
- $CC$  is the matrix with predicted stiffness for the validation points;

## Appendix E. ooDACE code, single model

There are two ways of creating surrogate models in ooDACE: automatic and manual. To create a surrogate model using automatic approach we used the following code:

```
k = oodacefit (data, C)
```

where

- $data$  is the matrix of sample points;
- $C$  is the matrix of the responses (stiffness) of the sample points;
- $k$  is a surrogate model constructed.

In this case the parameters of the surrogate model (regression and correlation functions, upper and lower bounds) in ooDACE are chosen and optimized automatically, thus a required code in ooDACE is shorter than that in DACE.

For more flexibility it is possible to input surrogate model parameters manually. For that case we used the following code:

```
opts = Kriging.getDefaults();
lb=[-10 -10 -10 -10];
ub=[5 5 5 5];
opts.hpBounds = [lb ; ub];
hyperparameters0=[-2 -2 -2 -2];
k = Kriging (opts, hyperparameters0, 'regpoly0', @corrgauss);
k = k.fit (data, C)
```

where

- $hyperparameters0$ ,  $lb$ ,  $ub$  are the parameters of the surrogate model;
- $data$  is the matrix of sample points;
- $@regpoly0$  is the regression model used (zero order polynomial in our case);
- $@corrgauss$  is correlation model used (Gaussian in our case);
- $C$  is the matrix of the responses (stiffness) of the sample points;
- $k$  is a surrogate model constructed.

We tried both approaches and we did not get better results using the manual approach, so for our next modeling we exploited the automatic one.

To return the predicted responses of rotational stiffness the following code is used:

```
CC = k.predict (VP)
C8=predictor ([260 10 200 8 80], modeIC)
```

where

- $VP$  is the matrix of the points of interest;

- $CC$  is the matrix with predicted stiffness for the points of interest;
- $C8$  is the stiffness predicted for the validation point No.8 (see Table 4.1).

## Appendix F. ooDACE code, multi model

To create a multi model the following code in ooDACE was used:

```
% first cycle separates data in accordance with chord width
[m,n] = size (data);
k100=1; k110=1; k120=1; k140=1; k150=1; k160=1; k180=1; k200=1; k220=1; k250=1;
k260=1; k300=1;
for i=1:m
    p=eval(['k',num2str(data(i,1))]);
    eval(['data',num2str(data(i,1)), '(p,:)', '=' data(i,:);']);
    eval(['k',num2str(data(i,1)), '=k',num2str(data(i,1)), '+1;']);
end
clearvars k100 k110 k120 k140 k150 k160 k180 k200 k220 k250 k260 k300 i m n p;

% second cycle separates responses matrices from sample point's matrices
A=[100 110 120 140 150 160 180 200 220 250 260 300];
for i=1:12
    eval(['C',num2str(A(1,i)),' = data',num2str(A(1,i)), '(:,5);']);
    eval(['data',num2str(A(1,i)), '(:,5)=[];']);
    eval(['data',num2str(A(1,i)), '(:,1)=[];']);
end

% third cycle creates surrogate models
for i=1:12
    eval(['k',num2str(A(1,i)), ' = oodacefit (data',num2str(A(1,i)), ', C',num2str(A(1,i)), ');']);
end
clearvars data100 data110 data120 data140 data150 data160 data180 data200 data220
data250 data260 data300;
clearvars A i C100 C110 C120 C140 C150 C160 C180 C200 C220 C250 C260 C300;
```

where  $data$  is a matrix of sample points and their responses represented as  $[b_0, t_0, \beta \varphi C]$ ;

To return the predicted responses of rotational stiffness the following code is used:

```
[m,n] = size(VP);
p(:,1)=VP(:,2); p(:,2)=VP(:,3); p(:,3)=VP(:,4);
for i=1:m
    eval(['C(i,1)=k',num2str(VP(i,1)), '.predict (p(i,:));']);
end
clearvars m n p i;
```

where

- $VP$  is a matrix of validation points represented as  $[b_0, t_0, \beta \varphi]$ ;
- $CC$  is a matrix with predicted responses for validation points.

## Appendix G. ooDACE code, complex model

Construction of the model presented quite a trivial task. Several surrogate models were collected in one Matlab file. Models  $k1$  and  $k2$  presented 1SM and 2SM respectively. Models

$k_{100}, k_{110}, k_{150}, k_{160}, k_{250}$  were taken from 1MM, 2MM or 3MM depending on their performance.

For validation of the complex model the following code was used:

```
[m,n]=size(VP);
p(:,1)=VP(:,2); p(:,2)=VP(:,3); p(:,3)=VP(:,4);
for i=1:m
    if VP(i,1)==200
        CC(i,1)=k1.predict (VP(i,:));
    else
        if VP(i,1)==120| VP(i,1)==140| VP(i,1)==180| VP(i,1)==220| VP(i,1)==260| VP(i,1)==300
            CC(i,1)=k2.predict (VP(i,:));
        else
            eval(['CC(i,1)=k',num2str(VP(i,1)),'.predict (p(i,:));']);
        end
    end
end
clearvars m n i p
```

where

- $VP$  is a matrix of validation points represented as  $[b_0, t_0, \beta \varphi]$ ;
- $CC$  is a matrix with predicted responses for validation points.

## Appendix H. ooDACE code, 3D graphs

These codes are valid only for single model. For multi model they are similar, more complicated though. We do not provide them here.

The following code was used to create a 3D plot of stiffness in respect to  $\varphi$  and  $\beta$ :

```
b0=150; t0=6; x1=0.5; x2=0.8; y1=30; y2=90;
VP=gridsamp ([x1 y1;x2 y2], 100);
m(:,3)=VP(:,1);
m(:,4)=VP(:,2);
m(:,1)=b0;
m(:,2)=t0;
CC=k.predict (m);
X=reshape (VP(:,2), 100,100);
Y=reshape (VP(:,1), 100,100);
CC=reshape (CC, size(X));

figure(1), surf (X, Y, CC)
colormap(hsv)
shading interp
xlabel ('\bf{\it{t}\varphi} [deg]', 'FontSize', 20)
ylabel ('\bf{\it{t}\beta}', 'FontSize', 20)
zlabel ('\bf{\it{k}\beta C} [kNm/rad]', 'FontSize', 20)
a1='{\it{t}\beta_0=}';
a2=num2str(m(1,1));
a3=' mm, {\it{t}\beta_0}=';
a4=num2str(m(1,2));
a5=' mm, {\it{t}\beta}=';
```

```

a6=num2str(x1);
a7='...';
a8=num2str(x2);
a9=', {\it\varphi}=';
a10=num2str(y1);
a11=num2str(y2);
a12='^o';
a=strcat (a1,a2,a3,a4,a5, a6, a7, a8, a9, a10, a7, a11, a12);
title (a, 'FontSize', 20)
axis([y1 y2 x1 x2])
a = get(gca, 'YTick');
set(gca,'YTickLabel',a,'FontName','Arial','fontsize',16)
set(gca,'YTickLabel', sprintf('%3.2f\n',a))
set(gcf,'Color','white')
axis square

```

```
clearvars m X Y x1 x2 y1 y2 VP a CC a1 a2 a3 a4 a5 a6 a7 a8 a9 a10 a11 a12 b0 t0
```

where

- $b_0$  and  $t_0$  are constant values of  $b_0$  and  $t_0$  respectively;
- $x_1$  and  $x_2$  are lower and upper values of  $\beta$  respectively;
- $y_1$  and  $y_2$  are lower and upper values of  $\varphi$  respectively.

The following code was used to create a 3D plot of stiffness in respect to  $t_0$  and  $\beta$ :

```

b0=300; x1=10; x2=12.5; y1=0.5; y2=0.8; phi=30;
VP=gridsamp ([x1 y1;x2 y2], 100);
m(:,2)=VP(:, 1);
m(:,3)=VP(:,2);
m(:, 1)=b0;
m(:,4)=phi;
CC=k.predict (m);
X=reshape (VP(:,2), 100,100);
Y=reshape (VP(:, 1), 100,100);
CC=reshape (CC, size(X));

figure(1), surf (X, Y, CC)
colormap(hsv)
shading interp
xlabel ('\bf{\it\beta}', 'FontSize', 20)
ylabel ('\bf{\it t_0} [mm]', 'FontSize', 20)
zlabel ('\bf{\it C} [kNm/rad]', 'FontSize', 20)
a1='{\it b_0}';
a2=num2str(m(1,1));
a3=' mm, {\it t_0}=';
a4=num2str(m(1,4));
a5=' mm, {\it \varphi}=';
a6=num2str(x1);
a7='...';
a8=num2str(x2);
a9=', {\it\varphi}=';
a10=num2str(y1);
a11=num2str(y2);
a12='^o';

```

```

a=strcat (a1,a2,a3,a6,a7, a8, a5, a10, a7, a11, a9, a4, a12);
title (a, 'FontSize', 20)
axis([y1 y2 x1 x2])
a = get(gca,'YTick');
set(gca,'YTickLabel',a,'FontName','Arial','fontsize',16)
set(gca,'YTickLabel', sprintf('%3.1f\n',a))
a = get(gca,'XTick');
set(gca,'XTickLabel',a,'FontName','Arial','fontsize',16)
set(gca,'XTickLabel', sprintf('%3.2f\n', a))
set(gcf,'Color','white')
axis square

```

```
clearvars m X Y x1 x2 y1 y2 VP a CC a1 a2 a3 a4 a5 a6 a7 a8 a9 a10 a11 a12 b0 phi
```

where

- $b_0$  and  $\phi$  are constant values of  $b_0$  and  $\varphi$  respectively;
- $x_1$  and  $x_2$  are lower and upper values of  $t_0$  respectively;
- $y_1$  and  $y_2$  are lower and upper values of  $\beta$  respectively.

The following code was used to create a 3D plot of stiffness in respect to  $t_0$  and  $\phi$ :

```

b0=300; x1=10; x2=12.5; beta=0.8333; y1=30; y2=90;
VP=gridsamp ([x1 y1;x2 y2], 100);
m(:,2)=VP(:,1);
m(:,4)=VP(:,2);
m(:, 1)=b0;
m(:, 3)=beta;
CC=k.predict (m);
X=reshape (VP(:,2), 100,100);
Y=reshape (VP(:,1), 100,100);
CC=reshape (CC, size(X));

figure(1), surf (X, Y, CC)
colormap(hsv)
shading interp
xlabel ('\bf{\it\phi}', 'FontSize', 20)
ylabel ('\bf{\it t_0} [mm]', 'FontSize', 20)
zlabel ('\bf{\it C} [kNm/rad]', 'FontSize', 20)
a1='{\it b_0}';
a2=num2str(m(1,1));
a3=' mm, {\it t_0}=';
a4=num2str(m(1,3));
a5=' mm, {\it \beta}=';
a6=num2str(x1);
a7='...';
a8=num2str(x2);
a9=' {\it \phi}=';
a10=num2str(y1);
a11=num2str(y2);
a12='^o';

a=strcat (a1,a2,a3,a6,a7, a8, a5, a4, a9, a10, a7, a11, a12);
title (a, 'FontSize', 20)
axis([y1 y2 x1 x2])
a = get(gca,'YTick');

```

```

set(gca,'YTickLabel',a,'FontName','Arial','fontsize',16)
set(gca,'YTickLabel', sprintf('%3.1f\n',a))
a = get(gca,'XTick');
set(gca,'XTickLabel',a,'FontName','Arial','fontsize',16)
set(gcf,'Color','white')
axis square

```

```
clearvars m X Y x1 x2 y1 y2 VP a CC a1 a2 a3 a4 a5 a6 a7 a8 a9 a10 a11 a12 b0 beta
```

where

- $b_0$  and  $\beta$  are constant values of  $b_0$  and  $\beta$  respectively;
- $x_1$  and  $x_2$  are lower and upper values of  $t_0$  respectively;
- $y_1$  and  $y_2$  are lower and upper values of  $\varphi$  respectively.

## Appendix I. Polyfitn code

For exploiting Polyfitn toolbox we used the following code:

```

p = polyfitn (data, C, n);
CC=polyvaln (p, VP)
polyn2sympoly(p)
polyn2sym(p)

```

where

- $data$  and  $C$  are the matrices of sample points and their responses respectively;
- $p$  is a polynomial regression model constructed;
- $n$  is the order of polynomial regression
- $VP$  and  $CC$  are the matrices of validation points and their responses, respectively.

*Polyn2sympoly* represents a conversion tool to generate a *sympoly* from the results of *polyfitn*. *Polyn2sym* represents a conversion tool to generate a symbolic toolbox object from the results of *polyfitn*. They allow to display and manipulate the resultant polynomials symbolically and both require *sympoly* toolbox to be installed.

The order of polynomial regression  $n$  is chosen by a user. We started from 1 and, increasing it gradually, came to the best result with  $n=6$ . For higher orders we noticed a growth in errors and had to stop the procedure.

## Appendix J. 3D plots

Here we presented several 3D plots showing how the final surrogate model behaves in respect to some pairs of variables. The codes for creating the plots are provided in App. H.

Figs. J.1-J.3 illustrate how the model behaves in respect to  $\varphi$  and  $\beta$ .

$$b_0=150 \text{ mm}, t_0=6 \text{ mm}, \beta=0.5 \dots 0.8, \varphi=30 \dots 90^\circ$$

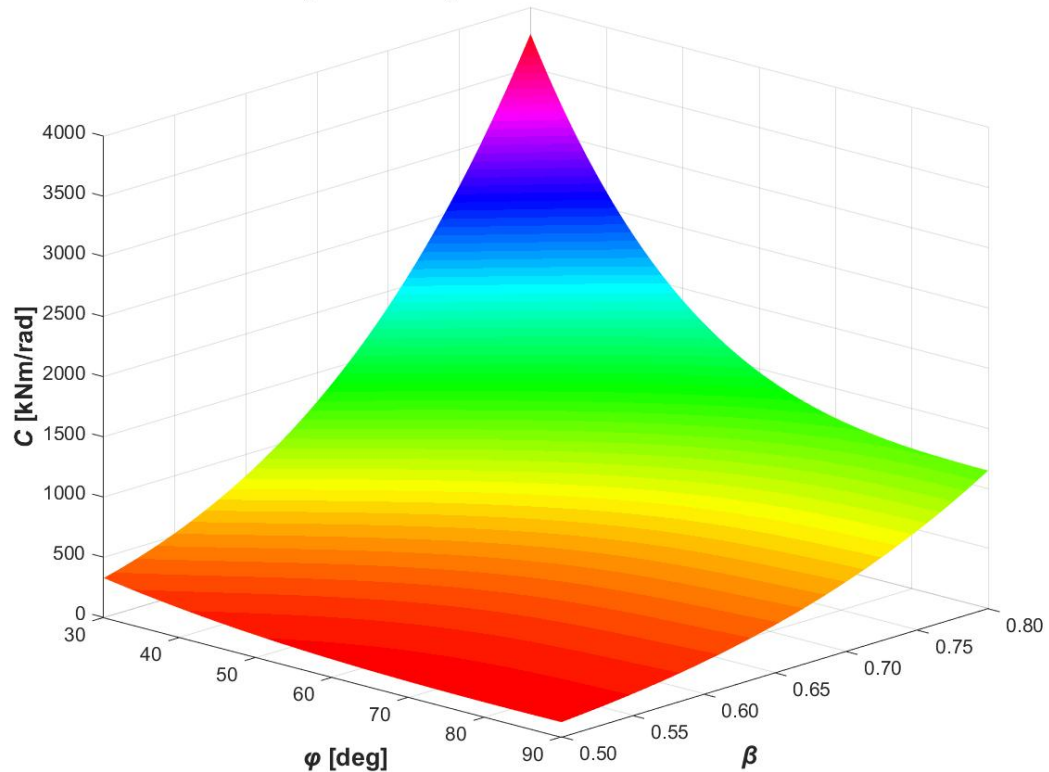


Figure J.1.  $C$ -( $\varphi+\beta$ ) response, case 1.

$$b_0=100 \text{ mm}, t_0=4 \text{ mm}, \beta=0.5 \dots 0.8, \varphi=30 \dots 90^\circ$$

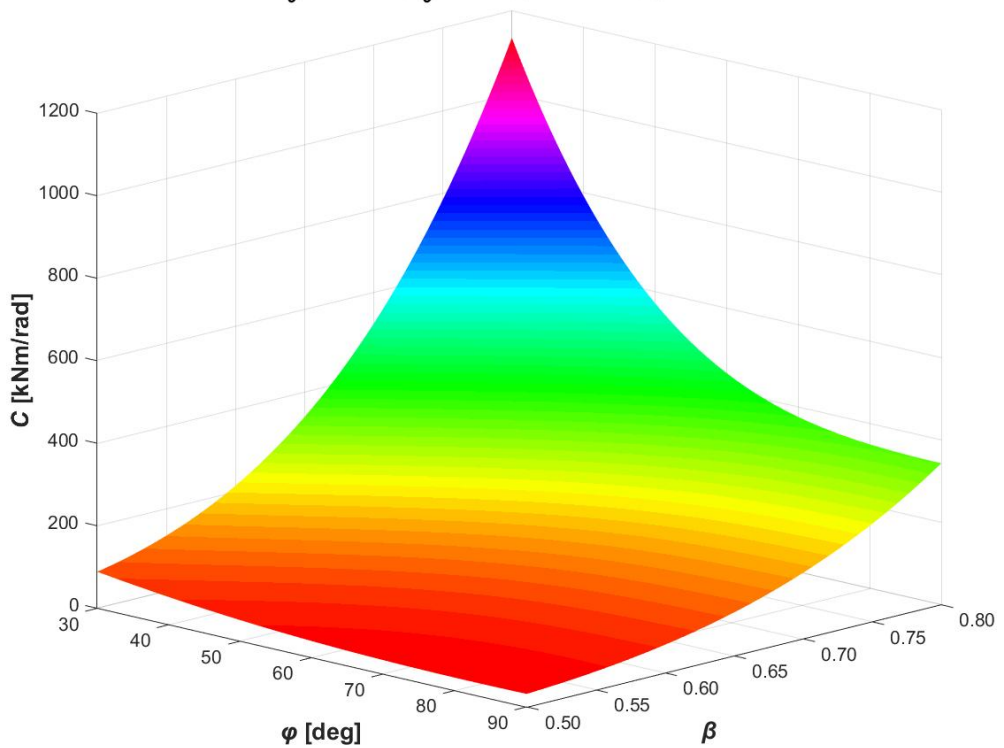


Figure J.2.  $C$ -( $\varphi+\beta$ ) response, case 2

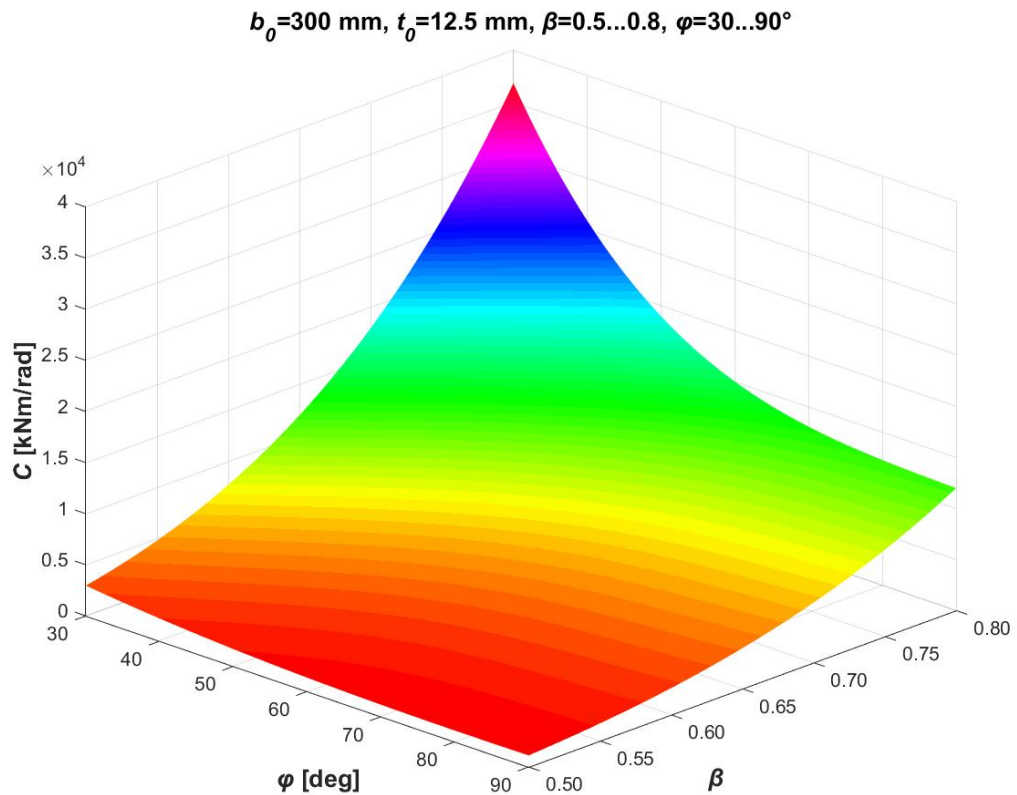


Figure J.3.  $C$ -( $\varphi+\beta$ ) response, case 3.

Figs. J.4-J.6 illustrate how the model behaves in respect to  $t_0$  and  $\beta$ .

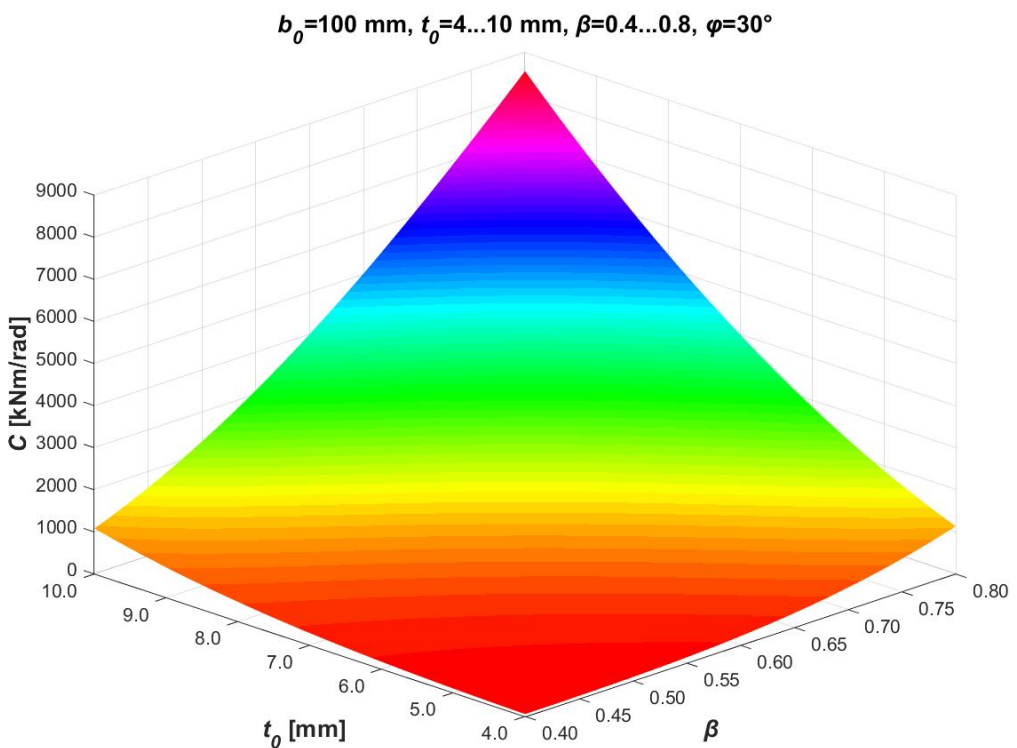


Figure J.4.  $C$ -( $t_0+\beta$ ) response, case 1.

$$b_0 = 150 \text{ mm}, t_0 = 6 \dots 12.5 \text{ mm}, \beta = 0.4 \dots 0.8, \varphi = 30^\circ$$

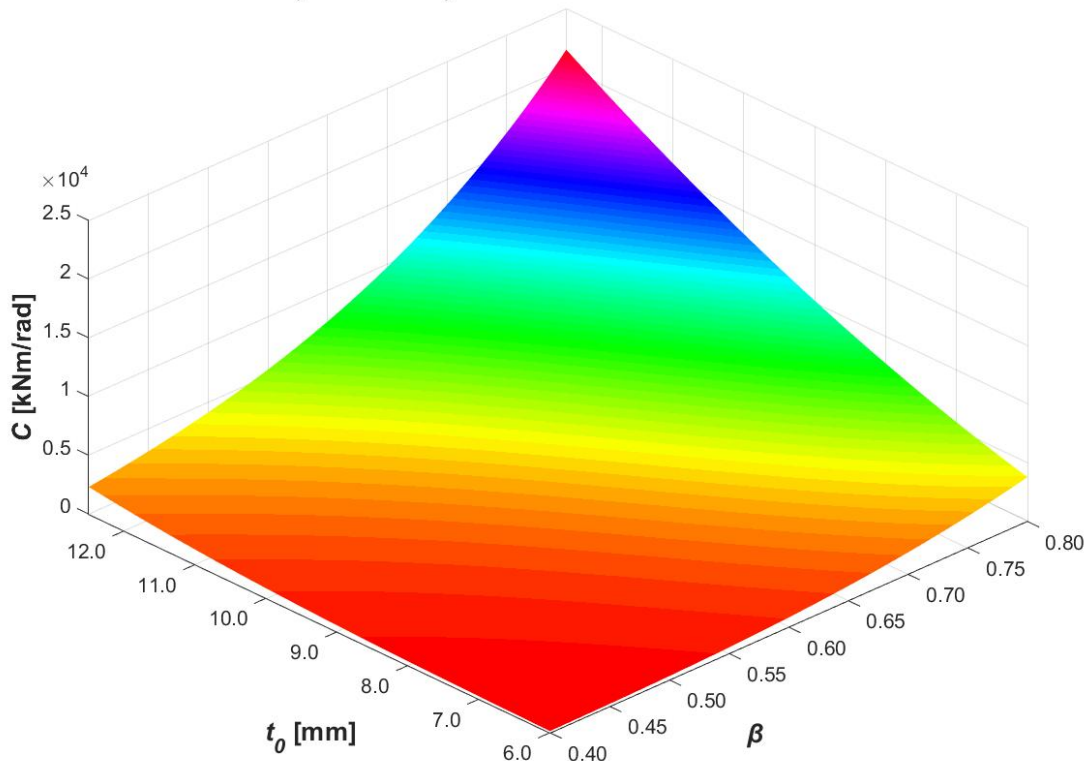


Figure J.5.  $C$ -( $t_0 + \beta$ ) response, case 2.

$$b_0 = 300 \text{ mm}, t_0 = 10 \dots 12.5 \text{ mm}, \beta = 0.5 \dots 0.8, \varphi = 30^\circ$$

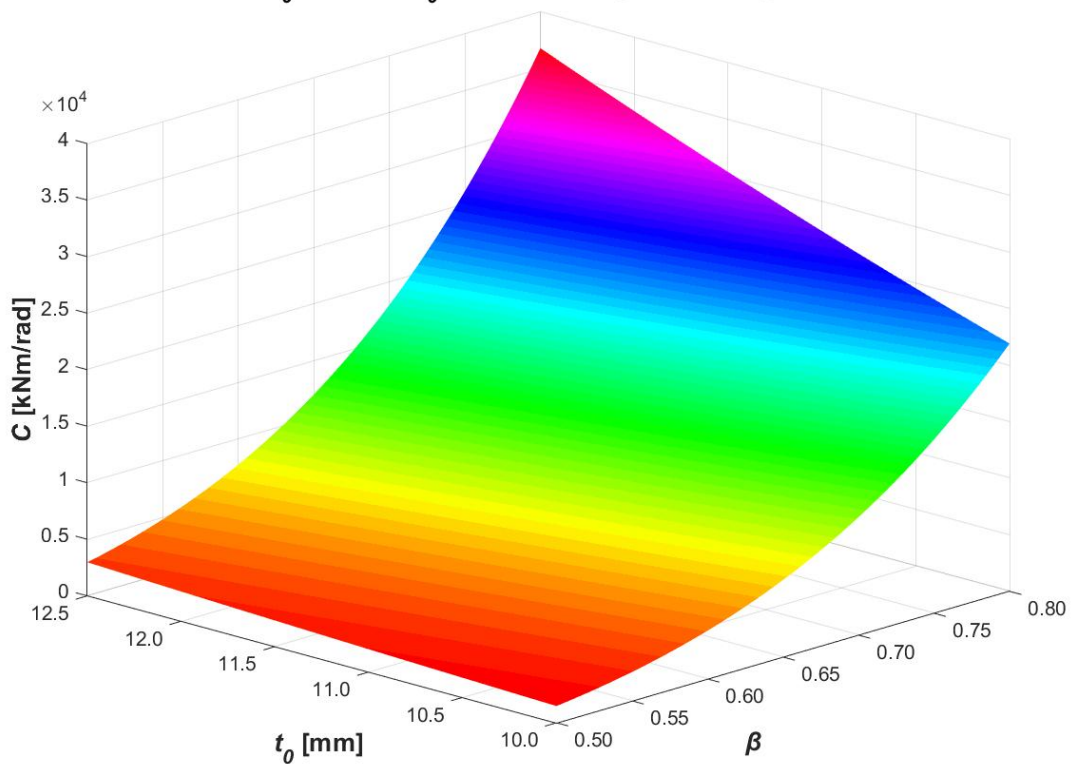


Figure J.6.  $C$ -( $t_0 + \beta$ ) response, case 3.

Figs. J.7-J.9 illustrate how the model behaves in respect to  $t_0$  and  $\varphi$ .

$$b_0=100 \text{ mm}, t_0=4 \dots 10 \text{ mm}, \beta=0.4, \varphi=30 \dots 90^\circ$$

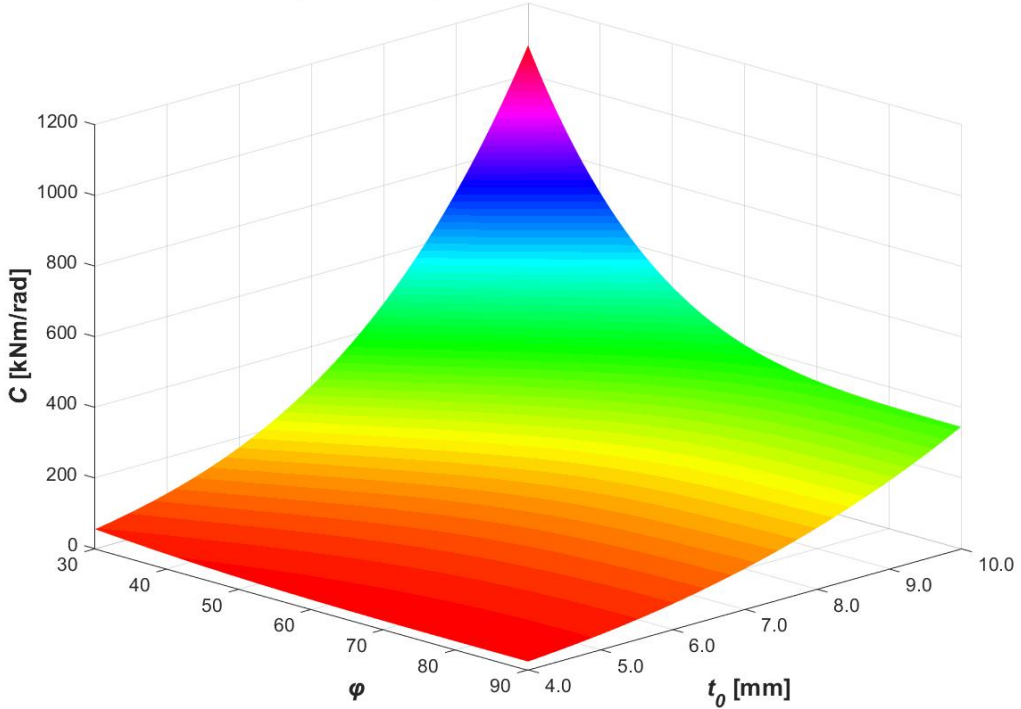


Figure J.7.  $C-(t_0+\varphi)$  response, case 1.

$$b_0=150 \text{ mm}, t_0=6 \dots 12.5 \text{ mm}, \beta=0.5333, \varphi=30 \dots 90^\circ$$

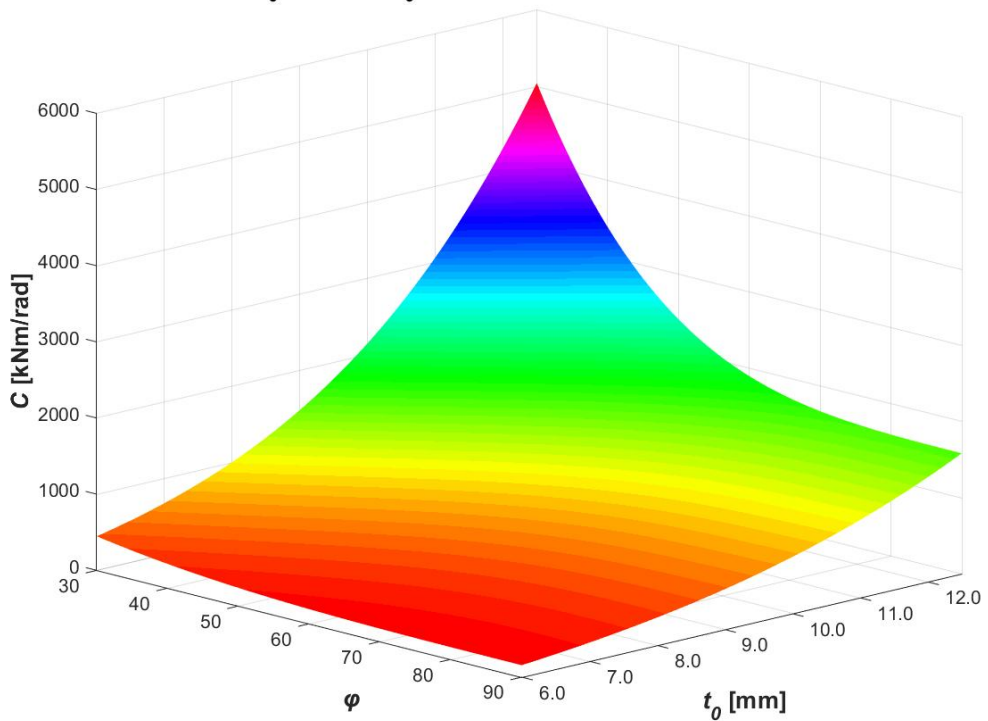


Figure J.8.  $C-(t_0+\varphi)$  response, case 2.

$$b_0 = 300 \text{ mm}, t_0 = 10 \dots 12.5 \text{ mm}, \beta = 0.8333, \varphi = 30 \dots 90^\circ$$

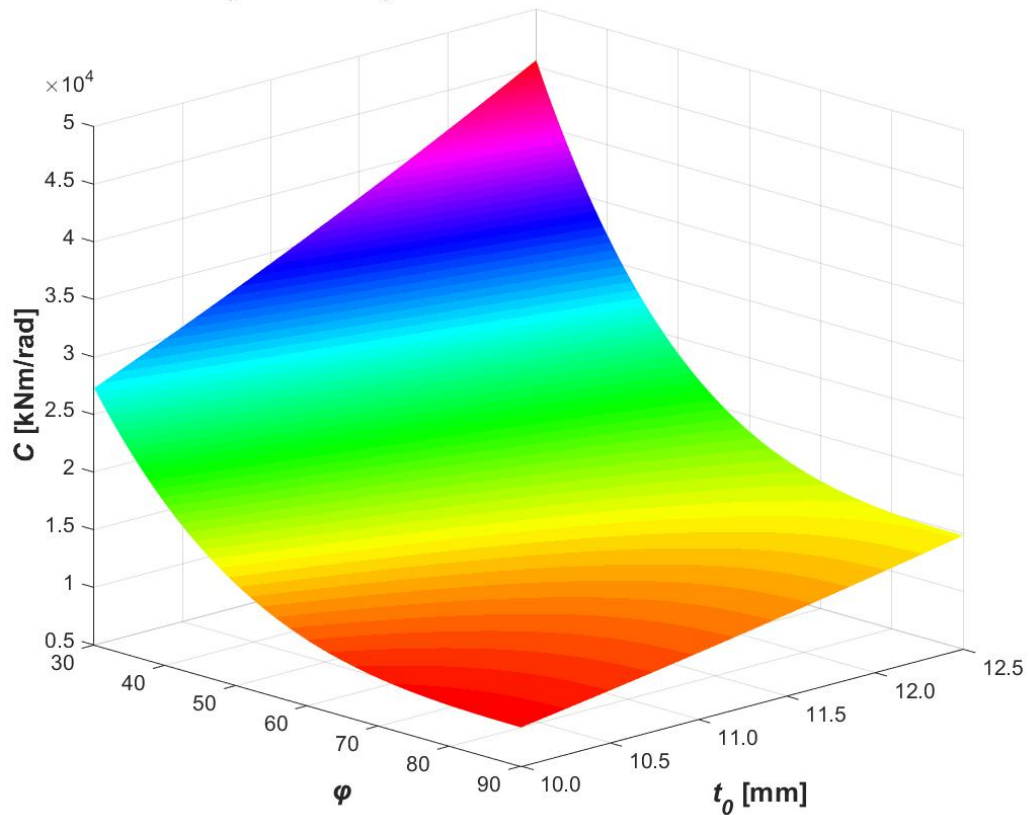


Figure J.9.  $C$ -( $t_0 + \varphi$ ) response, case 3.

Tampereen teknillinen yliopisto  
PL 527  
33101 Tampere

Tampere University of Technology  
P.O.B. 527  
FI-33101 Tampere, Finland

ISBN 978-952-15-3699-1 (printed)  
ISBN 978-952-15-3700-4 (PDF)  
ISSN 1797-9161